Newsletter of the Climate Variability and Predictability Programme (CLIVAR)

Exchanges

No 35 (Volume 10 No 4) October 2005

Southern Hemisphere Climate Variability

CLIVAR is an international research programme dealing with climate variability and predictability on time-scales from months to centuries.

CLIVAR is a component of the World Climate Research Programme (WCRP). WCRP is sponsored by the World Meteorological Organization, the International Council for Science and the Intergovernmental Oceanographic Commission of UNESCO.

The CLIVAR Newsletter Exchanges is published by the International CLIVAR Project Office
ISSN No: 1026 - 0471

Editors: Howard Cattle and Mike Sparrow
Layout: Sandy Grapes
Printing: The Print Centre, University of Southampton

Exchanges is distributed free of charge upon request (icpo@noc.soton.ac.uk)

If undelivered please return to:
International CLIVAR Project Office
National Oceanography Centre Southampton
University of Southampton Waterfront Campus
Southampton, SO14 3ZH, United Kingdom

Editorial

As you will see, this edition of Exchanges focuses on modes of Southern Hemisphere climate variability. It provides a follow-on to the CLIVAR/CliC/SCAR workshop on this topic which was held in Cambridge UK in June this year. The background to the workshop and the main themes of the presentations and discussions are summarised in the article by Ian Renfrew et al. following this Editorial. The result of the call for papers for this edition was overwhelming, resulting in submission of 34 papers in all – far more than we can actually include in this printed edition. In line with the intended title of the issue, therefore, we have decided to include most of the directly mode-based articles we received plus two commissioned papers in the printed copy. Other submitted articles will be found in the full colour pdf version which can be accessed via the CLIVAR home pages http://www.clivar.org/publications/exchanges/index.htm. There are many interesting papers included in the pdf version, so I would encourage all readers to take a look at it. Many thanks indeed to Mike Sparrow who has acted as guest editor and dealt with the checking and proof reading of all the papers and to Sandy Grapes for her extra work on the desktop publishing side of producing this expanded edition. It is indeed encouraging to see the wide variety of CLIVAR-relevant work on the Southern Ocean region.

On the wider hemispheric scale, I would draw attention to the 8th International Conference on Southern Hemisphere Meteorology and Oceanography which will be held from 24-28 April 2006 in Foz do Iguaçu, Paraná State, Brazil. Carolina Vera (VAMOS co-chair and Carlos Nobre are acting as programme co-chairs and the deadline for abstracts has just been extended to 31 October 2005. Further details will be found at http://www.ametsoc.org/AMS and http://www.cptec.inpe.br/SH_Conference.

The CLIVAR SSG Executive met from 15-16 September 2005 at ECMWF. Progress with CLIVAR was reviewed as well as our role in the new WCRP COPES strategy and plans for CLIVAR SSG-14 which will be held in Buenos Aires from 19-22 April 2006. On the COPES front, a new COPES brochure has just been published outlining the overall WCRP COPES strategy. It can be downloaded as a pdf or a hardcopy can be ordered from http://copes.ipsl.jussieu.fr/Publications/index.html.

This month has seen a meeting of the joint JSC/CLIVAR Working Group on Coupled Modelling. An account of the meeting will be published in next month's Exchanges (which will be joint with IGBP PAGES) but a clear and outstanding success discussed at the meeting has been the outcomes of the call for the community to participate in climate model analyses leading to participation in the IPCC Fourth Assessment Report (see CLIVAR Exchanges No. 30, June 2004). This is a type of activity the CLIVAR SSG is strongly supportive of and is keen to see extended e.g. to global model runs on seasonal, interannual and decadal timescales.

Finally I would like to repeat the call in the editorial of Exchanges 32 (January 2005) for suggestions for new members of CLIVAR Panels and Working Groups. If you are interested in taking part in their activities, please send your details, including a short paragraph of background, to icpo@noc.soton.ac.uk.

Howard Cattle

The Modes of Southern Hemisphere Climate Variability Workshop

I. Renfrew, K. Speer, S. Rintoul, D. Thompson, M. Sparrow
Corresponding Author: i.renfrew@uea.ac.uk

A workshop on Modes of Southern Hemisphere Climate Variability was held at the Scott Polar Research Institute, Cambridge, UK from 27-30th June 2005, in association with a CLIVAR/CliC/SCAR Southern Ocean Region Implementation Panel meeting. The goals of the workshop were to review the present understanding of the major modes of variability in southern hemisphere (SH) climate, to assess the potential for predictability of the climate at mid - to high-latitudes of the SH, to identify gaps in our understanding and to discuss field and modelling efforts to fill these gaps. The workshop was organized around invited talks by scientists spanning meteorology, oceanography, sea ice, remote sensing and paleoclimate, including both modelers and observers. Many of the invited speakers have produced an article for this special issue of Exchanges. The meeting program, list of speakers and copies of many of the talks are available online at http://www.clivar.org/organization/southern/Modes_meet.html. In this short note we summarize some of the main themes of the workshop presentations and discussions.

The southern annular mode and southern hemisphere climate

The Southern Annular Mode (SAM) is the primary mode of SH climate variability. The SAM owes its existence to eddy-mean flow interaction in the SH storm track. The impact of the SAM on land and ocean temperatures was discussed, and its role in recent SH climate change was reviewed. Measures of the SAM were also discussed, with no overall consensus on a preferred index. Instead it became clear that there are pros and cons of using an EOF-type analysis (likely most appropriate when reanalyses data are believable) or a zonal-index type analysis (simpler and perhaps more robust but unable to capture details of the large scale structure of the SAM).

There is clear evidence of a positive trend in the SAM in recent decades, with the largest trends in summer (Dec-Jan-Feb). A number of recent studies have attributed the trend to human influences, either changes in stratospheric ozone or greenhouse warming, although others have suggested the trend is within the range of natural variability. New analyses of climate model runs conducted for the IPCC 4th Assessment Report show that all of the models show a positive trend in the SAM when forced with the full suite of natural and anthropogenic forcings; that the SAM trend is outside the range of internal variability in the models; and that, while both greenhouse and ozone forcing tend to drive the SAM to its positive index state, ozone appears to be the stronger driver (at least in DJF). The dynamics of the SAM response to greenhouse forcing remain obscure.

The extent to which the SAM is linked to climate variability in the southern hemisphere continents north of Antarctica is not yet clear. Studies have suggested correlations between variations in the SAM and variations in rainfall in South

America, South Africa and southwestern Australia, presumably because changes in the SAM are associated with shifts in the location of the southern hemisphere storms. However, model studies suggest that translating this into predictable effects over land will be difficult.

The semi-annual oscillation (SAO) refers to a twice-yearly maximum in the magnitude of the sea level pressure gradient between mid- and high-latitudes (e.g. between 50S and 65S). The SAM and the SAO in a sense describe different aspects of the same phenomenon: both describe variations in the circumpolar flow, but the SAO describes variations in the amplitude of the annual cycle whereas the SAM describes variability about the annual cycle.

ENSO and southern hemisphere teleconnections

The Rossby wave teleconnection pattern in the southern hemisphere atmosphere, known as the Pacific South America (PSA) pattern, transfers climate signals from the tropics to high southern latitudes. Many fields have largest variance in the southeast Pacific, where Rossby wave trains generated in both the Indian and Pacific basins reach high latitudes. The PSA pattern is strongest in winter. Atmospheric model experiments with a circular continent displaced from the South Pole reproduce a "pole of variability" in the southeast Pacific, suggesting that orography plays a role in the asymmetric distribution of variability in high southern latitudes. While there is evidence for ENSO-related variability in many high latitude ocean and atmosphere fields, the nature of the connection between low and high latitudes varies with time. For example, during the 1980s, snowfall on the West Antarctic Peninsula was strongly positively correlated with the Southern Oscillation Index; during the 1990s the correlation was strong and negative. The response of the peninsula to the PSA depends strongly on the location of the PSA centre, as east-west shifts of the SLP anomaly can shift the flow over the peninsula from northerly to southerly. The existence of strong teleconnections between the tropics and high southern latitudes means that simulations of Antarctic climate are very sensitive to errors in tropical SSTs.

Ocean/ice responses to modes of variability

Sea ice extent and drift velocities are sensitive to the main modes of southern hemisphere variability, including the PSA, SAM, SAO and the wave number 3 pattern. One example is the Antarctic Dipole, a pattern of anomalies of opposite sign in the southeast Pacific and southwest Atlantic in sea ice and sea-level pressure. The dipole pattern is largely driven by the PSA pattern, although the persistence of the anomalies may indicate a role for ocean-ice dynamics. On a circumpolar scale, the SAO has a particularly strong correlation with sea ice extent, on a range of time-scales. Lag/lead relationships suggest that there is a feedback from the sea-ice distribution on sea-level pressure.

Satellite-derived sea ice drift products are now available that provide new insights into coupled dynamics in the sea ice zone. The combination of radar and laser altimeters and geodetic satellites, carefully validated with *in situ* observations, promises to deliver the first circumpolar estimates of sea ice thickness (and other properties) in the Southern Ocean. These remote sensing products will enable a substantial step forward in understanding the coupled dynamics in the sea ice zone and their influence on climate.

It was suggested that changes in the transport of the Antarctic Circumpolar Current were correlated with changes in the SAM, on time-scales from intra-seasonal to interannual (and perhaps longer). However, the magnitude of the transport response is relatively modest (e.g. a few Sverdrups for a one standard deviation change in the SAM index). This ocean-atmosphere interaction and variability was proposed to constitute a climate mode, though the coupling mechanism between the ocean and atmosphere for this mode is not yet evident.

Evidence from numerical simulations of the ocean/ice system suggests that modes of variability trapped to the Antarctic continent exist on decadal time scales and are of circumpolar extent. Mechanisms invoked include ice advection and the melt/freeze cycle, together with wind-driven effects. Antarctic ice cores provide a unique long-term perspective on the nature of the major modes of southern hemisphere climate variability, including proxies for ENSO, temperature, sea ice extent and circulation patterns such as the strength of the westerlies, the Amundsen Sea Low and the East Antarctic High. This resource has so far been under-utilised by oceanographers and meteorologists.

Several talks discussed the evidence for water mass variability in observations and models. There is clear evidence of changes in each of the major Southern Ocean water masses, but the short and discontinuous observational records make it difficult to describe and determine the causes of the variability. Models have an important role to play, but most models still have significant problems in reproducing the observed water mass structure in the Southern Ocean, so the interpretation of changes in model simulations requires some care.

There was a discussion on the utility of additional meteorological observations in the open ocean and sea-ice zone of the Southern Ocean. Recent work by King (2003) provided some evidence that the current generation of meteorological analyses are very good in a statistical sense over the Southern Ocean, especially in terms of mean sea level (msl) pressure (and hence geostrophic wind speed), due to the use of modern satellite sounder data. However it is likely they are less accurate for near-surface temperature and humidity, hence fluxes, especially over or close to the sea-ice zone.

Summary and open questions/challenges

A number of modes of variability in the atmosphere-ocean-ice system have been identified in the southern hemisphere. Some of the modes are inherent aspects of the high latitude southern hemisphere climate and others are forced by teleconnections from lower latitudes. While many of the modes have analogs in the northern hemisphere, the different continental geometry results in significant differences in the mean state and variability of the southern hemisphere atmosphere, ocean and sea ice. The modes of southern hemisphere variability described in the literature are not all independent and in some cases describe different aspects of the same physical phenomenon. Both models and observations reveal variability of the modes on a range of time-scales, but our understanding of the variability is increasingly primitive as the timescales increase, reflecting the short length of observational records and weaknesses in the models that are more severe at longer timescales.

The workshop provided an excellent summary of the present state of our understanding of southern hemisphere climate variability and identified a number of open questions: What is the dynamical explanation for the response of the SAM to enhanced greenhouse warming in climate models? Is there evidence for coupled modes of variability in the mid- to high-latitude southern hemisphere, or are the ocean and sea ice primarily responding to atmospheric variability? There is evidence for quasi-decadal variability in a number of climate parameters and relationships in high southern latitudes: does this reflect "reddening" of the stochastic forcing by the atmosphere, or do coupled dynamics play a role?

The International Polar Year (IPY) provides a unique opportunity to tackle many of these questions. The workshop was followed by a discussion of a number of IPY programs studying the role of the ocean, atmosphere and sea ice in past, present and future climate. More information on the developing plans for the IPY can be found on the Southern Ocean Panel's web site (http://www.clivar.org/organization/southern/).

We thank the speakers for their excellent and thought-provoking presentations, the workshop participants for their contributions to the discussion sessions, and the Scientific Committee on Antarctic Research, the most recent sponsor of the Southern Ocean panel, for hosting the workshop.

Reference

King, J. C., 2003: Validation of ECMWF Sea Level Pressure Analyses over the Bellingshausen Sea, Antarctica, *Weather and Forecasting*, Vol18, No. 3, pp536-540

Decadal Variability of the Antarctic–ENSO Teleconnection and its Association with the Southern Annular Mode

R. L. Fogt and D. H. Bromwich
Byrd Polar Research Center, Columbus, OH
Corresponding author: fogt.13@osu.edu

There is a need to better understand the decadal variability of the El Niño-Southern Oscillation (ENSO) signal in high southern latitudes. Results from Cullather et al. (1996) and Bromwich et al. (2000) indicate a strong shift in the correlation between West Antarctic (180°-120°W) precipitation minus evaporation and the Southern Oscillation index (SOI, an index that monitors ENSO variability and is the difference in the standardized mean sea level pressure between Tahiti (17.5°S, 149.6°W) and Darwin, Australia (12.4°S, 130.9°E)) using atmospheric reanalysis and operational analysis over the last two decades. The time series of precipitation minus evaporation was positively correlated with the SOI until about 1990, after which it became strongly anticorrelated, a relationship that persisted through at least 2000. Thus, there appears to be strong decadal variability of the ENSO signal in the South Pacific; however, the mechanisms forcing the variability remain undetermined.

To examine the decadal variability of the ENSO teleconnection to the high latitude South Pacific and to ascertain the mechanisms controlling it, correlations between the European Centre for Medium-Range Weather Forecasts (ECMWF) 40-year Reanalysis (ERA-40) and observations with the SOI are carried out over the last two decades. The decadal variability is observed in many fields including the annual mean sea level pressure and 500 hPa geopotential height; annual mean upper level wind and sea level pressure observations are also used to demonstrate the decadal variability and support the spatial representations produced by the ERA-40 reanalysis. Results in these annual mean fields indicate a weak teleconnection in the 1980s in a small region in the South Pacific (Fig. 1a) followed by a much stronger response during the 1990s shifted further south and east, lying across nearly the entire South Pacific and Amundsen/Bellingshausen Seas (Fig. 1b).

Analyzing the decadal variability by seasons demonstrates that the strong ENSO teleconnection seen in the annual mean plots is accounted for by the teleconnections during austral spring and summer. The reduced annual teleconnection during the 1980s is readily explained by the lack of a response during the spring in the 1980s; during the summer the teleconnection remains strong for both the 1980s and the 1990s although its spatial representation is different. The different spatial patterns between the 1980s and the 1990s in the summer help to explain the shifting of the correlation pattern seen in the annual mean plots. 500 hPa geopotential height anomaly composites that concentrate on ENSO events during spring and summer also confirm the decadal variability seen in the correlation plots.

Empirical orthogonal function (EOF) analysis, a statistical method that extracts dominant modes of variability, demonstrates that the patterns correlated with ENSO and the

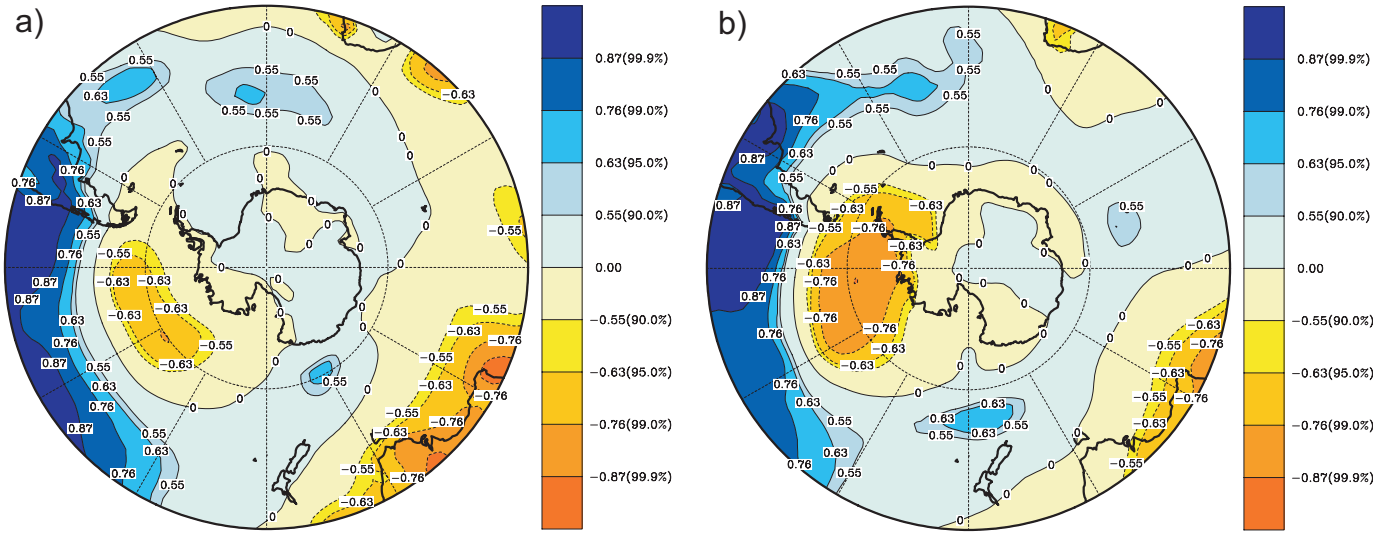

Figure 1. Spatial correlations of the annual mean ERA-40 mean sea level pressure and the SOI for a) 1980s and b) 1990s. Significance levels for correlation values are listed beside the key. Adapted from Fogt and Bromwich (2006).

Southern Annular Mode (SAM, a circulation pattern in the high southern latitudes which captures the variability in the north-south pressure gradient) have large loading centers in the South Pacific during austral spring and summer. As such, the high southern latitude ENSO teleconnection is amplified in the South Pacific when the SAM is positively correlated with the SOI, and is weakened during times of insignificant or negative correlation. During the austral spring, the SOI and the ERA-40 SAM are not significantly correlated during the 1980s, but are significantly (>95% confidence level) correlated during the 1990s, in agreement with the changes in the strength of the ENSO teleconnection during this season. During the austral summer, the SOI and the SAM maintain a significant correlation during both decades, which corresponds to the persistent teleconnection during this season. The shifting of the pattern during the summer is brought about by both the strong ENSO events of the late 1990s, which produced anomalies that were located further east towards the Antarctic Peninsula (Bromwich et al. 2004), and the marked strengthening of the SAM during this season (Marshall 2003), which moved the region of SAM / ENSO coupling farther south. Thus, the ENSO teleconnection to the high latitude South Pacific is governed by the coupling with the dominant Southern Hemisphere circulation captured by the SAM.

These findings, in combination with a growing body of literature, suggest that the tropical ENSO activity plays an important role in the forcing of the high southern latitude tropospheric circulation. It is unclear whether the coupling observed here between the high latitude Southern Hemisphere circulation and ENSO is part of natural climate variability or climate change; the quality of the available reanalyses limits the study to roughly the last two decades. However, the associations depicted in the 1990s are the strongest observed during this time period, in agreement with other recent studies (e.g., Bromwich et al. 2004).

References

Bromwich, D.H., A.J. Monaghan, and Z. Guo, 2004: Modeling the ENSO modulation of Antarctic climate in the late 1990s with Polar MM5. *J. Climate,* 17, 109-132.

Bromwich, D.H., A.N. Rogers, P. Kallberg, R.I. Cullather, J.W.C. White, and K.J. Kreutz, 2000: ECMWF analysis and reanalysis depiction of ENSO signal in Antarctic precipitation. *J. Climate*, 13, 1406-1420.

Fogt, R.L. and D.H. Bromwich, 2006: Decadal variability of the ENSO teleconnection to the high latitude South Pacific governed by coupling with the Southern Annular Mode. *J. Climate*, accepted.

Cullather, R.I., D.H. Bromwich, and M.L. Van Woert, 1996: Interannual variations in Antarctic precipitation related to El Niño-Southern Oscillation. *J. Geophys. Res*., 101, 19,109-19,118.

Marshall, G.J., 2003: Trends in the Southern Annular Mode from observations and reanalyses. *J. Climate,* 16, 4134-4143.

Modes of interannual Antarctic tropospheric circulation and precipitation variability

C. Genthon
Laboratoire de Glaciologie et Géophysique de l'Environnement, Saint Martin d'Hères, France
Corresponding author: genthon@lgge.obs.ujf-grenoble.fr

The SAM (Southern Annular Mode, also called the High Latitude Mode or Antarctic Oscillation) and ENSO are major components of the internannual climate variability in the southern hemisphere. This is, in particular, demonstrated by Empirical Orthogonal Functions (EOF) applied to meteorological analyses of the southern hemisphere atmospheric circulation (e.g. Kidson 1999). The spatial patterns of the main southern hemisphere EOFs, which show significant contributions of SAM and ENSO south of 60°S, suggest that Antarctic climate variability is embedded within that of the Southern hemisphere as a whole. By analysing the tropospheric circulation (and precipitation) in the Antarctic region alone, that is south of 60°S only, Genthon et al. (2003) confirm that the Antarctic climate variability is largely related to the southern mid- (SAM) and tropical (ENSO) latitudes: More than ~50% of the tropospheric variability (1st EOF) in the region is related to SAM, and an additional ~20% (2nd EOF) to ENSO (based on NCEP-NCAR analyses, ECMWF analyses, and climate model results). Much of this variability is concentrated in the western part of Antarctica (Figure 1).

Antarctic ENSO and precipitation

While an ENSO signature in the Antarctic atmospheric circulation is rather clear and unequivocal , hints of an ENSO signature in the Antarctic precipitation have been reported (e.g. Cullather et al. 1996) but challenged (e.g. Genthon and Krinner 1998). Antarctic precipitation is still very poorly known, yet this is the main positive term in the Antarctic ice sheet mass balance equation. The Antarctic ice sheet evolution in response to climate change may have significant contributions to sea-level, yet verifying whether climate models can predict ice sheet mass balance in the future is badly hampered by limited knowledge and understanding of Antarctic precipitation. In addition, that ENSO is reflected in Antarctic precipitation suggests that its signature can be recorded in ice cores, providing a way to reconstruct past ENSOs. It is thus important to decipher the characteristics of ENSO in Antarctic precipitation.

Short term forecasts based on meteorological analyses provide precipitation datasets with full spatial and temporal coverage, including over Antarctica. However, the observational control is poor on such data, which are thus largely model results. In addition, precipitation fields are much more noisy and irregularly distributed than circulation fields, with particularly strong spatial gradients in Antarctica. As a result, covariance-based EOF analysis of precipitation is much less convincing than for circulation. However, Genthon et al. (2003) and Genthon and Cosme (2003) show that various data sets (NCEP-NCAR, ECMWF, climate models) agree on a main mode of Antarctic precipitation variability, with again much of the variability concentrated in west-Antarctica (Figure 2). The contributions of SAM and ENSO to this mode, which appear mixed and cannot be separated by EOF analysis, is quite clear: A main pole of geopotential variability in the Amundsen sea sector (Figure 1) results in a dipole of precipitation variability in phase opposition between the Ross-Amundsen and the Bellingshausen-Peninsula sectors (Figure 2) due to air and moisture advection (Genthon et al. 2003, Genthon et al. 2005).

Are there any real observations to validate such a result? Kaspari et al. (2004) present firn core data in west Antarctica that resolve annual snow accumulation and which correlate

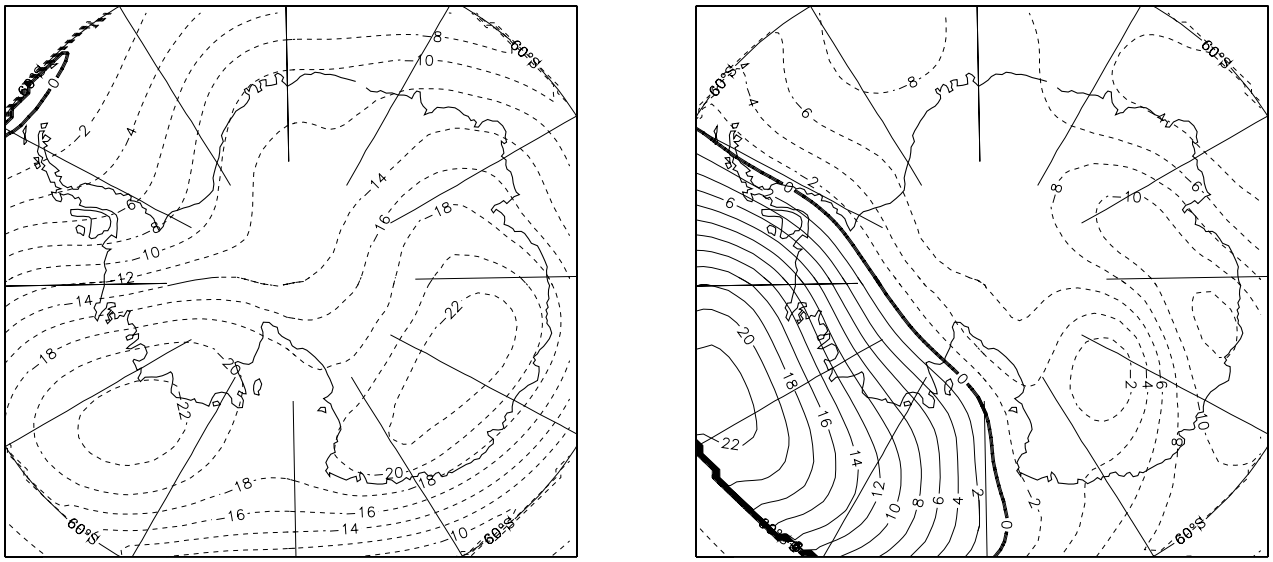

Figure 1: The first 2 EOFs of the 500 hPa geopotential height in the Antarctic region. 500 hPa data from NCEP-NCAR and ECMWF analyses and LMDZ climate model for 1979-1999, with 25-month Hanning filter. See Genthon et al. 2003 for details.

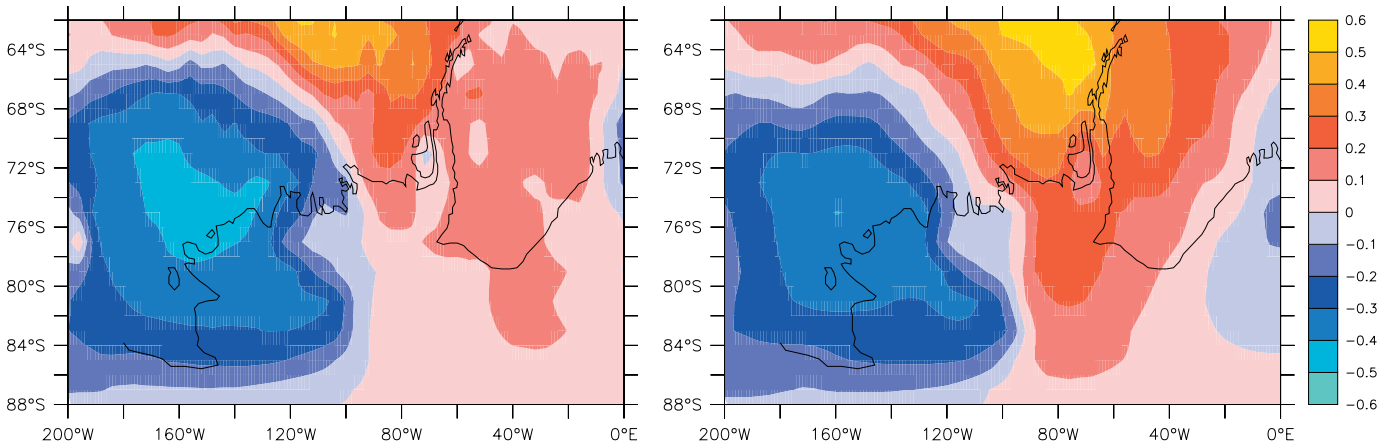

Figure 2: Major mode of variability of west Antarctic precipitation variability from EOF analysis, from ECMWF ERA40 forecasts (left) and HADCM3 climate model results (right).

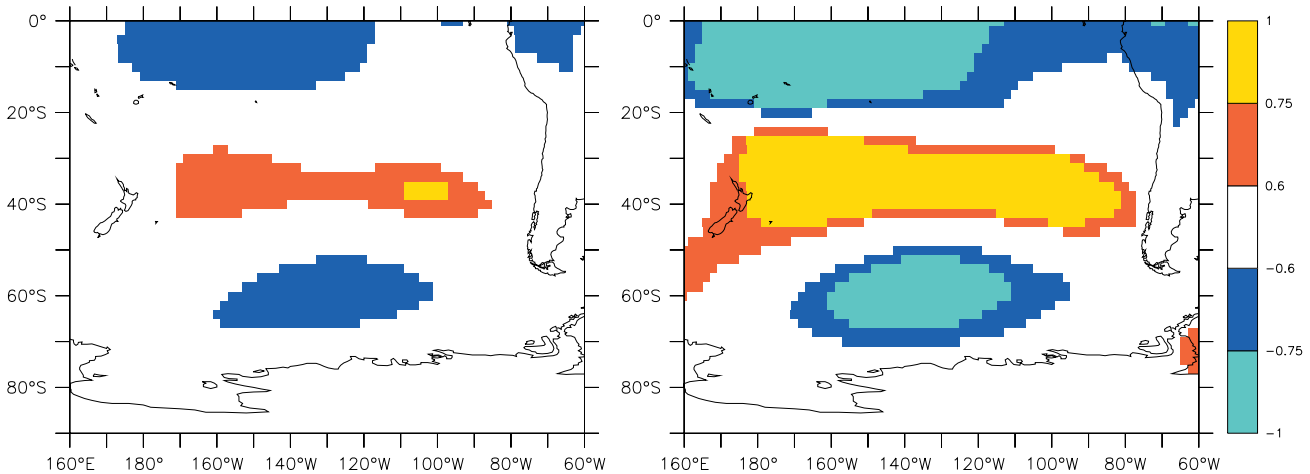

Figure 3: Correlation between ERA40 500 hPa geopotential height and the Southern Oscillation Index over 1958-2001 (left) and for a subset during which the ENSO signature in Antarctic precipitation is highest (right). The ENSO wave train is much stronger in the latter case.

differently with ENSO depending on ice core location. Genthon et al. (2005) show some agreement between meteorological analyses and model results and Kaspari et al. (2004)'s core data, but the comparison is limited, in particular, by the spatial significance of firn cores compared to that of model results. Additional field data of annual precipitation/accumulation (cores, stakes network, etc) are badly needed.

ENSO intermittency in Antarctica

A reason why the signature of ENSO in Antarctic precipitation, either in model results or field data, is elusive and resists robust characterization, may be that it is intermittent. Genthon et al. (2003) and Genthon and Cosme (2003) report that the magnitude of the contribution of ENSO to precipitation variability in west-Antarctica vary at approximately interdecadal time scales. The signature of ENSO in Kaspari et al. (2004)'s core data also vary with the period sampled (Genthon et al. 2005). Figure 3 shows that, in ECMWF ERA40 data, the propagation of the ENSO wave train from the troplical Pacific to west Antarctica is indeed stronger when the signature of ENSO in Antarctic precipitation is largest. Others (e.g. Bromwich et al. 2000) have found that the correlation between Antarctic precipitation and ENSO can change sign with time, although this is not confirmed by EOF analyses as presented here (but EOF is admittedly only an empirical linear covariance analysis), nor by firn core data (Genthon et al. 2005).

Conclusions / summary

From a climate variability point of view, Antarctica is not an isolated region. Much (~70%, a least) of the the interannual variability of the tropospheric circulation in the Antarctic region is related to that of regions in the mid- and even the tropical southern latitudes. It is thus not highly surprising that the signature of a major tropical signal, ENSO, can be traced in the Antarctic precipitation, mainly in west Antarctica. This signature shows as dipole of variability with phase opposition between the Ross-Amundsen and the Bellingshausen-Peninsula sectors. However, the detailed characteristics of this signature are still poorly known, verified and understood. In fact, it seems that the signature of ENSO in Antarctic climate and precipitation is intermittent, in relation to the variable strength of the dynamic link between the tropics and west Antarctica related to ENSO.

References

Bromwich, D. H., A. N. Rogers, P. Kallberg, R. L. Cullather, J. W. C. White, K. J. Kreutz, 2000: ECMWF analyses and reanalyses of ENSO signal in Antarctic precipitation, *J. Clim*. 13, 2673-2690.

Cullather, R.I., D.H. Bromwich, M. Van Woert, 1996: Interannual Variations in Antarctic Precipitation Related to El Niño - Southern Oscillation, *J. Geophys. Res*. 101, 19,109-19,118.

Genthon C., et G. Krinner, 1998: Convergence and disposal of energy and moisture on the Antarctic polar cap from ECMWF analyses and forecasts, *J. Clim*. 11, 1703-1716

Genthon C., G. Krinner, M. Sacchettini, 2003: Interannual Antarctic tropospheric circulation and precipitation variability, *Clim. Dyn*. 21, 289-307. DOI 10.1007/s00382-003-0329-1.

Genthon, C., and E. Cosme, 2003: Intermittent signature of ENSO in west-Antarctic precipitation, *Geophys. Res. Lett*., 30, 2081, doi:10.1029/2003GL018280.

Genthon C., S. Kaspari, and M. Mayewsky, 2005: Interannual variability of the surface mass balance of West Antarctica from ITASE cores and ERA40 reanalyses, *Climate Dyn*. 24, 759-770, DOI: 10.1007/s00382-005-0019-2.

Kaspari, S. , P. A. Mayewski, D. A. Dixon, V. B. Spikes, S. B. Sneed, M. J. Handley, G. S. Hamilton, 2004: Climate Variability in West Antarctica Derived from Annual Accumulation Rate Records from ITASE Firn/Ice Cores, *Ann. Glaciol*., 39, 585-594.

Kidson, J. W., 1999: Principal modes of Southern hemisphere low-frequency variability obtained from NCEP-NCAR reanalyses, *J. Climate*, 12, 2808-2830.

SAM–related variations in the Antarctic Peninsula from IPCC AR4 models

C. G. Menéndez[1] and A. F. Carril[2]
[1]Centro de Investigaciones del Mar y la Atmósfera/CONICET–UBA, Buenos Aires, Argentina
[2]Istituto Nazionale di Geofísica e Vulcanología, Bologna, Italy
Corresponding author: menendez@cima.fcen.uba.ar

1. Introduction

The Southern Annular Mode (SAM), a zonally symmetric and equivalent barotropic structure with synchronous pressure anomalies of opposite sign in mid- and high-latitudes, controls a significant proportion of the atmospheric seasonal to interannual variability in the southern extratropics (e.g. Thompson and Wallace, 2000). When pressures are below (above) average over Antarctica and westerly winds are enhanced (reduced) over the Southern Ocean, the SAM is said to be in its high (low) index or positive (negative) phase. Transient climate simulations in general exhibit a trend in the SAM towards its positive phase with a strengthening of the circumpolar vortex and intensification of the circumpolar westerlies (e.g. Kushner et al., 2001; Cai et al., 2003; Rauthe et al., 2004). The Antarctic Peninsula is a notable area where the observed warming during the second half of the 20th century has been a critical climatic change. This regional warming (~ 2°C), not captured by earlier climate models (Vaughan et al. 2001), is consistent with circulation changes associated with the trend in the SAM (Kwok and Comiso; 2002; Schneider et al.; 2004).

The region south of the Antarctic Circumpolar Current is the site of extensive seasonal sea ice cover, which is intricately involved with atmospheric variability and water mass modification processes. As a result, surface temperature varies greatly during the year and part of this seasonal variation could be connected with the SAM. The relationship between the positive phase of the SAM and surface features of the regional climate around Antarctica, through the analysis of simulations from a multimodel ensemble in the framework of the IPCC 4th Assessment Model Output experiment, was recently documented in Carril et al. (2005). The goal of the present study is to further explore the potential climate variations in the Antarctic Peninsula region associated with changes in the positive phase of the SAM under enhanced GHG forcing. In particular, we discuss aspects of the seasonal cycle of the SAM and its response.

2. Data and methodology

We analyse simulations of the 20th century climate (period 1970-1999) and of the 21st century climate using the SRES

A2 scenario (period 2070-2099). Our study includes a subset of seven IPCC AR4 models from seven modelling centres: CNRM-CM3, GFDL-CM2.0, GISS-ER, IPSL-CM4, MIROC3.2 (medres), MRI-CGCM2.3.2 and PCM. Documentation of these models is available on the PCMDI web site (http://www-pcmdi.llnl.gov). We consider four seasons, defined as JFM (January-March), AMJ (April-June), JAS (July-September) and OND (October-December). Input data are seasonal mean series. Series for the analysis are linearly detrended; anomalies are relative to the best straight-line fit linear trend from the input data. The SAM is defined as the leading mode of the empirical orthogonal function (EOF-1) obtained from anomaly series of 500 hPa geopotential heights, area weighted by the square root of cosine of latitude. The EOF domain is south of 20°S. We identify events during which the positive phase of the SAM is particularly strong (seasons in which the principal component, PC-1, is above one standard deviation of its mean value). We perform composites of anomalies of different variables and examine the associated climate response and its seasonal cycle in the Antarctic Peninsula region.

The EOF-1 of seasonal 500 hPa geopotential height anomalies explains 37% (JFM), 20% (AMJ), 22% (JAS) and 42% (OND) of the variability in the present climate, and 41% (JFM), 18% (AMJ), 25% (JAS) and 41% (OND) during 2070-2099. The spatial patterns of the EOF-1 in the two time slices are very similar (not shown), but the loadings derived from the SRES A2 scenario are somewhat higher, especially in the mid-latitudes, compared to the present climate.

3. Results

According to Carril et al. (2005) the sea-ice concentration ensemble-mean values are in rough accord with observational datasets. Models tend on average to produce too little sea ice cover (except along sectors of the sea-ice edge region where the sea-ice extent is slightly overestimated) and to amplify the amplitude of its seasonal cycle. But the large interannual variability and the large across-model scatter (especially in the Weddell Sea) make the comparison with observations difficult. The relatively good performance of the ensemble-mean results from the averaging of some models with too small sea ice cover and others with too large sea ice cover (Arzel et al., 2005).

The figure shows the ensemble-mean temperature anomalies for seasons characterised by a particularly strong positive phase of the SAM for both present and future climates. This phase is associated with strong circumpolar flow that tends to isolate the cold sub-antarctic seas from warmer air in the Southern Ocean. This leads in general to cooler temperatures around the continent, except in the Antarctic Peninsula region, where anomalous strong meridional winds lead to increased warm advection from the north. For the first time-slice (1970-1999, left panels), this pattern is especially visible during AMJ and OND. Weaker positive anomalies are also simulated in the Amundsen-Bellingshausen seas throughout the annual cycle. The central and eastern Weddell Sea presents negative anomalies.

In general, these patterns are reinforced during the second time slice (2070–2099, right panels). Under enhanced GHG forcing, anomalies intensify and a dipole pattern between the Antarctic Peninsula region and large areas in the Weddell Sea becomes more apparent (especially in AMJ and OND). During JAS the pattern is rather different, with strong cooling in the western Weddell Sea and warming in the Amundsen Sea. The asymmetry in the thermal response in winter is possibly imposed by the oceanic state: in winter the mixed layer depth

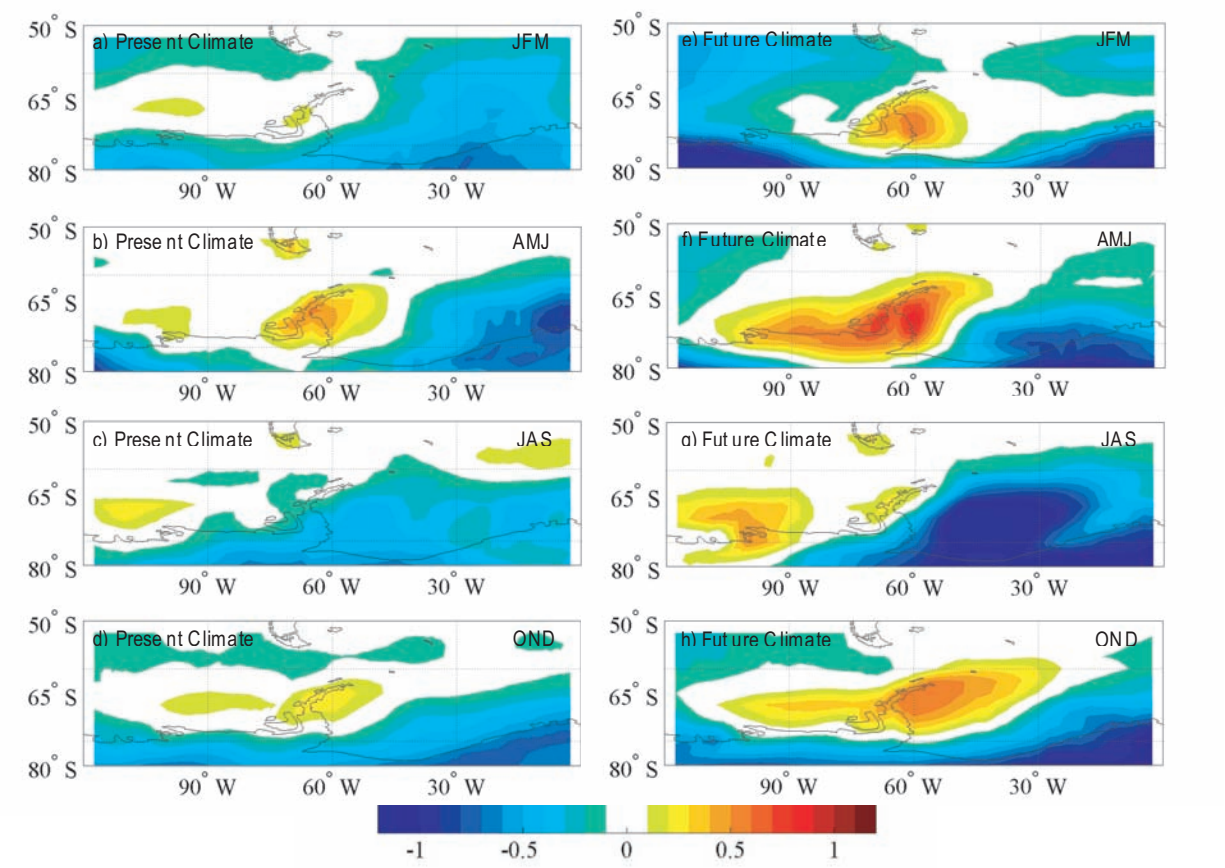

Figure 1: Composite anomalies of surface temperature [K] for the SAM positive phase. Left column is for the 20th century experiment and right column is for the SRES A2 experiment. Every panel illustrates a particular season

is deeper (Levitus and Boyer 1994, Yuan and Martinson, 2000). This seasonal cycle is associated with the sea ice response and its distribution and concentration in the region.

4. Final remarks

We show that the amplitude of the seasonal cycle of temperature anomalies associated with the positive phase of the SAM would increase in a warming climate. Perhaps more interestingly we find that, in contrast to previous TAR models, the ensemble created by this subset of IPCC AR4 models seems capable of simulating the Antarctic Peninsula warming induced by the positive phase of the SAM. As the surface temperature is determined by both the atmospheric circulation and the radiation balance and is sensitive to complex interactions within the coupled system, these results would suggest a general improvement in our simulation capacity. However, it should be highlighted that, even with the IPCC AR4 coupled models, the uncertainty in simulating the present-day sea ice coverage and thickness and in predicting sea ice changes remains large.

Acknowledgments.

We acknowledge the international modeling groups for providing their data for analysis, the Program for Climate Model Diagnosis and Intercomparison (PCMDI) for collecting and archiving the model data, the JSC/CLIVAR Working Group on Coupled Modelling (WGCM) and their Coupled Model Intercomparison Project (CMIP) and Climate Simulation Panel for organizing the model data analysis activity, and the IPCC WG1 TSU for technical support. The IPCC Data Archive at Lawrence Livermore National Laboratory is supported by the Office of Science, U.S. Department of Energy. This research was done in the framework of CLARIS EU project. A. F. Carril was partially supported by CLARIS (GOCE-CT-2003-01454) and by MERSEA IP project (SIP3-CT-2003-502885) and C.G. Menéndez by project PIP 5416 (CONICET, Argentina).

References

Arzel, O., T. Fichefet, and H. Goosse, 2005: Sea ice evolution over the 20th and 21st centuries as simulated by current AOGCMs. *Ocean Modelling*, submitted.

Cai, W., P.H. Whetton, and D.J. Karoly, 2003: The response of the Antarctic Oscillation to increasing and stabilized atmospheric CO2. *J. Climate,* 16, 1525-1538.

Carril A. F., C. G. Menéndez, and A. Navarra, 2005: Climate response associated with the Southern Annular Mode in the surroundings of Antarctic Peninsula: A multimodel ensemble analysis, *Geophys. Res. Lett.*, 32, L16713, doi:10.1029/2005GL023581.

Kushner, P.J., I.M. Held, and T.L. Delworth, 2001: Southern hemisphere atmospheric circulation response to global warming. *J. Climate*, 14, 2238-2249.

Kwok, R. and, J. Comiso, 2002: Spatial patterns of variability in Antarctic surface temperature: Connections to the Southern Hemisphere Annular Mode and the Southern Oscillation. *Geophys. Res. Lett.*, 29, 1705, doi:10.1029/2002GL015415.

Levitus, S., and T. Boyer, 1994: World Ocean Atlas 1994, Volume 4: Temperature. NOAA Atlas NEDSIS 4, U.S. Department of Commerce, Washington D.C.

Rauthe, M., A. Hense, and H. Paeth, 2004: A model intercomparison study of climate change signals in extratropical circulation. *Int. J. of Climatol.*, 24, 643-662.

Schneider, D.P., E.J. Steig, and J.C. Comiso, 2004: Recent climate variability in Antarctica from satellite-derived temperature data. *J. Climate,* 17, 1569–1583.

Thompson, D. W. J., and J. M. Wallace, 2000: Annular modes in the extratropical circulation, Part I: Month-to-month variability. *J. Climate,* 13, 1000–1016.

Vaughan, D., G. Marshall, W. Connolley, J. King, and R. Mulvaney, 2001: Devil in the detail. *Nature*, 293, 1777-1779.

Yuan, X., and D. Martinson, 2000: Antarctic sea ice extent variability and its global connectivity. *J. Climate*, 13, 1697-1717.

Southern Hemisphere Climate Modes and Their Relationships with Antarctic Sea Ice

X. Yuan
Lamont–Doherty Earth Observatory of Columbia University
Corresponding author: xyuan@ldeo.columbia.edu

1. Introduction

Numerous studies have suggested a strong link between the tropical El Niño-Southern Oscillation (ENSO) phenomenon and Antarctic sea ice variability (Simmonds and Jacka, 1995; Harangozo, 2000; Yuan and Martinson, 2000; 2001; Kwok and Comiso, 2002). The strongest tropical-polar teleconnection in the temperature and sea ice fields is the Antarctic Dipole mode with anomalous centres in the northeastern Ross Gyre, and the central Weddell Gyre. The Antarctic Dipole temperature anomalies present the largest ENSO signal outside of the tropical Pacific (Liu et al., 2002). It also represents the largest interannual variability in the Antarctic sea ice field. The changes of the basin-scale meridional circulation in the South Pacific and South Atlantic and stationary Rossby wave propagation associated with the ENSO variability are the main mechanisms for this tropical/polar teleconnection (Yuan, 2004). However, besides the ENSO impact, a number of distinct high latitude climate modes exist in the Southern Hemisphere at intra-seasonal to decadal time scales. These regional climate variabilities likely influence Antarctic sea ice but their impacts are less understood. Particularly, the relative importance of the impact from different climate modes has not been addressed before. This study systematically investigates the influences of high latitude climate variability on the Antarctic sea ice distribution at interannual time scales.

2. Southern Hemisphere Climate Modes

The climate variability examined here includes the following distinct climate modes in mid-high latitudes. First, the Southern Annular Mode (SAM) is marked by zonally symmetric but out-of-phase pressure anomalies between mid and high latitudes. It is a dominant climate mode in the Southern Hemisphere with maximum variability at a period of 10 days (Thompson and Wallace, 2000). The mechanism that causes and maintains this climate mode is a positive feedback between eddy activity in mid-high latitudes and zonal mean flow (Thompson, 2005). Hall and Visback (2002) in a modeling study showed that positive SAM means stronger westerlies, which creates a more northward ice transport resulting in thinner ice near the coast and thicker ice near the ice edge. Lefebvre et al. (2004)

in a different modelling study showed that the SAM index is modestly correlated with sea ice with marginal significance, and ice concentration response to SAM is out-of-phase in the Ross Sea and Weddell Sea rather than exhibiting a zonally symmetric response.

The second mode considered is the semi-annual oscillation (SAO), which describes another more-or-less zonally symmetric mode in the southern extra-tropics. The SAO is characterized by the twice-yearly enhancement in meridional gradients of temperature and pressure fields (van Loon, 1984, Simmonds and Jones, 1998). It is caused by differential solar heating at mid and high latitudes. The atmospheric convergence line with a strong half-year cycle exerts significant influence on the seasonal asymmetric behaviour of the ice extent: slowly advancing equatorward in fall/autumn and retreating fast in spring (Enomoto and Ohmura, 1990). The timing of the semi-annual migration of the Circumpolar Trough dynamically influences the timing of sea ice advance and retreat in the Western Antarctic Peninsular (Stammerjohn et al., 2003)

The third mode is the quasi-stationary wave-3 pattern in southern mid latitudes, a predominant winter mode in pressure/wind fields (van Loon, 1972). The land/ocean distribution in mid-latitudes of the Southern Hemisphere likely creates and maintains the wave-3 pattern. Yuan et al., (1999) showed that three southerly branches of the wave-3 pattern coincide with three northward maximum extent of sea ice edge during late winter 1996, suggesting the role of the wave-3 pattern in advancing the ice edge. Besides this case study, no thorough research has been done so far on the influence of wave-3 on sea ice in other seasons and at different time scales.

Lastly, the Pacific South America (PSA) pattern, which dominates climate variability in the subpolar region of the South Pacific, is considered. The PSA pattern is part of the stationary

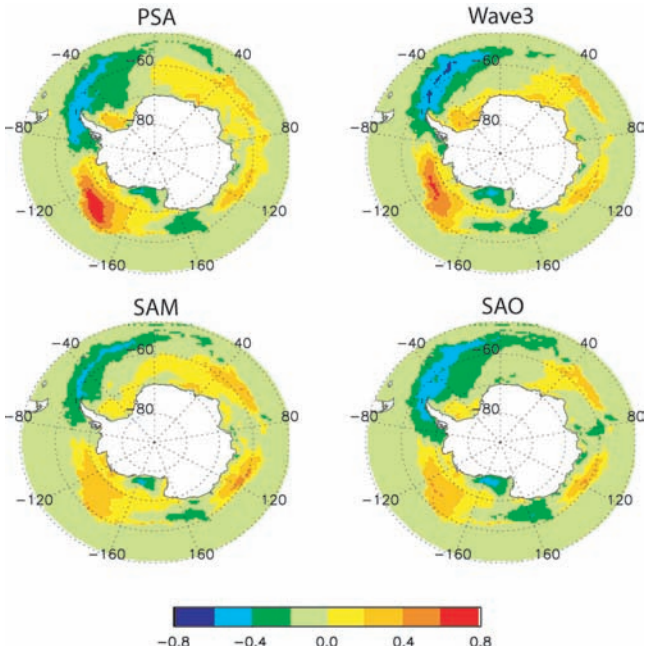

Figure 1. Correlation coefficients between Antarctic sea ice concentration anomalies (lag two months) and time series of the Pacific South American pattern (PSA), Wave-3 pattern, Southern Annular Mode (SAM) and Semi-Annual Oscillation (SAO), respectively.

Rossby wave train, which is usually generated by changes in tropical convection (Mo and Higgins, 1998). At the interannual time scale, the PSA pattern is associated with ENSO variability, creating persistent high (low) pressure centres in the southeast Pacific in response to ENSO warm (cold) events, respectively. The anomalous pressure centre consequently has a significant impact on the sea ice variability in the western hemisphere through thermodynamic and dynamic processes, creating the Antarctic Dipole in sea ice and surface temperature. (Kwok and Comiso, 2002, Yuan, 2004).

3. Impacts on Sea Ice

To systematically and comparatively examine the relationships between these climate modes and sea ice distribution, time series of these modes are constructed using monthly NCEP/NCAR reanalysis data. We either follow conventions used in earlier literature or choose the atmospheric variables that best represent these modes to define the indices of the modes. The PSA, by its nature, appears in pressure fields. The PSA index is then defined by monthly 500mb height anomalies at three anomalous centres east of New Zealand (H1), the Amundsen Sea (H3) and the southwest Atlantic (H2), respectively. This definition, IndexPSA= (H1+H2-H3)/3, is similar to the definition of the PNA in the Northern Hemisphere. Since the wave-3 pattern is most profound in meridional winds, the principle component of the leading EOF mode in surface monthly meridional wind provides the time series of the pattern. The lead EOF mode of sea level pressure describes the SAM variability, as used in earlier studies, which accounts for 28% of total variance of monthly SLP. Last, the index of SAO is defined by subtracting zonal mean SLP at 55°S by the zonal mean SLP at 65°S.

The time series of these four climate modes are then correlated with 24 years of monthly sea ice concentration anomalies around the Antarctic from ice lagging 6 months to leading 6 months. Figure 1 shows the correlations when ice lags the atmosphere by two months. The influences from the PSA pattern and wave-3 pattern on sea ice are stronger than that from the other two modes and are more profound in the western hemisphere. The SAM and SAO have relatively weaker but more evenly distributed correlations with sea ice around the Antarctic. Since all climate indices and sea ice concentration anomalies were detrended and filtered by a Gaussian filter with filter length of 13 months prior to the correlation, these correlations mainly represent the shared variance at interannual time scales. The correlation at each grid point is also tested for its confidence level and the percentage of the grid points that pass 99% confidence level for each correlation map is calculated. The results from this significance test suggest that the SAM has relatively less influence on sea ice than other climate modes. Moreover, sea ice usually responds to the atmospheric forcing with a two-month delay (figure 2).

4. Discussion

Although the physical or dynamical processes that create these climate modes are totally different, they are hardly independent from each other because of their interactions. As defined in this study, the SAM and SAO are quasi-zonally symmetric modes sharing 62% of the variance, while the PSA and Wave-3 are zonally asymmetric, sharing 36% of the variance. These interdependencies appear in the correlation maps (figure 1). In addition, these correlations mainly reflect the shared variance at interannual time scales. Some modes, such the SAO and Wave-3, have a stronger influence on sea ice at the seasonal time scale. In summary, the largest impact on sea ice comes from the PSA and Wave-3 patterns and occurs in the Antarctic Dipole regions. These modes are influenced by the remote ENSO forcing.

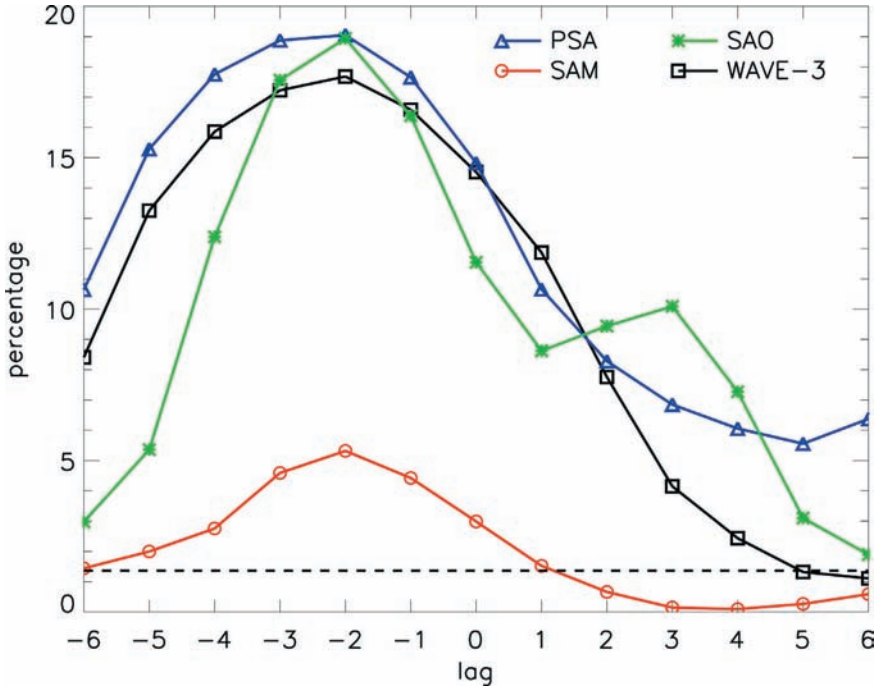

Figure 2. Percentage of grid points with significant correlation at 99% confidence level as a function of climate modes lagging months.

Acknowledgements.

This study is supported by the National Aeronautics and Space Administration through Grant NAG-12587 and Grant JPLCIT 1216483.

References

Enomoto, H. and A. Ohmura, The influence of atmospheric half-yearly cycle on the sea ice extent in the Antarctic. *J. Geophys. Res*., 95, C6, 9497-9511, 1990.

Hall, A, M. Visbeck, Synchronous variability in the southern hemisphere atmosphere, sea ice, and ocean resulting from the annular mode. *J. Climate*, 15 (21): 3043-3057, 2002.

Harangozo, S. A., A search for ENSO teleconnection teleconnections in the west Antarctic Peninsula climate in austral winter, *Int. J. Climatol*., 20, 663-678, 2000.

Kwok, R. and J. C. Comiso, Southern Ocean climate and sea ice anomalies associated with the Southern Oscillation. *J. Climate*, 15, 487-501, 2002.

Liu, J., X. Yuan, D. Rind and D. G. Martinson, Mechanism Study of the ENSO and Southern High Latitude Climate Teleconections. *Geophys. Res. Lett*., Vol. 29, No. 14, 1029/2002GL015143. 2002.

Mo, K. C. and R. W. Higgins, The Pacific-South America modes and tropical convection during the Southern Hemisphere winter. *Mon. Weather Rev*., 126, 1581-1596, 1998.

Simmonds, I. and T. H. Jacka, Relationships between the Interannual Variability of Antarctic Sea Ice and The Southern Oscillation. *J. Climate*, 8, 637-647, 1995.

Simmonds, I. and D. A. Jones, The mean structure and temporal variability of the semiannual oscillation in the southern extratropics. *Int. J. Climatol*., 18, 473-504, 1998.

Stammerjohn SE, M.R. Drinkwater, R.C. Smith, and X. Liu, Ice-atmosphere interactions during sea-ice advance and retreat in the western Antarctic Peninsula region. *J. Geophys. Res*. – Ocean, 108 (C10): Art. No. 3329, 2003

Thompson, D. W. J. Large scale climate variability in the Southern Hemisphere. Presentation at Modes of Southern Hemisphere Climate Variability & Southern Ocean Panel meeting, Scott Polar Research Institute, Cambridge, UK. July 27-30, 2005

Thompson, D. W. J. and J. M. Wallace, Annular modes in the extratropical circulation, part I, Month-to-month variability. *J. Climate*, 13, 1000-1016, 2000

van Loon, H., The Southern Oscillation, part 3, Associations with the trades and with the trough in the westerlies of the South Pacific Ocean. *Mon. Weather Rev*., 112, 947-954, 1984.

van Loon, H. Wind in the Southern Hemisphere. Meteorology of the Southern Hemisphere, Meteor. Monogr. No. 35, *Amer. Meteor. Soc*., 59-86, 1972.

Yuan, X., ENSO-related impacts on Antarctic sea ice: Synthesis of phenomenon and mechanisms. *Antarctic Sciences*, 16(4), 415-425, 2004.

Yuan, X. and D. G. Martinson, The Antarctic Dipole and its Predictability. *Geophys. Res. Lett*, Vol. 28, No. 18, 3609-3612, 2001.

The Southern Annular Mode and South African rainfall

C.J.C. Reason and M. Rouault
Dept. of Oceanography, University of Cape Town, South Africa
Corresponding author: cjr@egs.uct.ac.za

1. Introduction

Understanding South African rainfall variability and working towards improved long range forecasting is challenging because the region appears to be influenced by ENSO, the Southern Annular Mode (SAM), and SST patterns in the neighbouring South Atlantic and South Indian Oceans as well as by Antarctic sea-ice variability. Historically, most attention has focussed on the influence of the Indian Ocean and of ENSO (e.g., Lindesay, 1988; Walker 1990; Mason and Jury, 1997; Reason et al., 2000) since most of the country is dominated by summer rainfall with the major moisture source being the western Indian Ocean. In this note, we consider relationships between the Southern Annular Mode, South Atlantic SST and South African rainfall variability.

2. Winter rainfall variability

The west coast of South Africa contains the country's second largest city and is a mainly winter rainfall region. Analysis of South African Weather Service rainfall data for 1948-2004 indicates that 6 of 7 anomalously wet (6 of 8 dry) winters correspond to negative (positive) SAM phase (Reason and Rouault, 2005). Fig. 1 shows time series of winter rainfall over western South Africa (a winter rainfall dominated area) and a detrended index of the SAM obtained as the leading EOF of the NCEP re-analysis 700 hPa geopotential height. Both series have been smoothed with a 7 point running mean and the SAM index has been inverted for ease of comparison. The correlation between these series is 0.61 at zero lag (99.5% statistical significance) and increases slightly if the smoothed SAM index leads by two years. This result suggests that some indication of how the rainfall might change on interannual-decadal time scales may be obtained from the state of the SAM index for the previous few years. Such indications may be useful to water managers in the region who need to make decisions about the release of water from dams for irrigation and industrial purposes, and the planning of new urban developments to accommodate a rapidly growing and relatively poor population.

The mechanisms by which the SAM influences South African winter rainfall involve shifts in the subtropical jet, and changes in the low-level moisture flux and surface evaporation upstream over the South Atlantic, and in mid-level uplift, low-level convergence and relative vorticity over the region. In addition, experiments with the UKMO HadAM3 atmospheric general circulation model forced with various idealised SST anomalies over the subtropical and mid-latitude South Atlantic indicate that this ocean region has some influence on South African winter rainfall and that a SAM-like circulation anomaly is part of the model response (Reason and Jagadheesha, 2005) together with northward (southward) shifts in the subtropical jet and enhanced (reduced) low level westerly moisture flux over the South Atlantic during anomalously wet (dry) winters.

3. Summer rainfall variability

A link is also evident between the SAM and summer (JFM) rainfall over the Eastern Cape region of South Africa. This region is prone to drought and has a large and poor rural population. Previous work has found connections between summer rainfall here and SST in the South West Indian Ocean (Walker, 1990; Jury et al., 1993). Fig. 2 (over the page) shows the summer SAM index plotted against a summer rainfall index averaged over 32-34°S, 24-28°E after smoothing. The two series are correlated at -0.59. Spatial correlations of the raw data show values ranging from -0.4 to -0.6 over much of this region which remain stronger than -0.4 at two month lag. This result suggests that late summer / autumn rainfall over the Eastern Cape may have some predictability based on the state of the Southern Annular Mode earlier in the summer.

4. Summary

Evidence has been presented of relationships between a de-trended Southern Annular Mode (SAM) index and both winter rainfall over the west coast region of South Africa and summer rainfall over the southeast coastal region. Both regions are characterised by substantial interannual and interdecadal variability in rainfall. Although both these regions may be affected to some extent by ENSO, the influence of this mode is believed to be substantially less here than further north over the country (Lindesay, 1988; Reason et al., 2000) and the anomalously wet and dry years include both ENSO and neutral years. The mechanisms by which the SAM influences rainfall over South Africa appear to involve shifts in the subtropical jet and midlatitude storm tracks upstream over the South Atlantic and in the low level moisture flux advected towards the country which then tend to lead to increased (decreased) rainfall over western South Africa in winter and the reverse over the southeast coastal region in summer during the negative (positive) phase of the de-trended SAM.

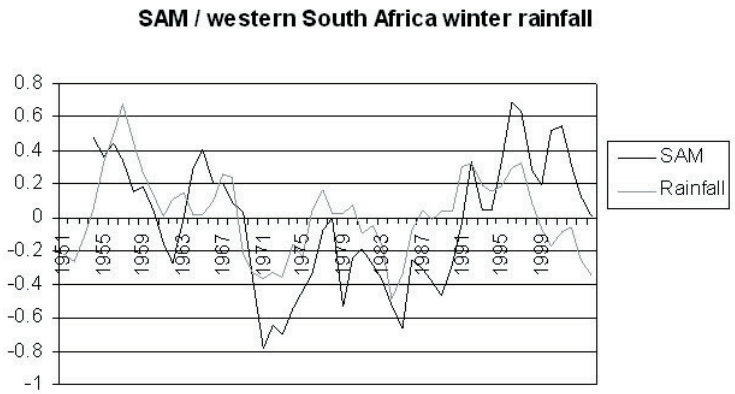

Fig. 1. Time series of winter (May-September) SAM index (de-trended) and rainfall over western South Africa. After Reason and Rouault (2005). The SAM index has been inverted for ease of comparison.

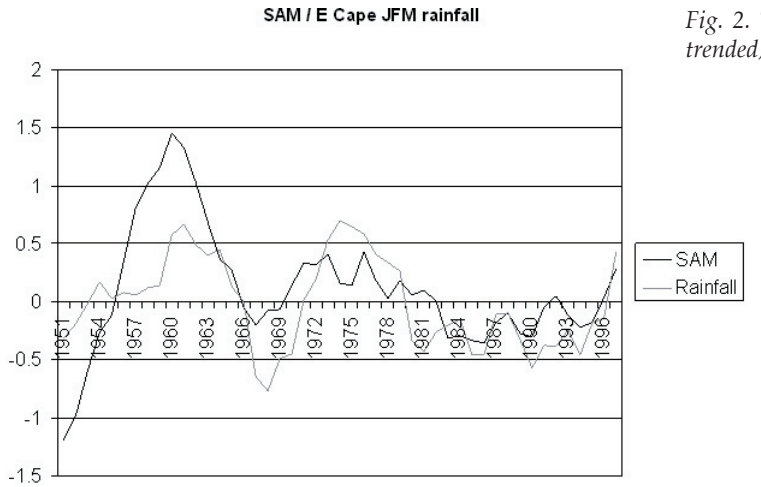

Fig. 2. Time series of summer (January-March) SAM index (detrended) and rainfall over the Eastern Cape region of South Africa

References

Lindesay J.A., 1988: South African rainfall, the Southern Oscillation and a southern hemisphere semi-annual cycle. *J. Climatology*, 8, 17-30.

Jury, M.R., H. Valentine and J.R.E. Lutjeharms, 1993: Influence of the Agulhas Current on the summer rainfall of the southeast coast of South Africa. *J. Appl. Met.*, 32, 1282-1287.

Mason S.J. and M.R. Jury, 1997: Climate variability and change over southern Africa: a reflection on underlying processes. *Prog. Phys. Geogr.*, 21, 23-50.

Reason, C.J.C., R.J. Allan, J.A. Lindesay and T.J. Ansell, 2000: ENSO and climatic signals across the Indian Ocean basin in the global context: Part I, interannual composite patterns. *Int. J. Climatol.*, 20, 1285-1327.

Reason, C.J.C. and D. Jagadheesha, 2005: Relationships between South Atlantic SST variability and atmospheric circulation over the South African region during austral winter. *J. Climate*, 18, 3059-3075.

Reason, C.J.C. and Rouault, M. 2005. Links between the Antarctic Oscillation and winter rainfall over western South Africa. *Geophys. Res. Lett.*, 32(7), L07705 , doi 10.1029/2005GL022419.

Walker, N.D., 1990: Links between South African summer rainfall and temperature variability of the Agulhas and Benguela current systems. *J. Geophys. Res.*, 95, 3297-3319.

Antarctic Sea Ice Drift Variability: Modes and Trends

M. R. Drinkwater[1] , C. Schmitt[2] and C. Kottmeier[2]
[1]European Space Agency, ESTEC, Earth Observation Programmes
Keplerlaan 1, 2201AZ, Noordwijk, The Netherlands
[2]Institut für Meteorologie und Klimaforschung, Universität Karlsruhe/Forschungszentrum Karlsruhe, Germany
Corresponding author: Mark.Drinkwater@esa.int

1. Introduction

Sea ice regulates atmosphere-ocean momentum transfer and ocean-atmosphere heat fluxes. In the austral winter, cold equatorward meridional winds blow off the Antarctic continent opening coastal polynyas and dilating the ice pack. Resulting ice divergence exposes the upper ocean to the atmosphere facilitating vigorous heat exchange and rapid sea-ice growth and brine rejection which destabilises the upper ocean. Conversely, poleward meridional winds cause sea-ice contraction towards the coast of Antarctica. Convergence of the ice pack compresses the ice into pressure ridges whose accompanying keels increase drag and momentum transfer from the atmosphere to the upper ocean and enhance mixing. Clearly, coupled models that do not faithfully reproduce the interplay between ice drift dynamics and thermodynamics are not expected to produce a realistic upper ocean response – nor realistic atmospheric feedbacks.

A number of recent studies highlight large-scale patterns of covarying Antarctic sea-ice extent (SIE) and concentration (SIC) and atmospheric parameters such as sea-level pressure (SLP), surface air temperature (SAT) and sea-surface temperature (SST), on seasonal to interannual to decadal timescales (Yuan and Martinson, 2000; and Kwok and Comiso, 2002). Their results indicate spatial patterns identified as the Antarctic Dipole (AD) and the Southern Annular Mode (SAM). A common weakness of such studies remains, however, in that satellite-derived ice concentration is used as the only index of sea-ice response to climate variability. Consequently, there remains the significant challenge to attribute observed sea-ice changes to growth/melt thermodynamic processes or ice dynamics, and thus to diagnose their respective impact on atmosphere-ice-ocean fluxes. To resolve ambiguities in interpretation, data on Antarctic sea-ice drift dynamics are essential.

Recent studies by Venegas et al, (2001), Venegas and Drinkwater (2001), Drinkwater and Venegas (2001) and Drinkwater et al. (2001) identify the role of Antarctic sea-ice drift (ID) dynamics in modulating SIE variability. They show the primary atmosphere-ice-ocean coupled mode reflected in ID variability has a dominant 3-5 year period. This "quasi-quadrennial" mode is driven by ENSO-related atmospheric variations with a primary "centre of action" receiving atmospheric stimuli in the South Pacific sea-ice sector, and is consistent with other published work.

The primary atmospheric mode of variability, SAM exhibits a strong decadal trend, yet no study would appear to have found any clear relationship between SIC and SAM. Recent modelling efforts speculate a response of the coupled system (e.g. LeFebvre et al, 2004) to SAM. But, some contradictions remain on the

nature of ocean-ice interactions due to the different model treatment of ice dynamics. Intuitively, ice concentration is not expected to exhibit any clear response to SAM due to its already annular configuration around Antarctica.

In an attempt to isolate dynamical connections with SAM we focus here on deviations from the typical long-term mean drift pattern. We highlight the interrelationships between ID, SIC, and SLP and SAT in the context of observed month to month sea-ice anomalies. Finally, we derive trends in ice-drift anomalies and indicate the significance of their spatial expression in relationship to SAM.

2. Data Set

Data shown here are from the Atlas of Antarctic Sea Ice Drift (www.imk.uni-karlsruhe.de/seaiceatlas) of Schmitt et al. (2004). Gridded time-series data contained in the Atlas database provide a comprehensive month to month view of seasonal to interannual Southern Ocean sea-ice drift dynamics, ice concentration data and NCEP reanalysis fields of lower atmosphere parameters. It provides a valuable reference source for the study of climate variability and coupled ocean-ice-atmosphere modeling due to the ability to directly compare sea-ice drift with synpotic scale atmospheric forcing and ice concentration conditions.

The Antarctic ID database comprises monthly records spanning almost two decades from 1979-1997 derived from automated tracking of sea ice in passive microwave images from the Nimbus-7 SMMR through the DMSP-SSMI instrument series on polar-orbiting satellites. It also contains an assembly of records from the WCRP International Programme for Antarctic Buoys (IPAB), PELICON sea-ice concentration data, and NCEP reanalysis product (NRP) lower atmospheric fields (SLP, SAT, U,V Wind). All products are rectified to the same grid and averaged to produce monthly mean products.

Monthly mean ice-drift velocity and drift variance statistics are calculated from the 2-day ice drift database using the values at each grid point. The 1979 – 1997 multiyear mean was also calculated for each month and removed from each year's monthly products to generate corresponding monthly anomaly fields. These data are used as the basis for investigating Antarctic ID dynamics.

3. Characteristics of Mean Ice Drift

The characteristics of sea-ice drift are illustrated by the mean daily ice velocity in July 1989. Figure 1 indicates a composite representation of ID vectors superimposed on the SIC, together with the accompanying SLP field. The large-scale winter sea-ice circulation in the Weddell and Ross Sea basins is governed predominantly by geostrophic winds, with ice drifting approximately parallel to the mean isobars. Higher-frequency, sub-daily drift fluctuations, caused by fast moving mesocylones (polar lows) and tidal forcing (over shallow-water continental shelf regions) is averaged out in the monthly mean plots, though statistics on the velocity variance are recorded for each monthly mean field.

As austral winter sets in, large-scale synoptic pressure patterns in the Eastern Weddell and Ross Seas establish the well-known gyre circulations, here reflected in the ice drift. Sea ice accelerates as it escapes the resistance offered by the coastlines of Victoria Land and the Antarctic Peninsula. As it becomes entrained in the Antarctic Circumpolar Current (ACC) it turns sharply eastwards - exporting ice into the Amundsen and Bellingshausen Seas. Consequently, the westward extent of the Ross Gyre is clearly delineated at around 170° E, while the climatological maximum sea-ice extent is observed at ~150° W in the location where ice drift constantly replenishes ice melting at the ice margin. A similar pattern occurs in the Weddell Sea, with sea ice turning and accelerating as it passes the northern end of the Peninsula. The ice drift sustains a broad maximum in ice extent from 45° W to 20° E.

An extensive comparison between two-day SSMI optimally-interpolated and collocated IPAB buoy ice drift data indicates a Gaussian distributed rms drift uncertainty of around 4 km/d and mean bias of -0.78 km/d over all seasons and buoy locations. Results also indicate that rms errors are reduced approximately in proportion to $1/\sqrt{n}$ when temporal averaging is performed, implying global mean rms uncertainty of ~1km/d for monthly climatologies (n=15). Significantly better tracking performance is evident in some specific locations and seasons (relative to the global statistics), while tracking performance is more uncertain in locations near to the coast (owing to the 25 km resolution of SSM/I), during surface melting (due to image decorrelation), and under rapid drift in the outer sea-ice margin (where eastward drift opposes the satellite orbit precession).

4. Variability about the Mean

Monthly anomalies were examined through the 18-year interval to document variability about the seasonal mean ice-drift pattern. Anomaly patterns were then compared with the SAM index to isolate the impact of the annular mode (see other papers in this issue for details regarding SAM). A SAM index is calculated using the normalized difference in the monthly zonal-mean sea level pressure (SLP) between 40 and 70°S (after Nan and Li, 2003). This modified index is preferred over the more traditional 65° limit: (a) to seek a more robust relationship between SAM and sea-ice drift south of 60°S; and (b) to mitigate any artificial bias introduced in the trend in the NRP-derived SAM index (Hines et al., 2000).

Figure 2 shows the July 1989 monthly ice drift anomaly with the accompanying SLP and SAT fields (with the zero degree contour highlighted in black). Notably, July 1989 follows a period of persistent positive spring and winter SAM index and the typical mean ice drift pattern is considerably reorganised in response to the large scale sea-level pressure anomalies. The eastward

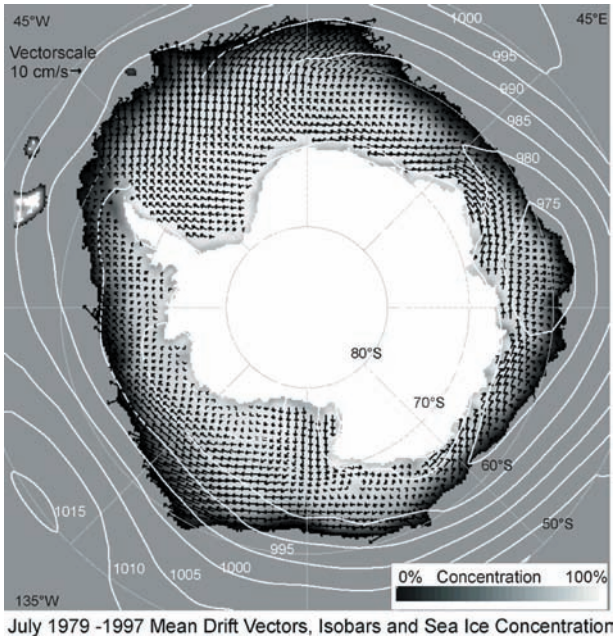

Figure 1: July 1979-1997 mean of Antractic sea-ice drift velocity superimposed on the PELICON sea-ice concentrations. NCEP sea-level pressure is indicated by isobars at 5mB intervals.

zonal ID component is enhanced in the northern Weddell Sea and Ross Sea sectors (between 60 and 70°S latitude), while the coastal drift in the southern Weddell and around a significant part of East Antarctica has decelerated. The typical feature of the SAM in the West Antarctic peninsula region is reproduced in the form of enhanced poleward warm air advection, though decorrelation in the surface radiometric signatures (by melt, rain, or snow) prevents robust sea-ice tracking during this period. The Weddell Sea experiences only a minor increase in the southward component of drift, though there is enhanced northerly ice drift over the entire Ross and Amundsen Sea sectors.

5. Ice Drift Trend Analysis

Regions with the largest proportions of the season over which ID is tracked are indicated in Figure 3a. To isolate significant trends in the 18-year ice drift record, locations with robust long-term statistics are selected (points 1-10). Each has continuous tracked drift over >75% of each year throughout the 18-year record. For each grid point, ID velocity and drift variance time series were derived.

It is hypothesised that regions experiencing the effects of a positive (increasing) trend in SAM index should respond with an increasing zonal component in ice-drift velocity. Though points 1, 2, 3 in the Weddell Sea indicate a weak (statistically insignificant) positive trend in eastward velocity, according to Figure 2a they are too far south to experience any significant effect. Relatively strong positive (equatorward) meridional trends are evident at locations 4, 5, 7, and 8. Interestingly, weak negative (poleward) meridional drift trends are observed at locations 1, 2, 3 and 10, perhaps in part due to small increases in the poleward component of surface winds in response to SAM in these locations.

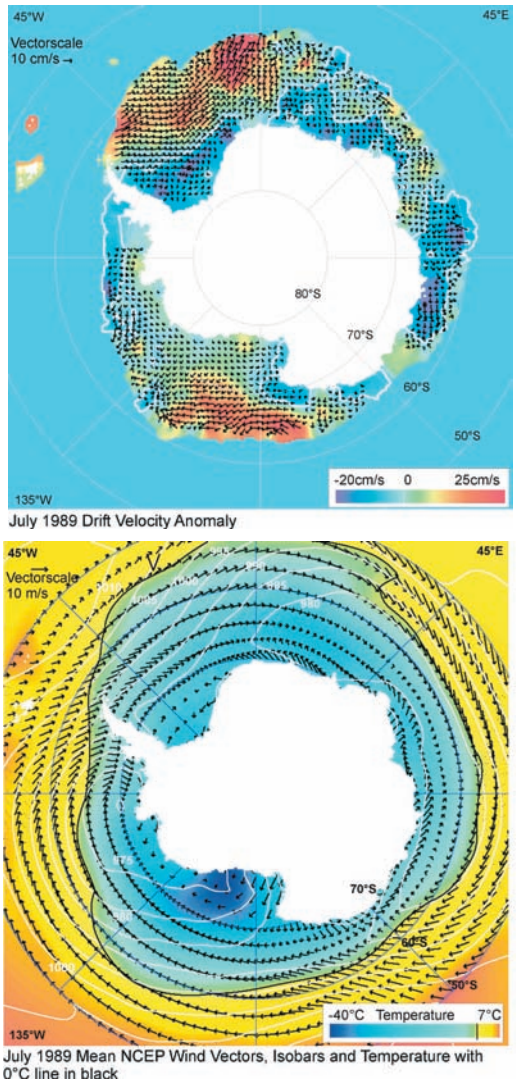

Figure 2. (a) July 1989 anomaly of daily ice drift and (b) atmospheric conditions for July 1989, during a period of high positive winter phase of the SAM index.

The highlight of the ID trend analysis is the observation of uniform long-term decreases in ice drift variance over the majority of the Southern Ocean. Drift variance statistics (derived from the 2-day drift products comprising monthly means) indicate the natural storm-imposed variability about the mean drift. Results indicate a robust, statistically significant downward trend in Antarctic sea-ice drift velocity variance at all of the points 1 – 10 over the 18 year interval, with the strongest negative trends observed at locations 1, 3, 4, and 5.

An example from location 3 is shown in Figure 3b since it allows direct comparison with historical in-situ buoy drift statistics. The point 3 time series shows a strong negative trend, indicating a reduction in sea ice velocity variance of -7.79 ±2.62 cm^2/s^2/ year over the 18 year interval. A direct comparison is made with velocity variance from all available Weddell Sea buoy drift statistics in Figure 3c over a 13 year interval from 1985-1998. IPAB buoy data provide confirmation of the trend, though the correlation is reduced due to extremely large values of velocity variance in the latter months. Peaks in the drift variance, such as in 1994, are isolated to buoys close to the seasonal ice margin which exhibit a higher mean velocity and greater range of velocity. In the central pack, fluctuations in variance mainly occur with abrupt velocity and direction changes due to passing low pressure systems.

6. Spatial Pattern in the 18-year Drift Trend

Figure 4 provides a spatial summary of trends from the linear regression fit to monthly sea-ice drift velocity and drift variance. The drift speed summary in Figure 4a indicates that Weddell Sea ice is almost uniformly slowing down over the last 18 years except for the outer ice margin. The pole of greatest slowing observed in the southernmost Weddell is likely an artifact of large grounded icebergs in the vicinity of Berkner Island. These have exerted a regional impact on ice drift by creating a fast ice barrier that retards inflow of ice into the southern part of the basin. Importantly the Weddell Sea and the western Amundsen - eastern Ross Sea sector exhibit a similar negative trend – whilst the West Antarctic peninsula area and large parts of coastal East Antarctica exhibit positive trends in velocity.

The spatial pattern in variance trends in Figure 4b is quite different, showing uniform reduction over most of the Southern ocean ice covered region, other than in the Bellingshausen and coastal Amundsen Sea, and the East Antarctic quadrant between 90E and 145°E along the Wilkes Land coast. The most striking aspect of this pattern is the dipole pattern of opposing trends on each side of the Antarctic Peninsula, and with the strongest positive trend in the location of the centre of action of SAM.

A combined positive trend in velocity and velocity variance in the west Antarctic Peninsula region implies greater storminess. This tendency corresponds with results suggesting that a positive trend in SAM may be responsible for storms delivering more heat in this region and thus the regional warming trend. Warming is expected to cause thinner and more mobile sea ice conditions, which coupled with stronger poleward meridional winds, may provide a dynamical explanation for observed ice extent anomalies, yet lack of corresponding ice concentration anomalies (Kwok and Comiso, 2002).

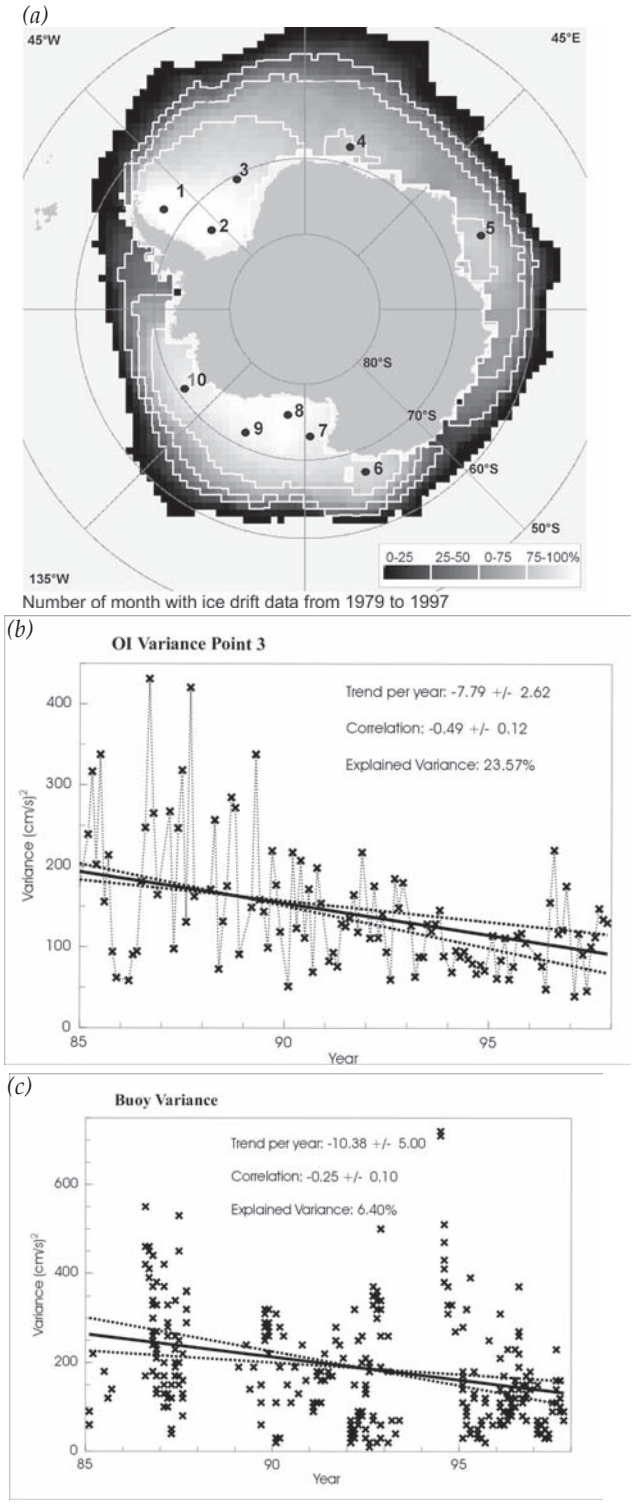

Figure 3 (a) Map of time-series locations; (b) Time-series example of ice drift variance trend from Weddell Sea compared with (c) time-series from Weddell Sea IPAB byoy data for the period of overlapping observations between 1985-1998.

The contrasting long term downward trend in ice drift variance observed over large parts of Antarctica imply a long term reduction in storminess or cyclonicity in over a significant portion of the sea ice cover. We speculate that this in turn may lead to a reduction in drift energy expended by opening and closing of leads and ridging and thus of dynamic thickening of the ice pack. There is also the possibility that reduced dynamical thickening may counterbalance any increase in thermodynamic thickening - as implied by coupled model SAM response simulations (Lefebvre et al., 2004). These preliminary results desire further detailed analysis.

7. Conclusions and Outlook

To-date no significant relationship has been observed between the primary mode of Atmospheric variability, SAM, and sea-ice concentration. In contrast, our sea-ice drift velocity statistics from the Antarctic Ice Drift Atlas provide a unique opportunity to investigate a direct dynamical response to modified atmospheric forcing. Our analysis of long-term ice drift statistics reveals a significant Southern Ocean wide reduction in ice-drift velocity variance, with a relatively weaker regional response in mean drift velocity.

It is speculated that the observed long-term reduction in ice drift velocity variance is related to an influence of increasing positive index of SAM on reducing Antarctic cyclonicity. A long term reduction in storminess or cyclone frequency is observed by Simmonds et al (2003). Meanwhile, Fyfe (2003) analysed the frequency of extra-tropical cyclones or low pressure centres in zonal bands around Antarctica, finding a statistically significant decrease in the number of cyclones in the Southern Ocean (between 40-60S), but a statistically significant increase over the sea-ice region (south of 60S). Thus, our results indicating localized positive trends in drift variance lend some support to the assertion that greater cyclonicity is observed in the Antarctic coastal region to the south of Australia (south of 60S), and in the Bellingshausen Sea – due to the positive trend in SAM.

Decreased cyclonic activity over the Southern Hemisphere sea-ice cover is not obviously consistent with an increase in the positive phase of the SAM in the last fifteen years or so. A more important question, therefore, is whether more or fewer extra-tropical cyclones occur with increased warming? Perhaps the key result validating a connection between warming and increased cyclonicity is the regional correspondence of positive trends in drift velocity and variance in the region of SAM centre of action (of greatest regional warming).

Studies of climate variability can now benefit from our Antarctic Ice Drift Atlas and its downloadable climatological databases. The accompanying error analysis makes these data relevant for sea-ice model performance verification activities. However, due to uncertainties and biases in tracking that limit the value of ice velocity on daily timescales, future activities will focus on the development of new satellite-based global sea-ice drift tracking products at high spatial and temporal resolution. Global-mode Advanced SAR data from the European Space Agency's Envisat satellite now facilitates Arctic- and Antarctic-wide coverage ice drift vector data recovery on a 1 or 2 km grid (see: www.icemon.org), and similar products shall become routinely available. This shall facilitate operational data assimilation on daily timescales, as well as ensuring the robustness and long-term quality of the data for use in scientific studies of the variability in sea ice and its response to climate.

Acknowledgments

C.S performed this work at the Institut für Meteorologie und Klimaforschung, Universität Karlsruhe with funding from the Deutsche Forschungsgemeinschaft (DFG) Project Ko924/3-1.

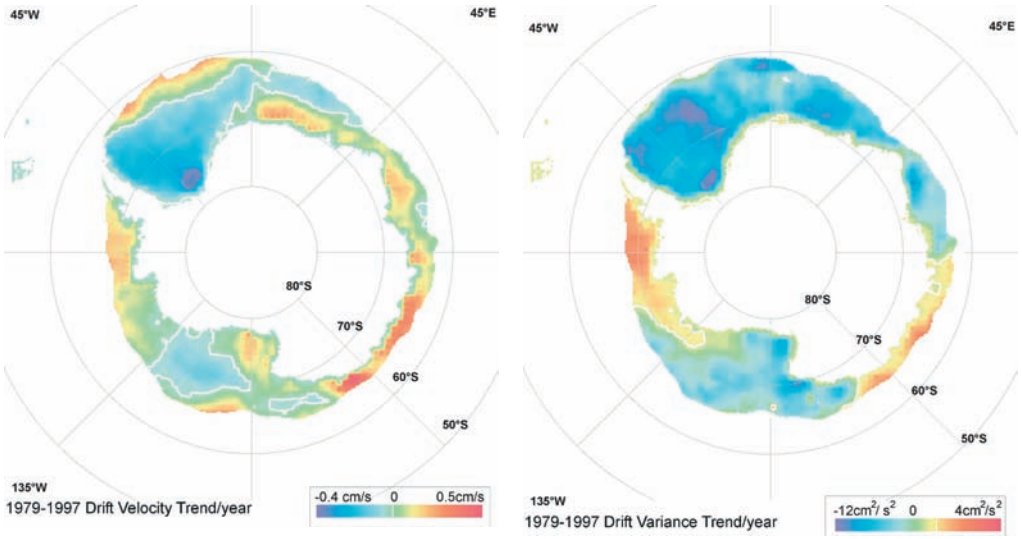

Figure 4. Spatial representation of ice drift speed and ice drift variance trends expressed as a mean trend/year over the interval from 1979-1997. White isolines seperate positive from negative trend values.

References:

Drinkwater, M.R., X. Liu., and S. Harms, Combined Satellite- and ULS-derived Sea-Ice Flux in the Weddell Sea, *Ann. Glaciol.*, 33, 125-132, 2001.

Drinkwater, M.R. and S. Venegas, Interannual Variations in Antarctic Atmosphere-Ice-Ocean Coupling, *EOQ*, 69, 14-17, 2001.

Fyfe, J.C., 2003: Extratropical southern hemisphere cyclones: harbingers of climate change? *J. Clim.*, 16, 2802-2805.

Hines, K.M., D.H. Bromwich, and G.J. Marshall, 2000: Artificial Surface Pressure Trends in the NCEP/NCAR Reanalysis over the Southern Ocean and Antarctica. *J. Clim.*, 13, 3940-3952.

Kwok, R. and J.C. Comiso, 2002: Spatial patterns of variability in Antarctic surface temperature: Connections to the Southern Hemisphere Annular Mode and the Southern Oscillation, *GRL*, 29, 14, 10.1029/2002GL015415.

LeFebvre, W., H. Goose, R. Timmermann, and T. Fichefet, 2004: Influence of the Southern Annular Mode on the Sea-ice-ocean System. *JGR*, 109, C09005, 10.1029/2004JC002403.

Nan, S., and J. Li, 2003: The relationship between summer precipitation in the Yangtze River valley and the previous Southern Hemisphere Annular Mode. *GRL* , 30(24), 2266, doi: 10.1029/2003GL018381.

Simmonds, I., K. Keay, and E.-P. Lim, 2003; Synoptic Activity in the Seas around Antarctica, *Mon. Weather Rev.*, 131, 2, 272-288.

Venegas, S., and M.R. Drinkwater, Sea Ice, Atmosphere and Upper Ocean Variability in the Weddell Sea, Antarctica, *JGR*, 106, C8, 16747-16766, 2001.

Venegas, S., M.R. Drinkwater, and G. Schaffer, Coupled Oscillations in the Antarctic Sea-Ice and Atmosphere in the South Pacific Sector, *GRL*, 28, 17, 3301-3304, 2001.

Yuan, X. and D.G. Martinson, 2001: Antarctic sea ice extent variability and its global connectivity. *J. Clim.* 13, 1697-1717.

Did a Prolonged Negative SAM produce the Weddell Polynya of the 1970s?

A. L. Gordon[1], M. Visbeck[2] and J.C. Comiso[3]
[1]Lamont-Doherty Earth Observatory, Palisades NY, USA
[2]Leibniz-Institut für Meereswissenschaften (IFM-GEOMAR), Kiel, Germany
[3]NASA Goddard Space Flight Center, Greenbelt, Maryland, USA
Corresponding author: agordon@ldeo.columbia.edu

With the advent of scanning passive microwave sensors on board polar orbiting satellites in late 1972, the polar community entered the era of viewing sea ice conditions poleward of the outer ice edge with nearly synoptic clarity. The waxing and waning of the seasonal sea ice cover in the Southern Ocean, whose northern ice edge had previously only been observed sporadically from ship, was now exposed in its entirety. The satellite sensors in their second full year of operation revealed a surprisingly large ice free region in winter near the Greenwich Meridian and 65°S that is now referred to as the Weddell Polynya (Zwally and Gloersen, 1977; Carsey, 1980; Gordon and Comiso, 1988; Fig 1a). The Weddell Polynya, averaging 250 x 103 km^2 in size, was present during the entire austral winters of 1974, 1975 and 1976. As the Weddell Polynya was observed near the very start of the satellite based time series one might have reasonably expected that a winter persistent Polynya was the norm, but since 1976 a persistent winter polynya has not been observed. What has been observed are much smaller (10 x 103 km^2), sporadic polynyas with characteristic time scale of 1 week in the vicinity of Maud Rise near 65°S, 2°E [Comiso and Gordon, 1987; Lindsey et al., 2004] induced by circulation-topographic interaction [Gordon and Huber, 1990].

The normal stratification within the Weddell Gyre is that of a thick layer of relatively warm, saline deep water drawn from the lower Circumpolar Deep Water. Along the southern limb of the Weddell cyclonic gyre, in which the Weddell Polynya was situated, the warm deep water is >1.0°C, with salinity >34.7. The warm deep water is capped by the ~100 m thick surface layer of near freezing temperature in the winter, separated from the warmer deep water by a rather weak pycnocline. A

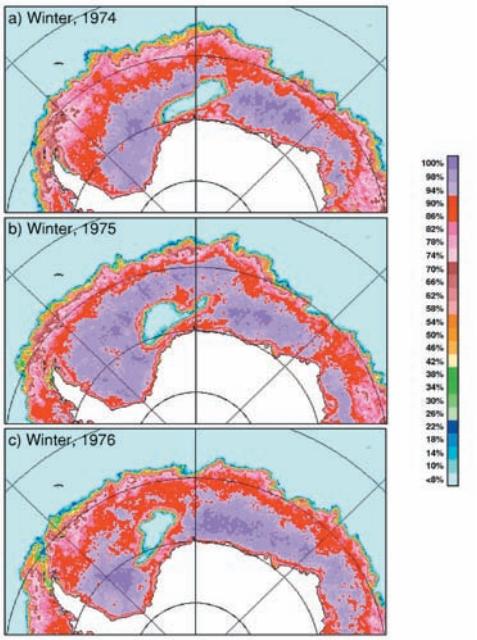

Figure 1a Colour coded sea ice concentration maps derived from passive microwave satellite data in the Weddell Sea region during (a) August 30, 1974, (b) August 30, 1975 and (c) August 29, 1976. The Weddell Polynya is the extensive area of open water (in blue) near the Greenwich Meridian roughly between 65°S and 70°S. [Adapted from Gordon and Comiso, 1988].

breakdown of this normal stratification is the likely cause of the Weddell Polynya [Gordon, 1978, 1982]. The Weddell Polynya was created as sea ice formation was inhibited by deep reaching ocean convection that injected relatively warm deep water into the winter surface layer. The ocean overturning left its mark on the deep water stratification down to 3000 m with significantly cooler and fresher deep water, a sign of massive intrusion of surface layer water into the deep, relative to the pre-polynya stratification (Fig 1b; Gordon, 1978, 1982). The deep water salt delivered into the surface layer by the convection insured a repeat performance of the polynya in the next winter. However the polynya "sensitized" regions slowly advected westward [~ 0.013 m/sec, the approximate barotropic flow within the Weddell Gyre] within the Weddell gyre flow into the western boundary current, where it was destroyed by shear. Estimate of the three-year average winter ocean heat lost to the atmosphere within the Great Weddell Polynya is 130 W/m^2.

What initiated the Weddell Polynya and why hasn't it occurred since the 1970s? Though observations within the Weddell gyre are sparse, there is convincing enough evidence that prior to the Weddell Polynya the surface water increased in salinity and the pycnocline isolating the cold surface later from the abundant heat of the deep water weakened [Fig 2]. We propose that this was the consequence of a prolonged period of negative Southern Annular Model [SAM]. During –SAM the Weddell gyre experiences colder and drier atmospheric conditions, making for saltier, denser surface water. This eventually led to a breakdown of the pycnocline stability, prompting deep reaching convection. Since the late 1970s SAM has been about neutral or in a positive state, inducing warmer, wetter conditions over the Weddell Sea and forestalling a repeat of the Weddell Polynya.

The weakened pycnocline was primarily a consequence of increased surface salinity. The surface layer [upper 100 m] salinity increases during the late 1960s and through the 1970s, levelled off in the 1980s and decreased in the 1990s, at a reduced rate since year 2000. The surface layer salinity for the decade before the Weddell Polynya is about 0.2, which require a decrease of freshwater input of 0.58 m over the 10 year interval, or about ~10-20% reduction of the estimated annual mean freshwater water input.

The atmospheric conditions associated with the SAM (or Antarctic Oscillation) is described by Gong and Wang (1999) and Thompson and Wallace (2000); and its impact on the ocean and sea ice by Hall and Visbeck (2002). Zonally symmetric fluctuations of the midlatitude westerly winds are caused by changes in the sea level air pressure difference between 40° and 65°S. SAM is the primary mode of atmospheric variability poleward of 30°S (Visbeck and Hall 2004), and may also account for much of the variability in ocean circulation and sea ice in this region. Hall and Visbeck (2002) use a coupled ocean-atmosphere model to explore how SAM influences ocean circulation and sea ice variability on interannual to centennial time scales. They find that the maximum westerlies shift southward during positive SAM and to the north in negative SAM. The atmosphere over the seasonal sea ice zone (between the maximum westerlies and Antarctica) becomes more convergent during the positive SAM, leading to an increase in rising motion within the air column, perhaps associated with poleward migration of cyclonic eddies, which would induce greater precipitation. During negative SAM the opposite condition prevails, that of reduced rising motion and drier conditions. In essence, during negative SAM the drier Antarctic high pressure conditions extend over the adjacent seas, such as the Weddell Sea. The results of Hall and Visbeck (2002) are in general agreement with the model findings of Lefebvre et al. (2004), showing that positive SAM spins up the meridional overturning circulation of the Southern Ocean, and the Weddell Sea experiences decreased sea ice with increased winds from the north (warmer), and negative SAM increases Weddell sea ice cover and induces slightly colder air with an increased southerly wind component.

Visbeck (unpublished) using air pressure records over the southern continents developed a SAM time series based on sea level pressure (SLP) indices for various sectors (Figure 3). An extensive period of negative SAM occurred from 1955 to1980, with a particularly strong period of negative SAM from 1965 to

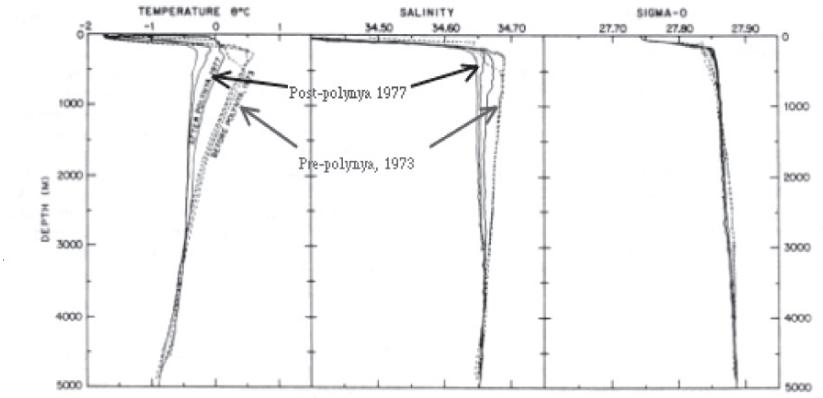

Figure 1b Profiles of potential temperature, salinity and density (sigma-0) within the area of the Weddell Polynya before and after the occurrence of the Polynya (adopted from Gordon, 1982).

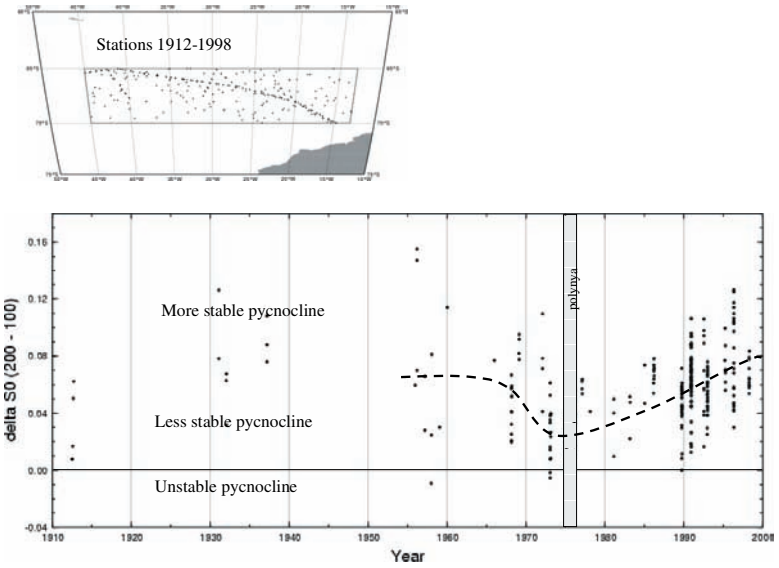

Figure 2 The pycnocline strength within the Weddell Polynya region of the Weddell Gyre (see map insert for data positions). "Delta S0 (200 m –100 m)" is the difference in sigma-0 density between 100 and 200 meters depth. The period of the Great Weddell Polynya is marked. Decreased pycnocline stability is observed in the early 1970s leading to the Weddell Polynya, since then the pycnocline strength has increased.

1978, represented by higher than normal SLP along the Antarctic margin and lower than normal SLP over both the African and South American sector, maximizing the response in the area of the Weddell Gyre. During the 1980s SAM was slightly positive, with a more substantial period of positive SAM since the late 1980s. In more recent years the strong SAM positive appears to be waning.

The relationship of SAM to precipitation since 1979, based on the CPC merged analysis of precipitation based on station observations and satellite estimates (CMAP, version 2, November 2004; Xie and Arkin, 1997) over the Weddell Sea reveals a positive, albeit weak, correlation of precipitation with SAM. For the central Weddell Gyre the regression imples 0.05 to 0.10 mm/day or 1.8 to 3.7 cm/yr less precipitation for a SAM index of –1. Over a decadal negative SAM period, as experienced in the mid-1960 into the mid-1970s, this could result in a deficit of freshwater of 20 to 40 cm. This is smaller, but probably not significantly so from the calculated decadal deficit of freshwater input of 58 cm, discussed above. Therefore it is reasonable to deduce that the negative SAM from the mid-1960s to the mid-1970s reduced the freshwater input to the Weddell surface water making the surface water saltier and denser, weakening the pycnocline, leading to deep reaching convection, and the Great Weddell Polynya.

We present the hypothesis that the Weddell Polynya of the mid-1970s resulted from a prolonged period of negative SAM. The –SAM starved the Weddell surface water of freshwater through a reduction of precipitation, making for a saltier surface layer. Winter cooling and increased sea ice production of this now saltier surface layer, destabilized the ocean pycnocline allowing the development of deep reaching ocean convection that delivered into the sea surface layer the "heat" of the Weddell deep water, thus inhibiting winter sea ice formation, resulting in the polynya state. ENSO may also have played a supporting role in that the strong La Niña of the 1970s produced a colder period over the Maud Rise region, allowing the destabilizing effect of more sea ice formation. We base our conjecture on observational data, which admittedly are sparse within the remote Weddell Sea, but we think sufficiently convincing to warrant further [most likely model based] research.

Will a winter-long Weddell Polynya happen again? One can say with a high degree of confidence that the answer is "yes". The conditions recorded at the beginning of the passive microwave data time series could not have been so unique that it caught a one time feature. The Weddell Polynya must have formed before the mid 1970s and will occur again, but when? According to our proposed mechanism, it will happen once the SAM enters into a period of prolonged negative phase, so as to build up the salinity of the surface layer. Coincidence with a strong La Niña event may help, or perhaps of significant is the interplay of the sequencing and relative strengthens of SAMS and ENSO. The Maud Rise forcing upwelling of warm deep water is the trigger, but the regional surface layer salinity needs to be high enough for the local trigger to produce a winter long persistent Weddell Polynya. So our advise to Maud Rise: Keep trying!

If the proposed link between SAM and the Great Weddell Polynya proves to be robust, then one can consider the consequences of the exposure to the polar winter atmosphere of the polynya's 250 x 103 km^2 surface ocean "hot" spot, to the regional synoptic scale meteorology or on the larger scale climate system.

References:

Carsey, F. D., 1980: Microwave observations of the Weddell Polynya. *Monthly Weather Rev*. 108: 2032-2044.

Comiso, J. C. and A. L. Gordon, 1987: Recurring Polynyas over the Cosmonaut Sea and the Maud Rise. *Journal of Geophysical Research-Oceans* 92(C3): 2819-2833.

Gong, D. and S. Wang, 1999: Definition of Antarctic Oscillation Index. *Geop. Res. Lett*. 26(4):459-462.

Gordon, A. L., 1978: Deep Antarctic Convection West of Maud Rise. *J. Physical Oceanography* 8(4): 600-612.

Gordon, A.L., 1982: Weddell Deep Water Variability. *J. Mar. Res*., 40: 199-217.

Gordon, A.L., and J. C. Comiso (1988: Polynyas in the Southern Ocean. *Scientific American*, 256(6): 90-97

Gordon, A.L., and B. Huber, 1990: Southern Ocean winter mixed layer. *J. Geophys. Res*., 95(C7): 11655-11672.

Hall, A. and M. Visbeck, 2002: Synchronous Variability in the Southern Hemisphere, Sea Ice, and Ocean Resulting from the Annular Mode. *J. Climate* 15(21): 3043-3057.

Lefebvre, W., H. Goosse, R. Timmermann, and T. Fichefet, 2004: Influence of the Southern Annular Mode on the sea ice-ocean system (DOI 10.1029/2004JC002403). *Journal of Geophysical Research*, 109, C09005.

Visbeck M. and A. Hall, 2004: Comments on ''Synchronous variability in the southern hemisphere atmosphere, sea ice, and ocean resulting from the annular mode'' - Reply *J. Climate* 17 (11): 2255-2258

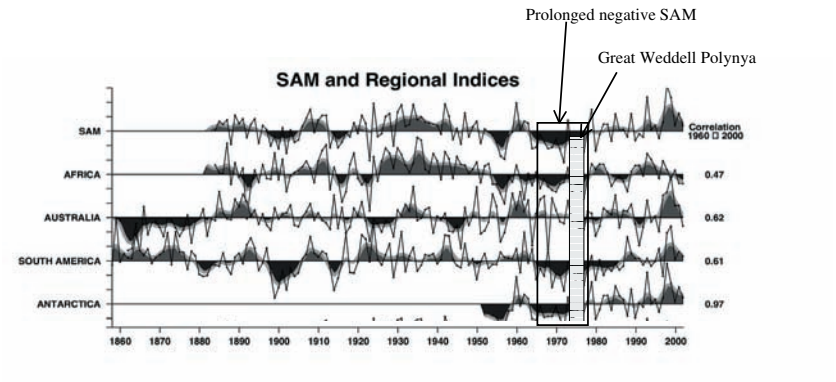

Figure 3. Southern Annular Mode, SAM, time series based on sea level air pressure (SLP) indices for various sectors of the southern ocean (Visbeck, unpublished). An extensive period of negative SAM occurred from 1955 to 1980, with a particularly prolonged period of negative SAM from 1965 to 1978 (marked on the figure, as is the period of the Weddell Polynya).

Lindsay, R. W., D. M. Holland, and Woodgate, R.A. , 2004: "Halo of low ice concentration observed over the Maud Rise seamount (DOI 10.1029/2004GLO19831)." *Geophysical Research Letters* 31(13): L13302.

Thompson, D. and J. M. Wallace, 2000 Annular modes in the extratropical circulation. Part I: month-to-month variability. *J. Climate* 13, 1000-1016.

Xie, P. and Arkin, P.A., 1997: Global Precipitation: A 17-Year Monthly Analysis Based on Gauge Observations, Satellite Estimates, and Numerical Model Outputs. *Bulletin of the American Meteorological Society*, 78, pp.2539-2558

Zwally, H. J. and P. Gloersen, 1977: Passive Microwave images of the polar regions and research applications, *Polar Rec*. 18, 431-450.

Response of the Antarctic Circumpolar Transport to Forcing by the Southern Annular Mode.

M. P. Meredith[1], C. W. Hughes[2] and P. L. Woodworth[2]
[1]British Antarctic Survey, Cambridge, U.K.
[2]Proudman Oceanographic Laboratory, Liverpool U.K.
Corresponding author: "Michael Meredith" <mmm@bas.ac.uk>

The Southern Ocean is unique in being zonally unbounded, and is home to the world's largest current system, the Antarctic Circumpolar Current (ACC). ACC transports from hydrographic sections are of order 130-140 Sv [e.g. Cunningham et al., 2003; García et al., 2002], and it is believed that this strong circumpolar flow (and associated transports of heat, salt etc) exerts a profound influence on global circulation and climate. Of interest to us is how the circumpolar transport around Antarctica changes over a range of timescales, and what impact these changes might have.

It is now well-established that the higher-frequency (subseasonal) circumpolar transport variability is dominated by a barotropic mode that follows contours of f/H almost everywhere, and that bottom pressure and sea level (corrected for the inverse barometer effect) close to the Antarctic continent provide good measures of the variability of this mode [Hughes et al., 1999]. Recently it was observed that sea level and bottom pressure around the entire instrumented part of Antarctica show high levels of coherence, with negligible lag [Aoki, 2002; Hughes et al., 2003], indicating the synchronous acceleration/deceleration of the circumpolar transport around the continent.

The different measures of sea level and bottom pressure at subseasonal timescales are strongly coherent with an index of the Southern Annular Mode (SAM) [Aoki, 2002; Hughes et al., 2003]. This is the dominant mode of atmospheric variability in the extra-tropical Southern Hemisphere, and is characterised by shifting of mass between a node centred over the Antarctic and an annulus encircling lower latitudes [Thompson and Wallace, 2000]. The changes in surface atmospheric pressure associated with variations in the SAM are also manifested as variations in the circumpolar eastward wind over the Southern Ocean. The lag between changes in forcing by the SAM and changes in bottom pressure / sea level around Antarctica is negligible, indicating a near-instantaneous response of the circumpolar transport (Figure 1; [Hughes et al., 2003]). That the changes in sea level are genuinely reflecting changes in ocean transport is further indicated by analysis of output from the Ocean Circulation and Climate Advanced Model (OCCAM). This is a global OGCM, run at 1/4° resolution and forced with ECMWF reanalysis winds [Webb, 1998]. Transport estimates from OCCAM on subseasonal timescales are also coherent with sea level and the SAM, again with negligible lag (Figure 1).

The seasonality in the SAM has received significant interest recently. The SAM has shown a marked trend toward a higher-index state (stronger circumpolar winds) over the past 30 years [Thompson et al., 2000], however this trend is not purely monotonic but is strongly modulated by season. It has been argued that anthropogenic processes such as greenhouse gas emissions and ozone depletion are important to this trend [e.g. Marshall, 2003; Thompson and Solomon, 2002]. Whilst we cannot examine directly the impact of the trend in the SAM on the circumpolar transport, we can investigate the impact of the changing seasonality of the SAM. Figure 2 shows the month-by-month trends in bottom pressure, as measured at the south side of Drake Passage during the 1990s [Meredith et al., 2004]. Also shown are the corresponding trends from the SAM index, plotted inverted and with their mean subtracted for comparison with the bottom pressure data. The similarity is striking, indicating that the changing seasonality of the SAM has indeed influenced the seasonality in the oceanic circumpolar transport. This also suggests a mechanism whereby humankind's activities can influence the large-scale ocean circulation [Meredith et al., 2004].

At longer (interannual) periods, simple barotropic dynamics are no longer applicable and significant baroclinic variability is expected. For these periods, there are few tide gauge records of sufficient length and of sufficiently high quality to be very useful. The most useful is Faraday/Vernadsky on the Antarctic Peninsula (Figure 1). Annual means of sea level from Faraday are significantly correlated with annual means of the SAM index, and also annual means of the total Antarctic circumpolar transport from OCCAM (Figure 3 [Meredith et al., 2004]), thus

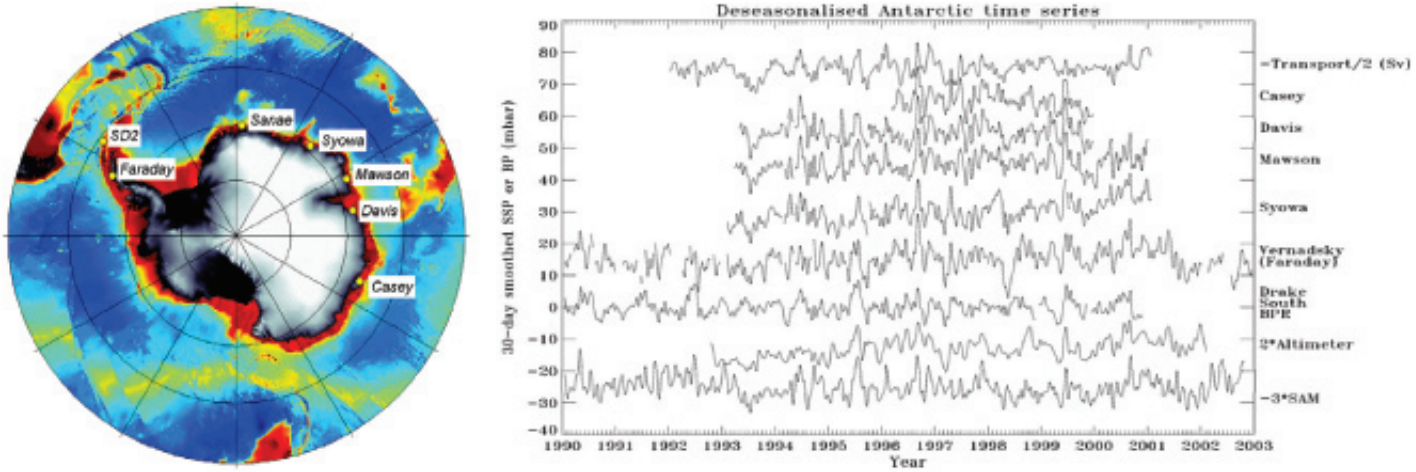

Figure 1(a) Locations of some key tide gauges/bottom pressure recorders around Antarctica (b) Deseasonalised time series from these gauges, along with transport from OCCAM (top line) and the SAM index (bottom line). [Hughes et al., 2003; Meredith et al., 2004].

even at interannual periods and in the presence of significant baroclinic variability, the transport around Antarctica is clearly responding to changes in forcing by the SAM. That sea level reliably reflects transport at this period is fortuitous, since the presence of significant baroclinic variability means that this need not be so. That it does implies that the transport changes are largely vertically coherent, if not fully barotropic.

Of particular interest is that the range in transport on interannual timescales is only around 7 Sv (Figure 3), whereas estimates from repeat hydrographic sections and other techniques show much larger ranges (~20 Sv [Cunningham et al., 2003; García et al., 2002]). The key to understanding this discrepancy is to note that the former is based on genuine annual means, where as the latter are based on sporadic (usually annual) sampling. To fully assess the impact of this aliasing, and to determine a minimum requirement for a sampling frequency, we subsampled the Faraday sea level series and OCCAM transport series at a range of different intervals, and derived the error from the true annual means due to aliasing [Meredith and Hughes, 2005]. We found that, to construct a time series of interannual variability of the circumpolar transport reliable at the 90-95% level requires sampling more rapidly than once per 10 days. This (already stringent) requirement is based on the sampling interval issue alone: additional uncertainty due to measurement error implies that even more rapid sampling is needed still. In practice, we find that data from fixed *in situ* sources (moorings, tide gauges, bottom-deployed equipment etc) are needed to fully resolve interannual transport changes in the circumpolar transport. Other techniques (such as repeat CTD sections, XBT/ADCP sections, satellite altimetry along a repeat groundtrack) will all be aliased, and whilst they can produce useful detail they do not circumvent the requirement for fixed *in situ* instrumentation.

As noted above, the SAM has shown a significant trend in the past 30 years, with associated stronger circumpolar winds. An obvious question to ask is whether the oceanic circumpolar transport has accelerated in response. However, this is not easily answerable. The tide gauge measurements used here each have their own trends, due to processes such as global sea level rise, land movements, and so on, and determining separately a trend due to acceleration of the circumpolar transport is not trivial. Other techniques, as noted above, suffer from problems with sampling intervals and aliasing, and simple calculations suggest these will be just as important for the ocean response to the long-term trend in the SAM as they are for its interannual variability. Efforts are now needed to design and implement a measurement system capable of reliably monitoring the circumpolar transport even on these very long periods.

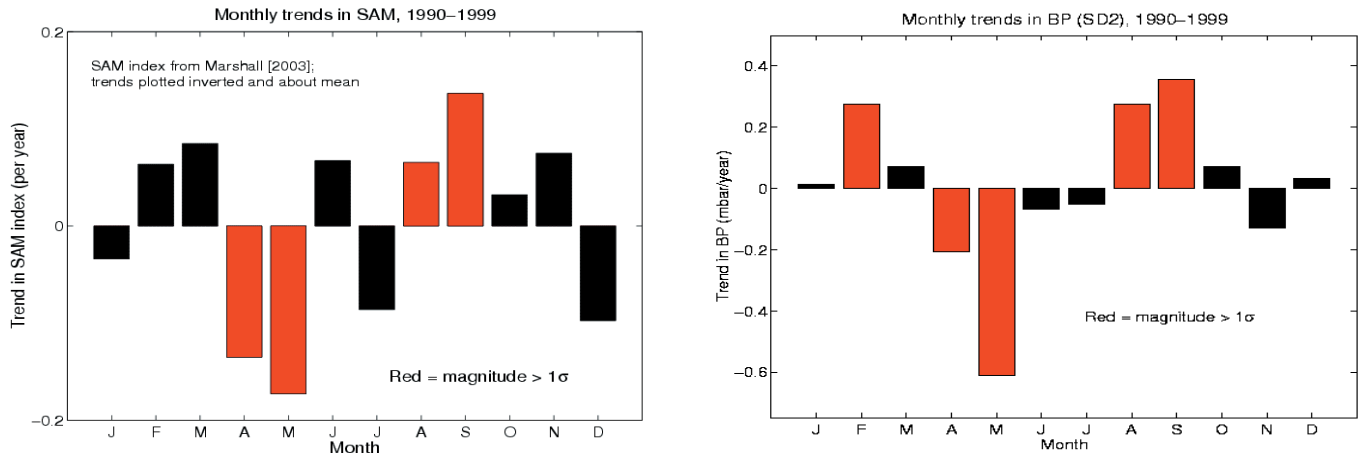

Figure 2(a). Monthly trends in the SAM index during the 1990s. Trends are plotted inverted and with mean subtracted, for comparison with bottom pressure data. (b) Monthly trends in bottom pressure data from southern Drake Passage during the 1990s [Meredith et al., 2004].

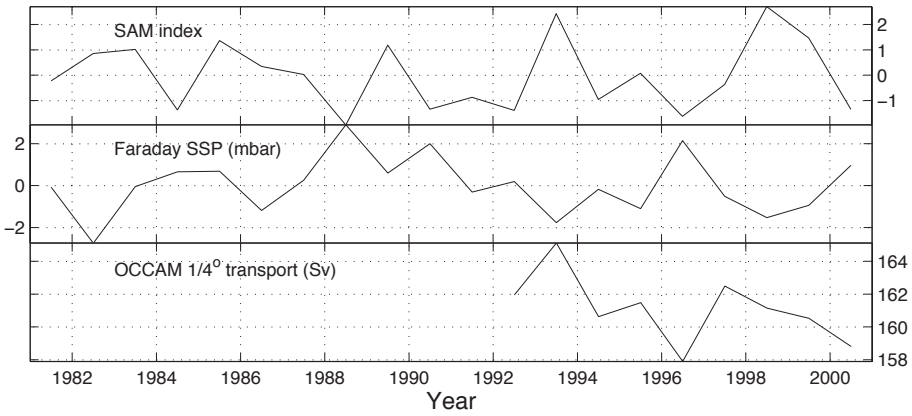

Figure 3. Annual means of SAM index (top), inverse-barometer corrected sea level from Faraday (middle) and OCCAM transport (bottom) [Meredith et al., 2004].

References

Aoki, S., Coherent sea level response to the Antarctic Oscillation, *Geophysical Research Letters*, 29 (20), 10.1029/2002GL015733, 2002.

Cunningham, S.A., S.G. Alderson, B.A. King, and M.A. Brandon, Transport and variability of the Antarctic Circumpolar Current in Drake Passage, *Journal of Geophysical Research*, 108, 10.1029/2001JC001147, 2003.

García, M.A., I. Bladé, A. Cruzado, Z. Velásquez, H. García, J. Puigdefàbregas, and J. Sospedra, Observed variability of water properties and transports on the World Ocean Circulation Experiment SR1b section across the Antarctic Circumpolar Current, *Journal of Geophysical Research*, 107 (C10), 10.1029/2000JC000277, 2002.

Hughes, C.W., M.P. Meredith, and K.J. Heywood, Wind-forced transport fluctuations at Drake Passage: a southern mode, *Journal of Physical Oceanography*, 29 (8), 1971-1992, 1999.

Hughes, C.W., P.L. Woodworth, M.P. Meredith, V. Stepanov, T. Whitworth III, and A. Pyne, Coherence of Antarctic sea levels, Southern Hemisphere Annular Mode, and flow through Drake Passage, *Geophysical Research Letters*, 30 (9), 10.1029/2003GL017240, 2003.

Marshall, G.J., Trends in the Southern Annular Mode from Observations and Reanalyses, *Journal of Climate*, 16, 4134-4143, 2003.

Meredith, M.P., and C.W. Hughes, On the sampling timescale required to reliably monitor interannual variability in the Antarctic circumpolar transport, *Geophysical Research Letters*, 32 (3), 10.1029/2004GL022086, 2005.

Meredith, M.P., P.L. Woodworth, C.W. Hughes, and V. Stepanov, Changes in the ocean transport through Drake Passage during the 1980s and 1990s, forced by changes in the Southern Annular Mode, *Geophysical Research Letters*, 31 (21), 10.1029/2004GL021169, 2004.

Thompson, D.W.J., and S. Solomon, Interpretation of recent Southern Hemisphere climate change, *Science*, 296, 895-899, 2002.

Thompson, D.W.J., and J.M. Wallace, Annular modes in the extratropical circulation. Part I: Month-to-month variability., *Journal of Climate*, 13, 1000-1016, 2000.

Thompson, D.W.J., J.M. Wallace, and G.C. Hegerl, Annular modes in the extratropical circulation. Part II: Trends, *Journal of Climate*, 13, 1018-1036, 2000.

Webb, D.J., The first main run of the OCCAM Global Ocean Model, Southampton Oceanography Centre, internal document, 34, 1998.

Evidence for the Antarctic Circumpolar Wave between the sub-Antarctic Islands of Gough and Marion during the past 50 years

J.-L. Mélice[12], J. R. E. Lutjeharms[1], and C. J. C. Reason[1]
[1]Department of Oceanography, University of Cape Town, 7700 Rondebosch, South Africa
[2]Institut de Recherche pour le Développement, Laboratoire d'Océanographie et du Climat: Expérimentations et Approches Numériques (LOCEAN), Université Pierre et Marie Curie, 4 place Jussieu, F-75252 Paris, France
Corresponding author: jmelice_sea_staff_sci_main_uct@mail.uct.ac.za

Abstract

Sea surface temperatures have been measured at the islands of Marion (47°S, 38°E) from 1949 to 1998 and Gough (40°S, 10°W) from 1956 to 1998. Evidence for the passage of the Antarctic Circumpolar Wave is apparent at each island, presenting one of the most extended documentation of this phenomenon to date. The highest, negative correlation between the anomalies in each island's sea surface temperature record and the sea ice extent anomalies is observed directly south of each individual island. The sea surface temperature anomalies at Gough lead those at Marion by about one year in average, with mean precession periods of 8.6, 8.9, and 10.4 years in the 60s, 80s and 90s, respectively. These precession periods can be compared to those observed in the sea ice extent anomalies.

1. Introduction

In recent years, several analyses of observed and modeled atmospheric and oceanic variables in the mid- to high latitudes of the Southern Hemisphere have revealed the existence of concurrent anomalies that appear to propagate eastward on interannual timescales. White and Peterson (1996) (hereafter WP96) were the first to report that anomalies in the Antarctic sea ice extent (SIE), sea surface temperature (SST), sea level pressure and winds propagate eastward around the Southern Ocean as a wave called the Antarctic Circumpolar Wave (ACW). The ACW as revealed by their analysis for the period 1982-1994, has a periodicity of 4-5 years at any location and takes approximately 8 to 10 years to encircle Antarctica. Some papers (Caril and Navarra, 2001; Connolley, 2003; Simmonds, 2003; Venegas, 2003) have shown that the ACW is modulated by interdecadal variability and that its character in terms of speed, spatial structure and mechanism of variability etc. is very dependant of the period analyzed, with even sometimes no clear sign of precession.

To study the variation of the ACW, it is desirable to use long-

Fig. 1 Locations of Gough (40°20'S, 10°0'W) and Marion (46°52'S, 37°51'E) islands

term records; unfortunately, the earliest NCEP-NCAR analyses are unreliable in this region, and it is only in the satellite era after 1979 that their quality becomes good (Fichefet et al., 2003). However, there are a few long-term records from individual stations that can be examined for longer-term variations (Connolley, 2003). Marion and Gough Islands are within the region generally considered to be influenced by the ACW (40°-60°S) and are sufficiently close to evaluate its longitudinal propagation. The original SST records at the two islands, together with the simulated SIE which will be described afterwards, provide therefore an opportunity to check for the existence, and to explore the characteristic of the ACW in the sub-Antarctic region for the last ~50 years. The reason why we will compare the SIE to the SST at the two islands is that there is a consistent ACW signal in the SIE (e.g. Simmonds, 2003). Moreover, there is a recent paper based on numerical simulations (Carril et al., 2004) in which the relevance of the SIE as an active component of the ACW is highlighted. This last paper stresses clearly the importance of the sea-ice variability as a component of the ACW.

SST has been measured at the two sub-Antarctic islands (Fig. 1) of Gough from 1956 to 1998 and Marion from 1949 to 1998 (Mélice et al., 2003). In this paper, we explore the relationships of the anomalies of the two ~50 years monthly averaged records with the Antarctic SIE anomalies over the period 1958-1998.

The SIE data used here consists of 240 time series (monthly values from 1958 to 1999) with 1.5° of resolution in longitude. They are the output of the Fichefet et al. (2003) hindcast simulation carried out with a global ice-ocean model driven by the NCEP-NCAR reanalysis daily surface air temperatures and winds. We have used these simulated SIE data instead of the observed SIE records because: (1) there are very few SIE observations before 1979 and the simulated data cover a period much longer than the observed series available, (2) the variability of the SIE is well reproduced by the hindcast simulation over the 1979-1998 period when satellite observations are available to verify it, (3) they can be used for exploring the associations between SIE and SST at Marion and Gough continuously from 1958 to 1998. We emphasis that there is a lack of data over the Southern Ocean during the early years of NCEP. For this reason, we will be careful to perform our analyses before and during the satellite period.

2. Evidence for the Antarctic Circumpolar Wave in the sea surface temperatures anomalies at Marion and Gough Islands

The highest correlation coefficient between Marion SST anomalies and the SIE anomalies is observed for the SIE signal at 32°E (Fig. 2a), thus relatively close to Marion's longitude (38°E). A positive anomaly at Marion SST corresponds to a SIE anomaly decrease south of Marion. The same holds for Gough, where the highest correlation coefficient between Gough SST anomalies and the SIE anomalies is observed for the SIE signal at 22°W (Fig. 2b), close to Gough's longitude (10°W).

We do not have too much confidence in the simulated SIE before 1979 because the reliability of the NCEP-NCAR reanalysis data used for the hindcast simulation is questionable before that date. For this reason, the same correlation analyses are also performed for period 1979-1998 when the variability of the simulated SIE was verified by satellites observations. For 1979-1998, the highest (negative) correlation of the SST anomalies with the SIE anomalies is at 31°E for Marion (Fig. 2a) and 15°W for Gough (Fig. 2b). These results indicate that, as for 1958-1998, the highest correlation is observed south of each island.

Figure 3 shows the Hovmöller plot of the 1958-1999 SIE anomalies, filtered to exclude periods less than 1.5 years. The dashed lines correspond to a precession speed of 45° per year. The ACW identified by WP96 is clearly seen from ~1980 to 1999. It can also be observed, but less clearly, from ~1958 to ~1970. From ~1970 to ~1980 there is no clear sign of ACW, and a pattern in the form of standing, or even westward propagating waves is sometimes observed. The significant inverse correlation between the SST series and the SIE south of the islands implies that the presence of the ACW in the simulated SIE is an indication of the potential existence of the ACW at Gough and Marion.

We investigate the eastward propagation of the SST anomalies from Gough to Marion by estimating the time-varying phase

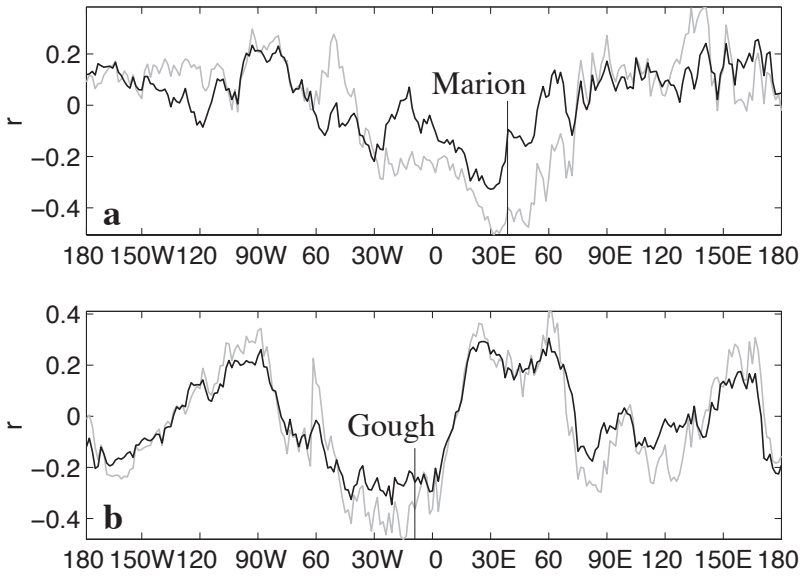

Fig. 2 (a) Correlation coefficient between the SST anomalies at Marion and the simulated Antarctic sea ice extent (SIE) anomalies for 1958-98 (black), and 1979-1998 (gray). Marion's longitude is indicated. (b) same as (a), but for Gough.

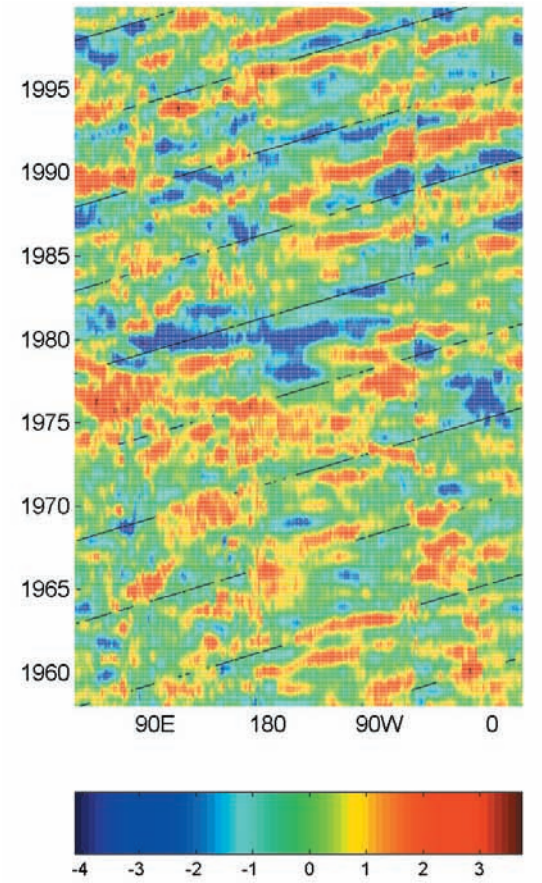

Fig. 3 Hovmöller diagram of the simulated Antarctic sea ice extent anomalies for 1958-1999.

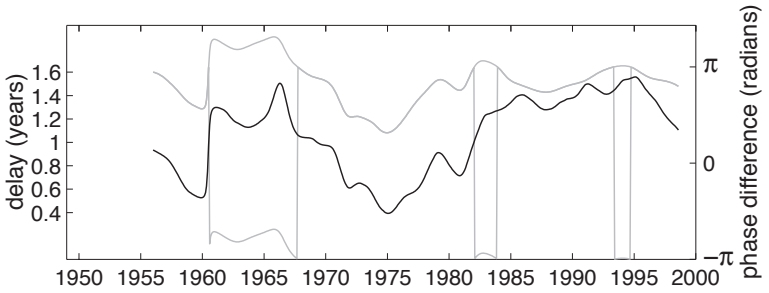

Fig. 4 Phase difference, unwrapped phase difference (gray), and delay (black) between the SST anomalies at Marion and Gough (positive when Gough leads).

difference and delay (Fig. 4) between the two SST anomalies series with the continuous cross-wavelet transform technique. The method is described in the appendix of of Mélice and Servain (2003). The mean delay for the 1956-1998 is 1.05 years. This corresponds to an eastward propagation taking 7.9 years to encircle Antarctica. The precession period varies strongly with time. The mean precession periods for the 50s, 60, 70s, 80s, and 90s are 5.5, 8.6, 5.0, 8.9, and 10.4 years, respectively. The two last periods agree well with the 8-10 years of the ACW precession period described by WP96. They are also in agreement with Carril and Navarra (2001) and Simmonds (2003) who found that the ACW was fast in the 80s and slower in the 90s. The low periods found in the 70s could be the result of interaction between two interannual signals with different frequency and structure as discussed in Venegas (2003), and are consistent with the lack of ACW seen prior to 1982 (Connolley, 2003). In the 60s, the 8.6 years period indicates a return to WP96 ACW-like conditions, as observed in White and Cayan (2000, Fig. 6). Finally, these different precession periods can be compared to those observed in the Hovmöller diagram of the simulated SIE anomalies (Fig. 3 page 24).

3. Conclusions

In the sub-Antarctic region, there are very few long-term records from individual stations that can be examined for long-term variations. The ~50 year long SST records at Marion and Gough islands are some of the longest of their kind in the sub-Antarctic and therefore provide a very important data set for investigating the climate variability of a large region of the mid-latitude Southern Hemisphere. Our analyses suggest the presence of the ACW in the SST anomalies at Gough and Marion, with mean precession periods of 8.6, 8.9 and 10.4 years in the 60s, 80s and 90s, respectively. We also observed that the highest, negative correlation between the anomalies in each island's SST record and the Fichefet et al. (2003) simulated SIE anomalies is observed directly south of each individual island. This correlation suggests that there may be a relationship between the SST anomalies in the sub-Antarctic and the sea ice extent anomalies, since both have the same ACW characteristics in terms of time-varying precession period. Our objective in the future is to use models to further study the physical basis of such correlations by investigating the impact of Southern Hemisphere climate modes on the Antarctic sea-ice ocean system and on the SST variability at Marion and Gough Islands.

References

Carril, A.F., and A. Navarra, Low-frequency variability of the Antarctic Circumpolar Wave, *Geophys. Res. Lett*., 28(24), 4623-4626, 2001.

Carril, A.F., A. Navarra, and S. Masina, Ocean, sea-ice, atmosphere oscillations in the Southern Ocean as simulated by the SINTEX coupled model. *Geophys. Res. Lett*., 31, L10309, doi:10.1029/2004GL019623, 2004.

Connolley, W. M., Long-term variation of the Antarctic Circumpolar Wave, *J. Geophys. Res*., 108(C4), 8076, doi: 10.1029/2000JC000380, 2003.

Fichefet, T., B. Tartinville, and H. Goosse, Antarctic sea ice variability during 1958-1999: A simulation with a global ice-ocean model, *J. Geophys. Res*., 108(C3), 3102, doi: 10.1029/2001JC001148, 2003.

Mélice, J.-L., and J. Servain, The tropical Atlantic meridional SST gradient index and its relationships with the SOI, NAO and Southern Ocean, Clim. Dyn., 20, 447-464, doi: 10.1007/s00382-002-0289-x, 2003.

Mélice, J.-L., J.R.E. Lutjeharms, M. Rouault and I. Ansorge, Sea-surface temperatures at the sub-Antarctic islands Marion and Gough during the past 50 years, *S. Afr. J. Sci*., 99, 363-366, 2003.

Simmonds, I., Modes of atmospheric variability over the Southern Ocean, *J. Geophys. Res*., 108(C4), doi: 10.1029/2000JC000542, 2003.

Venegas, S.A., The Antarctic Circumpolar Wave: A combination of two signals? J. Climate, 16(15), 2509-2525, 2003.

White, W.B., and D.R. Cayan, A global El Niño-Soutern Oscillation wave in surface temperature and pressure and its interdecadal modulation from 1900 to 1997, *J. Geophys. Res*., 105(C5), 11,223-11,242, 2000.

White, W.B., and R.G. Peterson, An Antarctic Circumpolar Wave in surface pressure, wind, temperature and sea-ice extent, *Nature*, 380, 699-702, 1996.

ENSO and the Southern Annular Mode driving sea surface temperature variability in the Southern Ocean

A. Verdy[1], A. Czaja[2], J. Marshall[3]
[1]MIT / WHOI Joint Program in Oceanography, Massachusetts Institute of Technology, USA
[2]Space and Atmospheric Physic group, Imperial College, UK
[3]Department of Earth, Atmospheric and Planetary Sciences, Massachusetts Institute of Technology, USA
Corresponding author: averdy@ocean.mit.edu

In the Southern Ocean sea surface temperature (SST) anomalies are observed to propagate around Antarctica in 8 to 10 years (White and Peterson, 1996). This decadal signal can be reproduced in numerical models (eg. Christoph et al., 1998). However the mechanisms controlling the spatial and temporal scales of SST variability are not well understood. Early studies argued for a coupled ocean-atmosphere phenomenon, implying that oceanic feedbacks have a dynamical impact on the atmosphere (White et al., 1998). Remote forcing by the El Niño-Southern Oscillation (ENSO) and local surface forcing by the Southern Annular Mode (SAM) have been suggested as potential triggers of SST anomalies (Cai and Baines, 2001; Hall and Visbeck, 2002). A recent paper by Verdy et al. (2005) examines the role of ENSO and SAM in driving air-sea heat fluxes, and concludes that SST variability along the Antarctic circumpolar current (ACC) is largely a passive response of the ocean mixed layer to atmospheric forcing. The main findings of that paper are reported here.

To study the generation and propagation of SST anomalies along the ACC, we employed surface data from the NCEP-NCAR Reanalysis over the period 1980-2004. Time series of monthly data are linearly detrended, and the variability is computed by removing the mean seasonal cycle. The path of the ACC is constructed from geostrophic streamlines evaluated by subtracting altimetric data from a reference geoid (see Figure 1).

Dominance of the South Pacific sector

Noticing that the magnitude of SST anomalies peaks in the Pacific sector of the Southern Ocean, we searched for zonally asymmetric air-sea interactions that could drive variability in that particular region. The surface signature of ENSO and SAM, shown in Figure 1, reveals that both affect the low-level atmospheric circulation in the South-East Pacific. The patterns are obtained by correlating time series of SLP anomalies with an index of ENSO variability (Niño3, an index based on Pacific SST) and another of SAM variability (estimated from atmospheric pressure, as defined by Thompson and Wallace, 2000). In both cases, large atmospheric pressure variations are found along the path of the ACC, allowing for possible interactions between ocean dynamics and atmospheric forcing patterns.

The surface pressure pattern associated with SAM has an annular shape, but it is not exactly zonally symmetric: it extends to lower latitudes in the Pacific sector (Figure 1). In that same region, the ACC bends toward the continent as the current flows through Drake Passage. As a result, the current intercepts a zone of strong zonal atmospheric pressure gradients, indicative of geostrophic advection of cold / warm air across the temperature front of the ACC. In contrast, the ENSO teleconnection is more localized to the eastern Pacific sector. El Niño events are associated with a high pressure center (low pressure during La Niña).

Statistical analysis indicates that the dominant mode of SST and SLP covariability along the ACC is centered in the South Pacific (not shown). The spatial patterns, identified by maximum covariance analysis, exhibit sharp peaks located around 100°W (SLP) and 145°W (SST). The maximum covariance is obtained when the temperature signal lags by 1 month; this time lag is consistent with the scenario of a passive response of the ocean to atmospheric forcing, in which SST is driven by SLP. As in White and Peterson (1996), we find that the SLP pattern is 45° (in longitude) downstream of the SST pattern. The position of the pressure maximum coincides with the location of ENSO- and SAM-induced SLP anomalies (Figure 1), suggesting that these surface patterns are linked to the generation of SST variability.

Mechanisms of external forcing

Generation of SST anomalies results principally from turbulent heat fluxes at the sea surface (Fs), as well as Ekman advection of heat in the ocean mixed layer (Fek). We obtain the turbulent (latent + sensible) heat flux data from the Reanalysis, and estimate the Ekman flow from the Reanalysis wind stress data to infer the anomalous advection of heat in the upper ocean. A simple model of SST forced by observed anomalous heat fluxes, and including advection by the ACC, suggests that Fs and Fek are equally important in generating the observed SST variability (Verdy et al., 2005). Patterns of atmospheric forcing associated with ENSO and SAM are identified in the heat flux

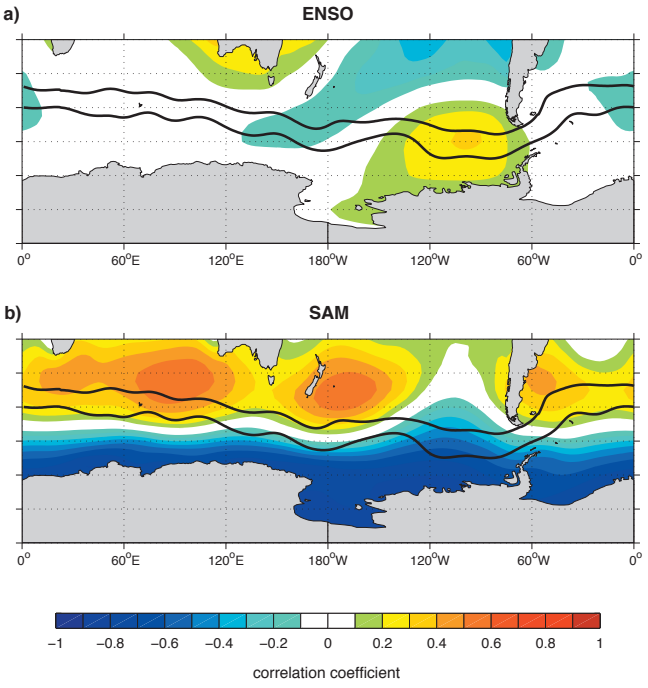

Figure 1 Patterns of anomalous sea level pressure (SLP) associated with a) Niño3 and b) SAM index. Color contours indicate the correlation between local SLP and the climate index. Thick black lines show the mean position of the ACC. In the ACC band, both signals exhibit a strong pressure anomaly in the South-East Pacific. The anomalous low-level circulation resulting from the pressure gradient drives air-sea turbulent heat fluxes and Ekman advection of heat in the oceanic mixed layer, leading to the generation of SST anomalies in the Pacific sector.

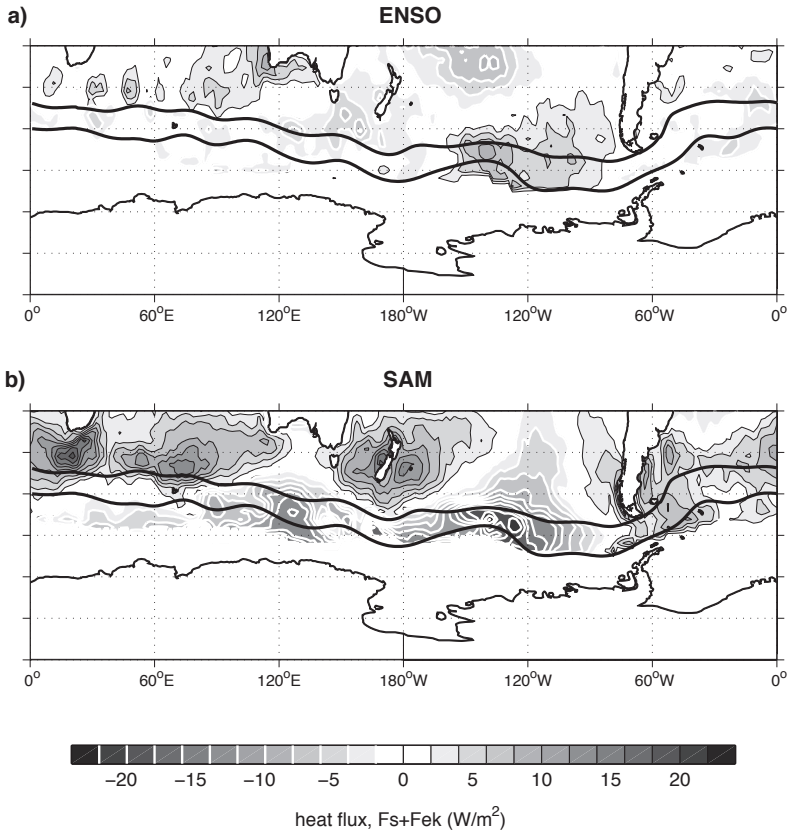

Figure 2 Regression of monthly heat flux anomalies (in W/m²) onto a) Niño3 and b) SAM index. The sum of surface turbulent heat fluxes, Fs, and oceanic Ekman advection, Fek, is plotted with black (white) contours indicating positive (negative) values. Heat fluxes are defined as positive when into the ocean. Along the path of the ACC (thick black lines), the amplitude of the heat fluxes peaks in the Pacific sector.

(Fs+Fek) signal. These surface forcing patterns, shown in Figure 2, are qualitatively consistent with the anomalous heat fluxes expected from the ENSO- and SAM-driven low-level circulation patterns (Figure 1). Most surface heat flux variability in the ACC occurs in the Pacific sector, where the atmospheric pressure gradients are largest.

Along the path of the ACC, anomalous meridional advection of air induced by ENSO warms the South-East Pacific (120°W) while it cools downstream of Drake Passage (60°W) and vice versa. At the same time, anomalous Ekman advection in the ocean occurs over a broad part of the South Pacific (160°W – 110°E), as a result of the meridional pressure gradients in that region. The total heat flux pattern peaks in the central Pacific (Figure 2a), where Fs and Fek interact constructively. This region coincides with the location where SST variance is observed to be a maximum. In an El Niño year, the heat fluxes induce warming of the upper ocean.

SAM displays a similar pattern of heat fluxes, with a maximum in the central Pacific (Figure 2b). The meridional advection of air leads to heat fluxes in the Indian as well as the East Pacific sector, where zonal pressure gradients are large. A zonally symmetric signal associated with oceanic Ekman advection is superimposed on the turbulent heat fluxes. The resulting heat flux pattern is efficient in driving cooling of the upper ocean in the ACC band during a positive phase of the annular mode. In the numerical model of Maze et al. (2005), Ekman advection in the ocean induced by SAM appears to be the main generator of SST anomalies. ENSO and SAM impact on SST variability

The importance of ENSO and SAM in driving SST variability is assessed by comparing the time series of the dominant mode of SST covarying with SLP (from the maximum covariance analysis) with Niño3 and the SAM index. The two indices are found to be strongly correlated with the SST signal (Figure 3 (over page). One observes a close correspondence between all time series, with the lagged cross-correlations peaking when ENSO and SAM lead in time; this is consistent with the hypothesis of the atmosphere driving SST variability. The correlation with Niño3 has a coefficient of 0.53, when the temperature lags by 1 month. The correlation with SAM has a coefficient of -0.38 for the same lag; the correlation is -0.47 when seasonal averages are considered. Together ENSO and SAM account for approximately 45% of the leading mode of SST covarying with the atmosphere (the fraction is given by the square of the correlation coefficient).

These results shed light on the nature of the air-sea interactions along the path of the ACC: SAM exists independently of ocean-atmosphere coupling, and the ENSO signal in the Southern Ocean is not affected by local ocean dynamics. Since ENSO and SAM are identified as the main generators of temperature anomalies along the path of the ACC, we suggest that SST

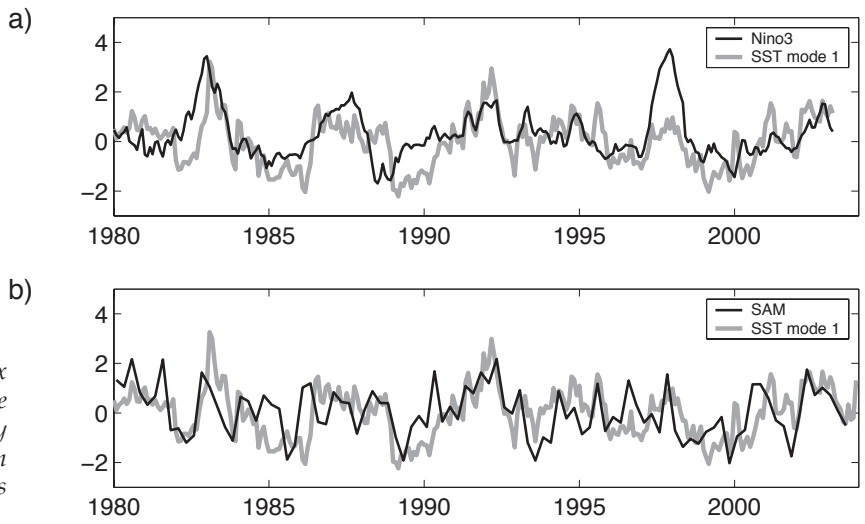

Figure 3 a) Niño3 (monthly data) and b) SAM index (seasonal averages), black line, plotted over the time series of the dominant mode of SST variability, gray line in both panels, obtained from the maximum covariance analysis of SST with SLP. Each index is normalized

variability in the Southern Ocean results primarily from a passive response of the oceanic mixed layer to atmospheric forcing, with ocean-atmosphere coupling playing a second-order role.

Acknowledgements

This research was funded by the Office of Polar Research of the National Science Foundation and the Office of Global Programs of the National Oceanic and Atmospheric Administration.

References

Cai W. and P.G. Baines, 2001: Forcing of the Antarctic circumpolar wave by El Niño-Southern Oscillation teleconnections. *J. Geophys. Res*. 106, 9019-9038

Christoph, M., T.P. Barnett and E. Roeckner, 1998: The Antarctic circumpolar wave in a coupled ocean-atmosphere GCM. *J. Climate* 11, 1659-1672

Hall, A. and M. Visbeck, 2002: Synchronous variability in the Southern Hemisphere atmosphere, sea ice, and ocean resulting from the annular mode. *J. Climate* 15, 3043-3057

Maze, G., F. D'Andrea and A. Colin de Verdière, 2005: Low-frequency variability in the Southern Ocean region in a simplified coupled model. Submitted to *J. Geophys. Res.*

Thompson D.W.J. and J.M. Wallace, 2000: Annular modes in the extratropical circulation, part I: month-to-month variability. *J. Climate* 13, 1000-1016.

Verdy A., J. Marshall and A. Czaja, 2005: Sea surface temperature variability along the path of the Antarctic Circumpolar Current. Submitted to *J. Phys. Oceanogr*.

White, W.B. and R.G. Peterson, 1996: An Antarctic circumpolar wave in surface pressure, wind, temperature and sea-ice extent. *Nature* 380, 699-702

White, W.B., S.-C. Chen and R.G. Peterson, 1998: The Antarctic circumpolar wave: a beta-effect in ocean-atmosphere coupling over the Southern Ocean. *J. Phys. Oceanogr*. 28, 2345-2361

The Causes of Full Ocean Depth Interannual Variability in Drake Passage

M Price[1], K Heywood[1], D Stevens[2], B King[3], A Naveira Garabato[3]
[1]School of Environmental Sciences, University of East Anglia, Norwich NR4 7TJ.
[2]School of Mathematics, University of East Anglia, Norwich NR4 7TJ.
[3]National Oceanography Centre, Southampton, SO14 3ZH.
Corresponding author: martin.price@uea.ac.uk

Introduction

In recent years a number of large scale modes of Southern Hemisphere climate variability have been observed, most notably the Southern Annular Mode (SAM, e.g. Thompson and Solomon, 2002), the Pacific South American modes (PSA, e.g. Mo and Peagle, 2001), the Antarctic Dipole (e.g. Martinson and Ianuzzi, 2003), the Antarctic Circumpolar Wave (e.g. White and Peterson, 1996), and of course the El Niño Southern Oscillation (ENSO). All have pronounced effects over or in the Southern Ocean, and may be expected to account for a significant part of the interannual variability observed there. Most studies analyse these phenomena from a large-scale point of view, often by extracting modes from Southern Hemisphere atmospheric and oceanic fields using various mathematical techniques. In this study we have taken an alternative approach, and tried to understand the causes of the full ocean depth variability in Drake Passage observed in the WOCE SR1b repeat hydrographic sections (Cunningham et al. 2003).

Variability in Drake Passage

Cunningham et al. (2003) find a mode of year-to-year variability in Drake Passage which is dominated by the north-south movements of the full-depth Polar Front. This is accompanied by vertically and laterally coherent shifts in isopycnal depth throughout most of the section. Figure 1 compares a set of isopycnal surfaces from the SR1b occupations in 1996 and 1997, Polar Front south and north years respectively. As the Polar Front moves north, isopycnals in the southern part of the section are on average elevated, and those in the north are depressed.

These vertically coherent shifts are well captured by satellite altimetry, since they have a clear effect on surface dynamic height relative to some deep level. We have found that altimetric sea level anomaly (SLA) extracted along the SR1b track is well correlated with surface dynamic height anomaly (r = 0.83, explaining 69% of the variance). As a consequence, Drake Passage SLA is a good proxy for the dominant mode of variability in SR1b, and can be used to examine full depth Drake Passage variability. The key advantage is greatly improved temporal resolution over the quasi-annual SR1b sections: we have used the ten-daily merged Topex / Poseidon and ERS-1/2 SLA data set. Figure 2 shows SLA averaged in the latitude band 56-58°S along the SR1b track, which is dominated by the north-south movements of the Polar Front and thus captures much of the dominant mode of variability in SR1b. While the time series contains some small amplitude and relatively rapid features, it is dominated by large amplitude variability

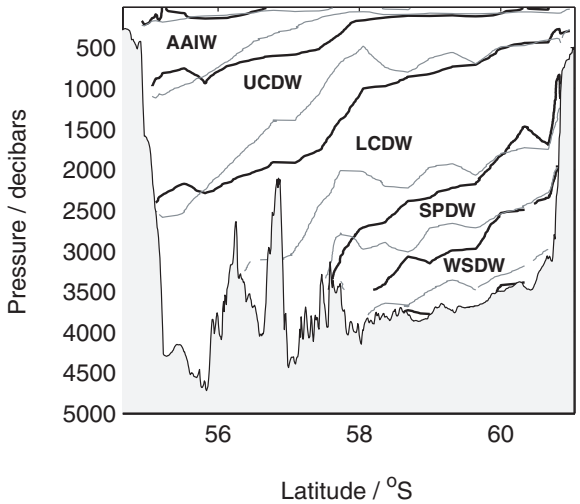

Figure 1: Isopycnal surfaces from SR1b 1996/7 (Polar Front south year, bold lines) and 1997/8 (Polar Front north year, faint lines). The contours are the boundaries in neutral density between the main water masses in the ACC, from top to bottom these are: Antarctic Intermediate Water, Upper and Lower Circumpolar Deep Water, Southeast Pacific Deep Water and Weddell Sea Deep Water

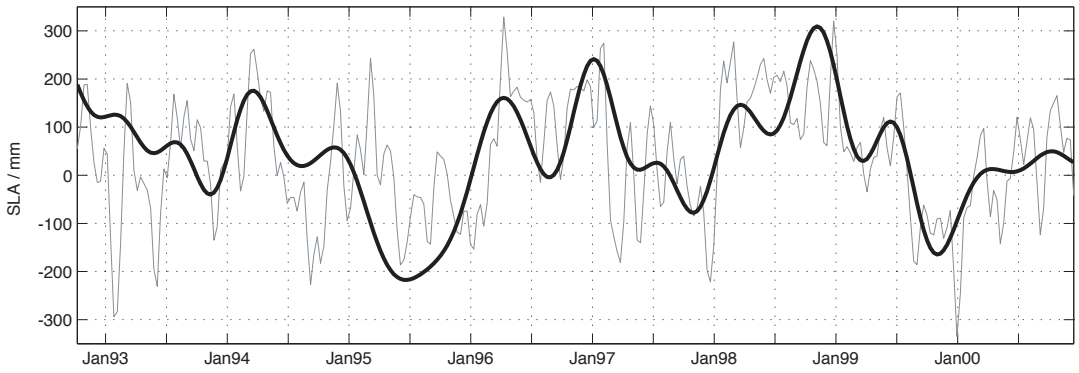

Figure 2: Sea level anomaly averaged 56-58°S along the SR1b track (faint line) and averaged over a larger region of Drake Passage (56-60°S, 56-68°W, bold line). The Drake Passage average series has been scaled up by a factor of three to make the comparison clear.

at interannual time scales. Figure 2 also shows a filtered Drake Passage average series of SLA, which captures essentially the same mode of interannual variability, so the vertically coherent mode in SR1b is not strictly local to the section, but is important in the whole region.

This Drake Passage averaged SLA series has been cross-correlated with Southern Hemisphere grid point SLA from the same data set to search for possible teleconnections forcing the vertically coherent mode in Drake Passage. A number of patterns emerge, the most significant of which is shown in Figure 3, which shows the correlation map at -10 months lag. There is a large region of positive correlation in the eastern tropical Pacific that extends southward along the west coast of South America. The whole lag-sequence of correlation maps shows the path of a Kelvin wave developing in the western equatorial Pacific, propagating along the equator, southward along the west coast of South America and into Drake Passage. The first part of this is clearly the path of a developing ENSO event, and the continued propagation of Kelvin waves along the coast of South America has been observed by others (e.g. Johnson, 1990). However the correlation coefficients seldom exceed the r = 0.56 level needed for 95% statistical significance (assessed using a Monte Carlo simulation), and similarly the number of locally significant correlations in this sequence never reaches the global significance level.

We have similarly searched for Drake Passage teleconnections in a wide range of oceanic and atmospheric data, including sea surface temperature, NCEP / NCAR reanalysis winds, sea level pressure, and EOFs of sea level pressure that are dominated by the SAM, PSA and ENSO modes. In every case there are hints at links between Drake Passage SLA and the large scale modes of Southern Hemisphere variability, but no globally significant teleconnection was found that could account for more than 20-30% of the variability in Drake Passage.

Locally generated variability?

While alternative or more sophisticated analysis techniques may be able to improve statistical confidence that teleconnections force SLA in Drake Passage, they are unlikely to increase significantly the percentage of variance explained. It seems likely that a significant part of the interannual SLA variability in Drake Passage is locally generated, probably by the interaction between the Antarctic Circumpolar Current and the topography in Drake Passage.

A simple zonally periodic channel model has been constructed using the Hybrid Co-ordinate Ocean Model (HYCOM). The model is 20° in latitude (centred on 60°S) by 120° in longitude, with 6 layers in the vertical and a lateral resolution of 0.25° latitude by 0.5° longitude. Layer interfaces slope upward from north to south to represent the density gradient across Drake Passage, and this interface slope is maintained by a relaxation at the side walls. The base configuration has a flat bottom at 4000 m depth with vertical side walls. In the run discussed here a Gaussian sea mount of height 500 m and diameter 440 km is added in the latitudinal centre of the channel at 20° longitude. The model ocean is driven by a steady eastward wind stress, which increases sinusoidally from zero at the side walls to a peak of 0.1 N/m^2 in the centre of the channel.

Even in this basic configuration the model generates large amplitude interannual variability in the region downstream of the sea mount. Figure 4 shows a time-longitude diagram of SLA from years 1 to 30 along a line running just north of the

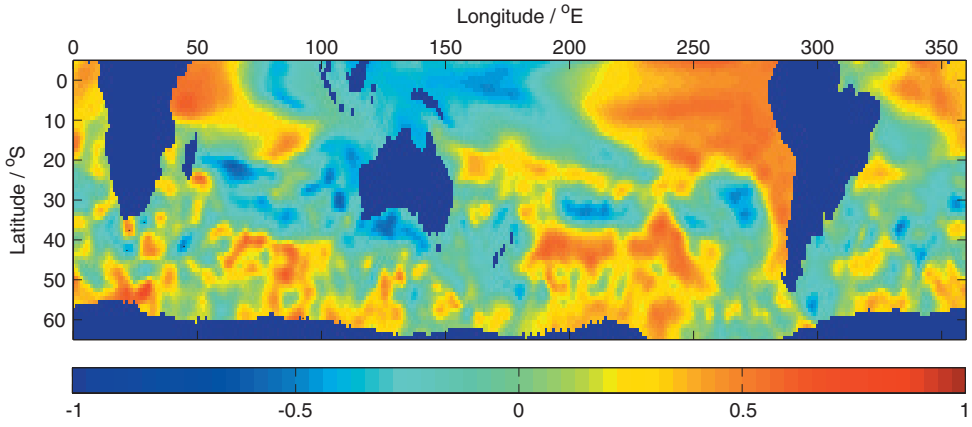

Figure 3: Correlation between Drake Passage SLA and Southern Hemisphere grid point SLA at –10 months lag.

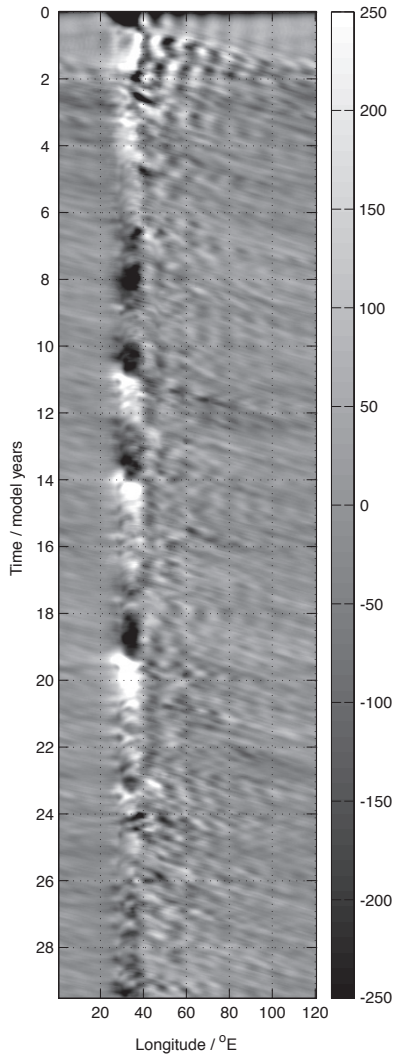

Figure 4: Time-longitude diagram of SLA (mm) in the HYCOM based zonal channel model along a latitude just north of the sea mount.

sea mount (where the variability is greatest). Downstream of the sea mount (which is at 20°E) SLA varies between low and high states with a period of 500-1000 days. The dominant flow feature in this region is a stationary Rossby wave, and the variability is caused by long period variations in its amplitude. In cross section the variability bears a strong resemblance to the variability seen in the SR1b hydrographic sections: high SLA in Figure 4 is accompanied by a southward redistribution of the flow and vertically and laterally coherent shifts in isopycnal depths. Runs with altered topography have confirmed that the amplitude of the variability depends on the meridional amplitude of the stationary Rossby wave, which in turn depends on the topography. In general topography with greater meridional extent generates larger amplitude variability. The mechanisms setting the time scale of the variability have not been clearly determined, but the advective time scale - the time taken to advect an anomaly right around the periodic channel - appears to play a role.

Aside from the simplicity of the model, there are key differences between the flow of the ACC through Drake Passage and the model described here. The similarities between the two should not be over emphasised, but the model does illustrate that flow-topography interactions can generate interannual variability without external forcing. It seems quite likely that variability will be generated dynamically by the flow of the ACC through Drake Passage, and at the least this locally generated variability complicates the question of how this region of the Southern Ocean will respond to the large scale modes of Southern Hemisphere variability like the SAM, ENSO, PSA modes and the ACW. Two papers are currently in preparation that will discuss the work described here in detail.

Acknowledgements

This work was carried out as part of a PhD at the University of East Anglia jointly supervised by Karen Heywood, Dave Stevens, Brian King and Alberto Naveira Garabato. Funding was provided by the National Oceanography Centre (NOC), Southampton. The altimeter products were produced by the CLS Space Oceanography Division as part of the Environment and Climate EC AGORA (ENV4-CT9560113) and DUACS (ENV4-CT96-0357) projects. WOCE SR1b hydrographic data were provided by Brian King of NOC and Mark Brandon of the Open University. Thanks to the HYCOM modelling group for providing their model code.

References

Cunningham, S. A., S. G. Alderson, B. A. King, and M. A. Brandon. Transport variability of the Antarctic Circumpolar Current in Drake Passage. *Journal of Geophysical Research*, 108(C5), art. no. 8084, 2003.

Johnson, M. A. A source of variability in Drake Passage. *Continental Shelf Research*, 10(7), pp. 629-638, 1990.

Martinson, D. G. and R. A. Iannuzzi. Spatial/temporal patterns in Weddell gyre characteristics and their relationship to global climate. *Journal of Geophysical Research*, 108(C4), art. no. 8083, 2003.

Mo, K. C. and J. N. Peagle. The Pacific-South American modes and their downstream effects. *International Journal of Climatology*, 21, pp. 1211-1229, 2001.

Thompson, D. W. J. and S. Solomon. Interpretation of recent Southern Hemisphere climate change. *Science,* 296, pp. 895-899, 2002.

White, W. B. and R. G. Peterson. An Antarctic Circumpolar Wave in surface pressure, wind, temperature and sea-ice extent. *Nature*, 380(6576), pp. 699-702, 1996.

Investigation of ACC transport and variability through Drake Passage using the simple ocean model BARBI

K. Lettmann and D. Olbers
Alfred Wegener Institute, Bremerhaven, Germany
Corresponding author: klettmann@awi-bremerhaven.de

Introduction

The determination of the transport of the Antarctic Circumpolar Current (hereafter ACC) through Drake Passage is one of the major tasks in studying the ocean climate of the southern hemisphere. Several studies (e.g. ISOS and WOCE) have tried to monitor the ACC transport and its variability. The mechanisms that balance the ACC transport are described e.g. in Olbers et al. (2004) and an overview of the measured transport values is given in Cunningham et al. (2003), who found no significant trend over the time period between 1975 and 2000.

With respect to the variability, Hughes et al. (1999) proposed that for periods between about 10 and 220 days the variability of the transport through Drake Passage is dominated by a barotropic mode that follows *f*/*h* contours at the rim of Antarctica. Furthermore, bottom pressure in the south of Drake Passage is a good indicator for monitoring the variability of the flow through Drake Passage. This view is supported further by Aoki (2002), Hughes et al. (2003) and Meredith et al. (2004). Additionally, they connected the variability of transport and pressure data with the Southern Annular Mode (hereafter SAM, see e.g. Thompson and Wallace 2000), which seems to be the dominant mode of atmospheric forcing in the southern hemisphere.

Here we investigate what the BARBI model (Olbers and Eden (2003)) yields about these issues of transport variability.

The BARBI model

BARBI is a two-dimensional simplified ocean general circulation model that is based on the vertically integrated primitive equations in Boussinesq form (further details in Olbers and Eden (2003)). The resulting model equation for the integrated velocity U is $\frac{\partial U}{\partial t} + fk \times U = -\nabla E + \tau + F$

where *h* is the depth of the ocean, *P* is the bottom pressure and *E* the baroclinic potential energy associated with the perturbation density. τ represents the surface forcing created by the wind stress (which is the only forcing in the model) and F stands for lateral friction. By using the rigid-lid approximation it is possible to introduce a transport streamfunction Ψ for the volume transport with $U=k\times\nabla\Psi$. The equations of heat and salt are combined into an equation for the perturbation density about a mean linear background stratification described in the constant Brunt-Väisälä Frequency N. A prognostic equation for the potential energy is derived, which is extended by a dissipation term $-\mu E$. For the sake of simplicity, this equation and the prognostic equation for the velocity moments are omitted in this abstract but can be found in Olbers and Eden (2003).

The following model parameters are used: the horizontal and vertical viscosities are $A_h=5\cdot10^4 m^2/s$ and $A_v=10^{-4}m^2/s$, the horizontal diffusivity is $D_h=2\cdot10^3 m^2/s$, the dissipation factor is $\mu=1.5\cdot10^{-10}s^{-1}$, the stratification frequency is $N=0.0015s^{-1}$. Only one baroclinic density and velocity moment is used, and the model domain is from 76°S to 20°S with a resolution of $\Delta X\cdot\Delta Y=2°\cdot1°$. Two different kinds of wind forcing are used: the first (type A) is a composition of a mean wind stress provided by the European Centre for Medium-Range Weather Forecasts (ECMWF) and the anomalies from NCEP/NCAR monthly wind data with a linear interpolation between the monthly values. The second (type B) are daily winds provided by NCEP/NCAR.

A trend in ACC Transport

Figure 1 shows the model transport through Drake Passage for wind forcing scenarios A and B during the time interval of the ISOS and WOCE studies. The time series are low-pass filtered to suppress periods less than 60 days. Furthermore, the estimated transport values from measurements, presented in Cunningham et al. (2003) (table 1), are plotted to compare them with the model transports. It is important to know that these values assume a level of no motion at 3000 dbar. The figure shows that the two time series of the model transports are quite similar and match the values of Cunningham et al. (2003) quite well.

On the basis of these data Cunningham et al. used a t-test with a 95% significance level to prove that the two sample means of the two time series (1975-1980, 1990-2000) are not different, and concluded that there is no trend in the ACC transport. Using the same procedure with the model data, the means of the two time intervals are significantly different. Taking the model data (NCEP daily forcing) only at those dates which are equal to the dates in Cunningham et al., the results are the same: the mean values are not significantly different. Therefore, these model data suggest that there is a trend from the mid 1970s until today, which can be estimated from the time series with NCEP daily forcing to be 0.30 Sv/y.

The model trend, shown in figure 2, is smaller for the NCEP daily forcing, which might be due to inertia of the system under the linear interpolated wind forcing of type A. Furthermore, an increasing trend is seen in the wind forcing which might cause the increasing model transport, because it seems reasonable that increasing the strength of the forcing increases the model response (ACC transport). The increasing wind stress could be related to the increasing SAM index.

Connection with SAM

Two different definitions of SAM indices are used here to relate them with the model transport. The first (hereafter SAM-1) is based on station data provided by Gareth Marshall (www.nerc-bas.ac.uk/icd/gjma/sam. html) and is displayed in the lower panel of figure 2. The second (SAM-2) follows Thompson and Wallace (2000) and has been derived from an EOF analysis of 700hPa geopotential height anomaly south of 20°S (www.cpc.ncep.noaa.gov/products/precip/Cwlink/ ENSO/verf/new.aao.shtml) .

Correlating the model transport under forcing B with SAM-1 results in r=0.55 and with SAM-2 results in r=0.60. These are quite similar but explain only about 36% of the observed variance. Therefore, these model results suggest that the SAM index might not be the best proxy for the transport variability through Drake Passage. The objection could be raised that the SAM isn't likely to be well characterised in the model, because only wind stress is used as forcing, which might not completely represent the SAM index. Using a linear regression model a change of SAM index of 1 standard deviation produces a transport change of 5.7 Sv for SAM-1 and 6.0 Sv for SAM-2 (for

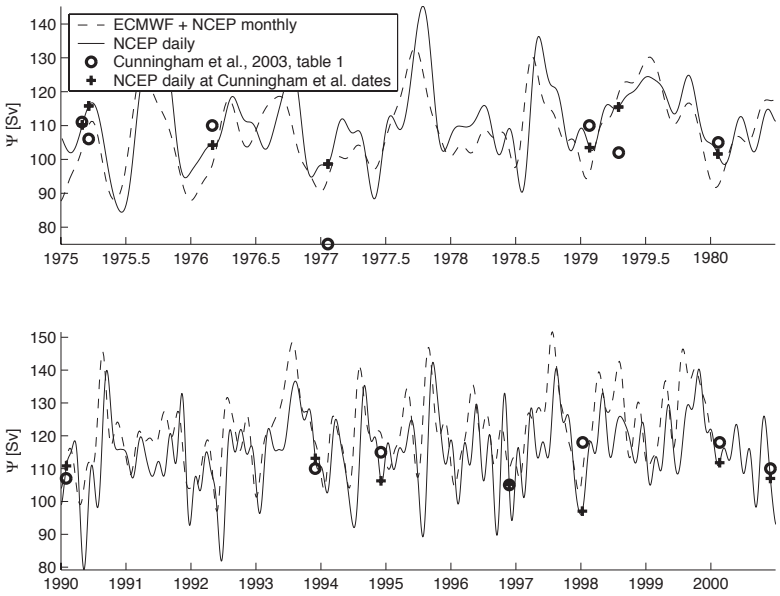

Figure 1: Comparison of model transport through Drake Passage with measurements listed in Cunningham et al. 2003.

comparison Hughes et al. (2003) find 3.5 Sv).

The bottom pressure as proxy

As mentioned in the introduction a good indicator of transport variability might be the bottom pressure around the rim of Antarctica. In figure 3 the correlation between transport through Drake Passage and bottom pressure at every grid point is plotted, showing the highest correlations along the *f/h* contours around Antarctica.

Borowski et al. (2002) and others showed the importance of the gradient of potential energy forcing the flow over the blocked *f/h* contours at Drake Passage. Therefore it seems interesting to investigate on which time scale potential energy comes into play. Figure 4 displays the coherence of transport through Drake Passage with the difference of potential energy across, and the bottom pressure in, the south of Drake Passage using the longer time series with forcing A. As can be seen, for periods up to four years the variability is dominated by bottom pressure peaking between 0.25 and 0.5 years.

Summary

From these results of the BARBI model it is suggested that for time scales of up to 4 years bottom pressure in the south of Drake Passage is a good proxy of ACC transport, whereas SAM index does not seem to be quite suitable.

Additionally, relying in the accuracy of the wind forcing a positive trend in transport through Drake Passage since the late 1970s seems plausible.

Acknowledgement

KL thanks the Alfred Wegener Institute, Bremerhaven, Germany for funding his trip to the Modes of Southern Hemisphere Climate Variability workshop in June 2005 at Scott Polar Research Institute.

References

Aoki S., 2002: Coherent sea level response to the Antarctic Oscillation. *Geophysical Research Letters*, 29(20), doi:10.1029/2002GL015733

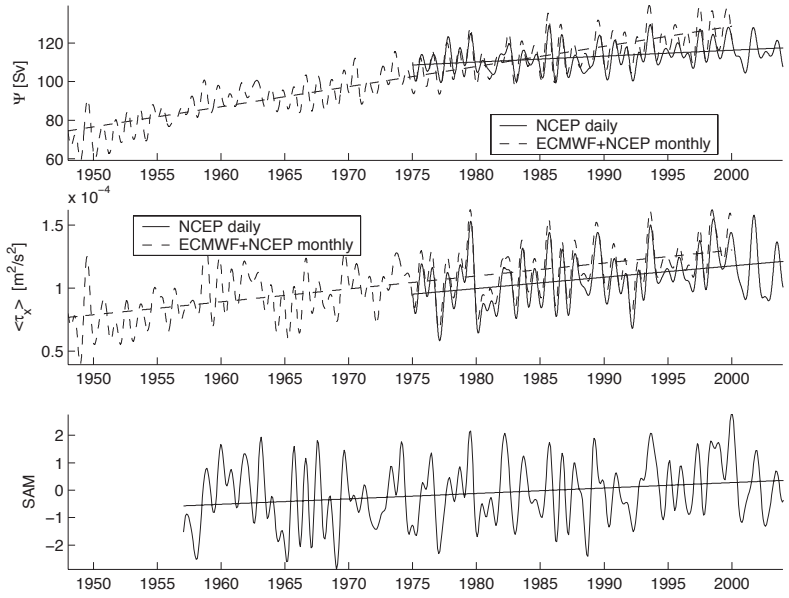

Figure 2: Upper panel: model transport through Drake Passage for wind forcing A and B. Middle panel: mean zonal wind stress between 68°S and 47°S. Lower panel: SAM index after Gareth Marshall

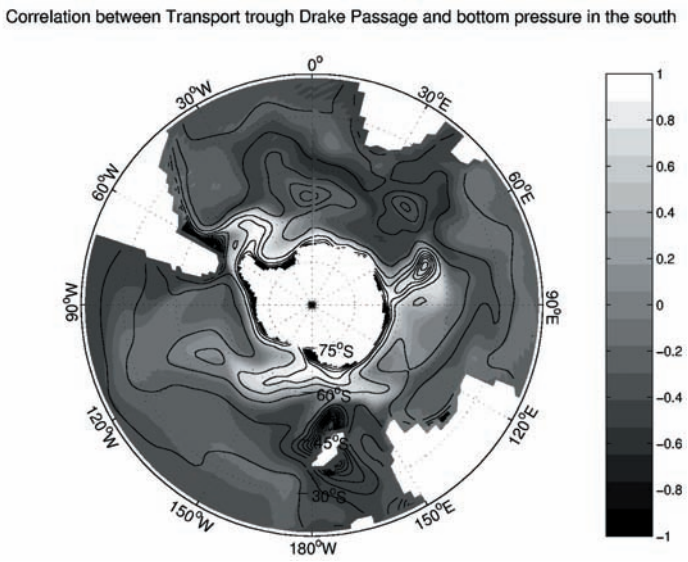

Figure 3: Correlation of transport through Drake Passage with bottom pressure at each grid point and geostrophic (f/h) contours in the model domain

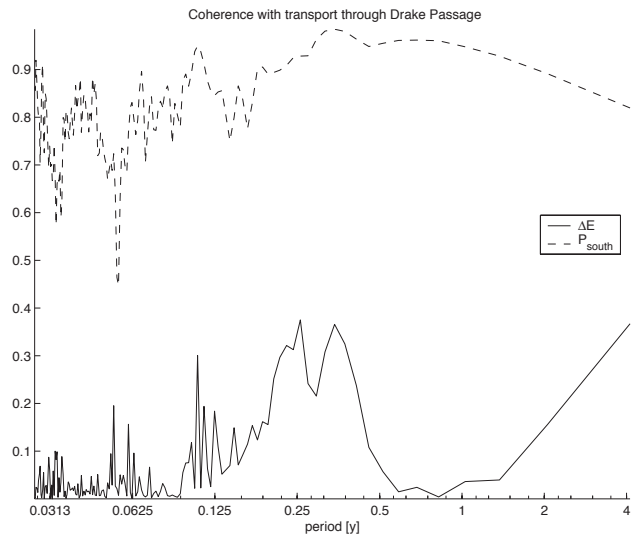

Figure 4: Coherence of transport through Drake Passage with bottom pressure in the south and with difference of potential energy across Drake Passage.

Borowski D., R. Gerdes , D.J. Olbers, 2002: Thermohaline and Wind Forcing of a Circumpolar Channel with blocked Geostrophic Contours. *Journal of Physical Oceanography*, 32, 2520-2540

Cunningham S.A., S.G. Alderson, B.A. King, M.A. Brandon, 2003: Transport and variability of the Antarctic Circumpolar Current in Drake Passage. *Journal of Geophysical Research*, 108, doi:10.1029/2001JC001147

Hughes C.W., M.P. Meredith, K. Heywood, 1999: Wind-Driven Transport Fluctuations through Drake Passage: A Southern Mode. *Journal of Physical Oceanography*, 29, 1971-1992

Hughes C.W., P.L. Woodworth, M.P. Meredith, V. Stepanov, T. Whitworth, A.R. Pyne, 2003: Coherence of Antarctic sea levels, Southern Hemisphere Annular Mode, and flow through Drake Passage. *Geophysical Research Letters*, 30(9), doi:10.1029/2003GL017240

Meredith M.P., P.L. Woodworth, C.W. Hughes, V. Stepanov, 2004: Changes in the ocean transport through Drake Passage during the 1980s and 1990s, forced by changes in Southern Annular Mode. *Geophysical Research Letters*, 31, doi:10.1029/2004GL021169

Olbers D., C. Eden, 2003: A simplified General Circulation Model for a Baroclinic Ocean with Topography. Part I: Theory, Waves and Wind-Driven Circulations. *Journal of Physical Oceanography*, 33, 2719-2737

Olbers D.J., D. Borowski, C. Völker, J.O. Wolff, 2004: The dynamical balance, transport and circulation of the Antarctic Circumpolar Current, *Antarctic science*, 16(4), 439-470.

doi:10.1017/S0954102004002251

Thompson D.W.J., J.M. Wallace, 2000: Annular modes in the extratropical circulation . Part I: Month-to-month variability. *Journal of Climate*, 13, 1000-1016

Optimum Multiparamenter Analysis of the Weddell Sea Water Mass Structure

R. Kerr, M.M. Mata and C.A.E. Garcia
Fundação Universidade Federal de Rio Grande, Rio Grande – Brazil
Corresponding author: pgofkerr@furg.br

1. Introduction

The Southern Ocean plays an important role in global climate as a result of complex interactions between ocean/atmosphere/ice, which eventually influence the global ocean circulation at different levels (e.g. Fahrbach et al., 1994; Orsi et al., 1999). One of the key regions of the Southern Ocean with respect to climate is the Weddell Sea (WS) as most of the bottom water that occupies the world ocean is likely to originate from this region (Orsi et al., 1999). Furthermore, those water masses acquire their signatures from air-sea processes and are therefore excellent indicators of alterations in climatic conditions.

Generally, four water masses occupy the water column in the Weddell Sea. The Surface Water (SW) is present in the top 200 m and experiences strong and variable atmospheric influences at different timescales. The Warm Deep Water (WDW) occupies the intermediate layer between 200-1000m and is derived from the modification of Circumpolar Deep Water (CDW) as it enters the Weddell Gyre around 20-30°E (Gouretski and Danilov, 1993). Moreover, the WDW is a source water mass for deep and bottom waters in the region. The Weddell Sea Deep Water (WSDW) occurs in the layer between 1000-4000m and is the main water mass exported from the WS, an important constituent of Antarctic Bottom Water (AABW) outside the Weddell gyre. Finally, the Weddell Sea Bottom Water (WSBW) is found near the ocean floor below 4000 m.

In this study, we address the distribution, mixing and some aspects of the variability of many of the water masses mentioned above. We dedicate special attention to 1990 and 1996, when positive (and negative) extremes of WSBW distribution were observed.

2. Methodology and data

An Optimum Multiparameter (OMP) analysis (e.g Tomczak and Large, 1989) is used to quantify the mixing between the major water masses present in the WS. The field data used was collected during the WOCE repeat line SR04 (in 1989, 1990, 1993, 1996 and 1998), which covers the WS central region from approximately 63°S to 71°S (Figure 1). The whole dataset is available at the WOCE Hydrographic Database (http://www.woce.org). Further details on the cruise data as well as many more references can be found in Fahrbach et al. (1994, 2004).

Due to strong seasonal variability we discarded the surface layer and only the following water masses were considered for the analysis: WDW, WSDW and WSBW. Table I shows the water mass definitions and weights utilized for model input (based on Robertson et al., 2002):

Table 1 - SWTs and paramet for model output

SWT / Parameter	WDW	WSDW	WSBW	Weight
θ(°C)	0.5	-0.3	-0.9	11.5
Salinity	34.70	34.66	34.64	11.5
DO (M)	212	234	263	11.9

3. Results and discussion

The general results (Figure 2, 1st column) show the presence of WDW in the intermediate layers up to 1000m, contributing 50-100% to mixing. The WDW reaches around 1500m deep with a contribution of about 30%. The deep layer shows the WSDW present between 1000-4000m, contributing around 50-100% to the mixing (Figure 2, 2nd column), while WSBW has more than a 60% contribution below 4000m along the deep basins (Figure 2, 3rd column).

With respect to the latter, the results from the OMP analysis show the same levels of contribution of WSBW hugging the northwestern slope, indicating the recently formed water mass, especially during 1990.

The WDW has an increased contribution during the years analyzed (not shown) and significant variability in its thermohaline properties as documented in the literature (Robertson et al., 2002; Farhbach et al, 2004), indicating a warming trend in this period that might be related to processes originating outside the Weddell Gyre. Fahrbach et al. (2004) suggest the possible factors that cause the WDW variability. They further argue that WDW temperature and salinity increase may explain the observed variability in WSBW.

The WSDW has a consistent distribution along the section during the years analysed. The core is shallower in the northwestern side of the section with the maximum (~100%) positioned between 2000-2500 m. An extreme event took place in 1990, when an anomalously vigorous decrease (increase) in WSDW (WSBW) contribution occurred. For that year, the analysis of the anomalies (not shown) indicates a decrease of about 30%, with respect to the average of all cruises, in the WSDW contribution to the mixing at the 3000 m layer. At the same time and depth, the WSBW contribution to the mixing increased by ~20%.

The peak contribution of WSBW to the water column in 1990 agrees with the Fahrbach et al (2004) analysis. They argue that during 1990 the atmospheric low-pressure centre was weaker and situated further to the east (see their figure 9). As a result, the wind regime changed and modified the Weddell Gyre structure and intensity. This anomaly significantly altered the Circumpolar Deep Water intrusions (source water mass for WDW). Here we add to the analysis of Fahrbach et al, showing that the anomaly signal also propagates to the WSDW layer and, in fact, the entire water mass structure of the Weddell Sea is changed. In 1990, for example, the core of WSDW is about 700 m shallower in the northwestern side of the gyre than observed in other years. We appreciate that the observed changes can be the result of alterations in the source water types. Nevertheless, those anomalies are felt throughout the water column in a single event, which is an important result.

The opposite was found during 1996, with a significant decrease in the contribution of WSBW. This event is matched with an increase in the positive anomaly of WSDW contribution, especially towards the bottom layers. Furthermore, the WSBW showed a decreasing trend during 1990s, with a small signal increase observed in the northwestern slope during the 1998 cruise.

Several mechanisms (remote and local) may be responsible for driving the deep and bottom water variability in the region. For example, Beckmann and Timmermann (2001) showed that seasonal, interannual and longer timescale variations in dense water volume in the WS are related to the frequencies of the Antarctic Circumpolar Wave. Atmospheric patterns of variability, like the Southern Annular Mode (Thompson and Solomon, 2002), probably also affect the WS deep and bottom water variability. For example, the strongest positive SAM index since 1950 was observed about 18 months before the 1990 positive anomaly of WSBW, but further investigation is needed to quantify that relationship. Furthermore, factors inside the Weddell Gyre may also be contributing to the observed variability as well. For example, a decrease in surface source waters (High Salinity Shelf Water or Ice Shelf Water) impacts the formation and hydrographic characteristics of WSBW (Fahrbach et al, 2004).

4. Summary

In this study we address the Weddell Sea water mass structure and variability based on an OMP analysis. The results identify two opposite extremes in the deep and bottom water mass distribution. The positive WSBW phase was observed during 1990, when a maximum concentration and distribution of this water mass was observed. This event occurred in conjunction with a significant decrease of the WSDW layer, showing that the anomaly was felt in the entire water column considered. The opposite phase was observed in 1996, when the minimum (maximum) of the WSBW (WSDW) contribution to the mixing was registered.

Acknowledgment:

This work was supported by the GOAL Project, part of the Brazilian Antarctic Survey (CNPq/PROANTAR/MMA). R. Kerr is supported by CAPES.

References

Beckmann, A. and R. Timmermann, 2001: Circumpolar Influences on the Weddell Sea: Indication of an Antarctic circumpolar coastal Wave. *J. Climate*, 14, 3785-3792.

Fahrbach, E.; R.G. Peterson; G. Rohardt; P. Schlosser and R. Bayer, 1994: Suppression of bottom water formation in the southeastern Weddell Sea. *Deep-Sea Res*. I, 41, 389-411.

Fahrbach, E.; M. Hoppema; G. Rohardt; M. Schröder and A. Wisotzki, 2004: Decadal-scale variations of water mass properties in the deep Weddell Sea. *Ocean Dynam*., 54,77-91.

Gouretski, V.V. and A.I. Danilov, 1993: Weddell Gyre: structure of the eastern boundary. *Deep-Sea Res.* I, 40, 561-582.

Orsi A.H., Johnson G.C., Bullister J.L., 1999. Circulation, mixing, and production of Antarctic Bottom Water. *Prog. Oceanogr*. 43: 55-109

Robertson, R.; M. Visbeck; A.L. Gordon and E. Fahrbach, 2002: Long-term temperature trends in the deep waters of the Weddell Sea. *Deep-Sea Res.* II, 49, 4791-4806.

Tomczak, M. and D.G.B. Large, 1989: Optimum multiparameter analysis of mixing in the thermocline of the eastern Indian Ocean. *J. Geophys. Res*., 94, 16141-16149.

Thompson, D.W.J. and S. Solomon, 2002: Interpretation of recent Southern Hemisphere Climate Change. *Science*, 296, 895-899.

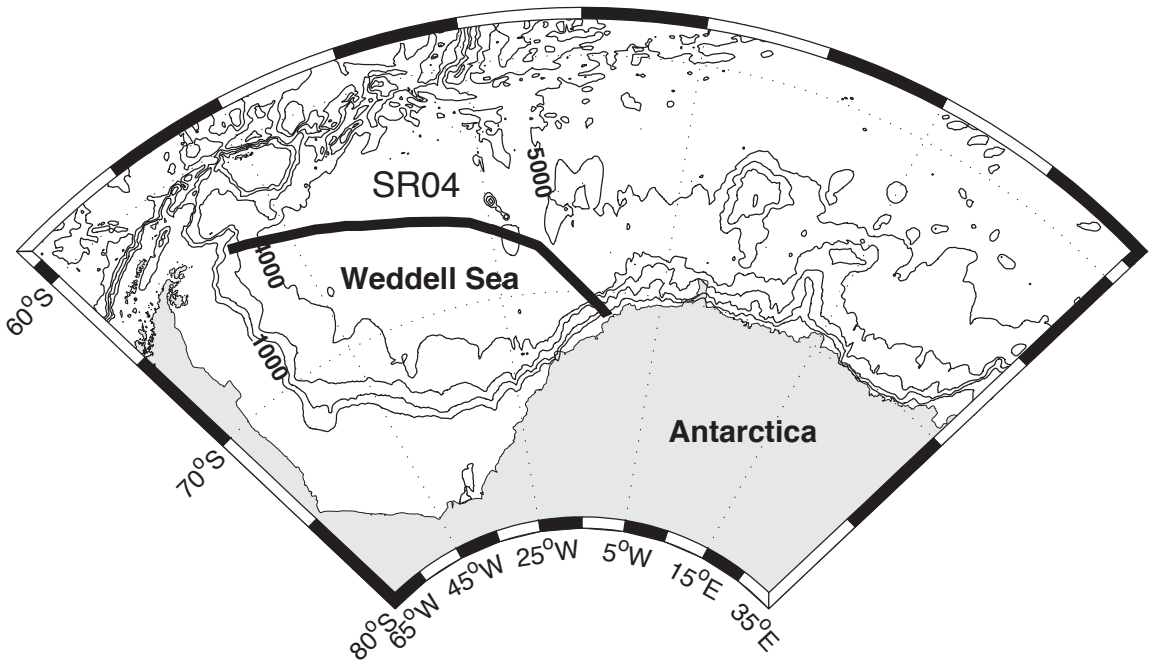

Figure 1 – Location of WOCE SR04 repeat hydrographic section.

Figure 2 – Weddell Sea Water Masses concentration (%): WDW (left column), WSDW (centre column) and WSBW (right column). Each line corresponds to a particular year which is indicated in the first box. Latitude limits vary slightly from cruise to cruise.

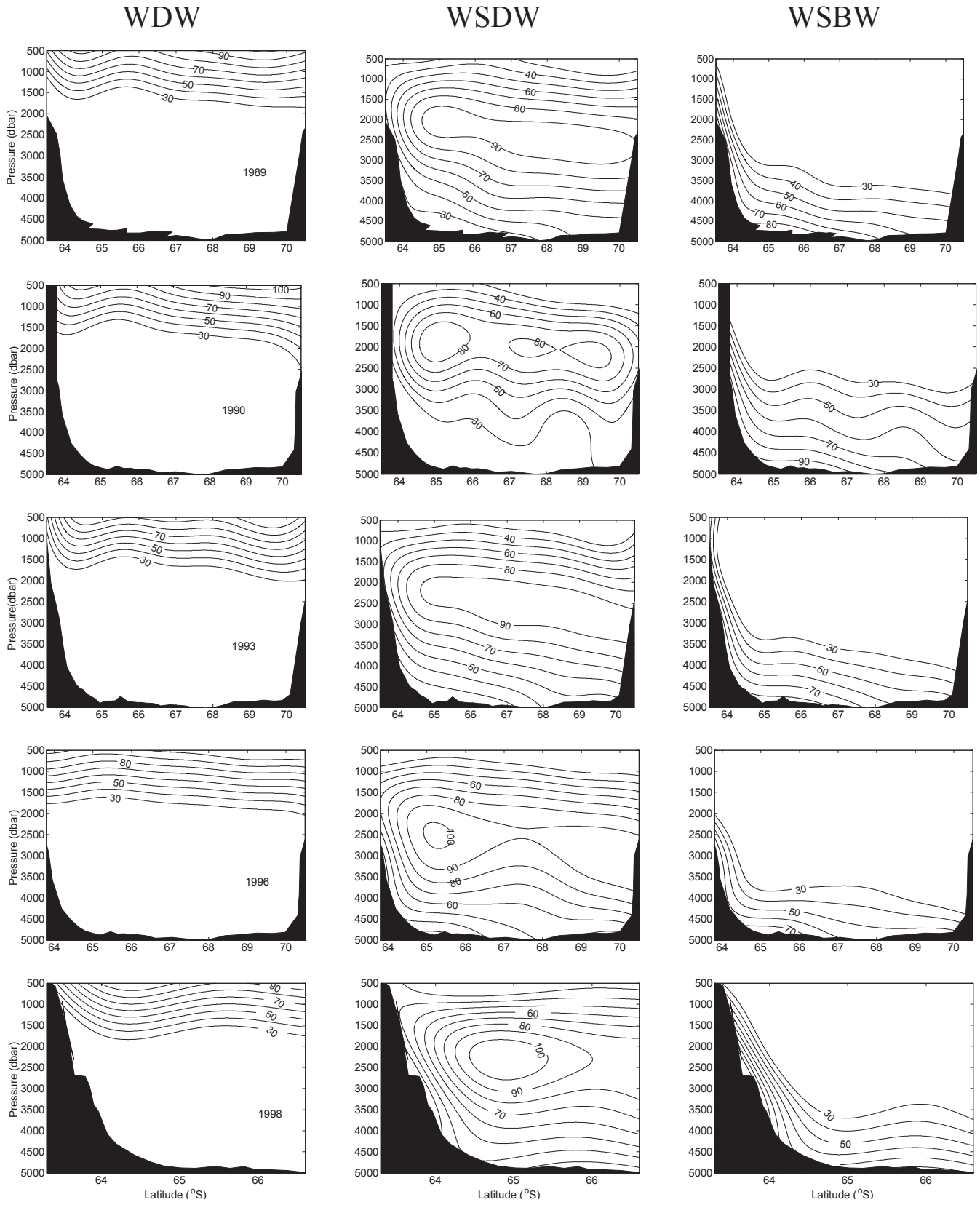

Surface layer heat flux variability in the Southeastern Indian Ocean

K. Speer[1], N. Wienders[1], J.B. Sallee[2], R. Morrow[2]
[1]Department of Oceanography, Florida State University, Tallahassee FL 32306–4320, USA
[2]LEGOS–UMR5566, 18 av Edouard Belin, 31401, Toulouse, France
Corresponding author: kspeer@ocean.fsu.edu

A major goal of climate studies is to understand the processes that control the heat content of the upper ocean. In particular, the heat content of mode water is of interest because the thermal anomalies in deep mixed layers tend to persist longer and might have a longer term effect on climate, through reappearance in winter or through subduction and interior mixing. Much effort is directed toward SST variability, but this does not necessarily represent substantial heat content, and studies of the mechanisms of heat transport and transport variability are needed.

Ekman advection and air-sea fluxes are thought to be dominant forcing contributions in the formation region of the Subantarctic Mode Water (SAMW), north of the Subantarctic Front in the Southern Ocean (Ribbe, 1999; Rintoul and England, 2002; Fig. 1). A recently submitted paper (Sallee et al, 2005) considers this matter by examining various terms in the upper ocean heat balance in the southern Indian Ocean. This article reports the air-sea and Ekman heat flux variability, since the interannual evolution of these two terms could reflect an interannual evolution of the SAMW characteristics.

We have estimated Ekman fluxes from satellite data and other sources (NCEP, COAPS winds, etc. – see Sallee et al., 2005). The derived Ekman fluxes from satellite data have shown substantial difference with those derived from the climatologies, but having made the calculations and with some understanding of the weaknesses of the climatologies we are now in a position to go back to the climatologies to infer long time scale variability, which is not possible with the short record from satellites. To illustrate the record, we plot the net air-sea heat flux, the Ekman heat transport, and their sum over the NCEP record 1948-2005 (Fig. 2). Before 1979 the analysis is considered to be less accurate because of the absence of satellite data (Hines et al., 2000; Marshall, 2003).

Post-1980, the variability is up to 20 W / m^2 in both the net air-sea heat flux and Ekman components, resulting in cooling ranging from near zero to -50 W / m^2. This is sufficient for temperature anomalies of up to 1 C or so in the mixed layer, consistent with the observed typical range of ± 0.5 C (Rintoul and England, 2002) south of Australia. There may be further agreement in the trend to cooler mode water over the period 1991 to 1995, when greater cooling occurred, but the trend is not consistent and the yearly differences in temperature are not quantitatively predicted. This situation is likely to be as much a mode-water sampling problem as a question of the accuracy of the fluxes or their averaging area and period.

Despite the uncertainties, the results do point to the influence of the net heat supply on mode water by the wind and air-sea exchange and its relevance as an indicator of climate variability. They also raise the question of the relationship between this variability and the major index of wind variability, the Southern Annular Mode (Thompson and Wallace, 2000). Ekman transport and air-sea flux depend directly on the surface wind, and would be expected to follow the variations of the Southern Annual Mode. Preliminary work (Fig. 3) suggests that while the SAM may explain some of the local variation, the connection between local Ekman heat flux forcing and the SAM is not entirely straightforward, partly because of longitudinal structure in both the atmospheric mode and SST fields, and propagation of SST in ocean currents.

References

K. Hines, D.H. Bromwich, and G.J. Marshall (2000) Artificial surface pressure trends in the NCEP-NCAR reanalysis over the Southern Ocean and Antarctica. *J. Climate*, 13:3940– 3952.

G.J. Marshall (2003) Trends in the Southern Annular Mode from observations and reanalyses. *J. Climate*, 16:4134–4143.

J. Ribbe (1999) On wind-driven mid-latitude convection in ocean general circulation models. *Tellus*, 51A:505–516.

S. R. Rintoul and M. H. England (2002) Ekman transport dominates air-sea fluxes in driving variability of Subantarctic Mode Water. *J. Phys. Oceanog.*, 32:1308–1321.

J.B. Sallee, N. Wienders, R. Morrow, and K. Speer (2005) Formation of Subantarctic Mode Water in the Southeastern Indian Ocean. *Ocean Dynamics*, submitted.

D.W.J. Thompson and J.M. Wallace (2000) Annular modes in the extratropical circulation. Part I : Month-to-month

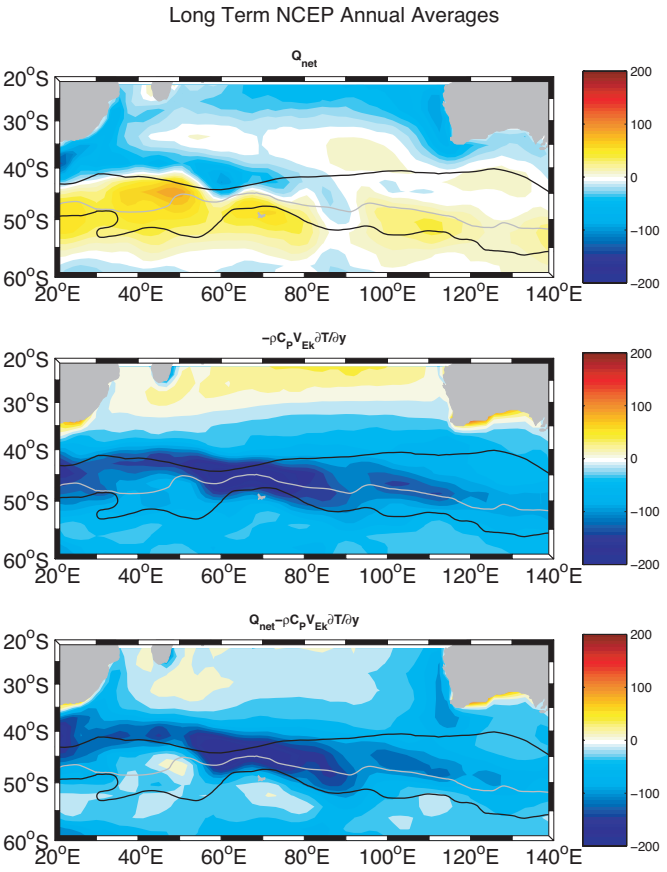

Fig. 1. Climatological average of net heat flux (upper), Ekman heat transport (middle), and their sum (lower), averaged over the entire NCEP record(1948-2005). Contours show the position of the STF, SAF (gray) and PF from Orsi et al. (1995).

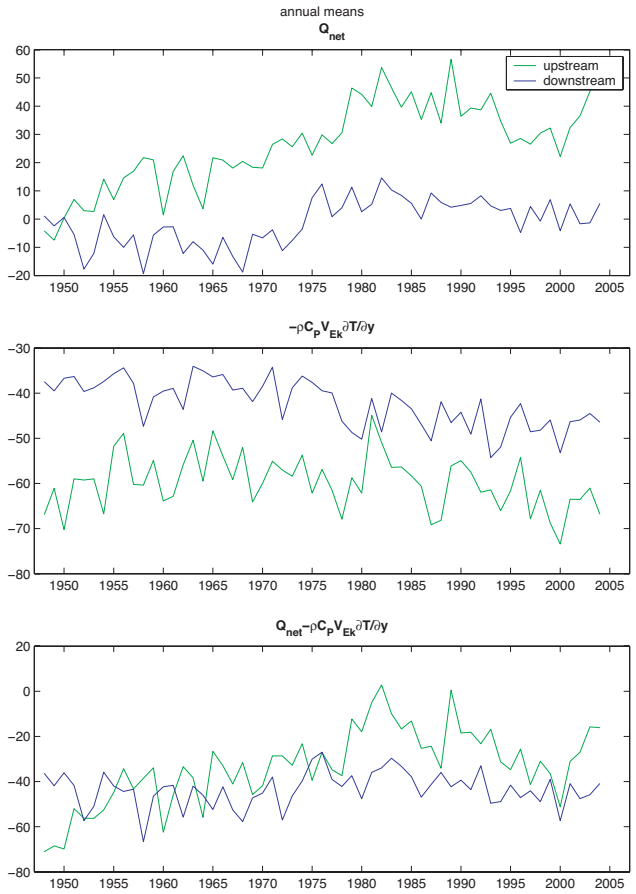

Fig 2. Time series of annual mean net heat flux (upper), Ekman heat transport (middle), and their sum (lower) from NCEP data over the period 1948-2005 in the southern Indian Ocean (regions between SAF and STF: upstream 20 - 70 E, downstream 70 - 140 E).

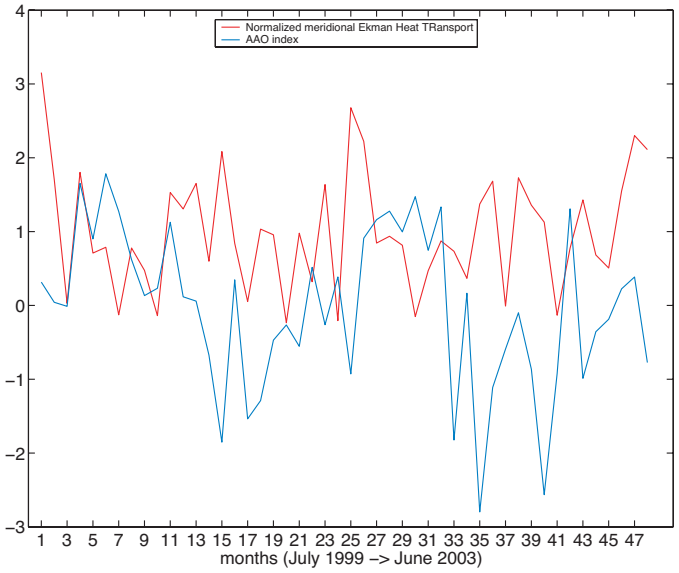

Fig. 3. Normalized meridional Ekman heat transport in the southern Indian Ocean between the Subantarctic Front and Subtropical Front for the period July 1999 to June 2003, and SAM or AAO index.

Feedbacks and uncertainties in a transient coupled simulation of the Weddell Sea

C.G. Menéndez[1] and S. Conil[2]
[1]Centro de Investigaciones del Mar y la Atmósfera/CONICET–UBA, Buenos Aires, Argentina
[2]Météo–France CNRM, Toulouse, France
Corresponding author: menendez@cima.fcen.uba.ar

We analyse the changes in the Weddell Sea region simulated by the Institut Pierre-Simon Laplace coupled climate circulation model (IPSL-CM2) in a transient global-warming scenario integration. Our aim is to describe possible mechanisms associated with abrupt swings in sea ice patterns and to discuss some related uncertainties, as a prelude to an improved understanding of the coupled climate system in this sector of the Antarctic periphery.

The IPSL-CM2 model is a state-of-the-art low-resolution coupled atmosphere-ocean-ice-carbon cycle model. After a 150 years spin up integration, two 241 years simulations (1860-2100) are performed without any flux corrections: a control simulation in which no CO_2 sources are considered and a climate change scenario simulation in which CO_2 emissions are prescribed following the IPCC SRES98 A2 scenario. The climatologies of both simulations can be examined at http://www.lmd.jussieu.fr/Climat/couplage/ipsl_ccm2/index.html. These simulations were extensively analysed to study the climate change and carbon cycle feedback (e.g. Dufresne et al, 2002). The control run displays no significant drift in the global mean surface temperature and atmospheric CO_2. The model is able to produce a stable multi-century control run as manifested by the time series of the large-scale heat and water balances. The drift of the zonal mean surface air temperature for the control simulation is about 0.5K at around 60°S since the year 100, and remains very small for the other latitudes of the Southern Hemisphere (SH).

The coarse resolution of the coupled model is potentially a serious shortcoming. Furthermore, there are processes that are not taken into account. As an example, the model neglects the wind-driven ice export because of the use of a thermodynamic sea ice model. Unfortunately, the precise impact of not using a dynamic sea ice model is difficult to estimate in the present framework. However, in a recent paper by Flato et al (2004) it was established that the errors in the ice climatology simulated by global models are not obviously related to the manner in which sea ice processes are represented. Overall, the area extent of SH sea ice and its seasonal variations are mostly well simulated by the IPSL-CM2 model. Sea ice extent is slightly overestimated in eastern Antarctica and underestimated in the western Weddell Sea (WWS) and in the Ross Sea. However, the simulated inner ice pack tends to be overestimated in the eastern Weddell Sea (EWS) and the Bellingshausen and Amundsen Seas.

The scenario simulation qualitatively captures some broad-scale patterns of observed changes in surface temperature around Antarctica (e.g. Vaughan et al., 2003), such as warming in the Antarctic Peninsula and WWS, cooling in the EWS and weaker, non-uniform changes in eastern Antarctica. A similar pattern also appears for the period 2000-2100. In particular, a strong warming of the WWS contrasts with a slight cooling in the EWS (anomalies with respect to the control run). In the following we will concentrate on the evolution of the Weddell Sea changes in the scenario simulation. Its eastern and western parts tend to exhibit contrasting behaviour during most of the simulation. This contrast has also been observed using satellite, reanalysed or observed data of the surface characteristics during the last decades (Venegas and Drinkwater, 2001; Parkinson, 2002).

Analysis of time series of different variables reveals that the climate of the Weddell Sea region exhibits extreme variability on interannual to interdecadal timescales. The large variability in both the control and transient simulations makes finding signals in the Antarctic Peninsula and Weddell Sea regions difficult. Figures 1 and 2 show the temporal evolution of the sea ice fraction and mixed layer depth averaged over the WWS and EWS. In both the EWS and WWS, major changes often occur abruptly rather than progressively. As an example, the event of the 2030s is clearly recognised by the abrupt and significant increase in sea ice concentration in the WWS. It is characterised by a period of vigorous ocean convection followed by strong ocean stratification, marking it as a major regional climate event.

The time evolution of surface air temperature (not shown) exhibits a generaly positive (negative) long-term trend in the WWS (EWS) throughout the simulation until the first part of the 21st century. Consistently, in the WWS a negative trend in sea ice fraction (figure 1) is manifested. In order to illustrate the possible feedbacks associated with a long-term oscillation in the WWS region, the 1980-2040 period is considered. During that interval, a positive long-term trend in surface temperature in 1980-2020 is followed by an abrupt negative trend in 2020-2040. During 1980-2020, progressively reduced ice concentration is associated with larger open water areas and a prevalent positive trend of the amount of heat released from the ocean to the atmosphere. Enhanced heat flux to the atmosphere implies destabilisation of the upper ocean mixed layer and increased overturning. This is a positive feedback in which warm deep water is brought to the surface, permitting more heat to be vented to the atmosphere. Consistently, the thermodynamic effect of the warm ocean waters tends to enhance ice melting as described in Gloersen and White (2001). It is likely that sea ice cover in the WWS is limited in its thickness and concentration by the introduction of warm and salty deep water into the winter mixed layer. On the other hand, the sea-to-air heat flux contributes to warming the atmospheric boundary layer over the region of thin ice concentration. In the WWS a negative precipitation trend and high evaporation rate during the first half of this period contribute to an increase in surface salinity, whereas the strong mixing and the ice melting have counteracting effects (i.e. contribute to the freshening). Small factors influencing the salinity budget can disturb it, causing large interannual variability in oceanic convection.

Lagged cross correlations (not shown) suggest that atmospheric forcing drives anomalous sea ice conditions in the WWS, while the sea ice anomalies in the EWS would be determined primarily by the water beneath. Our simulations highlight the possibility of large changes in oceanic convection associated with changes in the ocean and atmosphere coupling. In the control simulation most of the oceanic convection occurs in

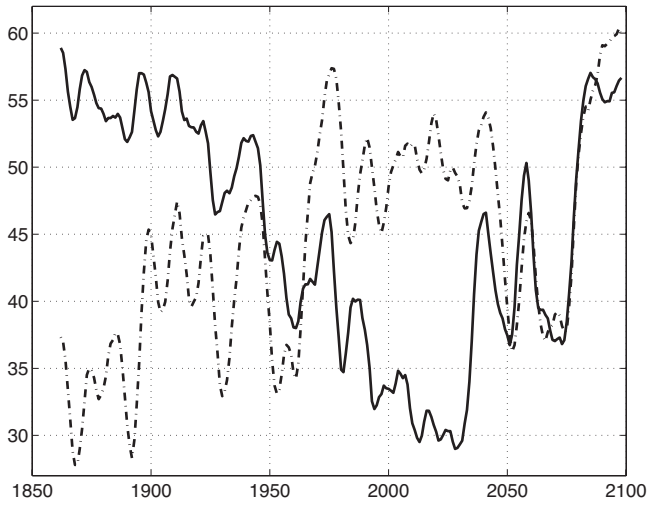

Figure 1: Time evolution of area-average sea ice fraction (%) for two regions: western Weddell Sea (WWS: 60°W/36°W 75°S/63°S, solid line) and eastern Weddell Sea (EWS: 28°W/4°W 66°S/56°S, dashed line). A 5 year running mean was applied.

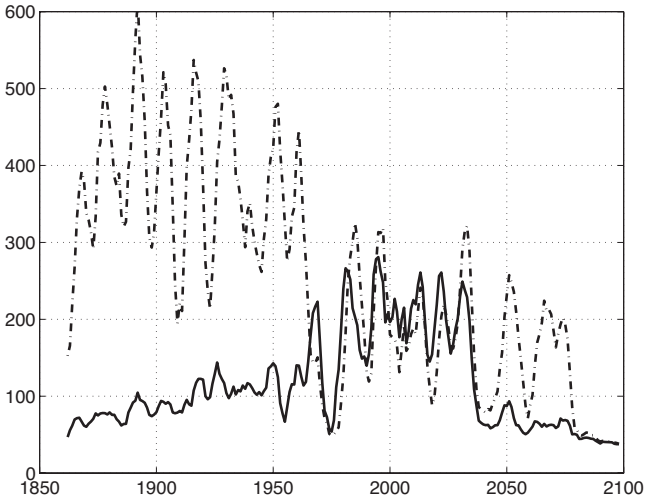

Figure 2: Identical to figure 1, but showing the mixed layer depth (unit: m).

the Ross Sea and in the EWS. In the scenario experiment, the response in the WWS is associated with a south-westward shift of the convective activity in the Weddell Sea. As convection is less active, the water in the EWS becomes more stratified. The increased stratification leads to a surface cooling and an extension of the sea ice promoting the slowing of the convection. During the second half of the 20th century, the convection becomes more efficient in the WWS, but a convection collapse occurrs in the 2030s in that region. We emphasise the importance of these abrupt swings in sea ice patterns because of their impact on the location, strength and depth penetration of the major sinking regions of the Southern Ocean.

The strong couplings and feedbacks among the atmosphere, ocean and sea ice allow the existence of long-term trends that can persist for periods of many decades. It is possible that a network of feedbacks maintains the thin layer of sea ice in a more-or-less stable configuration before the 2030s event. But this event stresses the possibility of quick changes in the coupled system. The precise timing of this event suggests that this might be the result of the atmospheric forcing. Unusually intense and

persistent southerly winds contribute to the large cooling in the WWS. Cold dry Antarctic winds blowing across the region of thin ice concentration can result in extremely large outward fluxes of sensible and latent heat and vigorous ice growth. Besides the atmospheric factor, the 2030s event highlights that the static stability between the mixed layer and deep water is quite weak and delicately balanced. It seems conceivable that, under simultaneous and favourable atmospheric and oceanic circumstances, the effects may be enhanced, leading to the generation of a large event.

The high variability in this region is related to the occurrence of intermittent convective events (Hirschi et al., 1999) and demands care in interpreting the results. The instability of the convection would be associated with changes of the convection pattern and mean climate drift in the Weddell Sea (Cai and Gordon, 1999). The development of erroneous convective ocean anomalies is a frequent occurrence in coupled model simulations. According to O'Farrell and Connolley (1998), the ocean noise caused by shifts in the regions of convection in the Weddell Sea and by convective events leads to localised spurious signals usually during the early part or the first decades of the control simulation. The time series of mixed layer depth for the control run (not shown) also exhibits large interdecadal variability but its long-term trend is much less pronounced than in the scenario simulation. In particular, we did not find any evidence of an abrupt change like the one discussed previously (a period of vigorous ocean convection abruptly followed by strong and stable ocean stratification).

The regional climate drift as well as the intermittent convection activity obscures the signal of climate change in the Weddell Sea. In particular, assessing the likelihood of future rapid regional changes remains uncertain. While the large-scale effects of the anthropogenic increase in greenhouse gases have likely participated in the regional response, the natural climate variations, as well as possible model shortcomings may also have contributed in a complex non-linear way. These concerns emphasise that the findings need to be viewed with caution, given known weaknesses in the simulations.

Acknowledgements:

We wish to thank J.L. Dufresne and H. Le Treut, from the Laboratoire de Météorologie Dynamique (France), for their support and useful discussions. This research was done in the framework of ECOS A04U02 and PIP/CONICET 5416.

References

Cai, W., and H. B. Gordon, 1999: Southern high-latitude ocean climate drift in a coupled model. *J. Climate,* 12, 132–146.

Flato, G. M. and participating CMIP modelling groups, 2004: Sea-ice and its response to CO2 forcing as simulated by gobal climate models. *Clim. Dyn*., 23, 229-241.

Dufresne, J.-L., P. Friedlingstein, M. Berthelot, L. Bopp, P. Ciais, L. Fairhead, H. LeTreut, and P. Monfray, 2002: Effects of climate change due to CO2 increase on land and ocean carbon uptake. *Geophys. Res. Lett*., 29, 10.1029.

Gloersen, P., and W.-B. White, 2001: Reestablishing the circumpolar wave in sea ice around Antarctica from one winter to the next. *J. Geophys. Res*., 106, 4391-4396.

Hirschi, J., J. Sander, T. F. Stocker, 1999: Intermittent convection, mixed boundary conditions and the stability of the thermohaline circulation. *Clim. Dyn*., 15, 277-291.

O'Farrell, S.P., and W.M. Connolley, 1998: Comparison of warming trends predicted over the next century around Antarctica from two coupled models. *Ann. Glacio*., 27, 576-582.

Parkinson, C.L., 2002: Trends in the length of the Southern Ocean sea-ice season, 2979-99. *Ann. Glacio*., 34, 435-440.

Vaughan, D., G. Marshall, W. Connolley, C. Parkinson, R. Mulvaney, D. Hodgson, J. King, C. Pudsey, and J. Turner, 2003: Recent rapid regional climate warming on the Antarctic Peninsula. *Climatic Change*, 60, 243-274.

Venegas, S.A., and M. Drinkwater, 2001: Sea ice, atmosphere and upper ocean variability in the Weddell Sea, Antarctica. *J. Geophys. Res*., 106, 16747-16766.

Southern Ocean Variability and Climate Change in HadCM3

S.Stark[1], C. Harris[1] and G. Richardson[2]
[1]Hadley Centre for Climate Prediction and Research, Met Office, Fitzroy Road, Exeter, Devon, EX1 3PB, UK
[2]School of Environmental Sciences, University of East Anglia, Norwich, UK
Corresponding author: "Stark, Sheila" <Sheila.Stark@metoffice.gov.uk>

The Southern Ocean is unique in being directly connected to all of the other ocean basins which allows the Antarctic Circumpolar Current (ACC) and other features of the region to impact on the global climate system. The Southern Ocean is also relatively data sparse which is one of the reasons that models are useful to understand processes and changes as well as predict what is likely to happen in the region in the future. The usefulness of models however is dependent on how well the region is simulated. We will look at the Southern Ocean simulation of the coupled climate model HadCM3 focusing on the simulation of Subantarctic Mode Water (SAMW) and Antarctic Intermediate Water (AAIW).

The ACC is the worlds largest current in terms of volume and transport and as with many other models (Stevens and Ivchenko, 1997) its transport is overestimated by HadCM3. The ACC had been observed most at Drake Passage with Whitworth and Peterson (1985) quoting a generally accepted mean transport of approximately 130Sv from bottom pressure measurements. In the HadCM3 control simulation (CTL), which has fixed preindustrial greenhouse gases, the transport at Drake Passage is 220 ± 7Sv, more than 50% larger than observed. Looking at the transport over 2000 years of the simulation reveals that a transport in excess of that observed is achieved very quickly and that the upward trend appears to reflect changes in the density structure. The meridional density gradient in HadCM3 across the Drake Passage latitudes is too strong when compared to the Levitus climatology (Levitus and Boyer, 1994). The wind stress and temperature fields in the region compare well with climatology but the model salinity gradient is much larger than observed (Figure 1), the model ocean being too salty at high latitudes and too fresh further north in the top 2500m.

To evaluate the water mass simulation in the model Southern Ocean the hydrography is compared with Levitus and the WOCE SR3 section south of Australia at 140°E. The SAMW pycnostad is evident in the Tasman Sea, but the model water

mass is both lighter and fresher than observed because of the initial drift of the model during spin up (Pardaens et al, 2003). The model also exhibits a strong salinity minimum representative of AAIW though as with SAMW it is both fresher and lighter than in observations. The simulation of the deeper water masses by HadCM3 however is less realistic. The Lower Circumpolar Deep Water (LCDW) that is evident in the Levitus climatology as a salinity maximum is not visible in the model salinity fields. LCDW is supplied by the export of North Atlantic Deep Water (NADW) from the Atlantic. In HadCM3 the NADW layer is too shallow and does not penetrate as far south which combined with the strong ACC erodes any deep water signal.

Antarctic Bottom Water (AABW) is formed in the ocean by small scale processes on the continental shelves, which are not resolved in HadCM3. Consequently any deep water is formed by open ocean convection rather than by cooling and brine rejection on the shelves. Results from a passive tracer experiment reveal that the dominant sinking areas in HadCM3 are in the Weddell and Ross Seas, Drake Passage and the Adelie coast which are similar regions to where AABW is thought to form in reality (Broecker et al., 1998). It is less clear however whether the model formation occurs in a physically realistic manner. For example a notable feature of the tracer distribution is the high concentration at depth in Drake Passage which is due to a numerical instability resulting from the narrowness of the passage. This convection at mid depths means Drake Passage is the primary formation site for AABW in HadCM3 and brings the model AABW production rate closer to that observed. Overall the lack of continental shelf processes leads to the model having a less than physically plausible representation of AABW.

Over the last 40 years observations throughout the Indo-Pacific have shown SAMW and AAIW to be cooling and freshening on isopycnals (Bindoff and McDougall, 2000; Wong et al, 1999). This freshening has been attributed to the warming or freshening of surface waters, however a cruise completed in 2002 at 32°S in the Indian Ocean shows SAMW getting saltier on isopycnals (Bryden et al., 2003). We make use of CTL and three HadCM3 forced ensembles, each of which is made up of four experiments started 100 years apart in CTL: NAT which is forced with historical records of solar irradiance and volcanic emissions, ANT with imposed changes in greenhouse gases, sulphur and ozone and ALL which has both. The first two members of the ANT ensemble which were continued to 2100 with IPCC SRES B2 scenario emissions (IPCC, 2001) are also considered.

During the 20th century both AAIW and SAMW are seen to freshen on isopycnals in experiments where the forcing included greenhouse gases (ANT and ALL). A return to more saline SAMW at 32°S in the Indian Ocean is not seen. At 32°S both NAT and CTL exhibit oscillating isopycnal salinity, however the variability in NAT is smaller than is observed. Salinity changes of the magnitude observed are seen in CTL and the model experiments suggest that the likely explanation of the observed changes is that they are due to internal variability. The B2 experiments show both SAMW and AAIW becoming fresher during the 21st century as greenhouse gases continue to increase (Figure 2). At the salinity minimum the isopycnal freshening can only be the result of changing freshwater input and HadCM3 does exhibit an increase in the balance of precipitation and evaporation at high southern latitudes during the 21st century (Figure 2). The continued isopycnal freshening of SAMW can be the result of either warming or freshening on pressure surfaces where the water mass outcrops. In HadCM3 the winter mixed

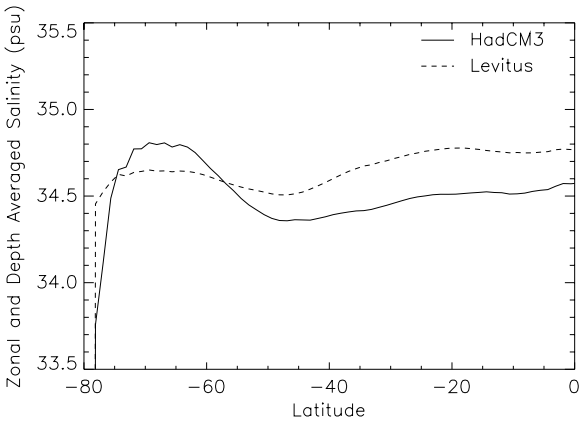

Figure 1. Zonally averaged salinity in the top 2500m for HadCM3 and the Levitus climatology.

layers where SAMW outcrops are seen to warm and freshen on z level surfaces. This is primarily as a result of an increased heat flux into the ocean (Figure 2) though there is also an increased Ekman advection of both heat and freshwater into the formation region. Isopycnal freshening of SAMW during the 21st century is consistent with heat content studies (e.g. Willis et al, 2004) which show there has been a strong, fairly linear warming trend in the Southern hemisphere centred at 40°S between 1993 and 2003. This trend combined with the results from the B2 experiments suggest that the reversal to more saline isopycnals is unlikely to persist.

To summarize we have shown that the Southern Ocean simulation of HadCM3 compares favorably with observations though the ACC is too strong and the simulation of AABW is not physically realistic. The model simulates both SAMW and AAIW well and our results suggest that the observed changes in SAMW properties are most likely due to internal variability. 21st century simulations indicate that both SAMW and AAIW will continue to freshen on isopycnals as greenhouse gas concentrations increase which highlights that continuing observations of these water masses, for example by ARGO floats, is necessary to allow a climate change signal to be detected.

Acknowledgements

This work was funded by the Department of Environment. Food and Rural Affairs under the Climate Prediction program (PECD 7/12/37).

References

Bindoff, N.L. and T.J. McDougall, 2000: Decadal Changes Along an Indian Ocean Section at 32°S and their Interpretation, *J. Phys. Oceanogr.*, 30, 1207-1222.

Broecker, W.S., S.L. Peacock, S. Walker, R. Weiss, E. Fahrbach, M. Schroeder, U. Mikolajewicz, C. Heinze, R. Key, T.-H. Peng and S. Rubin, 1998: How much deep water is formed in the Southern Ocean? *J. Geophys. Res.*, 103, 15,833-15,843.

Bryden, H.L., E. McDonagh and B.A. King, 2003: Changes in Ocean Water Mass Properties: Oscillations or Trends? *Science*, 300, 2086-2088.

IPCC Climate Change 2001: The Scientific Basis, Houghton et al. (Eds), Cambridge University Press, 2001.

Levitus, S. and T.P. Boyer, 1994: Temperature. Vol4, World Ocean Atlas 1994, NOAA Atlas NESDIS 4, 129pp.

Pardaens, A.K., H.T. Banks, J.M. Gregory and P.R. Rowntree, 2003: Freshwater transports in HadCM3, *Climate Dyn.*, 21, 177-195.

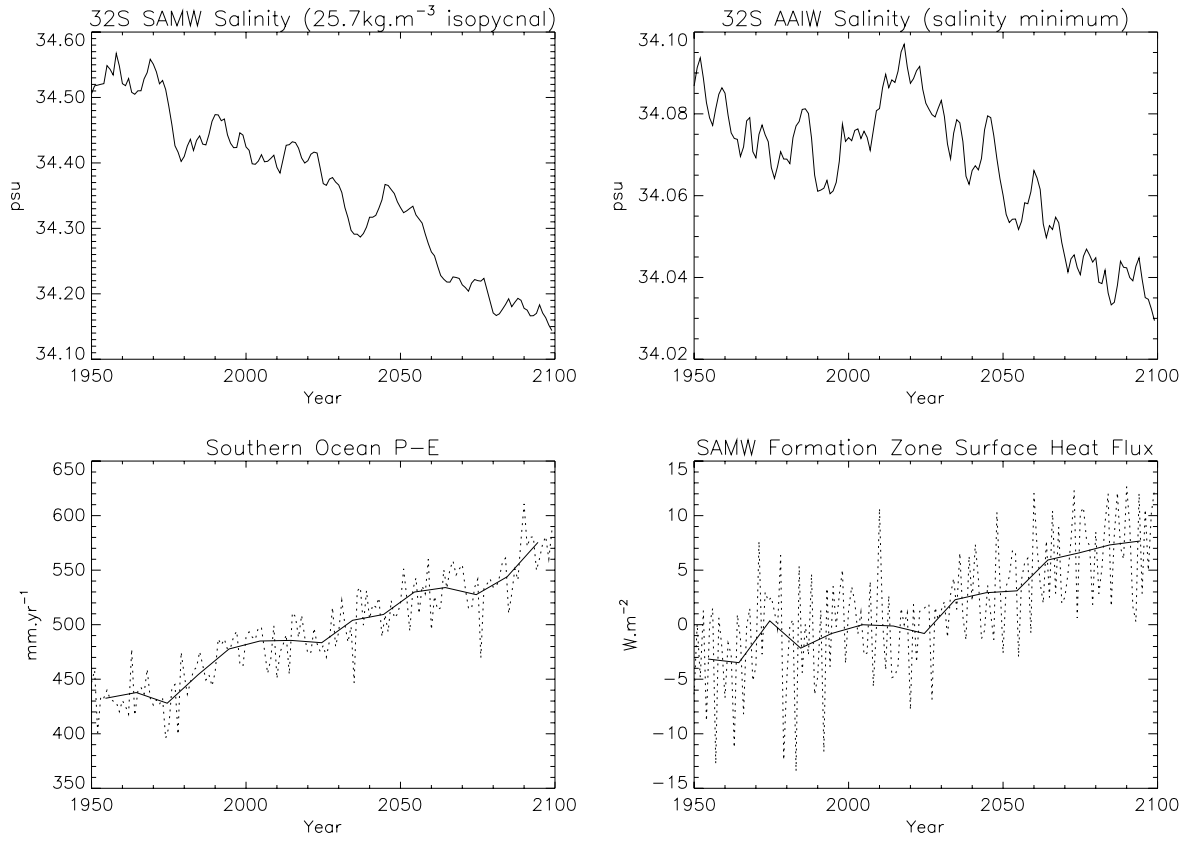

Figure 2. Timeseries of a) Isopycnal salinity at the core of the model SAMW at 32°S in the Indian Ocean b) AAIW salinity at 32°S, c) the balance of precipitation and evaporation between 55°S and 65°S and d) net surface heat flux where Indian Ocean SAMW ventilates in the 21st century under IPCC B2 scenario forcing. In the bottom two plots the annual data is shown by the dotted line with the decadal mean overlain.

Stevens, D.P., and V.O. Ivchenko, 1997: The zonal momentum balance in an eddy-resolving general-circulation model of the Southern Ocean, *Q.J.R. Meterolog. Soc.*, 123, 929-951.

Whitworth, T., III and R.G. Peterson, 1985: Volume Transport of the Antarctic Circumpolar Current from Bottom Pressure Measurements, *J. Phys. Oceanogr.*, 15, 810-816.

Willis, J.K., D. Roemmich and B. Cornuelle, 2004: Interannual variability in upper ocean heat content, temperature and thermosteric expansion on global scales, *J. Geophys. Res.*, 109, doi:10.1029/2003JC002260, 2004

Wong , A.P.S, N.L. Bindoff and J.A. Church, 1999: Large Scale Freshening of Intermediate Waters in the Pacific and Indian Oceans, *Nature*, 400, 440-443.

Circulation Anomalies Leading To Dry Periods In Buenos Aires

N.E. Ruiz and W.M. Vargas
Departamento de Ciencias de la Atmósfera y los Océanos, Facultad de Ciencias Exactas y Naturales, Universidad de Buenos Aires, Argentina
Corresponding author: "Nora E. Ruiz" <nora@at.fcen.uba.ar>

Abstract

The objectives of the present work are to explore the influence of mid-tropospheric circulation anomalies as factors in determining the local lack of precipitation for extended periods of one or two weeks in the Buenos Aires region, and to examine the circulation patterns leading to the initiation of a dry period. A couplet configuration with a WSW-ENE direction is evidenced through the climatological patterns associated with a dry week. The two phases of the height couplet are related with either a dry week period or with a week with at least one rainy day, respectively. When considering a somewhat more persistent dry period of two weeks, say initial drought circulation conditions, flow anomaly patterns become considerably significant showing particular large- and synoptic-scale characteristics associated with initial drought at Buenos Aires. A striking "triplet" pattern feature is observed, with the high or positive anomaly at 38°S to the west of the continent over the Pacific Ocean, and two strongly significant low anomalies. One of them is found in the south-western Atlantic region, including the Drake Passage, and the other conspicuous low anomaly is found at tropical latitudes west of 110°W. Anomalous cyclonic activity appears to be an important feature of the southern hemisphere circulation at subpolar latitudes at about 60°S in the south of the continent in association with initial drought at the humid pampas of Argentina. The presence of this triplet pattern may be considered as one of the responsible mechanisms of intense downward vertical motion and lack of precipitation at the Buenos Aires region over a fortnightly period.

Introduction

Dry periods in the humid and semi humid areas of Argentina undergo considerable non periodic variations, which may have

important impacts on the agriculture and farming of the country. Such precipitation variations stem from complex meteorological and climatological conditions. In previous studies, the influence of day to day weather events has been examined through the analysis of the relationships between variables representing mid tropospheric circulation over the southern part of South America and daily local precipitation (Ruiz and Vargas 1998, Ruiz 2004). One purpose of the present work is to explore the influence of circulation anomalies as factors in determining the lack of local precipitation for extended periods of one to two weeks for Buenos Aires, and to establish the circulation patterns leading to the initiation of a dry period in the region.

Data and methodology used

Daily objective analyses of 500 hPa height fields at 1200 UTC provided by the ECMWF covering a period of three years, 1983-1985, for the region from 120°W to 20°W and 15°S to 70°S, are employed. The colder months, May to October, are used here (552 days).

Daily precipitation data are those measured at three stations in the area of Buenos Aires: Villa Ortúzar, Ezeiza and Aeroparque. Precipitation is assumed to be a binary variable (occurrence or non-occurrence of a given event). In daily terms, the occurrence of a "dry day" event occurs when daily precipitation is on average less than 0.1 mm. In terms of a week, the occurrence of the event is defined depending on how many dry days there exist in the week: one or more dry days (case 1), two or more dry days (case 2), and so on up to seven dry days (case 7), i. e. a whole dry week. A similar analysis is made for the event of two weeks without precipitation.

To examine the circulation patterns associated with a completely dry week, biserial correlation fields as a specification technique of synoptic climatology (Yarnal, 1993) are constructed taking into account the occurrence or nonoccurrence of a given event (once the weekly event is specified, every day in that week is assigned the same binary variable). In this way, 500 mb geopotential height anomalies are examined in relation to the different dry events in a week, or a fortnight. Biserial correlation coefficients with an absolute value higher than 0.15 are statistically significant to the 99% level.

Results

The biserial correlation field associated with a completely dry week in Buenos Aires is shown in Fig. 1. From the synoptic-climatological point of view, positive anomalies in 500 hPa geopotential heights centered at about 38°S, 75°W over the Pacific coast covering the western side of Argentina and adjacent Pacific Ocean, and on the other side, low geopotential anomalies about 28°S, 45°W over the Atlantic Ocean and the south-eastern Brazilian coast are associated with a week without any precipitation at Buenos Aires, Argentina. A couplet pattern can clearly be seen in the WSW–ENE direction. The two phases of this height couplet are connected either with a whole dry week, or with a period of at least one day with precipitation in the week, respectively. A positive dipole or "high phase" of the dipole (500 hPa geopotential height higher than normal over the western continent and below normal over the western subtropical Atlantic Ocean) is associated with dry conditions over Buenos Aires, Argentina. A negative dipole or "low phase" of the dipole (opposite conditions) is related to wetter weekly conditions. During the positive phase of the dipole, mid-tropospheric anticyclonic circulation occurs to the west of Buenos Aires while cyclonic circulation anomalies take place to the east, generating southern south-eastern anomalous flow (not necessarily south-western anomalous wind, as generally supposed) in relation to weekly dry conditions over

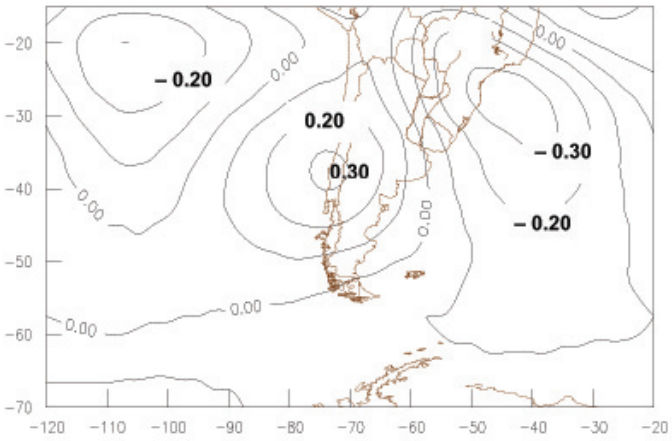

Fig. 1. Biserial correlation field between 500 hPa geopotential heights and a whole week without precipitation in Buenos Aires, for the cold semester (May-October). Correlation coefficient interval: 0.10.

Buenos Aires. It may also be understood as a weakening in the atmospheric zonal circulation at about 40°S in relation to this local dry event. It is worth noting that the above normal geopotential anomaly resulting in dry conditions over Buenos Aires is located more than 1300 km to the west. Under these conditions the mid-latitude circulation is modified and descending motion might be expected during the next seven days. Moreover, no height anomaly (zero correlation line) crosses over Buenos Aires (no particular anomaly is locally evidenced). The anomalously low heights over southeastern Brazil and the adjacent Atlantic coast may also have some influence, an area referred to as the South America convergence zone (Satyamurty et al 1998), with perhaps anomalous convection, upper-level outflow, and enhanced subsiding motion southwestward.

When considering a more persistent dry period of two weeks, say initial drought circulation conditions, flow anomaly patterns become considerably significant showing particular large- and synoptic-scale characteristics associated with initial drought at Buenos Aires (Fig. 2). A striking "triplet" pattern can be seen, with the high or positive anomaly at 38°S (the same latitude as for one dry week conditions, but shifted westward onto the Pacific Ocean) and two strongly significant low anomalies over both oceans. The anticyclonic anomaly is centered at the same latitude as the case for one dry week conditions, but shifted westward onto the Pacific Ocean. As a consequence, the southerly anomaly flux becomes southwesterly and more pronounced. One of the negative anomalies may be found at the southwestern Atlantic region including the Drake Passage, and the other conspicuous low anomaly at tropical latitudes west of 110°W. This "triplet" anomaly pattern associated with a two-week dry period clearly has a NW–SE propagation, showing a somewhat different progression and reinforcing negative anomalies with respect to those of a one-week period. Anomalous cyclonic activity appears to be an important feature of the southern hemisphere circulation at subpolar latitudes at about 60°S in the south of the continent in association with initial drought at the humid pampas of Argentina. Additionally, and in agreement with the results of Vincent et al (1997), anomalous cyclonic activity at tropical latitudes, perhaps in connection with anomalously strong convection over the Pacific Ocean at about 115°W seems to greatly influence the circulation pattern with upper tropospheric troughing in tropical Pacific giving way to ridging in the subtropical eastern Pacific and again anomalously low heights in southwestern Atlantic, showing a distinctive atmospheric Rossby wave pattern. This configuration seems

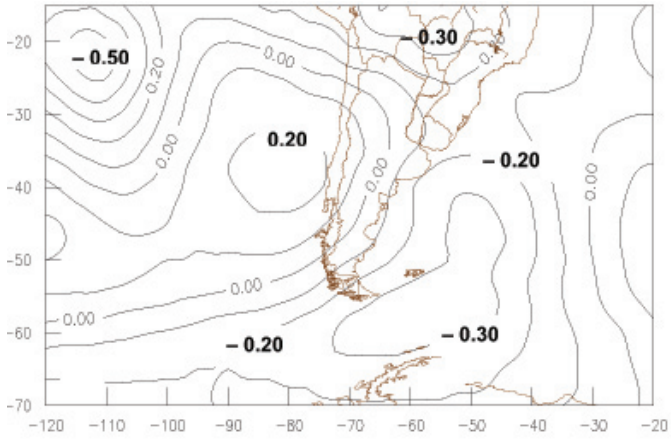

Fig.2. Biserial correlation field between 500 hPa geopotential heights and two dry weeks in Buenos Aires, for the cold semester.

to be propitiatory of downward vertical motion at the Buenos Aires region over a fortnight period. The persistence of these flow patterns would lead to longer dry periods in the eastern part of southern South America.

Acknowledgment.

This work is partially supported by the Universidad de Buenos Aires under grant X070 and X234.

References

Ruiz, N. E., W. M. Vargas, 1998: 500 hPa Vorticity Analyses over Argentina: Their Climatology and Capacity to Distinguish Synoptic-scale Precipitation. *Theor. Appl. Climatol.*, 60, 77-92.

Ruiz, N. E., 2004: Vorticity patterns for rainy and dry episodes in Argentina. *Meteorol. Atmos. Phys.*, 86, 45-62.

Satyamurty, P., C. A. Nobre, and P. L. Silva Dias, 1998: South America. *Meteorology of the Southern Hemisphere, Meteor. Monogr.* Vol. 27, No 49, D. J. Karoly and D. G. Dayton, Eds., Amer. Meteor. Soc., 410 pp.

Vincent, D. G., Ko, K. -C., and Schrage, J. M., 1997: Subtropical jet streaks over the South Pacific. *Mon. Wea. Rev.*, 125, 438-447.

Yarnal, B., 1993: S*ynoptic Climatology in Environmental Analysis*. Bellhaven Press, 195 pp.

Float Observations within the Weddell Sea

O. Klatt, O. Boebel, I. Núñez-Riboni, and E. Fahrbach
Alfred Wegener Institute for Polar and Marine Research
Postfach 120161, D – 27515 Bremerhaven, Germany
Corresponding author: oklatt@awi-bremerhaven.de

Introduction

The ARGO-project intends to continuously monitor temperature and salinity of the upper 2000 m of the global ocean. The project aims for an array of approximately 3000 autonomous, profiling floats on a 3° x 3° grid by 2006. This array will provide basin-wide hydrographic data in near real-time, forming the backbone of operational oceanography and climate research.

While the float coverage at low- and mid-latitudes is already moderate to good, float deployments at higher latitudes remained marginal until 2005, particularly in areas of at least seasonal ice-cover (Figure 1). This is due to the imminent danger of damage or loss of floats by collision with ice floes, as demonstrated by some early ARGO type floats deployed by the AWI in the eastern Weddell Sea. To enable ARGO type floats to operate within ice-covered regions a significant improvement in the floats' ice-resilience appeared mandatory.

To meet these demands, we adopted a three step process. The first and most important step was the implementation of the Ice Sensing Algorithm (ISA). This algorithm aborts the ascent when the likelihood of ice is high - rather than to abort

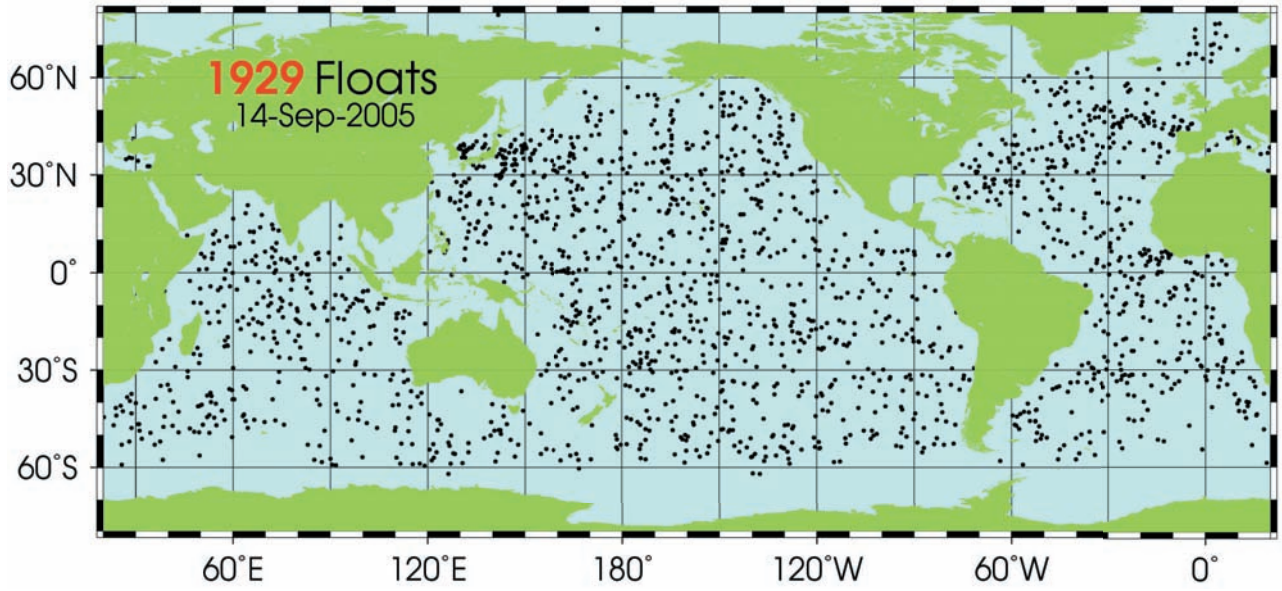

Figure 1: Current positions of the floats that surfaced within 30 days prior to 14 September 2005 [graph updated daily at: http://www-hrx.ucsd.edu/www-argo/statusbig.gif.

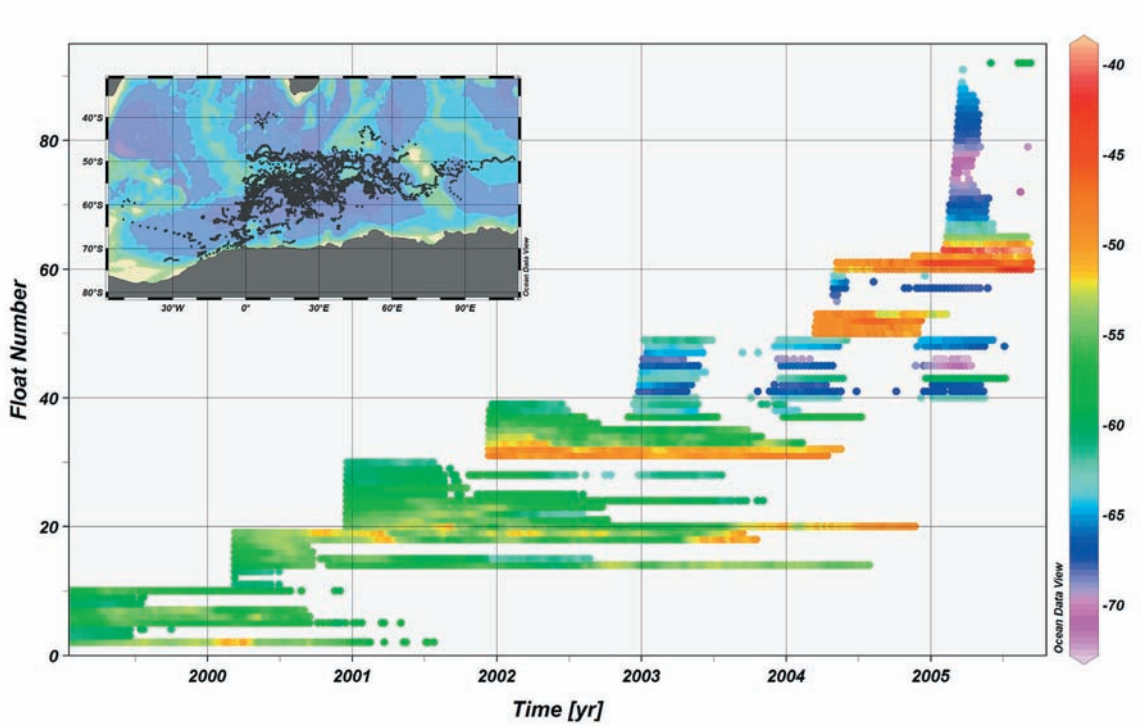

Figure 2: Overview of AWI-launched float surface events. Each dot represents a float surfacing and transmitting data. The colour of the dots represents the latitude of the respective profile. The inset shows the locations of the float profiles in the Weddell Gyre between 1999 and 2005.

(only) in the actual presence of ice. ISA was first proposed by AWI to the Webb Research Corporation in 2001 on the basis of temperature profiles from the few early Weddell Sea floats that happened to outlast the austral winter. The algorithm was implemented by Webb Research Corporation, USA, requiring only minor changes to the float's firmware and no modifications to its hardware. ISA is now available with the current line of APEX float.

The ISA algorithm uses two "OR" matched conditions to decide whether to abort an ascent. Aborts are triggerd if: a.) the median temperatures between 50 and 20 m depth lower is than 1.79°C, OR b) the surface pressure is not reached after twice the time required for ascent at 0.08 m/s (the expected vertical velocity of the float during the ascent) AND if the actual temperature is less than -1.79°C.

Since 2002, all AWI deployed floats were equipped with the Ice Sensing Algorithm. The successful timely abortion of the majority of ascents when in ice-infested water by ISA equipped floats is a likely reason that 13 of 18 of these instruments ISA equipped floats resurfaced after the first winter season, while 12 of these 13 resurfaced after the second winter season as well (Figure 2). Thus, the overall probability of ISA equipped floats to endure the winter season is about 80% (25 of 31 instruments).

Although ISA equipped APEX floats persevered in extended ice coved areas, they were not able to surface and transmit their data during this period and dumped the respective profile data. In the case of the southern Weddell Sea, this loss is likely to involve more than 50% of all profiles. Thus, step two in the development of an ice-resilient float was the implementation of an interim storage and later transmission of the data of the aborted profiles (iStore). This feature is currently being tested with nine NEMO (Navigating European Marine Observer) floats manufactured by Optimare, Germany.

When surface attempts are aborted, the positions of the stored profiles can currently only be estimated by interpolation between known surface positions. This might not pose a problem if one or two profiles are missing, but if the float stays beneath the sea ice for more than half a year, a more accurate way of fixing the float's position is necessary. Therefore, step three towards the ice-resilient ARGO floats was the implementation of RAFOS sensors to determine the subsurface profile position. RAFOS receivers are now available with both APEX and NEMO floats. For the Weddell Sea, sound coverage for the RAFOS navigation system is provided by 3 sound sources installed since 2003 (2 refurbished in 2005) and 3 in 2005. Sound coverage varies according to season, location and sound source manufacturer, though a range of 500 km can be safely assumed for planning purposes; for details see Klatt et al. (in prep.)

All three components (ISA, iStore and RAFOS) have been tested successfully (see Klatt et al. in prep) and are commercially available for the NEMO type floats. Further developments shall make use of high-speed acoustic modem connections between floats and moorings to transmit data in near real-time even when under the ice.

Methods And Observations

The mean subsurface velocities of the floats were calculated by taking the first surface position after the float's ascent and the last surface position before its descent. These velocities were interpolated to a regular grid by objective mapping (Bretherton et al., 1976; Hiller and Käse, 1983). The covariance function used in the objective mapping procedure was assumed Gaussian, with a covariance length of 4° and a variance of the climatological field of 3 cm s^{-1}, as attempted successfully in a similar study by Núñez-Riboni et al. (2005). The floats' parking temperatures (at about 750 m depth) were objectively mapped using the same covariance function. Interpolated data outside an area delimited by a Delaunay triangulation were neglected. For the velocity map, only data within triangles with their three sides shorter than the correlation length 4° were taken into account. For the temperature map the corresponding length was 6°. Both fields show the same structure (Figure 3), emphasizing the advective component of the heat transport.

At about 30°E, both temperature and flow fields show clearly the southward spreading of waters influenced by the ACC, resulting in an intrusion of warm water masses with temperatures of about 1°C into Antarctic waters. From about 60°S southward, these waters spread to the west as part of the southern branch of the Weddell Gyre. Their subsequent transformation into deep and bottom water feeds the global thermohaline circulation.

Additional southward float displacements are just about visible to the east of Conrad Rise at about 50°E. Possibly, warmer waters from the north are entrained here into the Weddell Gyre as well, which would be consistent with Park and Gambéroni (1995), who place the boundary of the Weddell Gyre as far east as 60°E, near the Kerguelen Plateau. In conjunction with the recirculation of the southern branch of the Weddell Gyre in the vicinity of the Greenwich Meridian, this observation supports the double cell structure of the Weddell Gyre as suggested by Mosby, (1934), Bagriantsev et al. (1989) and Beckmann et al. (1999).

References

Bagriantsev, N.V., A.L. Gordon, and B.A. Huber, 1989: Weddell Gyre: Temperature maximum stratum. *Journal of Geophysical Research,* 94: 8331-8334.

Beckmann, A., H.H. Hellmer, and R. Timmermann, 1999: A numerical model of the Weddell Sea: Large-scale circulation and water mass distribution. *Journal of Geophysical Research*, 104: 23375-23391.

Bretherton, F. P., R.E. Davis, C.B. Fandry, 1976: A technique for objective analysis and design of oceanographic experiments applied to MODE-73. *Deep-Sea Res*. 23 559-582.

Hiller, W., R.H. Käse, 1983: Objective Analysis of Hydrographic Data Sets from Mesoscale Surveys. Berichte aus dem Institut für Meereskunde an der Christian-Albrechts-Universität Kiel 116, 78 pp.

Klatt, O., O. Boebel, and E. Fahrbach, in preparation: A profiling float's sense of ice, to be submitted to Journal of Atmospheric and Oceanic Technology.

Mosby, H.; 1934: The water of the Atlantic Ocean. Scientific results of the Norwegian Antarctic Expedition 1927 – 1928, Vol. 11, 131pp., Oslo, Norway

Núñez-Riboni, I., O. Boebel, M. Ollitrault, Y. You, P. Richardson, R. Davis., 2005: Lagrangian circulation of Antarctic Intermediate Water in the subtropical South Atlantic. *Deep-Sea Research* II, 52, 545-564.

Park, Y.-H., Charriaud, E. and Craneguy, P., 2001: Fronts, transport, and Weddell Gyre at 30°E between Africa and Antarctica. *Journal of Geophysical Research,* 102(C2): 2857-2879.

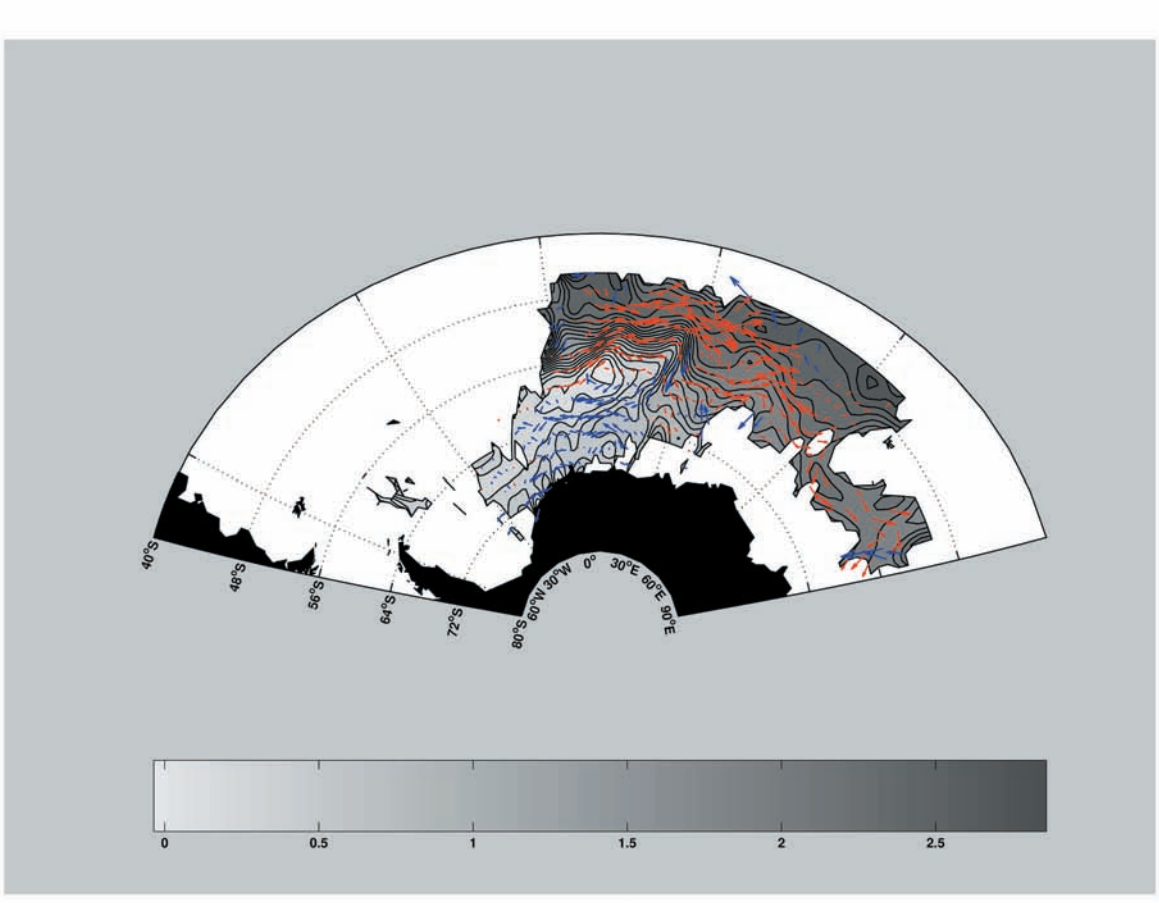

Figure 3: Temperature (grey shading) and velocity field (coloured vectors) at 750m depth in the Weddell Gyre. Blue (red) arrows represent currents with westward (eastward) zonal component.

Evaluation of the Weddell Sea Time Mean Circulation and Thermohaline Structure using the Ocean Component of the NCAR CCSM3–Coupled Climate Model: Preliminary Results

J. Pereira[1], I. Wainer[1] and M. M. Mata[2]
[1]Instituto Oceanográfico da Universidade de São Paulo, Brazil
[2]Fundação Universidade Federal de Rio Grande, Brazil
Corresponding author: janini@usp.br

Abstract

The Weddell Sea time-mean circulation and thermohaline structure along a transect between the Antarctic Peninsula edge and the Antarctic continent is investigated with the ocean component of the NCAR-CCSM3 coupled climate model (POP3). The model was forced with NCEP winds and corrected sub-ice fluxes. Preliminary results show for the integrated barotropic transport the double-core structure of the Weddell Gyre, but with a much stronger annual mean transport with respect to observations. The annual mean temperature profile along the transect shows a subsurface maximum of 1.1°C at ~800m. Bottom temperature values are warmer than expected (-0.3°C) due to insufficient model resolution to correctly resolve the bottom boundary layer transport of cold water from the continental shelves along the Antarctic Peninsula. The salinity field indicates a down slope transport on the northwestern side of the transect. Relatively fresh waters with salinities less than 34.67 reach down to 3000m.

1. Introduction

The Weddell Sea is considered an important source region for Antarctic Bottom Water (AABW) and thus one of the key regions contributing to the global thermohaline circulation of the world ocean (Mantyla and Reid 1983, Orsi et al. 1999, Hellmer et al. 2005). The characteristics of exported water masses are the result of complex interactions between surface forcing significantly modified by sea ice process, ocean dynamics at the continental shelf break and slope (Muench and Gordon 1995) and sub-ice shelf water mass transformations (Grosfeld et al. 1997).

Beckmann et al. (1999) performed the initial investigations with numerical ocean models, on the Weddell sector of the Southern Ocean. They used the Bremerhaven Regional Ice Ocean Simulations (BRIOS) a stand-alone ocean model, to represent many aspects of the Weddell Sea mean circulation and water mass distributions. Further modeling studies were carried out by Timmermann et al. (2002a,b), Schodlok et al. (2002), and Timmermann and Beckmann (2004). Schodlok et al. (2002) used a modified version of the primitive equation BRIOS, which had enhanced resolution near the sea surface and sea floor to investigate the water mass export from the Weddell Sea. Their results estimate the export rates of the Weddell Sea Deep Water through gaps in the South Scotia Ridge to be 6.4 Sv. In addition, Timmermann et al. (2002a,b) and Timmermann and Beckmann (2004) used the coupled ice-ocean model, BRIOS-2 (derived from BRIOS), based on a hydrostatic regional ocean circulation model and a dynamic-thermodynamic sea ice-model to investigate ice-ocean dynamics of the Weddell Sea.

In this paper, the Weddell Sea structure is investigated with the ocean only component of the NCAR-CCSM3 coupled climate model. The model description is summarized in Section 2. Section 3 contains the preliminary results and discussion. Concluding remarks are presented in Section 4.

2. Model Description

The ocean component of the NCAR-CCSM3 coupled climate model is based upon the POP Version 1.4.3, which was developed at Los Alamos National Laboratory. Gent et al. (2005) provide a detailed description of POP3. The horizontal grid has 320 (zonal) x 384 (meridional) grid points, with uniform (variable) zonal (meridional) resolution. In the southern hemisphere, the meridional resolution is 0.27° at the equator, gradually increasing to 0.54° at 33°S, and is constant towards higher latitudes. There are 40 levels in the vertical, whose thickness increases from 10 m near the surface to 250 m in the deep ocean. The minimum and maximum depths are 30m and 5.5km. The horizontal viscosity is an anisotropic Lapalcian operator (Smith and McWilliams 2003), which uses different coefficients in the east-west and north-south directions. The vertical mixing scheme is the K-profile parameterization (KPP) scheme of Large et al. (1994). Mesoscale eddies are parameterized following Gent and McWilliams (1990). The POP3 integration used here was forced by observed atmospheric fields from 1958-2000 with correct under ice fluxes, that are documented in Large and Yeager (2004). Further details of the CCSM3 ocean component can also be found in Smith and Gent (2004) and Danabasoglu et al. (2005).

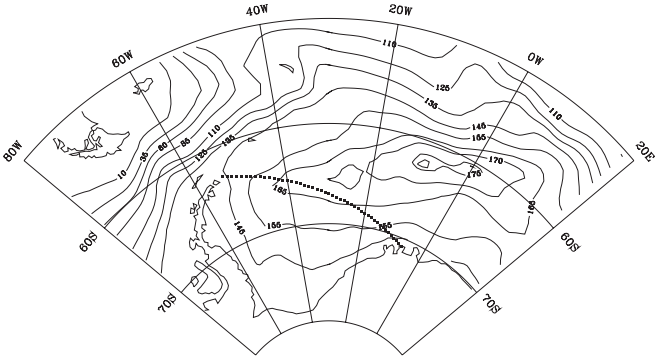

Figure 1 - Annual mean of the integrated barotropic transport from POP3. Contours intervals are from 15-125 (25), 125-165 (10), 165-175 (5) and 175-180 (1) in Sv. The dotted line marks the chosen transect.

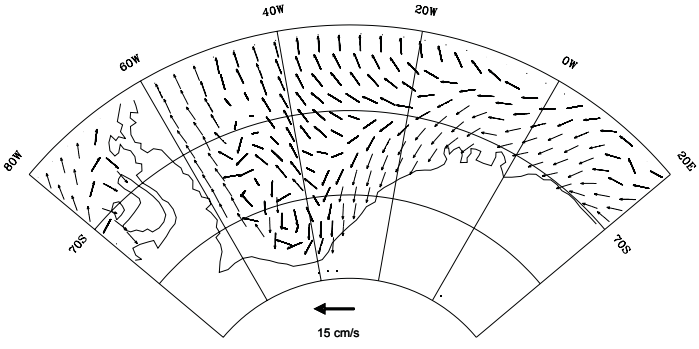

Figure 2 - Coastal-current field at the surface. Velocity unit is cm/s.

3. Results And Discussions

Figure 1 shows for the integrated barotropic transport a double-core structure of the Weddell Gyre, similar to that shown by Beckmann et al. (1999), Timmermann et al. (2002a) and Timmermann and Beckmann (2004), but with a much stronger annual mean transport, about 175 Sv. This is 3-5 times the expected magnitude of the Weddell Gyre transport (Fahrbach et al. 1994), and is most prominent in austral spring. The closed gyre circulation is well captured in the current field analysis (not shown) in the subsurface (500-1000m). The closed circulation associated with the Gyre is not evident at the surface because of the dominant influence of the large scale wind field. The surface coastal-current, with average velocities up to 3cms$^{-1,}$ is shown in figure 2.

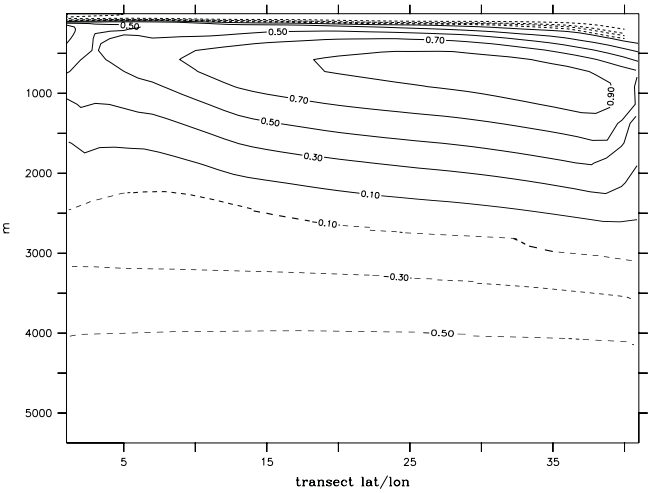

Figure 3 - Simulated annual mean potencial temperature (°C) for the transect. Intervals are 0.1°C

The annual mean temperature profile along the transect shows a subsurface maximum of 1.1°C at ~800m (Figure 3). Bottom temperature values are 0.2°C warmer than expected (Fahrbach et al. 2004). The same analysis using the SODA (Simple Ocean Data Assimilation) data set, for the same transect region, show at the east side temperature values of 0.3–0.4°C at ~1500m. At both sides of the section there is a downward slope of the surface isotherms towards the coast, due to onshore Ekman transport (Fahrbach et al. 1994).

In Figure 4, the salinity field suggests a down slope transport on the peninsula side of the transect. Relatively fresh waters with salinities <34.67 reach down to 3000m, suggesting the model is reproducing reasonably the deep ocean convection associated with the formation of Deep and Bottom water masses in the Weddell Sea.

4. Conclusions

The simulated annual mean vertically integrated transport shows a double-core structure of the Weddell Gyre, similar to that found by previous modeling studies (e.g. Beckmann et al. (1999), Timmermann et al. (2002a) and Timmermann and Beckmann (2004)). The double-core structure simulated for POP3 is displaced 5° to the west compared to Beckmann et al. (1999). Quantitatively, the simulated Weddell Gyre transport is overestimated compared with the calculations by Fahrbach et al. (1994) of 30Sv±10Sv and by Schroder and Fahrbach (1999) of 60Sv±10Sv.

At the surface the model current field distribution shows no recirculation in the northeastern part of the Weddell Sea as observed by Kottmeier and Sellmann (1996) and Beckmann et al. (1999). Below the surface (500-1000m) there is a single core structure with maximum values of 5cms^{-1}.

The simulated westward surface flow at the southern edge of the Weddell Gyre has peak average velocities of up to 3cms^{-1} within the coastal current. This time-mean velocity is close to the Fahrbach et al. (1994) measurements. At this resolution coastal current instabilities can not be resolved. However, the narrowness of the front is well represented and leads us to conclude that this ocean component (POP3) is adequate to simulate the general features of the Weddell Sea. The results described above are just a first step in the investigation of the influence of coupled air-sea-ice interactions in the Weddell Sea.

Acknowledgements.

The authors thank Gabriel Clauzet for his invaluable contribution and helpful discussions. The authors also wish to thank W. Large from NCAR for making the model output available. This research is supported by FAPESP nº 03/03054-2; CNP 300223/1993-5 and MMA.

References

Beckmann, A.; H.H. Hellmer and R. Timmermann, 1999: A Numerical model of the Weddell Sea: Large-scale circulation and water mass distribution. *J. Geophys. Res.*, 204(C10): 23375-23391.

Danabasoglu, G.; W.G. Large; J.J. Tribbia; B.P. Briegled and J.C. McWilliams, 2005: Diurnal ocean-atmosphere coupling. Submitted to *J Climate*.

Fahrbach, E.; G. Rohard; M. Schroder and V. Strass, 1994: Transport and structure of the Weddell Gyre. *Ann. Geophys.*, 12(9): 840-855.

Fahrbach, E.; M. Hoppema; G. Rohard; M. Schroder and A. Wisotzki, 2004: Decadal-scale variations of the water

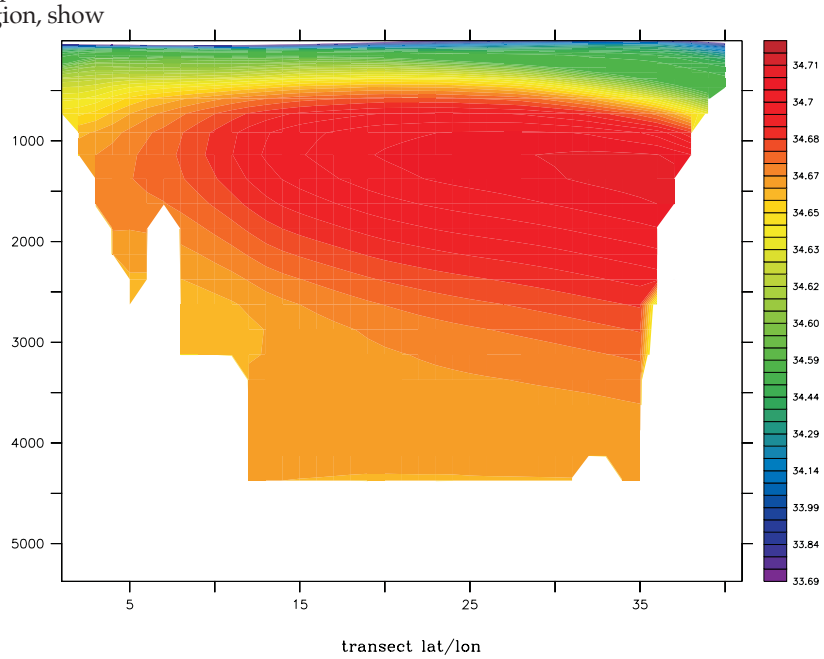

Figure 4 - Simulated annual mean salinity. Intervals are 0.005.

mass properties in the deep Weddell Sea. *Oc. Dynam.*, 54: 77-91.

Gent, P.R. and J.C. McWilliams, 1990: Isopycnal mixing in ocean circulation models. *J. Phys. Oceanogr.*, 20: 150-155.

Gent, P.R.; F.O. Bryan; G. Danabasoglu; K. Lindsay; D. Tsumune; M.W. Hecht and S.C. Doney, 2005: Ocean Chlorofluorocarbon and Heat Uptake During the 20th Century in the CCSM3. Submitted to *J Climate*.

Grosfeld, K.; R. Gerdes and J. Determann,1997: Thermohaline circulation and interaction between ice shelf cavities and the adjacent open ocean. *J. Geophys. Res.*, 102(C15): 15595-15610.

Hellmer, H.H.; M.P. Schodlok; M. Wenzel and J.G. Schroter, 2005: On the Influence of adequate Weddell Sea characteristics in a large-scale global ocean circulation model. *Ocean Dynam.*, 01(1900)

Kottmeier, C. and L. Sellmann, 1996: Atmospheric and oceanic forcing of Weddell Sea ice montion. *J. Geophys. Res.*, 101: 20809-20824 .

Large, W.G.; J.C. McWilliams and S.C. Doney, 1994: Oceanic vertical mixing: A review and a model with a nonlocal boundary layer parametrization. *Rev. Geophys.*, 32: 363-403.

Large, W.G. and S.G. Yeager, 2004: Diurnal to decadal global forcing for ocean and sea-ice models: The data sets and flux climatologies. NCAR Technical Note, 460.

Mantyla, A.W. and J.L. Reid, 1983: Abyssal characteristics of the World Ocean Waters. *Deep Sea Res.*-Part A., 30(8): 805-833.

Muench, R.D. and A.L. Gordon, 1995: Circulation and transport of water along the western Weddell Sea margin. *J. Geophys. Res.*, 100(C9): 18503-8515

Orsi, A.H.; G.C. Johnson and J.L. Bullister, 1999: Circulation, mixing and production of Antarctic Bottom Water. *Prog. Oceanogr.*, 43: 55-109.

Schodlok, M.P.; H.H. Hellmer and A. Beckmann, 2002: On the transport, variability and origin of dense water masses crossing the South Scotia Ridge. *Deep Sea Res.*, 49: 4807-4825

Schroder, M. and E. Fahrbach, 1999: On the structure and the transport of the eastern Weddell Gyre. *Deep Sea Res.*-Part A., 46: 501-527.

Smith, R.D. and J.C. McWilliams, 2003: Anisotropic horizontal viscosity for ocean models. *Oc. Model*, 5: 129-156.

Smith, R.D. and P.R. Gent, 2004: Reference manual for the Parallel Ocean Program (POP): Ocean component of the Community Climate System Model (CCSM2.0 and CCSM3.0). Technical Report, 02: 2484.

Timmermann, R., A. Beckmann and H.H. Hellmer, 2002a: Simulation of ice-ocean dynamics in the Weddell Sea. Part I: Model configuration and validation. *J. Geophys. Res.*, 107(C3): 10.1029/2000JC000741.

Timmermann, R., A. Beckmann and H.H. Hellmer, 2002b: Simulation of ice-ocean dynamics in the Weddell Sea. Part II: .Interannual variability 1985-1993 *J. Geophys. Res.*, 107(C3): 10.1029.

Timmermann, R. and A. Beckmann, 2004: Parametrization of the vertical mixing in the Weddell Sea. *Oc. Model*, 6(1): 83-100.

Deep and bottom water variability in the central basin of Bransfield Strait (Antarctica) over the 1980–2005 period

C.A.E. Garcia and M.M. Mata
Department of Physics, Fundação Universidade Federal do Rio Grande, Brasil
Corresponding author: dfsgar@furg.br and mauricio.mata@furg.br

Introduction

The Bransfield Strait (BS) is placed between the South Shetland Islands and the tip of the Antarctic Peninsula where several topographic barriers tend to isolate its waters from surrounding seas (fig 1). The strait is separated from the Weddell Sea to the east by a shallow plateau (depth < 750m) and from the southern Drake Passage to the northwest by several topographic barriers. The BS can be subdivided into three basins which are separated from each other by sills shallower than 1000 m. Islands, shallow sills and ridges to the north and west of the Bransfield Strait act as barriers and restrict the inflow of intermediate, deep and bottom waters from the Bellingshausen Sea. Most of the BS water masses therefore originate in the Weddell Sea, especially the deep and bottom waters.

The deep and bottom water properties of the central and eastern basins of the BS have been examined by several authors (Whitworth et al, 1994; Wilson et al, 1999; Gordon et al, 2000). These basins are mainly filled with Modified Warm Deep Water (MWDW, -1.4≤ θ< 0.1, 34.4≤S<34.6). Moreover, Gordon et al (2000) point out that bottom waters of the central basin are influenced by both High Salinity Shelf Water (HSSW, -1.88≤ θ < -1.7 , 34.56≤S<34.84) and Low Salinity Shelf Water (LSSW, -1.88≤ θ< -1.7 , 34.3≤S<34.4) drawn from the Weddell Sea around the tip of Joinville Island.

In this work we examine the thermohaline properties of cold (θ<-1.4 0C, the lower θlimit for MWDW) and deep (H>1000 m) waters of the Central Basin of the Bransfield Strait (CBBS) over the last 25 years (1980-2005). Interannual variability of the thermohaline properties of theses waters is expected since they are subject to temporal variations of source waters.

Data and Methods

Much of the data for the period (from 1980 to 1996) originated from the National Oceanic Data Centre (NDOC). In addition three oceanographic cruises conducted in 2003, 2004 and 2005 under the umbrella of the Brazilian Antarctic Program were also included. The Brazilian cruises were carried out on board the Brazilian Navy R/V Ary Rongel in January 2003, 2004 and 2005 when the BS waters were sampled for temperature, salinity, oxygen, nutrients, bio-optical properties, phytoplankton and zooplankton. The temperature and salinity data were collected using a Seabird CTD 911+ mounted on a 12 bottles (5 litres) carousel. Accuracies for temperature and salinity were about 0.002 ^{0}C and 0.003, respectively, for all Brazilian cruises. Only CTD thermohaline data from the deepest waters (H>1000m and θ≤ -1.40C) of the CBBS are considered in this work. The dataset comprise observations from the following periods: Dec 1980, Nov 1983, Dec 1984, Jan 1985, Nov 1987, Nov 1990, Dec 1996, Jan 2002, Jan 2003 and Jan 2005.

Results

Figure 2 shows the θ-S diagram for CBBS waters deeper than 1000m and colder than -1.4°C, which comprises the deepest waters in the BS. The main characteristic of these profiles is the

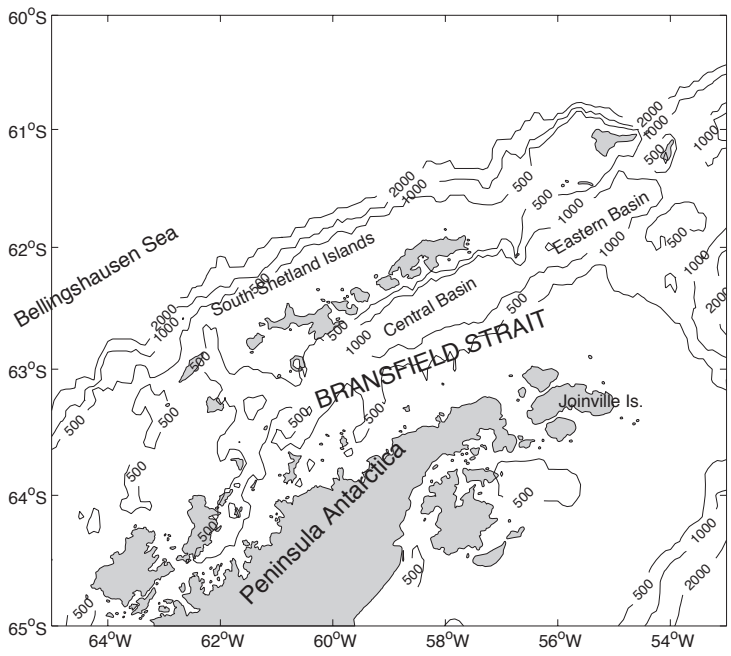

Figure 1. The Bransfield Strait and the surroundings seas. The Central Basin of the Bransfield Strait (CBBS) is highlighted for clarity.

significant influence of the High Salinity Shelf Water (HSSW), a major player in the formation of Weddell Sea Bottom Water. The minimum potential temperature was -1.767 0C in Jan 2005. The noise level present in the θ-S pairs differs from one year to another, however it is clear that lower noise levels are present in data gathered in recent years. The θ-S profiles during Jan 2003, Jan 2004 and Jan 2005 (Brazilian cruises) are shown in blue, green and red, respectively, to differentiate them from the NODC data.

We calculated the mean potential temperature ($\overline{\theta}$) and the mean salinity ($\overline{S}$) for the deep waters during the 25 years period. Figure 3 shows the property time series for both (a) potential temperature and (b) salinity. The $\overline{\theta}$ range was about 0.226 ^{0}C while the $\overline{S}$ range was 0.061. Care should be taken when analysing Dec 1984 and Jan 1985 years because they originate from the same austral summer. The $\overline{\theta}$ and $\overline{S}$ time-series also show high variability for the 2003-2005 period during the Brazilian cruises. The warming 1990-1996 period in the Warm Deep Water (WDW) and Weddell Sea Bottom Water (WSBW), observed by Fahrbach et at (2004, see fig 5 in their paper), also occurred in the deep waters of the Bransfield Strait (warming of 0.044 ^{0}C, fig 3a). During the 25 years, there is a marked decrease in salinity of about 0.0362 in CBBS (fig 3b) and an increase in potential temperature. A linear fitting shows salinity (r=-0.74, N= 10) and potential temperature (r=0.35, N= 10) gradients of -0.0014/year and 0.0027 ^{0}C/year, respectively. The above results are evidence that the observed change in salinity is more pronounced - and statistically more significant - than in temperature because the characteristics of the water sources of deep and bottom CBBS have changed over the years.

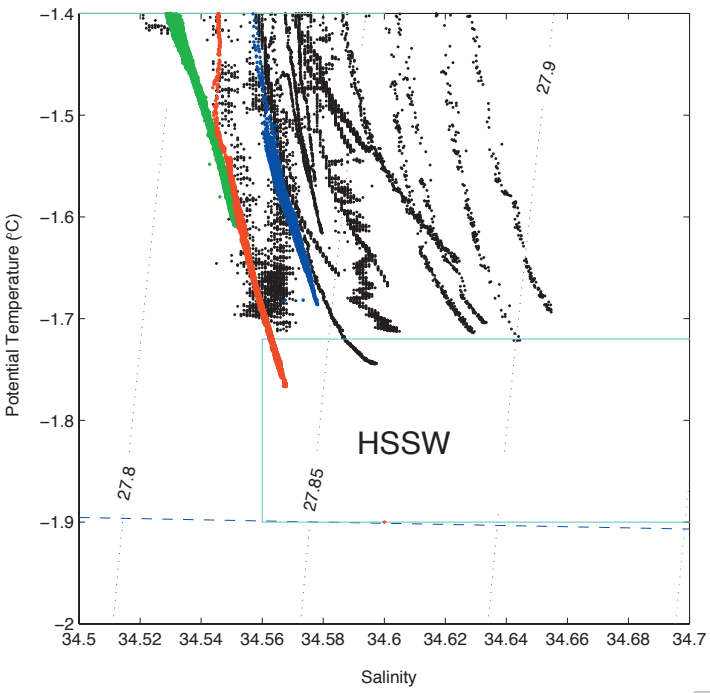

Figure 2. θ-S diagram for all profiles. NODC data are in black while Brazilian cruises are in blue (Jan 2003), green (Jan 2004) and red (Jan 2005). The High Salinity Shelf Water (HSSW) thermohaline indices are also shown for clarity.

The θ-S diagram of the $\overline{\theta}$-$\overline{S}$ pairs summarizes the results of the analysis performed here (fig 4). Over the 25 years period, there was a decrease in salinity but no significant trend was observed in potential temperature. According to Gordon et al (2000), the recipe for deep and bottom waters in the CBBS consists of about 60% of HSSW, 30% of LSSW and 10% of WDW (or MWDW). Near the freezing point, the potential sources are the LSSW and HSSW, which do not differ in temperature but do so significantly in salinity. The observed trend in salinity is likely to be associated with changes in the relative contribution of these shelf waters to the mixing or with a general freshening of the HSSW characteristics during the years considered. Conversely, the evidence of warming in the CBBS can also be due to modifications in the MWDW (or WDW), which is strongly influenced by remote as well as local conditions in the Weddell Sea which, for instance, presented a marked warming trend during the 1990s (Fahrbach et al, 2004). The changes in salinity are strong enough to decrease the density of the deep and bottom waters of the Bransfield Strait over the 25-years period (fig 4).

Conclusions

Thermohaline properties of the deep and bottom waters (H>1000m and $\theta \leq$-1.4°C) of the Central Basin of the Bransfield Strait have been used to examine their variability over the 1980-2005 period. A general trend of decreasing salinity of about 0.0362 is observed over the entire period. The analysis of the potential temperature reveals a warming trend during the same period, but less pronounced than the salinity change. Our results further suggest that the recipe of CBBS deep and water change during the years and that a general freshening of the HSSW flowing around the tip of Joinville island is also occurring. Another possible scenario is that these waters are becoming more influenced by the inflow of LSSW.

High interannual variability is observed in the 2003-2005 period during the Brazilian cruises. The warming of deep waters in the Weddell Sea during the early 90s is also observed in the deepest waters of the Central Basin of the Bransfield Strait. The overall result shows that the deep and bottom CBBS waters have become less dense over the 25 years period.

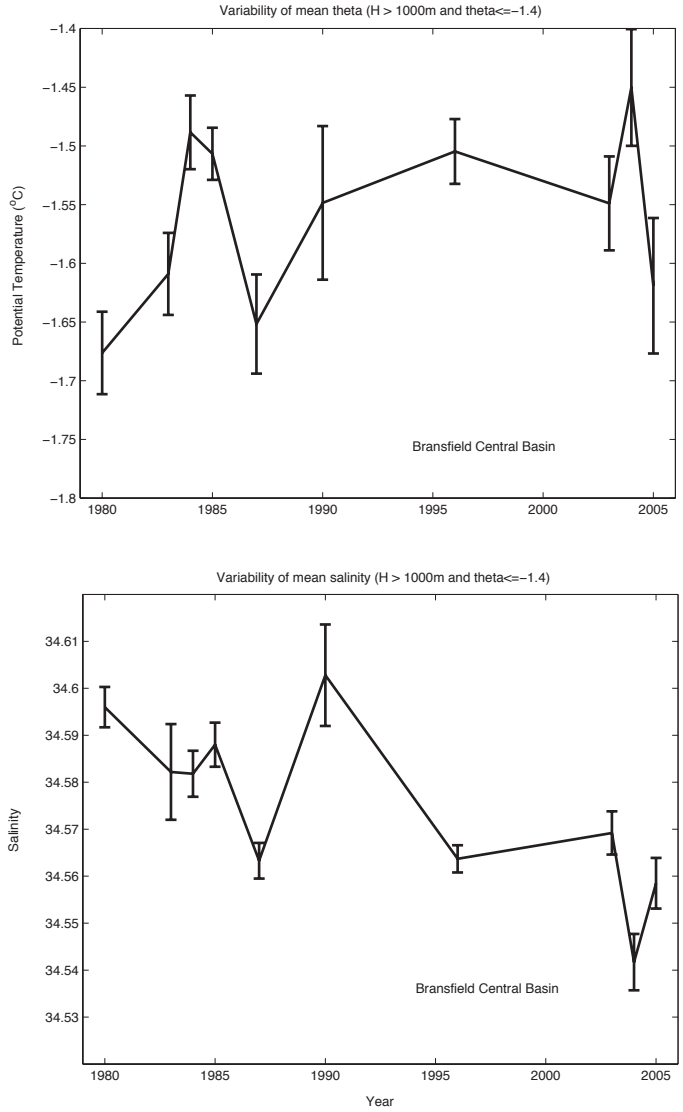

Figure 3. Time series of mean CBBS potential temperature and mean salinity over the 25 years. Data were taken only from waters deeper than 1000 m and colder than -1.4 ^{0}C.

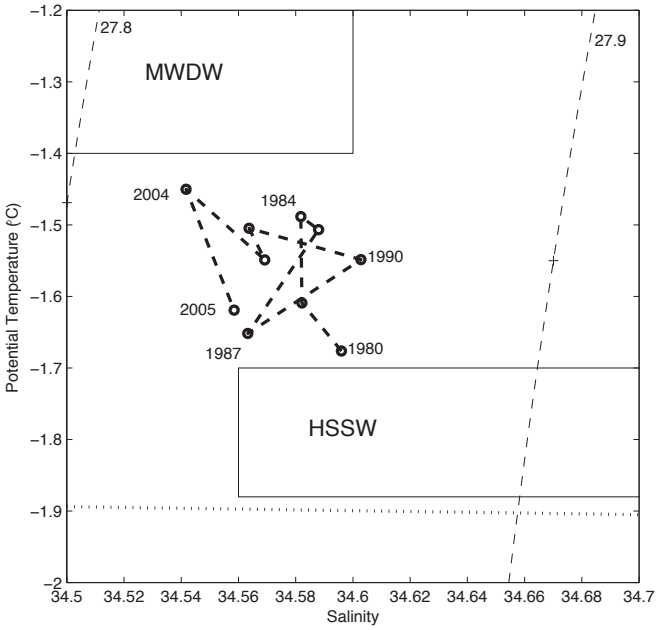

Figure 4. θ-S diagram for mean potential temperature and mean salinity over the last 25 years. The limits of TS indices for the High Salinity Shelf Water (HSSW) and Modified Warm Deep Water are shown. Dotted line is the seawater freezing point. Isopycnal (dashed lines) are drawn relative to sea surface.

Acknowledgment:

This work was supported by the GOAL Project, part of the Brazilian Antarctic Survey (/PROANTAR/MMA/CNPq).

References

Fahrbach, E., Hoppema, M., Rohardt, G., Schröder, V., Wisotzki, A., 2004. Decadal-scale variations of water mass properties in the Deep Weddell Sea. *Ocean Dynamics*, 54,77-91.

Gordon, A.L., Mensch, M., Dong, Z., Smethie Jr., W.M., de Bettencourt, J., 2000. Deep and bottom waters of the Bransfield Strait eastern and central basins. *Journal of Geophysical Research* 105 (C5), 11337–11346.

Whitworth III, T., Nowlin Jr., W.D., Orsi, A.H., Locarnini, R.A., Smith, S.G., 1994. Weddell sea shelfwater in the Bransfield strait and Weddell-Scotia Confuence. *Deep-Sea Research* I 41 (4), 629–641.

Wilson, C., Klinkhammer, G.P., Chin, C.S., 1999. Hydrography within the central and east basins of the Bransfield Strait, Antarctica. *Journal of Physical Oceanography* 29, 465–479.

Warm events near Maud Rise, Weddell Sea

M. Hoppema, E. Fahrbach, and G. Rohardt
Alfred Wegener Institute for Polar and Marine Research, Climate Sciences, Germany
Corresponding author: mhoppema@awi-bremerhaven.de

Introduction

Processes around Maud Rise, a topographic high centred at 65°S just east of the prime meridian, impact on water properties in the Weddell Sea (Bagriantsev et al., 1989). The great Weddell Polynya of the 1970s is thought to be associated with processes at the Rise (e.g., Holland, 2001). Circumpolar Deep Water (CDW) is the main source water of the Weddell Gyre. As part of the intermediate water of the westward flowing southern limb of the Weddell Gyre, it impinges on the seamount. While normally its subsurface temperature maximum reaches values of 1.2-1.3°C and occurs shallower than 300 m, it is lower than 0.6°C over the crest of Maud Rise and occurs deeper than 300 m (Bersch et al., 1992). The relatively isolated water column over Maud Rise is a Taylor column feature. To understand the processes by which it effects water mass formation and ice cover, long-time moorings are maintained close to Maud Rise at the prime meridian (see also Klatt et al., 2005). Here we present temperature and current velocity data of moorings AWI 229 at 64°S and AWI 230 at 66°S.

Water flow and temperature records

At AWI 229 – being situated in the abyssal plain NW at the base of Maud Rise– the water flow of the upper and deep layers is persistently southwestward, while the current velocities are high (Fig. 1). This complies with the main flow of the southern limb of the Weddell Gyre, which anti-cyclonically winds around Maud Rise. In contrast, the main flow direction at AWI 230 – situated SW of the crest on the lower slope – is northerly (Fig. 1), which places this mooring in a cyclonic inner recirculation around the Rise. During 1996-1998 the upper instrument of AWI 230 was lying at only 91 m depth, which is within the winter mixed layer. This is evidenced by the base level of temperature in winter, which lies at -1.85°C, i.e. the freezing point (Fig. 2). Superimposed are numerous peaks of high temperature; hereafter referred to as warm events. There is an accumulation of warm events in the spring and summer in 1996/1997 much more intense than in the same period one year later. But they also occur in the winter (July 1996; July and August 1997), reaching >0°C and even >1°C (in situ data), an increase of 2-3°C within a few days! The surface temperature record is coherent with temperature records in the vertical during all warm anomalies, i.e. also at depth a temperature increase was observed, albeit an order of magnitude smaller than in the surface layer (not shown here). There is no correlation of the warm events and the variations of the current velocity at AWI 230; for instance, the latter is certainly not higher during the spring and summer period. However, some single warm events do appear to correspond with peaks in the velocity, namely those of July 1996, July 1997 and November 1997.

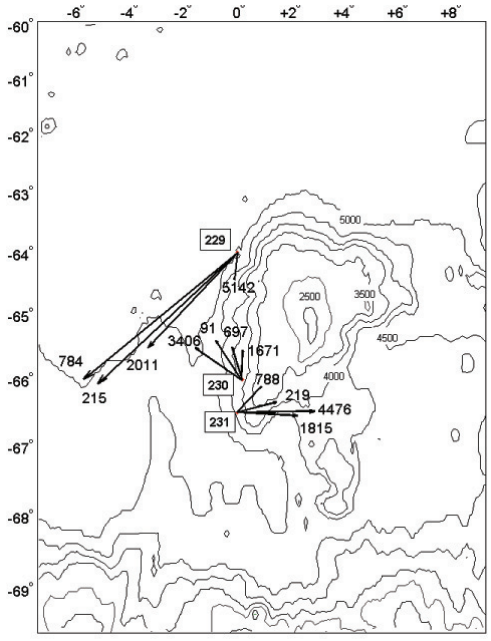

Figure 1

Map of the area of investigation around Maud Rise and the location of the moorings. Arrows show the flow direction at different depths (indicated by the number).

At AWI 229 in 215 m (the depth of the upper instrument), the temperature level generally lies in the range 0.5-1.3°C (Fig. 2). This corresponds approximately to the range of temperature maxima in the Weddell Gyre (Schröder and Fahrbach, 1999). AWI 229 is situated in the proximity of the boundary between the main flow of warm, deep water in the south and the much cooler deep water in the central, interior gyre (Bersch et al., 1992; Schröder and Fahrbach, 1999). Therefore, it is likely that the large temperature variability originates from frontal instabilities or meandering of this frontal structure. Numerous excursions towards low temperature beyond the usual level were observed, often as low as the freezing point (Fig. 2). These excursions occurred in the winter months, indicating that they represent convective deepening of the surface layer to at least 215 m depth. Since such deep mixed layer depths occur typically to the north in the gyre interior, they are indicative of influence from that region at the location of AWI 229. Comparing the temperature and current velocity records of AWI 229, it is striking that the low-temperature excursions appear to coincide with periods of specifically low current velocity (Fig. 2). Apparently, a low current velocity of the main westward gyre flow around Maud Rise leads to southward progress of water from the Weddell Gyre interior towards the Rise. Generally it can be stated that when temperatures in the range 0.5-0.7°C are observed (Fig. 2), this points to central gyre water with its low temperature maximum, whereas high temperatures (1-1.2°C) are indicative of the main flow around Maud Rise. Note that temperatures in the range 0.5-0.7°C generally correspond to current velocity minima.

Discussion

AWI 230 is placed in a frontal region that separates the water column centered over the crest of Maud Rise from the main gyre flow of warm subsurface water around the Rise. During warm events, the water characteristics appear to align with that of the main flow, i.e., a shallow pycnocline, at least shallower than 91 m! During the remaining time, the water characteristics seem to be similar to those over Maud Rise, namely a deep pycnocline (Bersch et al., 1992). Obviously, in November (1996 and 1997) a shift of regime occurred at the location of AWI 230, where

the water column with Maud Rise characteristics was being replaced by a water column with main flow characteristics. By the end of January, the shift took place in opposite direction. The same conditions were prevalent during relatively short periods of time in mid-winter in 1996 and 1997 (Fig. 2).

Many warm events at AWI 230 appear to correspond with low-temperature excursions at AWI 229 (Fig. 2), e.g. in July 1996, July 1997 and November 1997. The correlation is not perfect, where in particular the warm events in the summer do not have a corresponding event at AWI 229. If the cold excursions at AWI 229 and the warm events at AWI 230 have a common cause, this must be associated with a relatively low current velocity of the main flow. Note also that in summer the events do seem to correspond to a low current velocity at AWI 229. Near the northern, equatorward boundary of the main flow jet (i.e., near AWI 229), low velocities apparently tend to displace the flow jet to the south/polewards. A poleward displacement of the southern boundary of the jet in the transition region to the water column of Maud Rise (i.e., near AWI 230) would increase the influence of the main flow at that fixed location. Thus, part of the observations at AWI 229 and AWI 230 can be explained by a southward/poleward displacement of the main jet in times of a reduction of the current velocity.

The large-scale circulation of the Weddell Gyre is wind-driven, which implies that the main flow (as represented by AWI 229) is subject to this forcing. Thus variability of the wind regime will in the end cause the warm events. But can this also explain the warm events in the winter, when the Weddell Gyre is fully ice covered? It is important to keep in mind that momentum transfer by the wind on an ice-covered ocean is substantial. The wind speed reaches its annual maximum in winter, but usually a bimodal structure is observed with one peak in the beginning and another peak toward the end of the winter. We suggest that the relative minimum of the wind speed could cause a transient relaxation of the circulation in the Maud Rise region, leading to a lower current velocity in the main flow. This may explain the correlation of the low current velocity of the main flow on the one hand, and the low-temperature excursions (at AWI 229) and warm events (at AWI 230) on the other.

The temperature and current velocity records show a very large degree of variability. We can explain some remarkable peaks, but it is certain that the proposed mechanism cannot explain every single feature. Involved in a shift in the flow regime in the wider Maud Rise region will also be eddies, frontal instabilities, Taylor column modifications and mixing. Additionally, the variability of the main wind field is enormous, but also locally near Maud Rise it is extremely variable because Maud Rise is situated in the transitory region of east winds and west winds. These factors, being effective at different time scales, and their feedbacks all contribute to a large variability.

The warm events at AWI 230 are a spectacular observation, especially when they occur in the wintertime when the temperature may increase by up to 3°C within 1-2 days (Fig. 2). It is manifest that, if high temperatures occur in the surface layer under the pack ice, this is highly conducive to the melting of ice. In this regard, it is worthwhile noticing that there is an accumulation of warm events in spring and summer. It may not be a coincidence that this is also the time of the year that the ice pack opens, in the Maud Rise region earlier than in nearby regions. In addition, Lindsay et al. (2004) observed a halo of low ice concentration around Maud Rise, which could also be associated with warm events. Ice cover in the Maud Rise region is determined by many different factors; warm events, that is, heat from below, is only one of them. If warm events are significant in the reduction of ice cover, one would expect some kind of correlation with ice cover or ice concentration data. Upward Looking Sonar data, which measure the ice draft at our mooring locations, reveal that the annual mean effective ice draft, corrected for the occurrence of ice ridges, is significantly lower at AWI 230 (where the warm events occur) than at the nearby AWI 229 and one other nearby location south of AWI 230 (Hoppema et al., in prep.). Hence, this strongly suggests

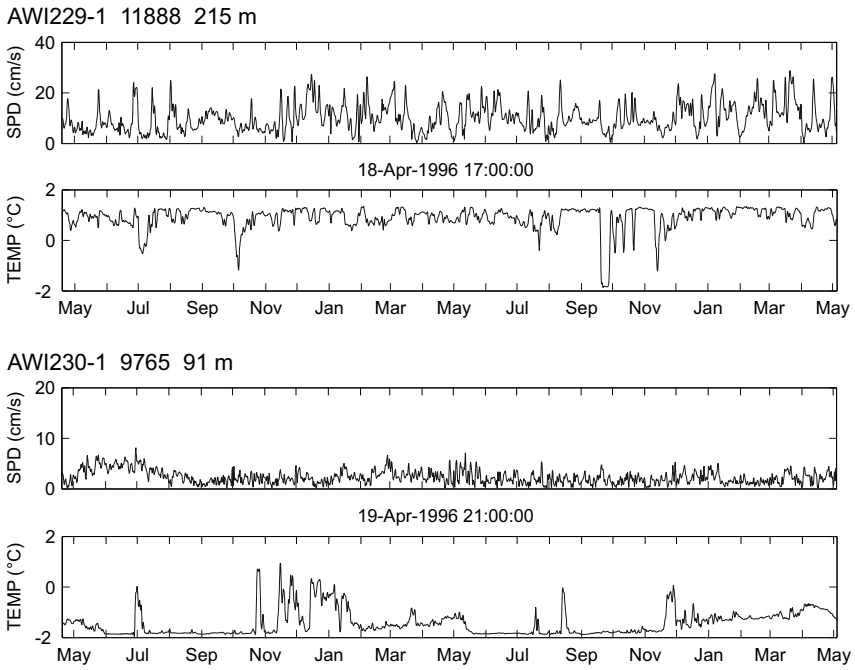

Figure 2
Time series (1996-1998) of temperature and current velocity at the shallowest depth of moorings AWI 229 and AWI 230.

that warm events play some role in melting the ice.

Concluding remarks

We have found strong indications that variation of the main southern limb flow of the Weddell Gyre, which winds around the northern reaches of Maud Rise in a relatively narrow jet, induces warm events at its lower flank. We conjecture that the generating of warm events in the oceanic surface layer plays an important role in removing the ice-pack and forming ice-free regions. It should be realised that the relatively warm intermediate water from the main flow around Maud Rise occurs at shallow depths, typically <100 m. What makes the warm events meaningful is that this already shallow warm water is further uplifted through circulation-topography interactions at the flanks of the Rise. If the warm events occur in winter, they have the potential to melt the pack ice and generate polynyas or, in early spring, open the pack.

References

Bagriantsev, N.V., A.L. Gordon, and B.A. Huber, 1989: Weddell Gyre: Temperature maximum stratum. *J. Geophys. Res*., 94, 8331-8334.

Bersch, M., G.A. Becker, H. Frey, and K.P. Koltermann, 1992: Topographic effects of the Maud Rise on the stratification and circulation of the Weddell Gyre. *Deep-Sea Res.,* 39, 303-331.

Holland, D.M., 2001: Explaining the Weddell Polynya - a large ocean eddy shed at Maud Rise. *Science,* 292, 1696-1700.

Klatt, O., E. Fahrbach, M. Hoppema, and G. Rohardt, 2005: The transport of the Weddell Gyre across the Prime Meridian. *Deep-Sea Res*. II, 52, 513-528.

Lindsay, R.W., D.M. Holland, and R.A. Woodgate, 2004: Halo of low ice concentration observed over the Maud Rise seamount. *Geophys. Res. Lett*., 31, L13302, doi: 10.1029/2004GL019831.

Schröder, M. and E. Fahrbach, 1999: On the structure and the transport of the eastern Weddell Gyre. *Deep-Sea Res*. II, 46, 501-527.

Circulation of Subantarctic Mode Water in the Indian Southern Ocean from ARGO and ALACE floats

K Speer[1], N. Wienders[1], J.–B. Sallee[2], R. Morrow[2]
[1]Department of Oceanography, OSB 435, Florida State University, Tallahassee FL 32306–4320, USA
[2]LEGOS–UMR5566, 18 av Edouard Belin, 31401 Toulouse cedex 9, France
Corresponding author: kspeer@ocean.fsu.edu

Abstract

Subantarctic Mode Water is the name given to the relatively deep surface mixed layers found directly north of the Subantarctic Front in the Southern Ocean, and their extension into the thermocline as weakly stratified or low potential vorticity water masses.

ARGO profiling floats provide estimates of temperature and salinity typically in the upper 2000 metres, and the horizontal velocity at various parking depths. Mode water circulation is determined with ARGO data, earlier ALACE float data, and climatological hydrography.

Introduction

Mode water is the name given to an ocean layer with physical properties (temperature, salinity) that are nearly homogeneous vertically and horizontally, covering an extended area in a given basin (a recent review is provided by Hanawa and Talley, 2001) and thus occupying a relatively large volume compared to other water types. They are one of the primary results of air-sea interaction (Speer et al., 1995), and serve to ventilate the interior of the upper ocean as they spread within gyres and boundary currents (McCartney, 1982; Hanawa and Talley, 2001).

In the Southern Ocean, the Subantarctic Mode Water (SAMW) forms in the deep winter mixed layers in the Subantarctic Zone (SAZ), north of the Subantarctic Front (SAF) and south of the Subtropical Front (STF).

Talley's (1999) map of mixed layer oxygen saturation shows an onset of higher oxygen in the southern Indian Ocean, at about 70°E, which supports the idea that the southeast Indian Ocean is a dominant source region of mode water; McCarthy and Talley (1999; see also Keffer, 1985) show a low potential vorticity (PV) pool near 26.8 sigma-theta centered near 90°W, 40°S which is generated by relatively deep winter mixed layers, spreads

into the subtropical Indian Ocean. The low PV pool also extends in a narrow tongue eastward south of Australia, a pattern that becomes more pronounced at slightly greater density.

Data

The ARGO float program has seeded the World Ocean for several years, and in particular, the Southern Ocean, which historically is poorly sampled. Good data coverage in the southern Indian Ocean started in late 2002, and this study focuses on the years 2003 and 2004. These data were collected and made freely available by the International Argo Project and the national programs that contribute to it. PALACE data (Davis, 2005) were combined with ARGO floats to compute the mean flow in the Southern Indian Ocean.

We obtained 8849 velocity components from the ARGO database and 11667 from the ALACE/PALACE database. The velocities were averaged into 2 degrees of longitude by 1 degree of latitude bins. We then mapped the velocity field and a stream function from the ARGO data in the Southern Indian Ocean using an objective analysis following Gille (2003). The mean 10-day current velocities estimated from ARGO data at the parking depth contain errors, mainly due to the float drift at the surface. Furthermore, the float drift during the descent and ascent phase is also unknown. A study on the error in the drifting velocity at the float parking depth by Ichikawa et al. (2002) estimates this error to be between 10 to 25 percent.

Our averaged, interpolated velocity field has substantial errors, formally of magnitude 50% or so, worse around the boundaries of the domain. However, other sources of error from sampling bias and unresolved flow probably dwarf this error locally.

Circulation of the southern Indian Ocean

Figure 1 shows a climatological average of velocities at 400 metre depth deduced from an objective analysis of ARGO and PALACE floats in the Southern Indian Ocean. We see a rich array of gyres embedded within the general flow of the ACC

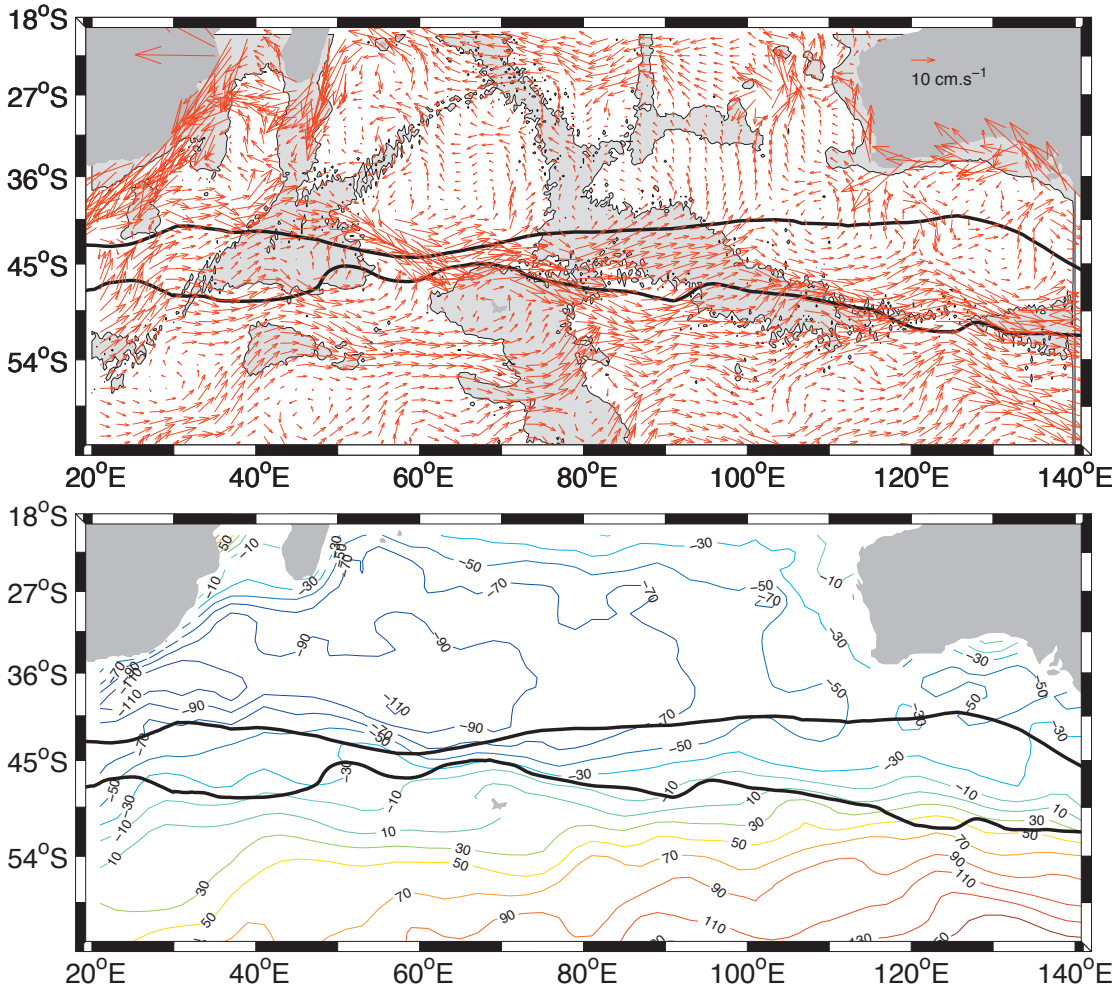

Figure 1: Averaged velocities at 400 metre depth deduced from an objective analysis of ARGO and PALACE floats in the southern Indian Ocean (upper). Bathymetry less than 3500 metres depth is shaded gray. Solid lines indicate the STF (north) and the SAF (south) from Orsi et al. (1995). A geostrophic streamfunction constructed from the same flow field is displayed for a smoother view of the circulation (lower).

and subtropical gyre. A geostrophic streamfunction view of the same flow field smoothes over some features but suggests a gyre south of Australia and others nested within the general subtropical gyre circulation.

The meandering Agulhas Retroflection is centered on about 40°S with velocities greater than 40 cm/s at 400 m depth. In this analysis, the Antarctic Circumpolar Current (ACC) bifurcates upstream of the Crozet Plateau at 40 S, the northern branch merging with the Agulhas Retroflection, and the southern branch continuing eastward. Further downstream, this eastward branch bifurcates again around the Kerguelen Plateau. A main southerly branch continues eastward across the plateau, merging with flow downstream of the plateau. The merging of ACC and Agulhas waters upstream of the two plateaus gives rise to strong lateral mixing.

Downstream of the Kerguelen Plateau near 80°E, the main fronts diverge; the STF moves northward, whereas the main branch of the SAF follows the northern flank of the Southeast Indian Ridge (Sandwell and Zhang, 1989). This is the region of deepest winter mixed layers described by Talley (1999), McCarthy and Talley (1999).

The northward spreading of mode water into the subtropical gyre is presumably due primarily to northward advection, itself a result of wind stress forcing and the fluxes that create mode water. Stramma (1992) showed that southeast of Africa the Subtropical Front (STF) is associated with a geostrophic transport of some 60 Sv (1 Sv = 106 m3/s) and that this transport is reduced to less than 10 Sv as Australia is approached. South of Australia the strength of the STF decreases further, reaching negligible magnitude near 130 E (Schodlock et al., 1997). The surface water between the STF and SAF becomes progressively cooler and denser as it moves east; this allows the development of northward thermal wind, thus gradually carrying away water from the northern side of the ACC and into the subtropical gyre.

Fine (1993) divided Indian Ocean SAMW into three density ranges: 26.65-26.7 sigma, which dominates in the southwestern region, 26.7-26.8 sigma, which dominates in the central region, and 26.8-26.85 sigma, which dominates in the south-eastern region. These divisions are presumably related to the large-scale wind-driven circulation, bathymetry, and the dynamics of mode water itself.

The mean wind stress curl (not shown) from QuikScat shows a complex spatial structure related to wind systems and flow over land, and also to SST; this tends to drive gyres at sub-basin scales.

Bathymetry clearly has a direct impact on the circulation in this region, creating large permanent meanders of the Agulhas Retroflection and the ACC, and limiting the latitudinal excursions of the hydrological fronts. North of the ACC distinct interior recirculation regimes exist apparently related to bathymetry that may set the primary mode water divisions.

Finally, strong eddy activity is associated with instabilities of the main currents and other dynamical fronts. The Agulhas Current System has the highest eddy kinetic energy (EKE) of the global ocean, and EKE maximums are located along the main axes of the meandering Agulhas Retroflection and the ACC (Le Traon and Morrow, 2001). Eddy mixing can be important in the diffusion of tracers, and in the transport of properties across the SAF.

In a separate study we investigate the primary sources of heat to mode water and the importance of eddies to the heat balance of mode water (Sallee et al. 2005).

Acknowledgements

The ARGO data were collected and made freely available by the International ARGO Project and the national programs that contribute to it. (www.argo.ucsd.edu, argo.jcommops.org). ARGO is a pilot program of the Global Ocean Observing System. This study was partially supported by the French PATOM and Coriolis programs, and by NSF grants OCE-0336697 and OCE-0117618 to KS.

References

R.E. Davis, 2005: Intermediate-depth Circulation of the Indian and South Pacific Oceans measured by autonomous floats. *J. Phys. Oceanog*., 35:583–707, 2005.

R.A. Fine. Circulation of Antarctic Intermediate Water in the South Indian Ocean. *Deep Sea Res*., Part I, 40:2021–2042, 1993.

S. T. Gille. Float observations of the Southern Ocean: Part 1. Estimating mean fields, bottom velocities, and topographic steering. *J. Phys. Oceanog*., 33:1167–1181, 2003.

K. Hanawa and L. Talley. Ocean Circulation and Climate, chapter Mode Waters, pages 373–386. G. Siedler and J. Church, editors, *International Geophysics Series*, Academic Press, 2001.

Y. Ichikawa, Y. Takatsuki, K. Mizuno, N. Shikama, and K. Takeuchi. Estimation of drifting velocity and error at parking depth for the ARGO float. Technical report, Argo Technical Report, FY2001, 2002.

T. Keffer. The ventilation of the world's oceans: maps of the potential vorticity field. *J. Phys. Oceanog*., 15:509–523, 1985. P.Y. Le Traon and R. Morrow. Satellite Altimetry and Earth Sciences, chapter Ocean currents and eddies, pages 171–215. Academic Press, 2001.

M. C. McCarthy and L. D. Talley. Three-dimensional potential vorticity structure in the Indian Ocean. *J. Geophys. Res*., 104:13251–13267, 1999.

M. S. McCartney. The subtropical recirculation of mode waters. *J. Mar. Res*., 40, suppl.:427–464, 1982.

A.H. Orsi, T. Whitworth III, and W.D. Nowlin Jr. On the meridional extent and fronts of the Antarctic Circumpolar Current. *Deep Sea Res*., Part II, 42:641–673, 1995.

J.B. Sallee, N. Wienders, R. Morrow, and K. Speer. Formation of Subantarctic Mode Water in the Southeastern Indian Ocean. *Ocean Dynamics*, in Review, 2005.

D. T. Sandwell and B. Zhang. Global mesoscale variability from the Geosat Exact Repeat Mission: correlation with ocean depth. *J. Geophys. Res*., 94:17971– 17984., 1989.

M P Schodlock, M Tomczak, and N White. Deep sections through the South Australian Basin and across the Australian–Antarctic Discordance. *Geophys. Res. Lett*., 24:2785–2788, 1997.

K. G. Speer, H.J. Isemer, and A. Biastoch. Water mass formation from revised COADS data. *J. Phys. Oceanog*., 25:2444–2457, 1995.

L. Stramma. The South Indian Ocean Current. *J. Phys. Oceanog*., 22:421–430, 1992.

L.D. Talley. The South Atlantic: Present and Past Circulation, chapter Antarctic Intermediate Water in the South Atlantic, pages 219–238. G. Wefer, W.H. Berger, G. Siedler and D. Webb, Springer-Verlag, 1999.

The Carbon Cycle In Mode Waters Of The Southern Indian Ocean: Anthropogenic Vs. Natural Changes

C. Lo Monaco and N. Metzl
Laboratoire d'Océanographie et du Climat: (LOCEAN/ IPSL CNRS) Université P. et M. Curie, France
Corresponding author: lomonaco@ccr.jussieu.fr

Introduction

The ocean carbon cycle is closely linked to climate. The ocean's uptake of anthropogenic CO_2 regulates the increase of this greenhouse gas in the atmosphere and thus global warming. In turn, the rate of the ocean's uptake of CO_2 is affected by climate-induced changes in biogeochemical and physical ocean processes. Global models have shown that the Southern Ocean is of particular interest here both because it is where most anthropogenic CO_2 enters the ocean and because it will be particularly sensitive to future climate change. However, the Southern Ocean is also the region where the highest disagreements exist among different ocean carbon models (Orr et al., 2001) and between models coupling the global carbon cycle with climate change (Friedlingstein et al., 2003). In that context, long-term observations of carbon dioxide in the Southern Ocean and data-based studies of the carbon uptake and its variability represent important steps to validate current ocean carbon models and to reduce uncertainties attached to climate change predictions. As part of the long-term observational OISO project, started in 1998 onboard the R.S.S. Marion-Dufresne (IPEV), several hydrographic stations were conducted in the Southern Indian ocean and corresponding Antarctic sector (figure 1). One aim of the project was to complement WOCE stations occupied in 1995 in this area, to reoccupy historical stations (GEOCECS, INDIGO) and investigate the seasonality of the oceanic carbon properties (summer and winter data). In this note, we focus on recent results obtained in mode waters in this region. Both the spatial and temporal evolution of anthropogenic carbon accumulated by the ocean are analyzed.

A large-scale view of anthropogenic carbon in mode waters

Subantarctic Mode Water (SAMW) is formed during the deep winter mixing that occurs north of the Subantarctic Front (45-50°S) and sinks at intermediate depth (500-800m) towards low latitudes, thus providing a privileged path for the penetration of anthropogenic CO_2 into the ocean interior. Current observation-based methods for estimating the ocean's uptake of anthropogenic carbon (C^{ant}) agree on a large accumulation of C^{ant} in SAMW, both for cumulated uptake since the pre-industrial period (20-40 μmol/kg, Sabine et al., 2004; Lo Monaco et al.,

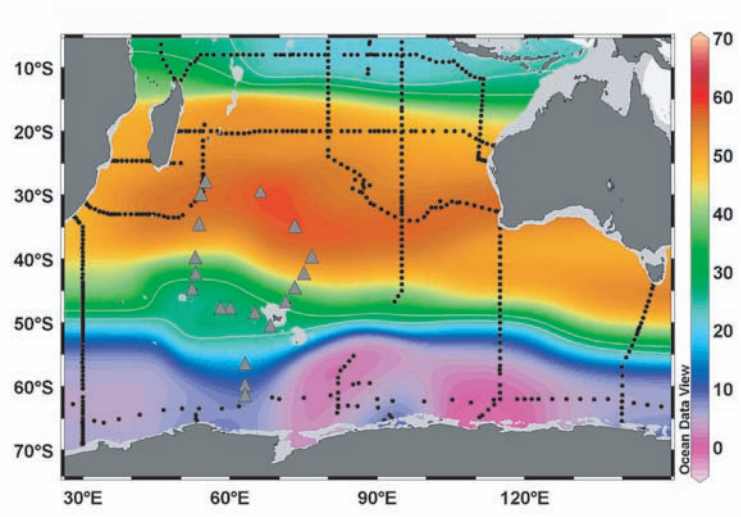

Figure 1: Distribution of anthropogenic carbon (C^{ant}) in the Indian Ocean at 500m. For this map we have merged the WOCE 1995-1996 data (Key et al., 2004; black circles) and observations obtained during OISO cruises (1998-2001, triangles). High C^{ant} concentrations are detected in the Subtropical/Subantarctic band (20-45°S), corresponding to the spreading of mode waters (STMW in the west and SEI-SAMW in the east). A strong C^{ant} gradient follows the circumpolar frontal system shifted southward from South-Africa to Tasmania (white lines = 25 and 30 µmol/kg). South of the Polar Front (50°S-55°S) C^{ant} concentrations at 500m are much lower than north of the front. The back-calculation method used to derive C^{ant} is described by Lo Monaco et al. (2005a)..

2005a,b) and for decadal increase (20-25 µmol/kg over the last three decades, McNeil et al., 2001). An example of the basin-scale distribution of anthropogenic carbon at 500m depth is presented in Figure 1. The inclusion of new OISO data in the South-West Indian Ocean highlights the link between the C^{ant} distribution and well known frontal/circumpolar features. For example, C^{ant} values around 25-30 µmol/kg (white lines on figure 1) follow the southward shift of the Subantarctic/Polar Fronts system from 50°E to 150°E. High concentrations of anthropogenic carbon at latitude 20-40°S are closely linked to the spreading of mode waters. In the Indian Ocean, both Subtropical Mode Waters (STMW) in the west and South-Eastern Indian Subantarctic Mode Waters (SEI-SAMW) in the east have been well identified (Hanawa et Talley, 2000). Since characteristics and formation rates of mode water are linked to natural variabilities or controlled by climate change forcing (Wong et al., 1999), one might expect the oceanic carbon cycle to also be subject to changes in this region (rapid changes or trends). However, C^{ant} data-based methods do not account for natural or climate-induced changes in biogeochemical and physical processes. Instead, one must consider variations of dissolved inorganic carbon (DIC) which result from both the increase in C^{ant} and changes in the ocean carbon cycle.

Temporal variation of anthropogenic carbon in SAMW

In order to investigate the decoupling between anthropogenic uptake by the ocean and carbon cycle natural variability, we have analyzed changes in DIC and C^{ant} by comparing data collected in the Subantarctic Zone of the central Indian region (75-80°E) during INDIGO (1985) and OISO (1998-2000) cruises. In this area, near the mode water formation region, observations indicate that very deep mixing occurs in winter (up to 520m around 40°S in 1998, Figure 3) and one might expect to observe a relatively large anthropogenic signal and perhaps variabilities linked to natural or climate change processes. The potential temperature-salinity diagram shows no difference in SAMW over 15 years (density = 26.75-26.9), while changes are observed in the mixed layer (warming) and in Antarctic Intermediate Water (freshening). In the same zone, below the seasonal mixed layer, we observed an increase of 7 µmol/kg for DIC concentrations over the 15-years period. The increase in C^{ant} over the same period is estimated to be around 14 µmol/kg (Figure 3). Different methods were used to estimate C^{ant} (see details in Lo Monaco et al., 2005b) all leading to the same conclusion: the accumulation of anthropogenic carbon in SAMW from the mid-eighties to the end of the nineties was larger than the observed DIC changes. The difference between

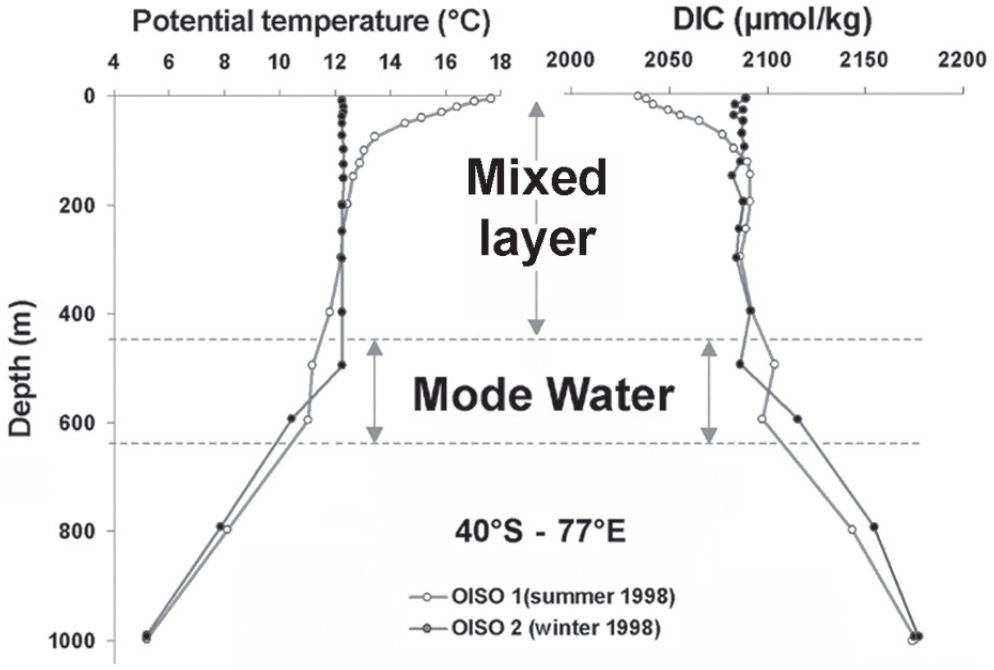

Figure 2 : Profiles of potential temperature and DIC measured during summer and winter 1998 in the Subantarctic Zone of the Central Indian Ocean (OISO cruises). In this region, the winter season is characterized by a deep mixing (up to 520m at the end of august 1998). This results in an homogeneous layer persisting around 500-600m during summer, the Subantarctic Mode Water (SAMW)..

direct DIC measurements and indirect C^{ant} calculations (-7 μmol/kg) represents a rather low residual relatively to the precision of DIC measurements (2 μmol/kg at best). However, one may also interpret this difference as a record of recent natural variability, such as an imprint of biological activity changes in the Subantarctic Zone where it has been suggested that primary productivity has decreased since the eighties (Gregg et al., 2003). Changes in water mass formation or winter deep mixing due to recent warming may also play a role in explaining the differences between the anthropogenic carbon signal and natural or climate-induced variability of DIC. These preliminary results present important issues. First, observed changes of the ocean carbon cycle must not be interpreted only as anthropogenic carbon, otherwise this could create significant errors in global ocean anthropogenic carbon inventories. Secondly, the separation between the observed total carbon variations and the anthropogenic signal will help to determine the effect of external forcing and/or climate change impact on the complex ocean carbon cycle. We believe this could only be achieved through a very close coupling between observationalists and modellers. For these issues, specifically addressed in the Southern Ocean region, CLIVAR, SOLAS and IPY programs will hopefully help different communities to work together.

Acknowledgements

The long-term observational project OISO is supported by three Institutes in France, INSU, IPEV and IPSL. We would like to thanks the directors of these Institutes for supporting this project over many years. Thanks to captains and crews onboard the R.S.S. Marion-Dufresne and TAAF operational chiefs during the windy winter cruises. Warm thanks to many colleagues at IPEV, LBCM and LOCEAN for their help during the cruises. This work was also recently supported by the national program PNEDC-CLIVAR (CANTEMS project).

References

Friedlingstein, P., J.-L. Dufresne, P.M. Cox, and P. Rayner, 2003: How positive is the feedback between climate change and the carbon cycle? *Tellus*, 55B, 692-700.

Gregg, W.W., M.E. Conkright, P. Giroux, J.E. O'Reilly, and N.W. Casey, 2003: Ocean primary production and climate: global decadal changes. *Geophys. Res. Letters*, 30(15), 1809.

Hanawa, K., and L.D. Talley, 2000: Mode Waters. *Ocean Circulation and Climate*. Editors G. Siedler and J. Church, International Geophysics Series, Academic Press.

Key, R.M., A. Kozyr, C. Sabine, K. Lee, R. Wanninkhof, J. Bullister, R. Feely, F. Millero, C. Mordy, and T.-H. Peng, 2004: A global ocean carbon climatology: Results from Global Data Analysis Project (GLODAP). *Global Biogeochem. Cycles*, 18(4), doi:10.1029/2004GB002247.

Lo Monaco, C., N. Metzl, A. Poisson, C. Brunet, and B. Schauer, 2005a: Anthropogenic CO2 in the Southern Ocean: distribution and inventory at the Indian-Atlantic boundary (WOCE line I6), *J. Geophys. Res*., 110, doi:10.1029/2004JC002643.

Lo Monaco, C., C. Goyet, N. Metzl, A. Poisson, and F. Touratier, 2005b: Distribution and inventory of anthropogenic CO2 in the Southern Ocean: comparison of three data-based methods. *J. Geophys. Res*., 110, doi:10.1029/2004JC002571.

McNeil, B.I., B. Tilbrook, and R.J. Matear, 2001: Accumulation and uptake of anthropogenic CO2 in the Southern Ocean south of Australia between 1968 and 1996. *J. Geophys. Res*., 106, 31431-31445.

Orr, J.C., et al., 2001: Estimates of anthropogenic carbon uptake from four three-dimensional global ocean models. *Global Biogeochem. Cycles*, 15, 43-60.

Sabine, C., et al., 2004: The oceanic sink for anthropogenic CO2. *Science*, 305, 367-371.

Wong, A.P., N.L. Bindoff, and J.A. Church, 1999: Large-scale freshening of intermediate waters in the Pacific and Indian oceans. *Nature*, 400, 440-443.

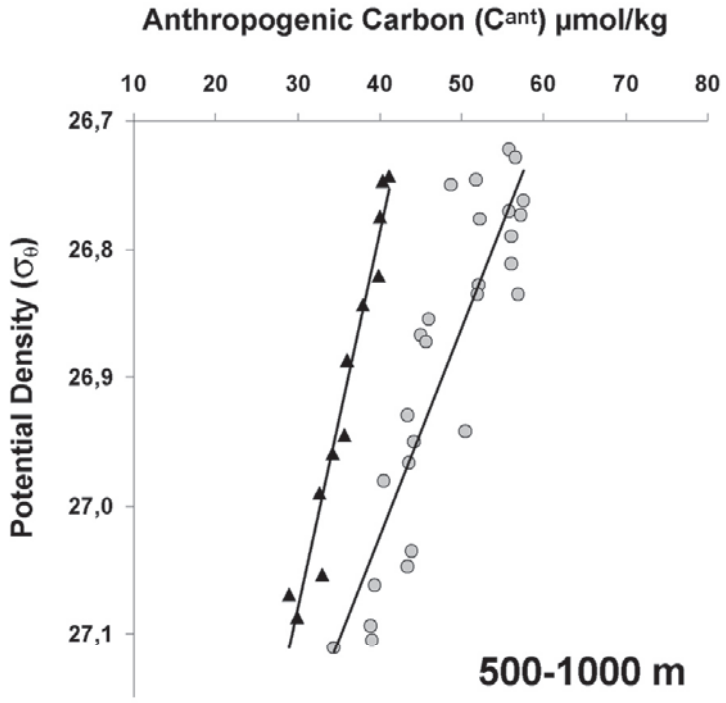

Figure 3 : Temporal evolution of anthropogenic carbon (C^{ant}) as a function of density estimated in the South Indian Ocean (region 30-45°S, 70-80°E). In SAMW, below the winter mixed layer, C^{ant} increase from about 40 µmol/kg in 1985 (INDIGO, triangles) to 54 µmol/kg in 1998-2001 (OISO, circles).

Evaluation of the Latent and Sensible Heat Fluxes Simulated by RegCM3 over the South Atlantic from 1990 to 1994

M. Simões Reboita, R. Porfírio da Rocha and T. Ambrizzi
Department of Atmospheric Sciences, University of São Paulo, Brazil
Corresponding author: reboita@model.iag.usp.br

1. Introduction

The main mechanism for extratropical cyclone development is primarily baroclinic instability. However, the contribution of upper level dynamic forcing, and air-sea interaction can produce explosive deepening of marine cyclones (Nuss and Anthes, 1987). Studies such as Neiman and Shapiro (1993) have shown that these kind of cyclones, called bomb cyclones, can be strongly influenced by the turbulent transfer of heat, moisture and momentum from the ocean surface to the atmosphere.

Over South America, Gan and Rao (1991) observed two regions with a maximum of cyclogenesis in the ocean: one near to Uruguay and another around 42,5°S. Reboita et al. (2005) confirmed the first region using relative vorticity to identify the cyclones, while in their study the second appears to displaced to the south (48°S). A new cyclogenetic area was also identified, located over the subtropics (Reboita et al., 2005). These results used the vorticity threshold that includes smaller intensity cyclogenesis. At present, there is not yet a complete dynamic explanation for the preferential formation of the cyclones in the above mentioned areas. However some hypotheses have been suggested, for instance, Saraiva and Silva Dias (1997) showed that the horizontal sea surface temperature (SST) gradients due to the Brazil and Malvinas current confluence can contribute to maximum cyclogenesis activity. Vera et al. (2001) pointed out that the presence of the warm waters associated with the Brazil current can be an additional source of heat and moisture that reduces the low level static stability, thus contributing to cyclogenesis in this area.

The difficulties in understanding the processes that favor cyclogenesis over the South Atlantic (SA) may be related to the poor data availability in this region. There are few studies in the literature that have used instrumental measures of vertical turbulent fluxes. Weill et al. (2003) reviewed all the experiments that measured these fluxes over the entire Atlantic Ocean and only found five. All these were carried out over the North Atlantic, with four of them in middle latitudes. Thus, the coefficient of turbulent change usually used to estimate the latent and sensible heat fluxes is more representative of these particular regions.

The main data sets that represent the atmospheric conditions over the SA come from information obtained from satellites and numerical model results, or by a combination of both, as for the WHOI - Woods Hole Oceanographic Institution data set (Yu et al., 2004).

The focus of this study is to evaluate the latent and sensible heat surface fluxes simulated by a Regional Climate Model (RegCM3) over the SA. The skill is assessed by comparing the mean simulated values with the data set of WHOI and ECMWF (European Centre of Medium Range Weather Forecasting) analyses for the period 1990 to 1994.

This work is organized as follows: In section 2 there is a brief description of the simulation design and the data sets used. Section 3 presents the main results and the conclusions are discussed in section 4.

2. Data and Methodology

The RegCM3 model used in this study is a limited area model and a detailed description can be found in Elguindi et al. (2004). The simulations were done for the SA domain (60°S-5°S and 84°W-15°E) from September 1989 to December 1994. Due to the spin-up time, the first three months of the simulations were excluded. A 60 km horizontal resolution and 18 vertical sigma levels are used. The initial and boundary conditions for the simulations were provided by the NCEP-DOE (National Centers for Atmospheric Research; Kanamitsu et al., 2002) reanalysis. The SST was specified by the mean monthly dataset of Reynolds and Smith (1995).

The WHOI and ECMWF data sets were used to validate the simulated values. The WHOI data set covers the Atlantic Ocean (64.5°S-64.5°N and 100.5°W-25.5°E) and correspond to daily averages with 1° of horizontal resolution from 1988 to 1999 (Yu et al., 2004). The variables obtained from the WHOI data set are a combination of the satellite data and NCEP and ECMWF analyses. From ECMWF, the ERA-40 global reanalysis (Simmons and Gibson, 2000) monthly means with 2.5° of horizontal resolution were used.

The turbulent flux parameterizations in the RegCM, WHOI and ECMWF data sets follow bulk aerodynamics algorithms developed, respectively, by Zeng et al. (1998), Fairall et al. (2003) and Beljaars (1995). These fluxes are calculated from near surface air temperature, specific humidity, wind velocity and SST. The equations to determine the turbulent fluxes are:

$$SH_0 = -\rho_0 c_p C_h U_r (T_r - T_s) \quad (1)$$

$$LH_0 = -\rho_0 L C_e U_r (q_r - q_s) \quad (2)$$

where the subscripts r and s indicate the height reference and surface values; ρ_0 is the air density; C_p is the specific heat at constant pressure, L is the latent heat of vaporization; C_h and C_e are the heat and moisture exchange coefficients, respectively; q_s is the saturation specific humidity at the surface. The reference height to the wind velocity (U) is 10 m and to air temperature (T) and specific humidity (q) is 2 m. The conventions used in (1) and (2) indicates that positive fluxes represent energy transfer from sea to atmosphere.

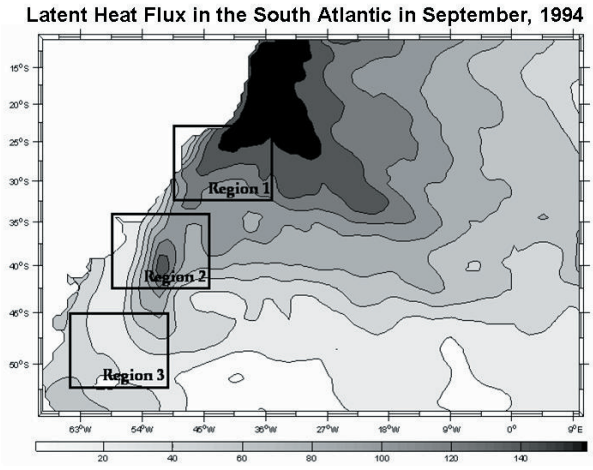

Figure 1. Mean latent heat flux from RegCM3 simulation for September 1994 over the SA domain. The boxes 1, 2, and 3 indicate the favourable regions to cyclone development. The RegCM values over the continent were not included in the averages.

Monthly mean values from 1990 to 1994 for the analysis (WHOI and ECMWF) and simulated results were calculated for a large area over the SA (69.5°W - 10.5°E and 54.5°S - 10.5°S) and also for the sub domains indicated in Fig. 1. These small regions represent the main areas favourable to cyclogenesis (Reboita et al., 2005) and correspond to: region 1 (32.5°S – 23.5°S and 49.5°W - 35.5°W) the south and southeast coast of Brazil; region 2 (42.5°S - 33.5°S and 59.5°W - 45.5°W) the area of the confluence of the Brazil and Malvinas ocean currents; region 3 (43.5°S - 52 .5°S and 51.5°W – 65.5°W) the Gulf of São Jorge to the east of the Argentine coast. The variables to be considered in the analysis are: latent and sensible heat fluxes, air temperature, specific humidity, wind intensity and SST.

3. Results

Figures 2 and 3 show the annual cycle of six variables averaged from 1990 to 1994 and for the SA Ocean main domain and the three small regions indicated in Fig. 1, respectively.

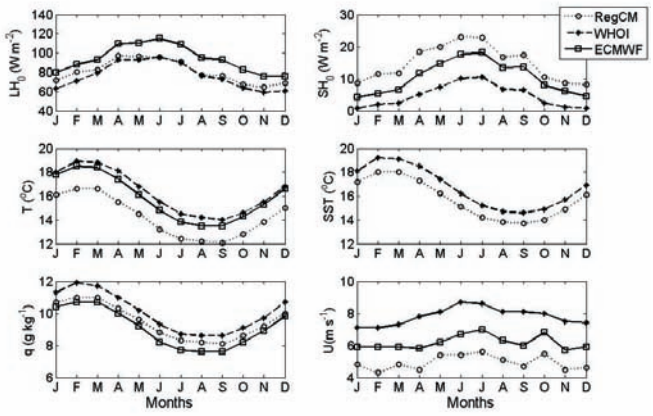

Figure 2. Monthly mean, from 1990 to 1994, of the: a) latent heat flux (W m–2), b) sensible heat flux (W m–2), c) 2 m air temperature (°C), d) SST (°C) - except for ECMWF, see text, e) 2 m specific humidity (g kg^{-1}), and f) 10 m wind intensity (ms^{-1}) for RegCM3 (dot line), WHOI (dashed line) and ECMWF (continuous line).

One important result observed from Fig. 2 is that the RegCM was able to simulate the WHOI and ECMWF annual cycle for all variables, though with different intensities. By the end of the austral winter and beginning of the spring (August-September) the simulated and analyzed latent and sensible heat fluxes (Fig. 2a-b) are almost constant over the South Atlantic Ocean. Throughout the year the RegCM latent heat flux intensity is similar to the WHOI but lower than the ECMWF analysis. On the other hand, the sensible heat flux is overestimated by the RegCM (Fig. 2b) though it has an annual cycle very similar to the other two datasets. The modeled latent heat flux has its maximum in April while for the WHOI and ECMWF it occurs in July. The RegCM air temperature (Fig. 2c) is colder than both analyses while the specific humidity (Fig. 2e) is more moist than ECMWF and drier than WHOI data set. An important difference of around ~1°C is apparent between WHOI and RegCM SST data (Fig. 2d). This difference may occur because of the different methodologies used in the generation of the WHOI and Reynolds and Smith (1995) SST data. As will be discussed in the next section, this difference may influence the general results of the heat flux calculated by the model. Throughout the year the RegCM underestimates the wind intensity when compared to the WHOI and ECMWF analysis, reaching its minimum during the summer.

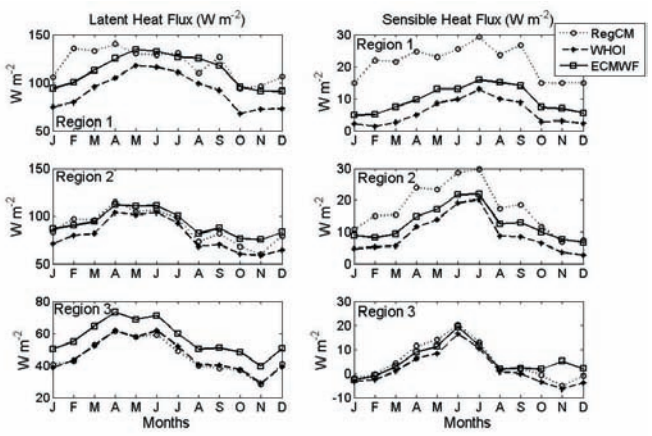

Figura 3. Monthly mean, from 1990 to 1994, of the latent and sensible heat fluxes (W m^{-2}) of the RegCM3 (dot line), WHOI (dashed line) and ECMWF (continuous line) for the regions 1 to 3 indicated in Figure 1.

For the three-cyclogenetic regions (see Fig. 1) the most notable differences between the simulated and analyzed sensible heat fluxes (Fig. 3 b-d-f) occur at lower latitudes where the RegCM shows large intensities. At middle latitudes (Fig. 3f) the simulated values are very close to both analyses, but from October to February there is indication of energy transfer from the atmosphere to the ocean in the RegCM and WHOI data sets (Fig. 3f). For latent heat fluxes, at lower latitudes the RegCM values are closer to ECMWF (Fig 3a) and at middle latitudes are more similar to the WHOI (Fig. 3c), showing intermediate values in the region 2 (Fig. 3b).

Table 1 shows the annual latent and sensible heat flux bias for the three cyclogenesis areas. In general the RegCM overestimates WHOI latent heat flux in the sub-tropics and underestimates the ECMWF data in middle latitudes.

Table 1. Annual latent (LH_0) and sensible (SH_0) heat flux bias (W m-2) for the selected cyclogenesis areas depicted in Fig.1.

Regions	Bias WHOI		Bias ECMWF	
	LH_0	SH_0	LH_0	SH_0
Region 1	27.7	15.5	7.5	11.5
Region 2	8.8	8.2	-3.9	4.7
Region 3	-0.5	2.9	-11.2	-0.4

As mentioned before, for the SA domain (Fig. 2) the differences in the RegCM sensible heat flux are relatively larger than the latent heat flux when compared to the other two datasets. However they seem to decrease when one moves to higher latitudes as shown by Figs 3b-d-f. In fact, the differences between the simulated and analyzed sensible heat fluxes at the various sub regions (Fig. 3) and for the SA domain (Fig. 2), in accordance with equation (2), could be attributed to three factors: wind intensity, turbulent exchange coefficient or temperature vertical gradients. As shown in Fig. 2 and for the sub regions 1 to 3 (Figs. not shown), the simulated wind intensities are smaller than the WHOI and ECMWF analyses. Therefore, according to eq. 2 this would lead to a less intense simulated sensible heat flux. In order to explain the high sensible heat flux values and assuming that Ch does not vary

too much it is the temperature vertical gradient that will play the most important role.

The differences between 2 m air temperature and SST (Tr - SST) for the WHOI and RegCM datasets for the SA domain and the three sub regions are presented in Fig. 4. The ECMWF data were not included because the SST is unavailable at the present. From Fig. 4 one can clearly see that the temperature vertical gradient in the WHOI data set is much smaller than in the RegCM for the SA and regions 1 and 2, respectively, explaining the large values of the simulated sensible heat flux. However, for region 3, the temperature vertical gradients are similar which explain the closeness of the values found before in the model simulation and WHOI analysis (Fig. 3f).

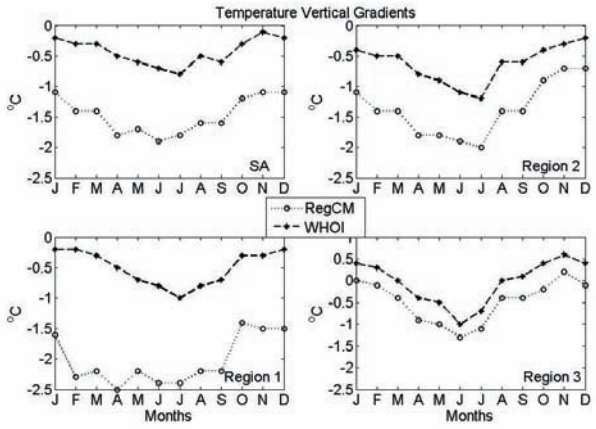

Figura 4. Temperature vertical gradient of the RegCM3 (dots line) and WHOI (dashed line) to the SA domain and the regions 1 to 3.

4. Conclusions

The latent and sensible heat fluxes estimated from WHOI and ECMWF analyses were compared to the simulated values from the RegCM model. Monthly mean data from 1990 to 1994 over the South Atlantic Ocean, and for three cyclogenetic selected areas were used. The analysis of such fluxes is important if one wants to better understand and simulate cyclogenesis near to the South American coast.

The annual cycle was well simulated by the model when compared with the WHOI and ECMWF analyses. For the SA domain, the intensity of the latent heat flux is more similar to the analyses values than the sensible heat flux. When compared to the WHOI data set, the sensible heat flux is overestimated by the model. However it is shown that this result is due to more intense vertical temperature gradients found in the model simulations because of the different intensities in the SST data sets used.

The simulations seem to have a latitudinal dependence. Large differences are found in relation to the WHOI and ECMWF data sets at low latitudes, but they become smaller in the middle latitudes.

Although the simulations of the RegCM3 have shown good skill when compared with the datasets used in the present diagnostics, one must be very cautious before drawing any general conclusions, since the real model validation can only be made with observed data. However, the present study is important, for example to provide confidence on the current cyclogenetic modeling studies under development in the GrEC/USP (Climate Studies Group – University of São Paulo).

5. Acknowledgments

The authors would like to acknowledge Prof. Dra. Jacyra Soares for some helpful suggestions during the development of this study and the WHOI and ECMWF for providing the data sets. We also thank FAPESP -04/02446-7 and CNPq - 475281/03-9 for financial support. The RegCM3 was provided by the Weather and Climate Physics Group of the ICTP (International Centre for Theoretical Physics).

6. References

Beljaars, A. C. M., 1997: Air-sea interaction in the ECMWF model. Proc. Seminar on Atmosphere-Surface Interaction. Reading, United Kingdom, ECMWF, 31-52.

Elguindi, N., X. Bi, F. Giorgi, B. Nagarajan, J. Pal, and F. Solmon, 2004: RegCM Version 3.0 User's Guide. PWCG Abdus Salam ICTP, 48 pp.

Fairall, C. W., E. F. Bradley, J. E., Hare, A. A. Grachev, and J. B. Edson, 2003: Bulk Parameterization of Air-Sea Fluxes: Updates and Verification for the COARE Algorithm. *J. Climate,* 16, 571-591.

Gan, M. A., and B. V. Rao, 1991: Surface Ciclogenesis over South America. *Mon. Wea. Rev.*, 119, 293-302.

Kanamitsu, M., W. Ebisuzaki, J. Woollen, S. –K. Yang, J. J. Hnilo, M. Fiorino, and G. L. Potter, 2002: NCEP-DOE AMIP-II Reanalysis (R-2). *Bull. Am. Met. Soc.*, 83, 1631-1643.

Neiman, P. J., and M. A. Shapiro, 1993: The Life Cycle of an Extratropical Marine Cyclone. Part I: Frontal-Cyclone Evolution and Thermodynamic Air-Sea Interaction. *Mon. Wea. Rev*., 121, 2153-2176.

Nuss, W. A., and R. A. Anthes, 1987: A Numerical Investigation of Low-Level Processes in Rapid Cyclogenesis. *Mon. Wea. Rev*., 115, 2728-2743.

Reboita, M. S., R. P. Rocha, and T. Ambrizzi, 2005: Climatologia de Ciclones sobre o Atlântico Sul Utilizando Métodos Objetivos na Detecção destes Sistemas. In: IX CONGREMET, Congresso Argentino de Meteorologia, Buenos Aires, AR, October 3-7, 2005.

Reynolds, R. W., and T. M. Smith, 1995: A High Resolution Global Sea Surface Temperature Climatology. *J Climate*, 8, 1571-1583.

Saraiva, J. M. B., and P. L. Silva Dias, 1997: A case study of intense cyclogenesis of the southern coast Brazil: Impact of SST, stratiform and deep convection. Preprints, Fifth Conf. On Southern Hemisphere Meteorology and Oceanography, Pretoria, South Africa, *Amer. Meteor. Soc.*, 368-369.

Simmons, A. J., and J. K. Gibson, 2000: The ERA-40 Project Plan. ERA-40 Project Report Series No 1, ECMWF.

Vera C. S., P. K. Vigliarolo, E. H. Berbery, 2002: Cold Season Synoptic-Scale waves over Subtropical South América. *Mon. Wea. Rev.*, 130, 684-699.

Yu, L., R. A. Weller, and B. Sun, 2004: Mean and Variability of the WHOI Daily Latent and Sensible Heat Fluxes at in Situ Flux Measurement Sites in the Atlantic Ocean. *J. Climate*, 17, 2096-2118.

Weill, A., and Coauthors, 2003: Toward a Better Determination of Turbulent Air–Sea Fluxes from Several Experiments. *J. Climate,* 16, 600-618.

Zeng, X., M. Zhao, and R. E. Dickinson, 1998: Intercomparison of Bulk Aerodynamic Algorithms for the Computation of Sea Surface Fluxes Using TOGA COARE and TAO Data. *J.Climate*, 11, 2628-2644

Monitoring of Bottom Water Formation in the Southern Weddell Sea

S. Østerhus
Bjerknes Centre for Climate Research and Geophysical Institute, University of Bergen, Norway
Corresponding author: svein.osterhus@gfi.uib.no

The coldest and densest bottom water in the Southern Ocean abyss is produced in the southern Weddell Sea, Antarctica (see Fig. 1), making Antarctic Bottom Water (AABW) the densest water mass in the world oceans. The southern Weddell Sea is believed to contribute to at least 50% of the bottom water formed in the Antarctic (Orsi et al 1999, Foldvik et al 2004). Cooling and freezing on the shallow shelves produce High Salinity Shelf Water (HSSW) at the freezing point. Some of the HSSW cascades down the continental slope and contributes directly to bottom water production (see Fig. 2). In addition, some of the HSSW penetrates underneath the floating Ronne - Filchner Ice Shelf in the Southern Weddell Sea (Foldvik et al 2001) (see Fig.2 and 3). This water mass, termed Ice Shelf Water (ISW), becomes super-cooled and is observed to overflow the sill of the Filchner Depression at a rate of about 1.6 Sv (1Sv = 10^6 m^3s^{-1}) (Foldvik et al 2004). As it flows down the continental slope it forms a bottom plume which is deflected westwards because of the Coriol's force (see Fig.3). Here we believe that the bottom topography may give rise to different pathways; the upper part will descend at a moderate angle with the isobaths due to friction (Killworth 2001). Deep canyons and ridges (Fig.4) provoke other branches to descend more rapidly towards the deep Weddell Sea.

On its path down the slope the ISW plume mixes with overlaying water masses. These mixing processes are not well understood, but supercritical plume speeds and associated hydraulic jumps are believed to be important (Holland et al., 2002). On its way down the cold bottom plume increases its volume transport to more than 4 Sv. This is an upper estimate of the total production of Weddell Sea Bottom Water (WSBW) believed to be formed in the whole region. WSBW is a precursor to AABW.

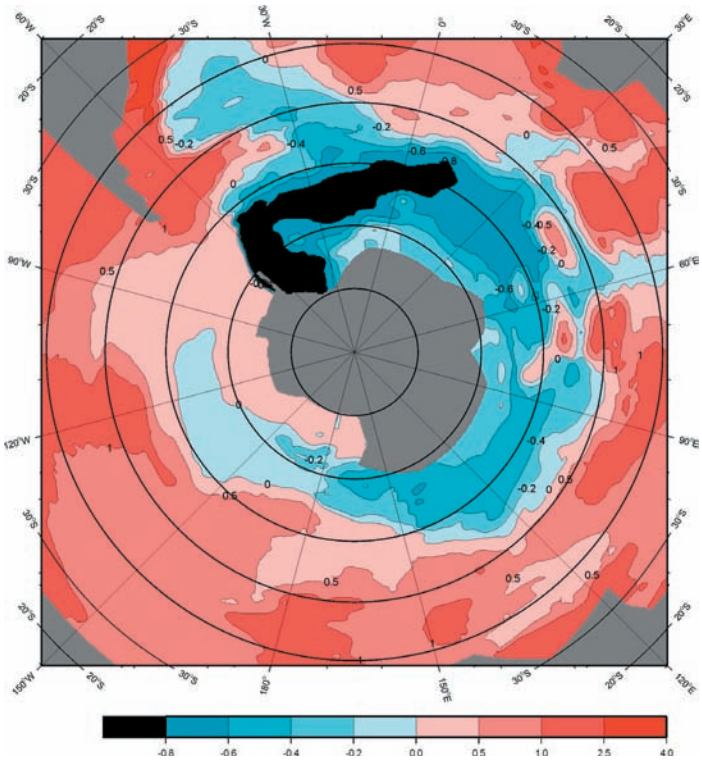

Fig. 1. Bottom temperature in the Southern Ocean (modified from early version of Orsi et al (2005))

To monitor the flow of the dense water from its formation areas toward the abyss of the world oceans is a key issue for climate research. For the Weddell Sea this means monitoring the formation of HSSW on the Ronne and Berkner shelf (Fig 3), the transformation to Ice Shelf Water (ISW) underneath the floating Filchner-Ronne ice shelf, the flux of ISW overflowing to the deep Weddell Sea, and its fate as it forms WSBW, and finally AABW.

In cooperation with British Antarctic Survey (BAS) we operate a number of instrumented moorings in the southern Weddell Sea. The monitoring system builds upon techniques and methods developed during several decades and has a proven record of high data return (Foldvik et al. 2004, Nicholls and Østerhus, 2004, Nicholls et al. 2004).

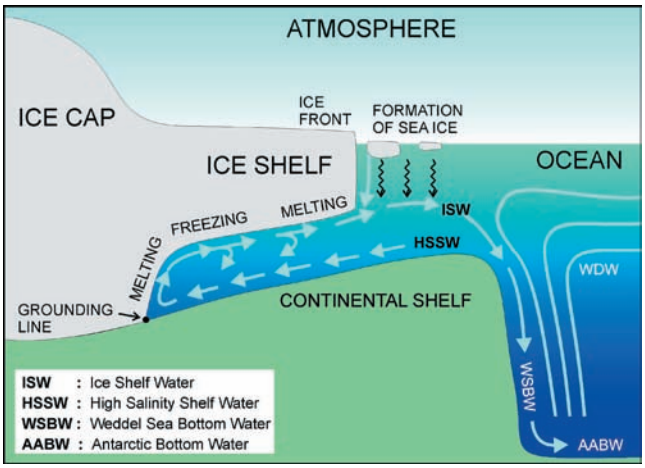

Fig 2. Schematic of the water masses formation, transformation and circulation

For the years to come we intend to integrate, extend, and operate our existing monitoring systems to increase our knowledge of the natural variability of the southern Weddell Sea, and to allow early identification of possible changes of regional or global importance. One such scenario may be the impact of a changing Antarctic Ice Sheet on the cooling of the world oceans, through changes in the formation of the extremely cold and dense water that ventilates the world ocean abyss.

The Ronne Ice Shelf monitoring

The ocean cavity beneath the Filchner-Ronne Ice Shelf is studied by a group of instrumented moorings deployed by hot water drilling through the ice shelf (Fig. 3).

Two sites were established by BAS in January 1999 (Fig. 1). At Site 4 (80°59.1'S. 051°36.4'W) and Site 5 (80°20.0'S, 054°36.4'W) the ice thickness were 941 m and 763 m underlain by 621 m and 402 m of water, respectively (Nicholls et al., 2001). The sites were instrumented with current meters and temperature and conductivity sensors. Results from the multiyear time series support the importance of monitoring the sub ice shelf processes and their sensitivity to changes in the ocean condition on the

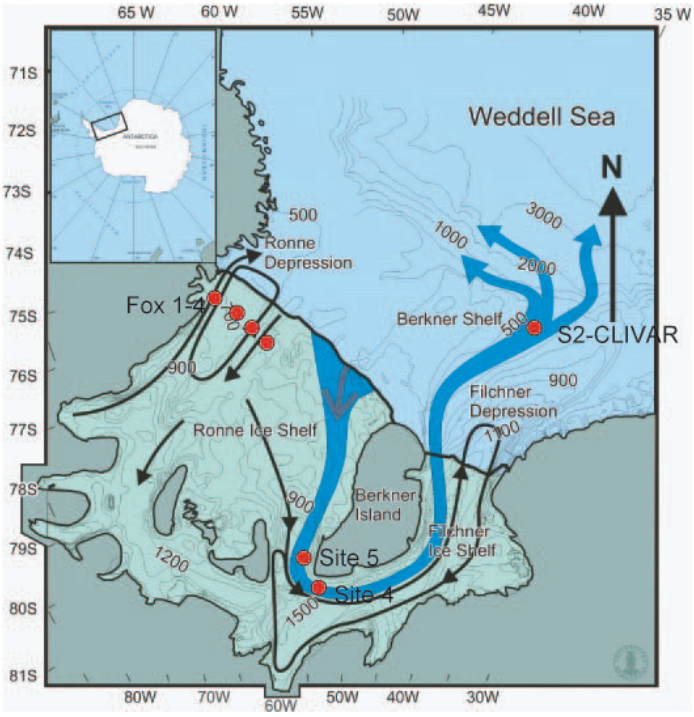

Fig 3. Bathymetric map of the southern Weddell Sea, Antarctica showing the vast shallow shelves in the Southern part. The arrows indicate simplified circulation in the cavity beneath ice shelf and the pathways for the ISW. The monitoring sites Site 4 and 5, Fox 1 to 4, and the S2 CLIVAR mooring on the Filchner sill.

Ronne shelf (Nicholls and Østerhus 2004). The Site 4 and 5 measurements were terminated in 2004 but new deployment may be proposed for the IPY.

The outflow of ISW at the ice front must have the same flux as the HSSW inflow, enhanced slightly by the admixture of glacial melt. ISW north of Filchner Ice Shelf has been observed flowing down the continental slope with a flux of the order of a Sverdrup (see Foldvik et al., 2004). An open question is what controls the strength of the flow? Nicholls et al. (2003) have shown that the rate of production of HSSW over the continental shelf appears not to be the primary limiting factor on the flow of HSSW into the cavity. Even at the end of summer HSSW dominates the Ronne Depression north of the ice front, one of the principal regions of HSSW inflow into the sub-ice shelf cavity. During the Antarctic season 2002/03 BAS made four (Fox 1-4) access holes through the ice shelf, allowing oceanographic instruments to be deployed (Nichols et al., 2004). The site locations were selected to be far enough south to avoid complex dynamical effects due to the presence of the large step-change in water

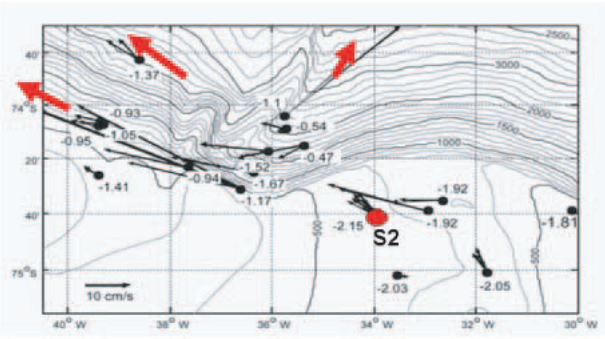

Fig. 4. Mean current vectors and bottom temperature from moored instruments.

column thickness imposed by the ice front. Using the ice shelf as a platform offers the logistical advantage of removing the need for repeat ship visits to service moorings in a region awkward to access because of difficult sea ice conditions. An additional advantage is that the moorings are safe from being dredged by icebergs. All sites are equipped with Aanderaa current meters and Sea Bird TS sensors (MicroCat), and are transmitting data in real time using ARGOS. Fox 3 and 4 are also equipped with thermistor strings to study the melting and freezing on the ice shelf base.

Long term monitoring of ISW overflow

After the discovery and mapping of the ISW overflow, instrumented moorings were deployed during the Norwegian Antarctic Expedition 1977/78, see Fig. 4 (Foldvik et al. 1985). The position for the mooring S2 proved to be a key site for monitoring the ISW overflow and is selected to be a part of the global net of monitoring sites under CLIVAR (www.clivar.org) and OceanSITES (www.oceansites.org).

Since the establishment of the S2 mooring a number of year-long time series (Foldvik et al. 2004) have been obtained. From 2003 the mooring is served on a biannual basis by the BAS ships supplying the Halley station.

We aim to continue and expand these measurements by replacing the old instrumentations by a new state of the art instrumented mooring. The mooring will be equipped with high quality sensors for water velocity, sea ice thickness and movement, temperature, salinity, and dissolved oxygen and at a later stage we will add sensors to measure carbon fluxes. The mooring will also be designed to carry an auto sampler (e.g. SF6).

References

Foldvik, A., T. Gammelsrød, and T. Tørresen (1985). Hydrographic observations from the Weddell Sea during the Norwegian Antarcic Research Expedition 1976/77. *Polar Research*, 3, 177--193.

Foldvik, A. and Gammelsrød, T. and Nygaard, E. and Østerhus, S. Current measurements near Ronne Ice Shelf: Implications for circulation and melting (2001), *Journal of Geophysical Research* 106, C3, 4463-4477.

Foldvik, A., T. Gammelsrød, S. Østerhus, E. Fahrbach, G. Rohardt, M. Schröder, K. W. Nicholls, L. Padman, and R. A. Woodgate (2004). Ice shelf water overflow and bottom water formation in the southern Weddell Sea. *Journal of Geophysical Research*, 109, C2, 10.1029/2003JC002008, C02015.

Killworth, P. D. (2001). On the rate of descent of overflows. *Journal of Geophysical Research*, 106, 22267--22275.

Nicholls, K.W., S. Østerhus, K. Makinson and M.R. Johnson, 2001. Oceanographic conditions south of Berkner Island, beneath Filchner-Ronne Ice Shelf, Antarctica. *J. Geophys. Res.*, 106(C6), 11,481-11,492

Nicholls K.W., L. Padman, M. Schröder, R. A. Woodgate, A. Jenkins, and S. Østerhus. (2003). Water mass modification over the continental shelf north of Ronne Ice Shelf, *Antarctica*, 108 , C8 3260, doi:10.1029/2002JC001713.

Nicholls K. W., L. Padman, and R. A. Woodgate (2004). Ice shelf water overflow and bottom water formation in the southern Weddell Sea. *Journal of Geophysical Research*, 109, C2, 10.1029/2003JC002008, C02015.

Nicholls, K. W. and Østerhus, S. (2004). Interannual variability and ventilation time scales for the ocean cavity beneath Filchner-Ronne Ice Shelf, Antarctica. *Journal of Geophysical Research*, C04014, doi:10.1029/2003JC002149.

Orsi, A. H., G. C. Johnson, and J. L. Bullister (1999). Circulation, mixing, and production of Antarctic Bottom Water. *Progress in Oceanography*, 43, 55-109.

Orsi, A.H., T. Whitworth III, Hydrographic Atlas of the World Ocean Circulation Experiment (WOCE). Volume 1: Southern Ocean (eds. M. Sparrow, P. Chapman, J. Gould), International WOCE Project Office, Southampton, U.K. ISBN 0-904175-49-9. 2005

Climate of Antarctica and the Southern Ocean (CASO): A Strategy for Climate Research for the International Polar Year

S. R. Rintoul
Antarctic Climate and Ecosystems Cooperative Research Centre, CSIRO Marine and Atmospheric Research
Corresponding Author: steve.rintoul@csiro.au

Southern Ocean processes have global reach. Ocean circulation and water mass formation in the Southern Ocean regulate the ocean storage and transport of heat, freshwater and anthropogenic carbon dioxide; link the upper and lower limbs of the global overturning circulation; and return nutrients to the surface ocean to support a large fraction of global productivity. Changes in Southern Ocean currents and sea ice can drive significant climate feedbacks. The circulation of the Southern Ocean reflects complex interactions between the atmosphere, ocean and ice, including the effect of oceanic and atmospheric teleconnections between low and high latitudes. The ice of Antarctica provides a unique record of climate variations on time-scales from 1-100,000 years. While the past decade has seen a rapidly growing appreciation of the role of the Southern Ocean and Antarctica in the global climate system, a lack of observations continues to hinder attempts to understand how the region drives and responds to climate change and variability.

The International Polar Year (IPY) provides an unprecedented opportunity to fill this gap. The Climate of Antarctica and the Southern Ocean (CASO) program provides a strategy to integrate climate research activities during the IPY. By pooling resources and taking advantage of new technologies, CASO aims to obtain the first synoptic, multi-disciplinary snapshot of the Southern Ocean region (including atmosphere, ocean, cryosphere and aspects of the biosphere).

The Climate of Antarctica and the Southern Ocean (CASO) program is organized into five themes, with the following objectives:

1. Antarctica and the Southern Ocean in the global water cycle: To quantify the high-latitude contributions to the global water cycle, determine the sensitivity of the water cycle to climate change and variability, and identify the impact of changes in the high latitude water cycle on the rest of the globe.
2. Southern hemisphere teleconnections: To understand the climate connections between low and high latitudes, including both atmospheric and oceanic pathways; determine the role of air-ice-ocean interactions in southern hemisphere variability and change; and assess the sensitivity of the modes of variability to future change.
3. Climate processes at the Antarctic continental margin: To improve our understanding and models of ocean-ice-atmosphere interactions and ice shelf stability; obtain a snapshot of the circumpolar distribution of the complex system of coastal, shelf and slope currents; quantify the production rate of Antarctic Bottom Water and implement an observing system; measure the circumpolar volume of sea ice.
4. Climate – ecosystem – biogeochemistry interactions in the Southern Ocean: To understand the impact of climate variability and change on Southern Ocean ecosystems, biodiversity and biogeochemical cycles, including the role of the Southern Ocean in the CO_2 cycle.
5. Records of past Antarctic climate variability and change: To use proxy records to determine the natural modes of climate variability on time-scales from years to millennia and improve our understanding of the mechanisms of abrupt climate change in the past, including the role of northern versus southern hemisphere.

Implementation

The scope of CASO is extremely broad and a more focused approach is required for implementation. IPY activities have been grouped into a number of clusters. CASO is taking the lead in the Antarctic Ocean Circulation cluster. The CASO cluster will be integrated closely with other clusters, including programs studying ocean circulation near the Antarctic margin (SASSI), biogeochemistry (GEOTRACES), sea ice, meteorology (ACAC), ecology (ICED-IPY) and paleoclimate (IPICS-IPY). The CASO cluster includes 25 individual projects and involves scientists from 18 nations.

The specific goals of the CASO ocean circulation cluster are:

1. To obtain a synoptic circumpolar snapshot of the physical environment of the Southern Ocean (collaboration with other IPY activities will extend the snapshot to include biogeochemistry, ecology, and biodiversity).
2. To enhance understanding of the role of the Southern Ocean in past, present and future climate, including connections between the zonal and meridional circulation of the Southern Ocean, water mass transformation, atmospheric variability, ocean-cryosphere interactions, physical-biogeochemical-ecological linkages, and teleconnections between polar and lower latitudes.

The field program to meet these goals will include:

1. A circumpolar array of full-depth multi-disciplinary hydrographic sections and XBT/XCTD sections, extending from the Antarctic continent northward across the Antarctic Circumpolar Current, including key water mass formation regions.
2. An enhanced circumpolar array of sea ice drifters, measuring a range of ice, ocean and atmosphere parameters.
3. Profiling floats deployed throughout the Southern Ocean, including acoustically-tracked floats in ice-covered areas.
4. Current meter moorings and pressure gauges to provide time series of ocean currents and water mass properties at key passages, in centres of action of dominant modes of variability, and in areas of bottom water formation and export.
5. Direct measurements of diapycnal and isopycnal mixing rates in the Southern Ocean.
6. Automatic weather stations, flux measurements in the

boundary layer and drifters to measure atmospheric variability (pressure, winds, heat and freshwater flux).

7. Environmental sensors deployed on marine mammals.

The observations will be integrated closely with modelling studies using a variety of approaches (coupled climate models; high resolution ocean-ice models; atmospheric models; tidal models; Lagrangian diagnostic studies).

Legacy

The legacy of CASO will include improved climate predictions, from models that incorporate a better understanding of southern polar processes; proof of concept of a viable, cost-effective, sustained observing system for the southern polar regions (including the ocean, atmosphere and cryosphere); and a baseline for the assessment of future change.

Further information

More information on IPY activities can be found at http://www.ipy.org . CASO plans and updated maps of proposed field work can be found on the Southern Ocean panel's web site http://www.clivar.org/organization/southern .

Synoptic Antarctic Shelf–Slope Interactions Study (SASSI) A project for IPY coordinated by iAnZone

K. J. Heywood
Chair, International Antarctic Zone programme (iAnZone), School of Environmental Sciences, University of East Anglia, Norwich NR4 7TJ, U.K.
Corresponding author: k.heywood@uea.ac.uk

Introduction

The SASSI project will conduct the first synoptic study of the Antarctic continental shelf and slope, as a multi-national contribution to the International Polar Year (IPY) (2007-2009). This is a critical and under-observed region for physical processes determining global climate. SASSI will be coordinated by the International Antarctic Zone (iAnZone) programme, a SCOR- and SCAR-Affiliated organisation. iAnZone's goal is to advance our understanding of climate-relevant processes within that region of the Southern Ocean poleward of the Antarctic Circumpolar Current. We maintain close cooperation with the CLIVAR/CliC/SCAR Southern Ocean Region Panel. The iAnZone website http://www.ldeo.columbia.edu/res/fac/physocean/ianzone/ provides further information.

SASSI was initiated at a three-day iAnZone open workshop in August 2004. An Expression of Interest (EoI) was submitted to the International Polar Year (IPY) in December 2004. SASSI was chosen to lead a cluster of 10 EoIs in preparation of a full bid, which was submitted in June 2005. The other EoIs enhanced the original project by adding other disciplines and techniques. A workshop to further develop SASSI was held at the iAnZone biennial meeting on 9th October 2005 in Venice, just prior to the Ross Sea conference (http://www.ross-sea.org/).

Background

The Antarctic continent, with its vast ice sheets that sequester much of the world's freshwater, is separated from the ocean by a complex peripheral system of coastal, shelf and slope currents and fronts. Freshwater that passes from the continent northward through this boundary influences the global ocean through its impact on formation of sea ice and of the dense water that drives shallow and deep modes of the meridional ocean circulation (MOC). These processes have a strong impact on global climate, both through the ocean (influencing the strength and properties of the MOC) and through the atmosphere (influencing the heat released to the southern hemisphere atmosphere). Quantitative knowledge of the moisture/freshwater budget is one of the greatest uncertainties in climate modelling, particularly in the southern hemisphere.

The few historical sections across the marginal ocean systems that surround Antarctica have shown varying characteristics. Some reveal simply a westward coastal current, others a complex system of coastal current, shelf break currents, and current jets deeper down along the continental slope. The currents and associated fronts, resulting from lateral gradients in temperature, salinity and density, form dynamic barriers that can control cross-shelf flow of properties. They influence turbulent mixing in the ocean over the continental slope and, by so doing, impact the depths to which dense bottom waters can penetrate. Strong tidal currents further interact with these currents and associated turbulent mixing. Through transport of heat beneath ice, these flows influence the rate of ice melting. These systems influence the intensity and distribution of the meridional fluxes of volume, heat and freshwater. In short, the Antarctic continental margins present both physical and dynamical barriers that impact oceanic meridional fluxes related to the Antarctic freshwater budget. Even existing coarse resolution coupled climate models now indicate a significant impact of Antarctic freshwater on global climate on time scales from months to centuries.

Despite considerable scientific interest and a strong conviction that the resident processes play significant roles in global climate, the Antarctic margins are neither quantitatively well documented nor dynamically well understood. Our present understanding is based on highly non-synoptic data obtained from widely different regions from different years under the auspices of projects having different, or even disparate, scientific goals. Obtaining synoptic data would be a polar science breakthrough, avoiding the confusion of spatial and temporal variability. Interannual variability, such as that associated with the El Nino-Southern Oscillation, Southern Annular Mode, or the Antarctic Circumpolar Wave, as well as secular change, means that adjacent years can exhibit completely different ocean, ice and wind fields, forcing different coastal systems and fluxes. The vast majority of the available data have been collected during the austral summer, when withdrawal of the seasonal sea ice cover allows access for non-ice-strengthened research vessels. Although seasonal coverage has been extended through the use of moorings and drifting buoys, winter shipboard programmes have been largely restricted to the Weddell Sea. Our documentation of seasonality in the shelf and slope currents and frontal systems is limited. Finally, geographical spacing of samples has frequently been too great to allow adequate assessment of the dynamically important features. IPY therefore offers a unique opportunity to focus our efforts on obtaining a synoptic data set that resolves, for the first time, the critical processes for climate.

Objectives

The SASSI objectives will be to:

1. Obtain a circumpolar synoptic view of Antarctic shelf and slope oceanography.

2. Assess quantitatively the properties and amount of inflow of warm, saline deep water onto the continental shelf, with a focus in regions known to be active sites for water transformation.
3. Assess the role of onshore oceanic heat transport in melting sea ice and ice shelves.
4. Determine where, when and how this oceanic inflow is transformed, through net cooling and freshwater fluxes during the seasonal sea ice melting/freezing cycle over the shelf domain into dense Shelf Water and its subsequent derivative Antarctic Bottom Water.
5. Assess the importance of ice shelves in the net upper ocean freshening process including iceberg calving and melting, and determination of basal melt rates.
6. Assess the importance of coastal polynyas to water mass transformations.
7. Better understand the dynamics of the coastal current and slope front systems, and how they influence the exchanges between sea ice, glacial ice, coastal and deep ocean waters.
8. Quantify freshwater transports around Antarctica through both currents and atmosphere-ocean-ice interaction.
9. Determine down-slope dynamics and associated meridional transports, integrating physical, geological and geophysical records with the currents in the bottom boundary layer.
10. Assess the degree to which present coupled ocean-ice models represent the shelf system and its variability.
11. Design a long-term monitoring system over the Antarctic continental margins that can act as an early indicator of global climate-related changes.
12. Identify key Antarctic shelf/slope processes that should be included or parameterised in future climate models.
13. Explore and document the geology, chemistry and biology of underwater volcanic hot vents.
14. Obtain a swath bathymetry map of the Antarctic continental shelf and slope, including beneath ice shelves.
15. Assess the role of the microbial biomass and processes in regulating the carbon biological pump efficiency for the carbon sequestration on the Antarctic continental shelf.
16. Understand the bio-optical processes that affect the ocean colour signal in the Southern Ocean.

Implementation Plan

Short synoptic transects will be undertaken circumpolarly radiating outwards across the Antarctic continental shelf and slope (Figure 1). To be as synoptic as possible, all sections should be undertaken within the target austral summer period of January-March 2008. Winter coverage will be achieved through mooring array deployments (Figure 2; recoveries in early 2009) and remote sensing, where possible. The sections will link on the landward side with any IPY transcontinental transects that may be undertaken for glaciological and meteorological studies. Coordination with these land transects will be appropriate in order to best encompass ice shelf processes. On the seaward side, the SASSI sections will be coordinated with CASO transects (see previous article) proposed for monitoring the Antarctic Circumpolar Current (ACC). (Indeed it is likely that in some instances the same shiptime and scientists will accomplish both, and we will encourage that). Station spacing will be sufficiently tight – similar to or less than the internal radius of deformation in the shelf-slope region – to identify, and resolve where feasible, pertinent shelf and slope features. Of special interest will be the possibility to detect and estimate the transport of newly-formed dense bottom waters flowing westward along the continental slope, to better understand the connections between known deep water sources and the locations where deep water leaves the slopes to flow north. Transects will incorporate insofar as possible:

* Closely-spaced full depth CTD/ADCP stations plus profiles of PAR irradiance, bio-optical properties and fluorescence.
* Collection throughout the water column at stations of water samples for tracer, chemical and biological analyses including oxygen isotopes, carbon parameters, inorganic and organic nutrients and trace gases, and for biomass on deck incubation experiments to evaluate auto and heterotrophic activities.
* Deployment of moored instruments along each transect to measure temperature, salinity, current velocities, sedimentary fluxes and sea level for at least one year.
* Deployment on the shelf of autonomous water samplers to collect weekly samples for tracer analyses.
* Deployment of ice-hardened surface ocean drifters across the coastal and slope break current systems, measuring temperature, salinity, sea level pressure and location.
* Air-sea heat and freshwater flux and meteorological measurements.
* Swath bathymetric surveys of the complex shelf and slope terrain, both to assess local circulation and mixing processes, and to detect geological/glaciological phenomena such as iceberg scour.
* Sedimentological observations including coring and biostratigraphy.
* Turbulent mixing measurements.
* Continuation of hydrographic sections poleward beneath ice shelves and/or sea ice using autonomous underwater vehicles (AUVs) and hot-water drilled access holes.
* Use of AUVs to measure sea ice thickness distribution on the Antarctic shelf and slope.
* Use of autonomous underwater vehicles and/or instrumented pelagic marine mammals to penetrate beneath sea ice and ice shelves to measure hydrographic and dynamical properties, marine geological, chemical and biological characteristics.

Additionally:

- We will deploy subsurface Lagrangian floats to be tracked acoustically beneath the seasonal sea ice throughout the winter. These will provide profiles of temperature and salinity, and geographical location, every 10 days. Plans are already in hand to ensonify the Weddell Sea, the offshore region of the Wilkes-Adelie Land and the western margin of the Antarctic Peninsula, to enable use of such floats. Extension of this tracking network to other regions surrounding Antarctica will be undertaken through SASSI to provide polar coverage to the global Argo programme.
- Visible, passive microwave and synthetic aperture radar remote sensing will be used to assess the seasonal/interannual variability of circumpolar coastal polynyas and of phytoplankton biomass. SAR, passive microwave and Cryosat altimetry will allow large scale monitoring of sea ice.
- Numerical models will be developed to quantitatively study heat & freshwater fluxes and water mass transformations, and impacts of large iceberg calving events, processes of exchange between ice shelves and the open ocean, tides,

biogeochemical cycling of C, N and P, short-term mesoscale instabilities, mixing processes and mass transports associated with gravity plumes across sloping bathymetry. Coupled ice-ocean models will be analysed, and will assist in developing parameterisation for climate models.

- Hot-water drilling through floating ice shelves will allow sub-ice-shelf CTD profiling and mooring deployment, together with acoustic determinations of basal melt rate.

Conclusions

SASSI will leave a legacy of a design for an observing system on the Antarctic margin for future multidisciplinary studies; the first circumpolar synoptic data set on the Antarctic continental margin against which future changes can be assessed; the first simultaneous circumpolar time series including winter; and a network of links between iAnZone and other disciplines to foster future science.

We will particularly welcome nations new to Antarctic research who wish to use IPY to develop their own expertise, for example by participating in short sections on their own vessels or those of other nations. Those with limited resources might wish to participate simply by contributing floats or drifters. The short hydrographic sections are specifically designed so that nations with only limited science time or expertise available on Antarctic supply vessels can make a full and important contribution. If you are interested in getting involved in SASSI, please contact me. To subscribe to the ianzone mailing list, send a message to majordomo@ldeo.columbia.edu with the following 2-line message:

subscribe ianzone

end

Updated versions of the map showing planned sections and mooring deployments are being maintained at http://www.uea.ac.uk/~e280/sassi.html, together with other useful links.

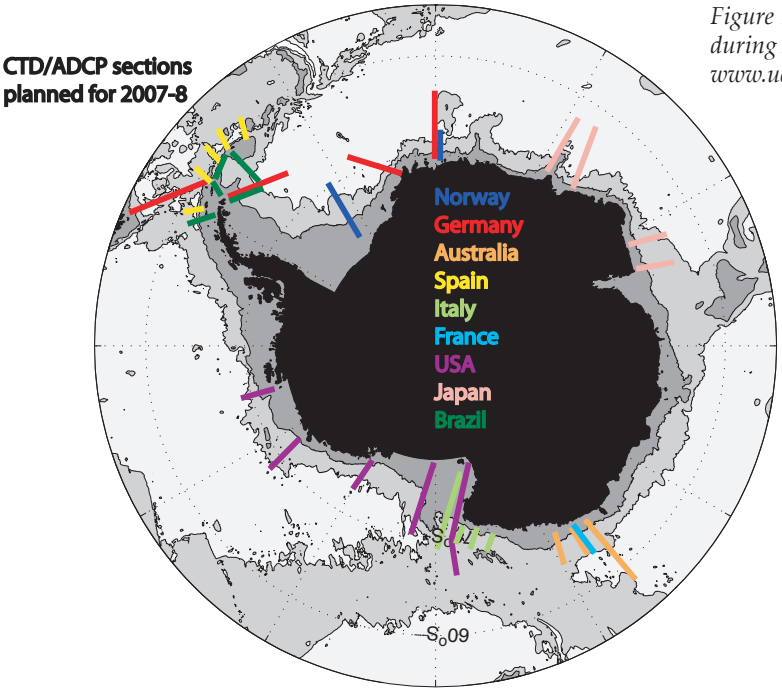

Figure 1. Plans for SASSI CTD/ADCP sections around Antarctica during 2007-2008. An updated version is being maintained at http://www.uea.ac.uk/~e280/sassi.html.

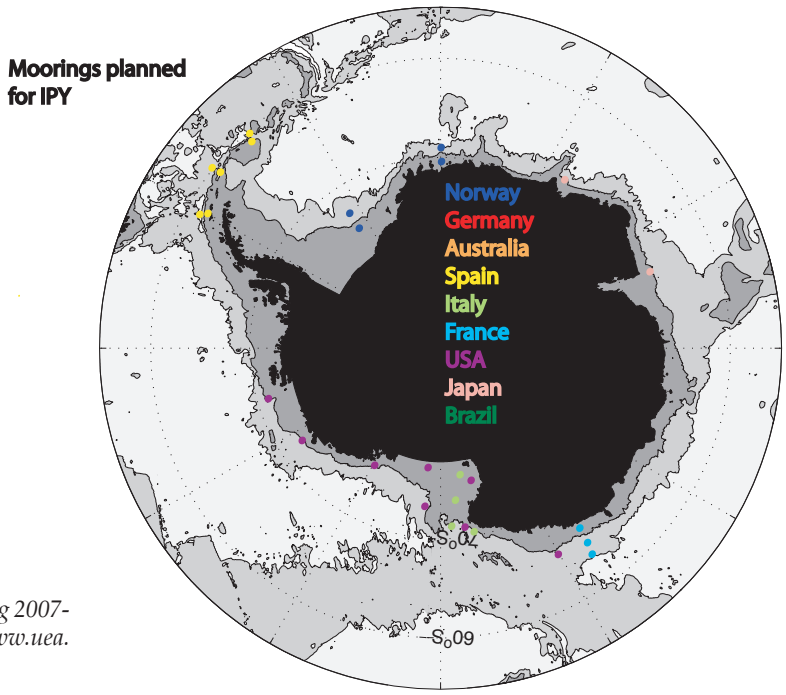

Figure 2. Plans for SASSI moorings around Antarctica during 2007-2009. An updated version is being maintained at http://www.uea.ac.uk/~e280/sassi.html.

The Surface Ocean Lower Atmosphere Study (SOLAS) and the International Polar Year

R.G.J. Bellerby[1], C. Ryan[2], J. Hare[3] and P. Liss[3]
[1]Bjerknes Centre for Climate Research, University of Bergen, Norway.'
[2]School of GeoSciences, University of Edinburgh, Edinburgh, UK
[3]SOLAS International Project Office, School of Environmental Sciences, University of East Anglia, UK
Corresponding author: richard.bellerby@bjerknes.uib.no

In readiness for the International Polar Year (IPY), the Surface Ocean Lower Atmosphere Study (SOLAS) is co-ordinating international plans to optimise high latitude SOLAS research. Although bi-polar in ambition, the SOLAS IPY activities will initially be co-ordinated from individual perspectives: large parts of SOLAS IPY science are being co-ordinated through the OASIS program (http://www.oasishome.net/) and Antarctic SOLAS IPY through this present initiative. It is planned to later amalgamate the information from the two to form a complete high-latitude picture of SOLAS research.

The aim of SOLAS is to "achieve quantitative understanding of the key biogeochemical-physical interactions and feedbacks between the ocean and the atmosphere, and of how this coupled system affects and is affected by climate and environmental change" (SOLAS, 2004). This objective will be achieved through the foci and activities detailed in Figure 1.

The current objective of the central SOLAS IPY plan is to gather together the jigsaw pieces of planned SOLAS activities to form a coherent picture from which we can integrate actions to provide a holistic and synoptic understanding of high latitude ocean-atmosphere interactions. Importantly for the most effective use of research platforms, through collaboration with other international research programmes it will be possible to co-ordinate cross-disciplinary research such that SOLAS scientists complement, and profit from, science done under other work programmes.

Due to the multidisciplinary nature of research performed under most ocean and atmosphere studies, there will be also be opportunities for utilising information gained under non-SOLAS umbrella IPY programs that may be used to obtain a complete picture of Antarctic processes. Accordingly, the SOLAS IPY would benefit from input from other IPY frameworks identifying where proposed research would augment the research foci detailed in Figure 1. For example, agreement has been made with the SASSI (http://www.uea.ac.uk/~e280/sassi.html) and CASO (http://www.ipy.org/development/eoi/proposal-details.php?id=132) projects to liaise during further project development to facilitate the identification of mutually beneficial research and the possible inclusion of SOLAS activities. Other planned IPY projects are encouraged to contact the corresponding author to determine potential research collaboration.

References

SOLAS Scientific Steering Committee. 2004. The Surface Ocean - Lower Atmosphere Study: Science Plan and Implementation Study. Stockholm, Sweden :IGBP Secretariat , 85 p. (IGBP Report ; 50).

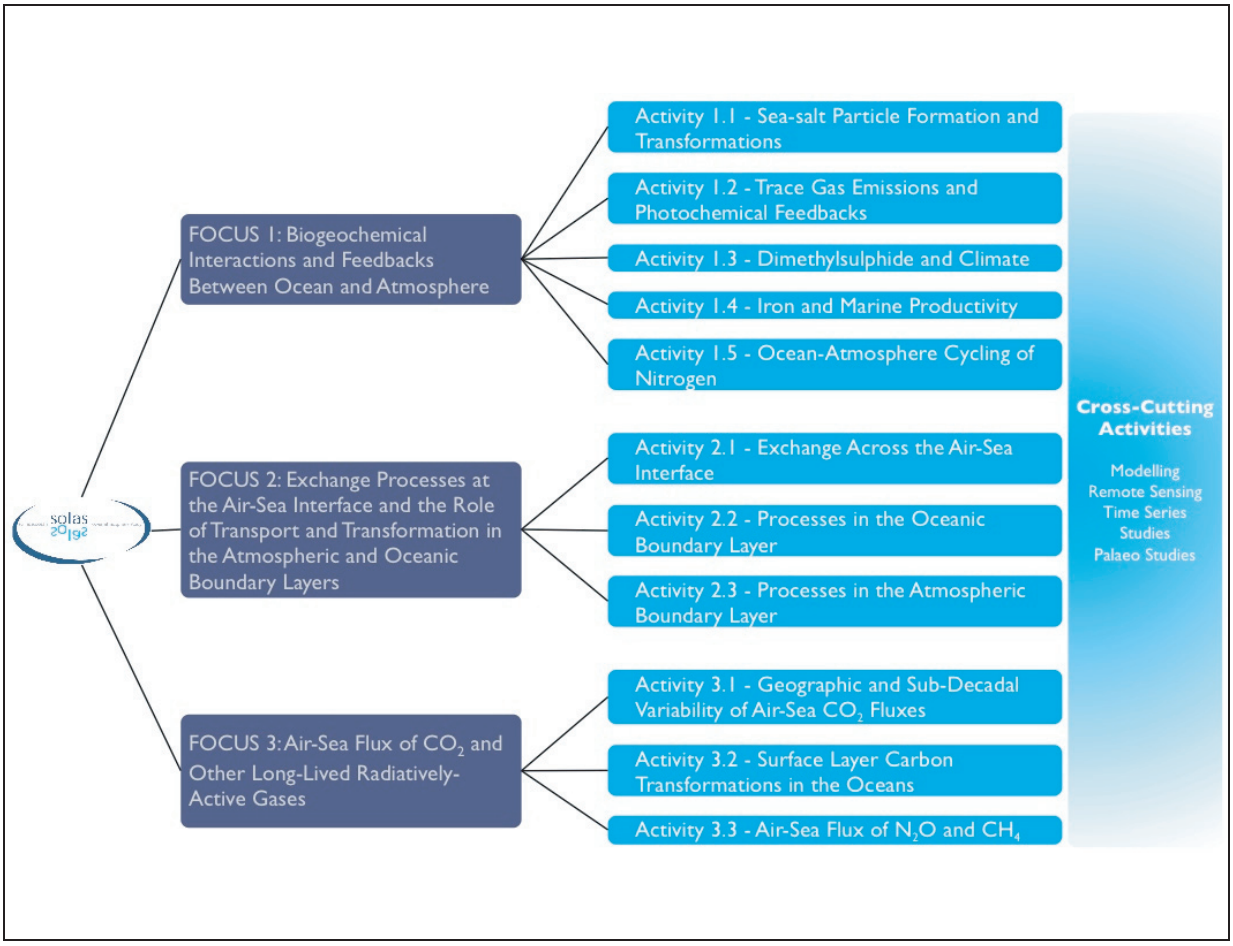

Southern Ocean Carbon Dioxide Studies

W.R. McGillis
Geochemistry and Earth and Environmental Engineering Columbia University, USA
Corresponding author: Wade McGillis (wrm2102@columbia.edu)

Goal:

To understand air-sea flux of CO_2 and other long-lived radiatively active gases

Natural and anthropogenic changes in climate and global biogeochemistry will alter the air-sea exchange of CO_2 and other long-lived radiatively active gases, which may cause changes in the rate of uptake by the oceans. Understanding physical and biogeochemical processes at the air-sea interface is critical for predicting the air-sea exchange of gases and determining how these processes will affect and be affected by global change.

Major Scientific Questions:

The following questions address major issues that require resolution in the SOLAS Science Plan and Implementation Strategy:

- What is the sensitivity of air-sea CO_2 flux to climate-related changes in physical forcing?
- How do biogeochemical cycles and air-sea CO_2 fluxes respond to the dominant modes of interannual variability?
- How do biogeochemical cycles and air-sea CO_2 fluxes respond to changes in individual components of the meridional overturning circulation (e.g., bottom water formation; intermediate/mode water formation; cross-frontal exchange).

Project Description:

The Southern Ocean south of 46°S covers 16% of the world's oceans and ventilates about half of the deep ocean waters. Regional measurements based on measurement of surface water pCO_2 suggest this region is a large sink of carbon (Takahashi et al., 2002; Figure 1), but atmospheric inversions suggest significantly smaller sink of only 0.4 Pg C yr-1 (Gurney et al., 2002). Currently large uncertainties in the air-sea flux of CO_2 prevent an accurate quantification of the partitioning of anthropogenic CO_2 between the ocean and the terrestrial biosphere on interannual timescales, based on surface water measurements. This limits our ability to realistically model future atmospheric CO_2 levels. Uncertainties of ~50% are associated with the current global and regional air-sea flux estimates because of inadequacies in the gas transfer parameterizations. Prognostic model estimates are equally uncertain. Aside from uncertainty in the gas transfer parameterization, significant uncertainty stems from the paucity of measurements in the Southern Ocean. Consequently, the Southern Ocean is of vital importance for the study of air-sea gas exchange and there is a need to concentrate on measuring CO_2 fluxes directly in the marine air boundary layer and to elucidate the physical, chemical, and biological processes that will allow for parameterizations of gas exchange from physical forcing. Physical forcing data such as wind, wave slope, and wind stress for the region can be obtained through remote sensing and sustained in situ observations.

Until recently, the gas transfer velocity was determined exclusively from indirect measurements based on mass balance techniques in the surface mixed layer. The techniques utilized natural or deliberate tracers that yielded gas transfer velocities averaged over periods of days to weeks. The successful improvement of direct flux techniques now makes it possible to measure the flux and determine gas transfer velocity from collocated ΔpCO_2 measurements on the timescale of the variability of the forcing (on the order of 1 hour). Fairall et al. (2000) demonstrated important technical improvements that now allow direct flux measurements of CO_2 over the ocean, alleviating previous shortcomings as described in Broecker et al. (1986). Advances in direct flux measurement techniques and airside gradient and covariance measurements have decreased the temporal scale to hours and spatial scale to below 1 kilometer. Successful examples include the ocean-atmosphere direct covariance method for CO_2 (McGillis et al., 2001a; McGillis et al., 2004;) and the gradient method for DMS (dimethylsulfide) (McGillis et al., 2001b). The ability to measure transfer velocity locally in the field now provides the tools to properly relate the gas transfer to the appropriate forcing function. However, wind parameterizations will continue to be used extensively in the near future, both because wind is an important driver of surface turbulence controlling gas transfer and because synoptic measurements and assimilation

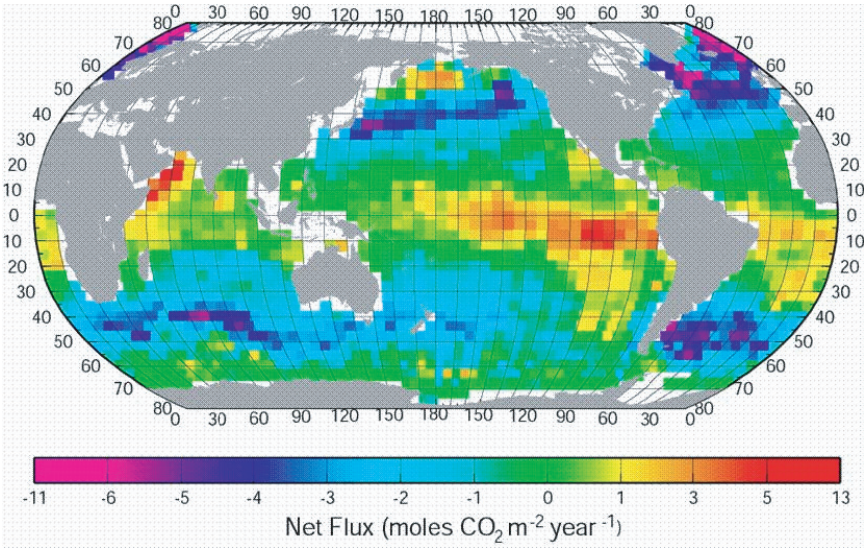

Figure 1: Air-sea CO_2 fluxes from Takahashi et al., (2002).

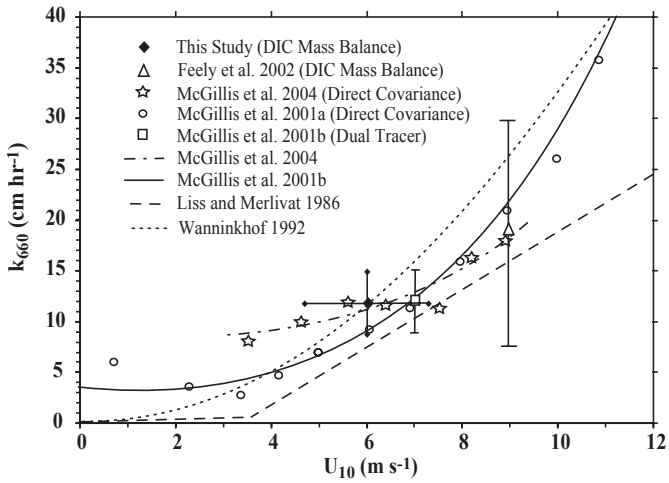

Figure 2: Comparison of gas exchange measurements and models.

products of wind speed are readily available. Improvements in these parameterizations, especially in our ability to apply the relationships, are critically needed for the high-wind regimes of the Southern Oceans.

Previous process studies to improve quantification of air-sea CO_2 fluxes and gas transfer velocity were initiated in the late 1990s by NSF and NOAA and focused on the determination of gas transfer velocities on a regional scales. For example, the GASEX-98 experiment occurred in the CO_2 sink region of an anticyclonic warm core ring in the eastern North Atlantic during May and June of 1998 (Wanninkhof and McGillis, 1999; McGillis et al., 2001a; McGillis et al., 2001b; Feely et al., 2002). A second study, GasEx-2001, took place in the eastern Equatorial Pacific in February and March, 2001 (McGillis et al., 2004; Sabine et al., 2004). The contrasting conditions of a large CO_2 sink and high winds in the North Atlantic, and low annual mean wind speeds and high ΔpCO_2 values in the Equatorial Pacific, offered a unique opportunity to compare the fluxes in these environments and to elucidate the factors controlling the flux. Although the measurements show some agreement at low wind speeds, there is considerable variability in the transfer rates at high wind speeds (Fig 2). These differences result in a large uncertainty of the Southern Ocean CO_2 sink.

The overall objective for the gas exchange study is to quantify air-sea gas fluxes over the unique range of oceanographic, atmospheric, and biogeochemical conditions in the Southern Ocean. This includes obtaining an improved understanding of processes governing air-sea fluxes to adequately constrain and predict the fate of CO_2 in the surface ocean and lower atmospheric boundary layers. This effort will improve the measurement, modeling, and remote-sensing capability in the Southern Ocean CO_2 region. Table 1 provides a list of the research components for a gas exchange study.

To address these issues we propose an experiment to be carried out in the Southern Ocean focusing on two primary objectives:

Target 1: Quantify the net air-sea CO_2 flux in the Southern Ocean.

The critical issue is to improve coverage of the regional estimates of air-sea CO_2 fluxes and to establish factors regulating ΔpCO_2 (i.e., deep winter convection; warming/cooling/mixing of surface waters; biological utilization of nutrients) and CO_2 flux (i.e., bubble production and turbulence, near surface shear and micro breaking, Langmuir circulations, stratification, and surfactants). The Southern Ocean gas exchange experiment should focuses on enhancing the understanding of air-sea CO_2 fluxes and the processes controlling them. The primary goal is to measure air-sea CO_2 fluxes, the surface physical processes, and the surface biogeochemical processes controlling CO_2 fluxes over short (≈hourly) time scales. This effort will provide necessary knowledge for remote sensing and modeling efforts by understanding how gas transfer could be parameterized at small time and space scales. Of the available techniques for measuring air-sea CO_2 fluxes, atmospheric boundary layer micrometeorological CO_2 flux approaches (direct covariance and gradient methods) are best suited for measuring fluxes over short time scales. In these methods, the gas flux is measured directly with averaging times on the order of 0.5 hrs to 3 hrs. The field study using micrometeorological measurements (direct covariance, gradient flux and eddy accumulation methods) would also be aided by water column methods of measuring gas exchange with purposeful and/or natural tracers that yield flux

Table 1. Southern Ocean Air-Sea CO_2 Flux Experiment

	Research Project Component	Process and Method Components
1	Biological Measurements	Primary production; New production
2	Surface pCO2 Variability	Surface CO2 and O2 variability; carbon modeling; SAMI; CARIOCA; free rising temperature profiler
3	Core CO2 and Hydrographic Measurements,	DIC; pCO2; CTD, spatial and temporal CO2 flux footprint.
4	Sea Surface Roughness	Shipboard Radars. Buoy based small–scale waves.
5	Bulk Meteorology and Turbulent Fluxes	Atmospheric boundary layer physics/meteorology; turbulent fluxes of momentum, Water vapor, temperature, IR, Solar
6	IR Remote Sensing	IR heat flux; ocean skin temperature; microbreaking processes. Active Infrared techniques
7	Shipboard CO2 Fluxes	Air–sea gas flux systems; ship mast
8	Surface Ocean Processes	Directional wave field; currents; atmospheric CO2 gradients; oceanic surface turbulence, oceanic shear, oceanic stratification, bubbles, large waves, Langmuir cells, aerosols.
9	Nutrients	Nutrient and oxygen
10	Deliberate Tracers	SF_6 and ^3He

estimates on daily to weekly timescales. Modeling components could be proposed and begun at any time.

Target 2: Determine the sensitivity of Southern Ocean CO_2 uptake to climate variability and climate change, particularly in response to anticipated increase in stratification.

The approach is to design and deploy an early detection system of physical and chemical parameters that will collect records of sufficient length to distinguish between climate change and climate variability. This sustained phase of the study will include the deployment of moorings, gliders and floats capable of making the appropriate physical and biogeochemical measurements required to detect secular trends and provide input into prognostic models. The data will be utilized to provide reliable projections of future trends through model development and model-data comparisons. Verification on a regional scale will be accomplished by comparing outputs of oceanic and atmospheric inverse models which yield estimates of fluxes based on oceanic and atmospheric measurements, respectively. The results of this study will also be used in data assimilation routines. The technology for the field program is presently available, and the experiment could take place with a two-year lead-time.

International Interactions:

Many of the activities proposed in this effort are complementary to a number of international program objectives, in particular CLIVAR, IMBER and LOICZ. Each of the programs addresses a specific issue of ocean carbon within the framework of other ocean science topics. For example, SOLAS focuses on the air-sea exchange of CO_2, CLIVAR focuses on large-scale climate variability and physical ocean feedbacks, IMBER focuses on carbon transport, storage, and transformations, and LOICZ focuses on coastal carbon fluxes.

Needs Required For Research:

- NOAA RV Ronald H. Brown

Project Authors:

Richard A. Feely (Richard.A.Feely@noaa.gov)

Wade McGillis (wrm2102@columbia.edu)

Chris Sabine (Chris.Sabine@noaa.gov)

Rik Wanninkhof (Rik.Wanninkhof@noaa.gov)

Possible Funding Sources:

NSF (Atm Chem); NOAA (OGP); NASA; DOE; IOC.

Reference:

McGillis, W. R.; J. B. Edson; C.J. Zappa; Ware, J. D.; McKenna, S. P.; Terray, E. A.; Hare, J. E.; Fairall, C. W.; Drennan, W.; M.Donelan; DeGrandpre, M. D.; R.Wanninkhof; Feely, R. A., Air-sea CO_2 exchange in the equatorial Pacific. *J. Geophys. Res* 2004, 109, doi:10.1029/2003JC002256.

Update on GEOTRACES

P.N.Froelich[1], R. Anderson[2], G.M. Henderson[3],
[1]Dept of Oceanography, Florida State University, USA
[2]Lamont–Doherty Earth Observatory, USA
[3]Environmental Earth Sciences, Oxford University, UK
Corrresponding author: froelich@magnet.fsu.edu

The International GEOTRACES Project began as an outgrowth of marine geochemists' desire to extend the legacy of the GEOSECS program of the 1970s - to expand our knowledge of the biogeochemistry and chemical cycles of trace elements and isotopes (TEIs) that were impossible to measure in the ocean thirty years ago. GEOSECS (Geochemical Ocean Sections) led directly to important breakthroughs in understanding ocean circulation using geochemical tracers, plus the broader cycles of carbon, nutrients and a few trace elements. By demonstrating the power of ocean tracers, GEOSECS was the grandfather of projects such as TTO, WOCE, and JGOFS. The advent of new analytical technologies to measure vanishingly small concentrations of trace elements and their isotopic signatures, plus clean ocean sampling techniques to provide faithful samples for measurement, provides a timely opportunity to describe the global distributions of the biologically-important trace elements, their isotopic signatures, and the processes controlling their distributions. The importance of many TEIs as tracers of oceanic processes, as co-factors for critical biological processes, and also as monitors for operation of the carbon cycle, is now well accepted. Yet for many TEIs our knowledge of their first-order oceanic distributions and the processes controlling these distributions is virtually non-existent. To develop the full power to utilize these new generation biogeochemical TEI distributions to infer past and future changes in ocean biogeochemical processes and oceanic health requires a global assessment of the current patterns.

The primary motivations for GEOTRACES are thus to:

- determine the role of micronutrients in ocean biogeochemistry (N, P, Si, Fe, Zn, Mo, Cd....)
- establish the impact of these trace elements on the carbon cycle and on rates of carbon cycle processes
- develop new tracers of ocean processes – vertical and horizontal mixing, benthic boundaries, submarine groundwater inputs, mineral dust infalls, etc.
- establish the transport and fate of both trace micronutrients (iron) and toxic agents (lead, mercury) to the ocean, especially via the atmosphere
- obtain ground-truth proxies of past ocean environments and the ocean's response to global change in order to correctly assess its future health

Preparations are currently in the planning stages, with the program expected to participate in the International Polar Year during 2007-2009. Core activities during 2008-2013 will involve 12-15 ocean sections chosen to address the maximum number of processes run by various countries but with international representation, plus preparations for initiation of several process studies. Final ocean sections plus parallel and follow-up process studies through 2018 will focus on estuaries, shelf processes, the distal northern and southern limbs of the meridional overturning circulations, submarine groundwater fluxes, etc., generally tied to the ends of ocean sections. The program is designed to rely on and coordinate with important

global scale programs such as SOLAS, CLIVAR, IMBER, IPY, LOICZ, ORION/GOOS and IMAGES/PAGES.

GEOTRACES is currently sponsored by SCOR and various national funding agencies. The members of the international planning group, the July 2005 science plan draft, and additional information is available on the GEOTRACES website: http://www.ldeo.columbia.edu/res/pi/geotraces/ (also accessible via www.geotraces.org) Co-chairs of the planning group are Bob Anderson (US - Lamont) and Gideon Henderson (UK - Oxford).

Ice Core Reconstruction of Antarctic Climate Variability Over the Last 200–2000 Years (ITASE)

P.A. Mayewski,
Chair ITASE, Climate Change Institute, University of Maine, USA
Corresponding author: Paul Mayewski <Paul.Mayewski@maine.edu>

Purpose of Ice Core Reconstructions

Antarctica plays a critical role in the dynamic linkages that couple the spatially and temporally complex components of the Earth's system. However, our knowledge of the functioning of Antarctica within the global system and the spatial and temporal complexity of Antarctic climate is poor, largely due to the limitations and the short period (typically 30-50 years) of observational and instrumental data on Antarctic climatic variables. Further, Antarctica exhibits significant regional contrasts, including decoupling of climate change on decadal scales between different parts of the continent. Large areas of the interior of the ice sheet are influenced by the continental temperature inversion while other portions of the interior and the coastal regions are influenced by the incursion of cyclonic systems that circle the continent. As a consequence these coastal regions are mainly connected with lower tropospheric transport whereas high altitude regions in the interior are more likely influenced by vertical transport from the upper troposphere and stratosphere. As a result the coastal regions experience higher climatic variability than regions in the interior. Further, high frequency climatic changes impact both Antarctica and the surrounding Southern Ocean. Some are related to the El Niño Southern Oscillation (ENSO) and other local to regional to global scale climate features such as: atmospheric blocking, sea-ice variations and volcanic event induced atmospheric shielding. Over time periods longer than the instrumental era ice core studies demonstrate that Antarctica experienced millennial to decadal scale climatic variability that is associated with significant changes in temperature, snow accumulation, wind-blown dust, sea-salt loading and methane composition.

ITASE (International Trans Antarctic Scientific Expedition) – A Continent-Wide Array of Ice Cores

The multi-national consortium included within ITASE has, since its inception in 1990, sampled an extensive portion of the Antarctic ice sheet, including many of the proposed deep ice core drilling sites and much of the topography and climate of the Antarctic ice sheet (Figure 1). To date ITASE research has resulted in the collection of more than 240 cores (Figure 2) (for a total length of ~7,000 m), greatly expanding the pre-ITASE ice core inventory over Antarctica, and >20,000 km of associated ground penetrating radar (GPR) coverage. Several properties were identified as part of the original ITASE sampling program, notably: isotopes, major anions and cations, trace elements, hydrogen peroxide, formaldehyde, organic acids, 10m temperatures, stratigraphy, and GPR-GPS. Additionally, ITASE oversnow traverses have provided opportunities for the installation of automatic weather stations, and the measurement of, for example, atmospheric chemistry, ice dielectric, and ice core microparticles plus the deployment of experiments valuable for ground truth in remote sensing missions and geophysical measurements for crustal investigation.

Examples of ITASE Contributions to the Understanding of Climate Variability Over Antarctica and the Southern Ocean

Although full-scale reconstructions of past climate over Antarctica have yet to be finalized, ITASE has pioneered calibration tools and reconstruction of climate indices and evidence for climate forcing using single-sites through to multiple arrays of sites. Initial syntheses of combined ITASE and deep ice core records demonstrate that inclusion of instrumentally calibrated ITASE ice core records allows previously unavailable reconstruction of past regional to continental scale variability in atmospheric circulation and temperature. Emerging results demonstrate the utilization of ITASE records in testing meteorological reanalysis products. Connections are now noted between ITASE climate proxies and global scale climate indices such as ENSO in addition to major atmospheric circulation features over the Southern Hemisphere such as the Amundsen Sea Low, East Antarctic High, and Antarctic Oscillation. Large-scale calibrations between satellite-deduced surface temperature and ITASE ice core proxies for temperature are also now available. ITASE is developing proxies for sea ice, a critical component in the climate system, through comparison of marine emissions records captured in ice cores and sea ice extent data. ITASE research is also focused on understanding the factors that control climate variability over Antarctica and the Southern Ocean, through, for example, the documentation of the impact of solar forcing on zonal westerlies at the edge of the polar vortex.

The greatest unknown in the determination of the mass balance of the Antarctic ice sheet, and its potential role in sea level and ice dynamics, is the surface mass balance (the resultant accumulation of snow - the precipitation minus sublimation and wind-blown snow). ITASE research reveals high variability in surface mass balance and that single cores, stakes, and snowpits do not represent the geographical and environmental characteristics of a local region. Field observations show that the interaction of surface wind and subtle variations of surface slope have a considerable impact on the spatial distribution of snow at short and long spatial scales and that spatial variability of surface mass balance can be higher than its temporal variability at some timescales. Advances in the understanding of mass balance are being made through the tracking of ice core dated isochrones determined from continuous surface GPR measurements. These measurements capture local to regional scale changes in mass balance.

The growing ITASE database has the potential to explore temporal variability and recent evolution of Antarctic climate utilizing an unprecedented spatio-temporal array. Data extraction and validation activities are an essential preliminary to the synthesis task. Such activities, together with development of instrumental calibration techniques have been a significant

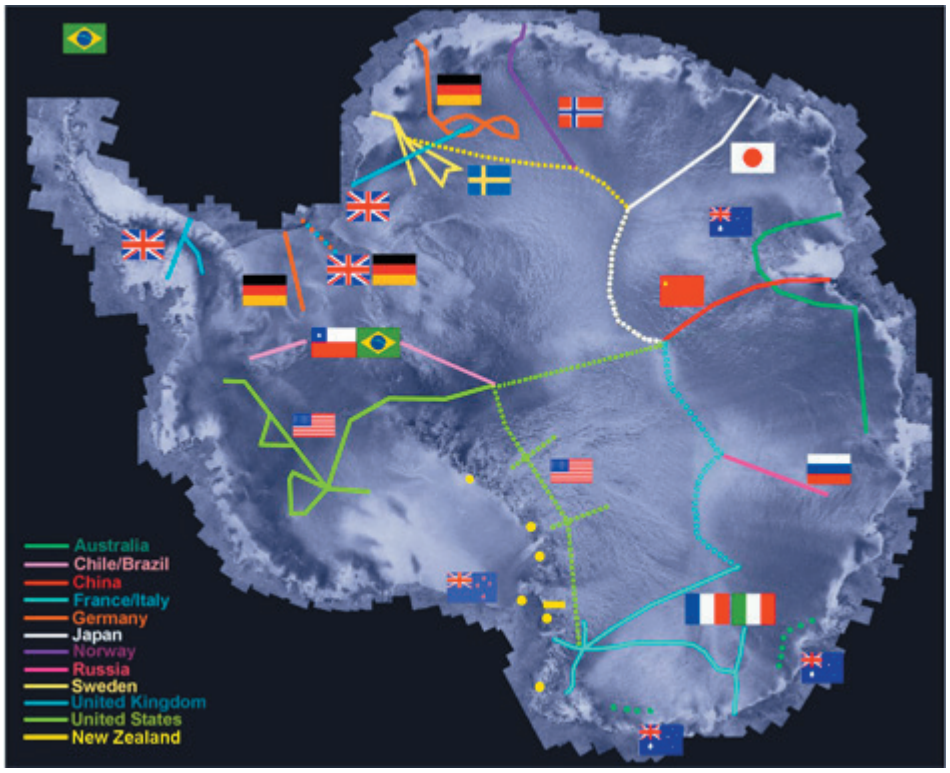

Figure 1 – ITASE traverse routes superimposed on a RADARSAT image. Solid lines indicate completed traverses and dashed those planned for the future.

component of ITASE studies. Maps of the surface distribution of chemical species indicate the unprecedented scope for exploring climate variability as extended time-series become available over broad regions through ITASE and deep ice core drilling projects.

Antarctica is Earth's largest storehouse of buried climate archives (ice cores) and ITASE has already changed this continent from the most poorly sampled of continents, with respect to climate, to the most highly resolved for periods extending beyond the instrumented record of climate. This remarkable accomplishment is essential to unraveling the role of Antarctica in the global climate system. Future ITASE traverses will be essential in completing this goal.

Funding in support of ITASE comes from national funding agencies. For more information including: the ITASE Science and Implementatyion Plan, national reports, publications, and core metadata see www.ume.maine.edu/itase. The SCAR ITASE Project Office is maintainned at the University of Maine www.climatechange.umaine.edu.

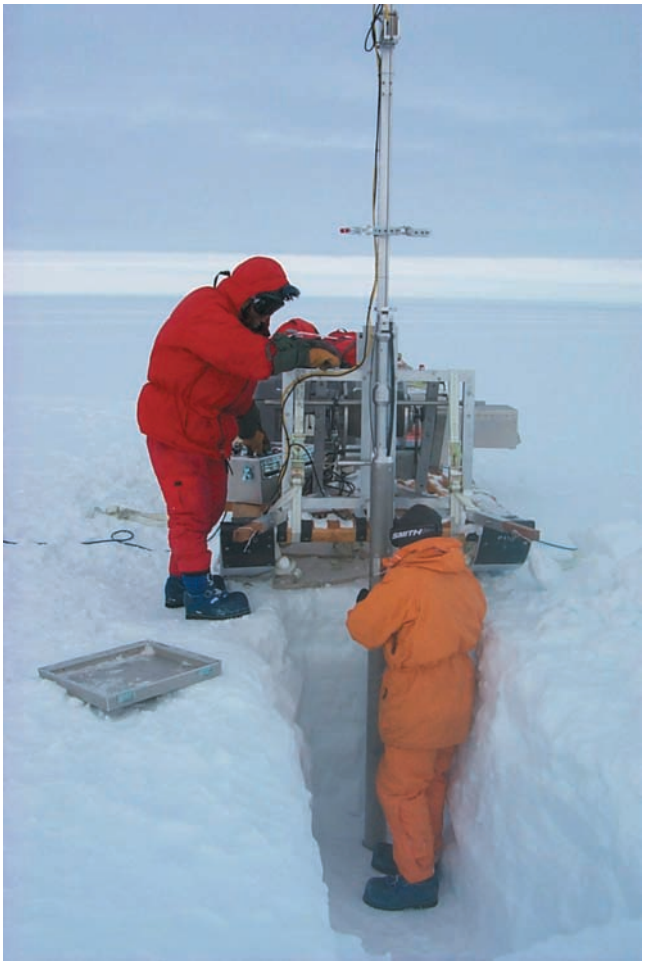

Figure 2 – Ice coring in West Antarctica

Antarctic Circumpolar ice–ocean modelling – status and perspectives

A. Beckmann
Division of Geophysics, Department of Physical Sciences, P.O.Box 64, 00014 University of Helsinki, Finland.

The hydrosphere and marine cryosphere of the Antarctic Marginal Seas are characterised by a number of unique processes. Interactions between atmosphere, ocean, sea ice and ice shelves, lead to complex chains of water mass transformation and exchanges between the surface and deep ocean which are, at least in some regions, strongly affected by tides and episodically subject to freshwater input through drifting and melting icebergs (Figure 1).

The realism of numerical simulations of this system has greatly improved during the past decade, mostly due to the efforts of modelling groups in the US, UK, Belgium and Germany. The representation of key processes has been investigated, both in idealized high resolution configurations (e.g., Schodlok et al., 2002, Holland et al., 2003, Dinniman et al., 2003) and in more complete regional simulations (Beckmann et al., 1999, Timmermann, 2002, Assmann et al., 2003, Assmann and Timmermann, 2005). As a result, a number of algorithmic and parameterizational requirements have been identified as crucial for the success of these models. The main lessons learned are:

(1) it is essential to use a vertical model coordinate that faithfully represents bottom topography and bottom boundary layer dynamics; the large scale circulation, the shelf-deep sea exchange along the Antarctic continental margins depend critically on topography and near bottom processes. There are many areas with strong topographic control and individual topographic features like Maud Rise (Beckmann et al., 2001), may have consequences for sea ice and climate. Drastically increased resolution alone may not be sufficient (Sasai et al., 2004), and is not practical for many applications. Available alternatives are partial step topographies, generalized s-coordinates and isopycnic coordinates, which in fact greatly enhance the performance of the models (see Figure 2).

(2) the use of an oceanic vertical mixing parameterization that preserves the overall thermohaline structure of the Weddell and Ross Gyres in decadal-long integrations is crucial. In particular, the near-surface mixing in seasonally ice covered parts of the Southern Ocean needs to be able to handle salt input from ice formation without producing excessive open ocean convection. The wide-spread practice of surface salinity restoring needs to be abandoned. Investigations like in Timmermann and Beckmann (2004) demonstrate that the problem can be cured by proper parametrization.

(3) the fresh water input from melting ice shelves needs to be included in order to approach the observed water mass products (e.g., Hellmer, 2004), stratification, circulation and spreading of tracers (Schodlok et al.,2001). Options include the addition of the major ice shelf cavities (Beckmann et al., 1999, Timmermann et al., 2002, Holland et al., 2003) or the use of an ice shelf melting parametrization (Beckmann and Goosse, 2001).

(4) both previous issues have to be considered also in connection with the implementation of a coupling algorithm between ocean and cryosphere that avoids the use of a flux correction which limits the applicability of the model results

(5) resolution seems to be less critical than often assumed, as many large scale features (e.g., Beckmann and Timmermann, 2001) can be represented with 0(50) km grid spacing quite well, if the above points are observed.

Nowadays, CLIVAR relevant scientific questions about interannual and interdecadal variability and about the distribution transport of biogeochemical quantities in the Southern Ocean are being addressed with global models, which however, have mostly not been designed to specifically represent the processes in Antarctic Marginal Seas. This means that some of the above issues will be suboptimal in these models.

This calls for renewed activities for rigorous validation of global models with respect to the Southern Ocean and Antarctic Marginal Seas, before (or at least as) these models are used for the analysis, synthesis and interpretation of e.g., IPY results. With new data products becoming available (e.g. sea ice thickness data), we may be able to make a significant step forward.

For the foreseeable future, we have to live with the fact that

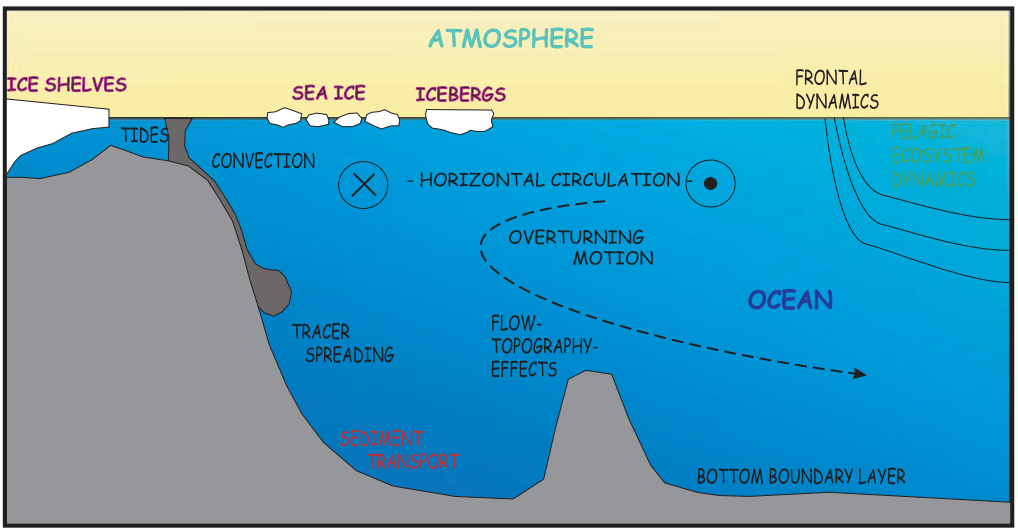

Figure 1: Schematic overview of ice-ocean processes in the Southern Ocean with emphasis on the Antarctic Marginal Seas.

each coupled ice-ocean model represents a unique system and specific changes that appear crucial in one model may not have a significant effect on the results of another. Still, I believe that the knowledge and methodology (as well as appropriate validation data sets) are available to significantly improve the performance of global models in the Antarctic Marginal Seas (see, e.g., Hellmer et al., 2005)

At the same time, however, we should not forget the unresolved issues: the addition of the fresh water effects due to ice shelf calving and iceberg melting (Lichey and Hellmer, 2001, Gladstone, 2001); the addition of mixing and rectification effects by tides (Pereira et al., 2002, Padman et al., 2002) and the development and implementation of parameterizations for polynya coastal dynamics (Marsland et al., 2004).

References:

Assmann, K., Hellmer, H. H., Beckmann, A. (2003). Seasonal Variation in Circulation and Watermass Distribution on the Ross Sea Continental Shelf, *Antarctic Science*, 15(1), 3-11. DOI: 10.1017/S0954 102003001007

Assmann, K. M., Timmermann, R.(2005). Variability of dense water formation in the Ross Sea , *Ocean Dynamics*, DOI: 10.1007/s10236-004-0106-7

Beckmann, A., H.H. Hellmer, and R. Timmermann, 1999: A numerical model of the Weddell Sea: Large scale circulation and water mass distribution. *Journal of Geophysical Research*, 104, 23375-23391.

Beckmann, A., Timmermann, R. (2001). Circumpolar Influences on the Weddell Sea: Indication of an Antarctic Circumpolar Coastal Wave, *Journal of Climate*, 14, 3785-3792

Beckmann, A., Timmermann, R., Pereira, A. F., Mohn, C. (2001). The Effect of Flow at Maud Rise on the Sea Ice Cover - Numerical Experiments, *Ocean Dynamics*, 52, 11-25

Beckmann, A., Goosse, H.(2003). A Parameterization of Ice Shelf-Ocean Interaction for Climate Models, *Ocean Modelling*, 5, 157-170.

Dinniman, M.S., J.M. Klinck and W.O. Smith, Jr., 2003. Cross shelf exchange in a model of the Ross Sea circulation and biogeochemistry, *Deep-Sea Research* II, 50, 3103-3120.

Gladstone, R., G. R. Bigg and K. Nicholls, 2001: Icebergs and fresh water fluxes in the Southern Ocean, *Journal of Geophysical Research*, 106, 19903-19915.

Hellmer, H. H.(2004). Impact of Antarctic ice shelf melting on sea ice and deep ocean properties, *Geophysical Research Letters*, Vol. 31, No. 10, L10307. DOI: 10.1029/2004GL019506

Hellmer, H. H., Schodlok, M. P., Wenzel, M., Schröter, J. G.(2005). On the influence of adequate Weddell Sea characteristics in a large-scale global ocean circulation model, *Ocean Dynamics*. DOI: 10.1007/s10236-005-0112-4

Holland, D.M., S.S. Jacobs, and A. Jenkins, 2003: Modeling Ross Sea ice shelf - ocean interaction. *Antarctic Science*, 15, 13-23.

Lichey, C., Hellmer, H. H. (2001). Modeling giant iceberg drift under the influence of sea ice in the Weddell Sea, *Journal of Glaciology*, 158, 452-460.

Marsland S.J., N.L. Bindoff, G.D. Williams, W.F. Budd, 2004: Modeling water mass formation in the Mertz Glacier Polynya and Adelie Depression, East Antarctica. *Journal of Geophysical Research*, doi:10.1029/2004JC002441

Madec, G., Madec, G., P. Delecluse, M. Imbard and C. Lévy, 1999. OPA 8.1 Ocean General Circulation Model reference manual. Notes du Pôle de modélisation, Institut Pierre-Simon Laplace, N°11, pp 91.

Padman, L., H. A. Fricker, R. Coleman, S. Howard, and S. Erofeeva, 2002. A new tidal model for the Antarctic ice shelves and seas, *Ann. Glaciol.*, 34, 247-254.

Pereira, A. F., Beckmann, A., Hellmer, H. H. (2002). Tidal mixing in the southern Weddell Sea: results from a three-dimensional model, *Journal of Physical Oceanography*, 32(7), 2151-2170.

Sasai, Y., A.Ishida, Y.Yamanaka, and H. Sasaki, 2004:

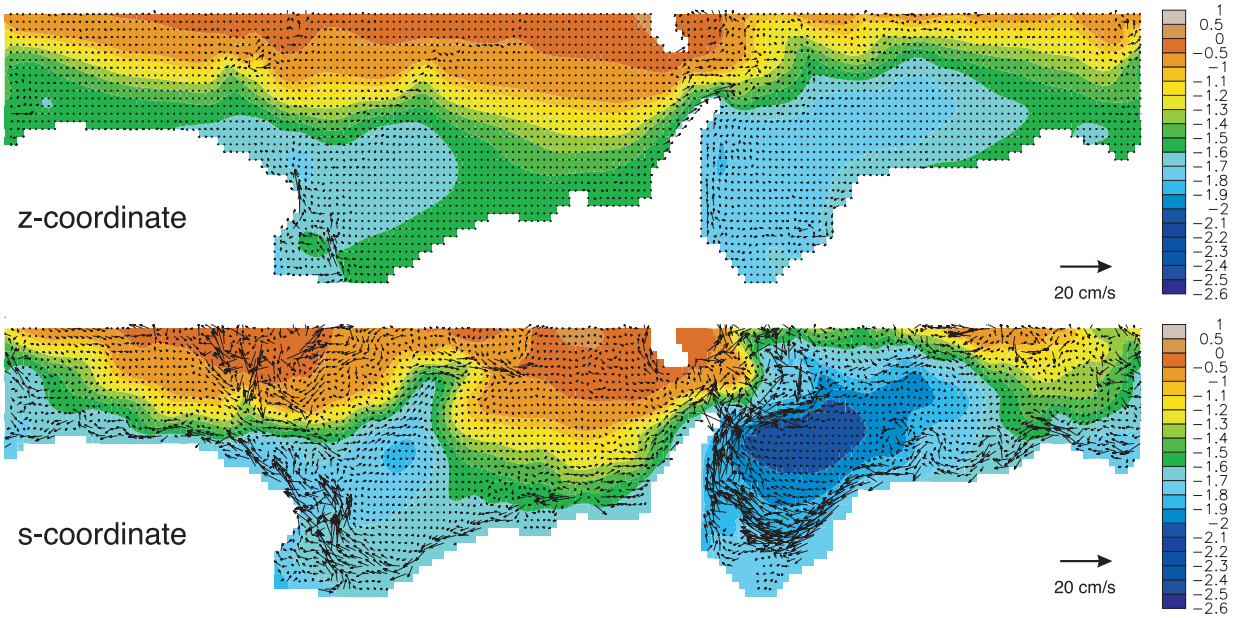

Figure 2: Bottom layer flow field in the Southern ocean south of 50S, on top of the sea surface height (in m) for two otherwise identical simulations of a global coupled ice-ocean model (ORCA2-LIM, Madec et al., 1999) with standard z-coordinate (upper panel) and generalized s-coordinates (lower panel). Note the almost continuous coastal current signature in the latter simulation, along with a more pronounced Weddell Gyre, which both correspond much better to observations.

Chlorofluororcarbons in a global ocean addy resolving OGCM: pathways and formation of Antarctic Bottom Water. *Geophysical Research Letters*, doi:10.1029/2004GL0129895

Schodlok, M.P., Rodehacke, C.B., Hellmer, H.H., Beckmann, A. (2001). On the origin of the deep CFC maximum in the eastern Weddell Sea - numerical model results, *Geophysical Research Letters*, 28, 2859-2862

Schodlok, M.P., H.H. Hellmer, and A. Beckmann, 2002: On the transport, variability and origin of dense water masses crossing the South Scotia Ridge. *Deep-Sea Research* II, 49, 4807-4825.

Timmermann, R., Beckmann, A., Hellmer, H. H.(2002). Simulation of ice-ocean dynamics in the Weddell Sea. Part I: Model configuration and validation, *Journal of Geophysical Research*, 107(C3), 10.1029/2000JC000741.

Timmermann, R., Beckmann, A.(2004). Parameterization of vertical mixing in the Weddell Sea, *Ocean Modelling*, 6(1), 83-100.

Timmermann, R., Goosse, H., Madec, G., Fichefet, T., Ethe, Ch.and Dulière, V., 2005: On the representation of high latitude processes in the ORCA-LIM global coupled sea ice–ocean model. *Ocean Modelling*, 2005, 175-201

Regional Reanalysis for Middle and High Latitudes of the Southern Hemisphere: A Proposal

D.H. Bromwich[1] and K. Speer[2]
[1]Byrd Polar Research Center, The Ohio State University, USA
[2]Department of Oceanography, Florida State University, USA
Corresponding author: bromwich@polarmet1.mps.ohio–state.edu

The Southern Ocean and Antarctic continent are among the most remote parts of our planet but are intimately connected to elsewhere via the atmosphere and ocean on a wide variety of space and time scales. Notable and variable climate changes are taking place in these latitudes, presenting a challenge to understanding whether anthropogenic forcing from increasing concentrations of greenhouse gases is implicated. Global atmospheric reanalyses are primary tools to investigate the behavior of the atmosphere and ocean in this data sparse region. Reanalyses merge all available atmospheric observations from the surface, atmosphere and space with a short-term weather forecast to produce a three-dimensional, time-dependent description of atmospheric behavior. The two most popular global reanalyses (ERA-40 and NCEP-NCAR) span roughly the International Geophysical Year (1957-1958) to today. Yet these reanalyses suffer from many shortcomings related in part to the strong temporal trend in the quantity and quality of observations available for use by a fixed data assimilation scheme (e.g., Bromwich and Fogt, 2004). Trends and variability of reanalysed atmospheric parameters are suspect for a large fraction of the reanalysis period. A huge increase in the number of observations over the Southern Ocean occurred around 1979 at the start of the comprehensive polar orbiting satellite program by the National Oceanic and Atmospheric Administration ("modern satellite era") and this is reflected by improved reanalysis skill after this time.

Following the example provided by the North American Regional Reanalysis (http://wwwt.emc.ncep.noaa.gov/mmb/rreanl/), a regional atmospheric reanalysis is proposed for the middle and high latitudes of the Southern Hemisphere, probably poleward of 35°S. The goals are to provide higher resolution in space and time than the global reanalyses (~100 km at 6-h intervals) and to yield more detailed and comprehensive descriptions of the energy, momentum, and freshwater fluxes between the atmosphere, ocean, and ice sheet. Improved resolution in space and time will capture phenomena characterized by strong spatial variability and rapid change, especially mesoscale circulations associated with complex terrain or frontal zones in the atmosphere and ocean.

Other issues that have surfaced with global reanalyses concern the assimilating model's climatology that governs the reanalysis solution when limited data are available to constrain the assimilation and the use of model parameterizations that are optimized for lower latitudes. The latter most often impacts reanalysis variables derived from short-term forecasts, such as precipitation, clouds, and radiation fluxes. A regional reanalysis using an assimilating model optimized for high latitudes can minimize these limitations.

More detailed descriptions of the surface temperatures over the ice-free ocean and of the sea ice characteristics can be prepared to constrain the regional reanalysis at the lower boundary. As a prelude to the reanalysis, a sustained effort is needed to uncover and quality control all available observations from ground-based platforms such as research vessels and from space. This is needed because global reanalyses have omitted a surprising amount of "conventional observations". The regional reanalysis will certainly span 1979 to present. Less accurate but still useful descriptions could be produced back to the International Geophysical Year when the Southern Ocean was not well monitored but Antarctica was sampled by a data network similar to today. It is anticipated that an intensive focus on reanalysis for middle and high southern latitudes will produce realistic trends and variability of atmospheric parameters spanning many decades, and will help to address the role of these areas in global climate variability and change.

Reference

Bromwich, D.H., and R.L. Fogt, 2004: Strong trends in the skill of the ERA-40 and NCEP/NCAR reanalyses in the high and middle latitudes of the Southern Hemisphere, 1958-2001. *J. Climate,* 17, 4603-4619.

Contents